

The background of the cover features a microscopic image of human adult stem cells, showing a dense network of fibrous structures and several large, circular cells with prominent nuclei. The image is rendered in shades of orange and blue, creating a textured, organic appearance.

John R. Masters
Bernhard Ø. Palsson
Editors

Human Cell Culture 7

Human Adult Stem Cells



Springer

HUMAN CELL CULTURE
Volume VII: Human Adult Stem Cells

Human Cell Culture

Volume 7

For further volumes:
<http://www.springer.com/series/6058>

Human Cell Culture

Volume VII

Human Adult Stem Cells

edited by

John R. Masters

University College London, London, UK

and

Bernhard Ø. Palsson

University of California, San Diego, CA, USA

 Springer

Editors

Dr. John R. Masters
University College London
67 Riding House Street
London
United Kingdom W1W 7E
j.masters@ucl.ac.uk

Prof. Bernhard Ø. Palsson
University of California, San
Diego
Dept. Bioengineering
9500 Gilman Dr.
La Jolla CA 92093-0412
USA
bpalsson@bioeng.ucsd.edu

ISSN 1389-2142

ISBN 978-90-481-2268-4

e-ISBN 978-90-481-2269-1

DOI 10.1007/978-90-481-2269-1

Springer Dordrecht Heidelberg London New York

Library of Congress Control Number: 2009926880

© Springer Science+Business Media B.V. 2009

No part of this work may be reproduced, stored in a retrieval system, or transmitted in any form or by any means, electronic, mechanical, photocopying, microfilming, recording or otherwise, without written permission from the Publisher, with the exception of any material supplied specifically for the purpose of being entered and executed on a computer system, for exclusive use by the purchaser of the work.

Cover design: Boekhorst Design BV

Printed on acid-free paper

Springer is part of Springer Science+Business Media (www.springer.com)

Preface

The aim of this volume is to provide protocols for isolating and maintaining human adult stem cells in culture and methods for directing differentiation into specialized cell types.

Human adult stem cells from each tissue are potentially capable of differentiating into all the cell types within that tissue. Consequently there is considerable interest in using these cells for the treatment of a wide variety of medical conditions. Careful consideration needs to be given to the relative value of embryonic (described in Human Cell Culture Volume 6), induced pluripotential stem cells and adult stem cells. The development and optimization of techniques for growing human adult stem cells are crucial for the clinical application of these cells and are the focus of this volume.

Contents

1 Neural Progenitors	1
Dustin R. Wakeman, Martin R. Hofmann, Yang D. Teng and Evan Y. Snyder	
2 Multipotent Stromal Cells (hMSCs)	45
Margaret Wolfe, Alan Tucker, Roxanne L. Reger and Darwin J. Prockop	
3 Endothelium	73
Sangmo Kwon and Takayuki Asahara	
4 Lung	91
Rabindra Tirouvanziam, Megha Makam and Bruno Péault	
5 Eye	113
Maria Notara, Yiqin Du, G. Astrid Limb, James L. Funderburgh and Julie T. Daniels	
6 Colon	143
F. Iovino, Y. Lombardo, V. Eterno, P. Cammareri, G. Cocorullo, M. Todaro and G. Stassi	
7 Spermatogonia	157
Makoto C. Nagano, Jonathan R. Yeh and Khaled Zohni	
8 Hair Follicle Pluripotent Stem (hfPS) Cells	171
Robert M. Hoffman	

9 Pancreas 183
Fang-Xu Jiang and Grant Morahan

10 Prostate 197
C. Foley, K.T. Brouillette, C. Kane, H. Patel, H. Yamamoto
and A. Ahmed

Contributors

A. Ahmed Division of Surgery and Interventional Sciences, Charles Bell House Laboratories, Prostate Cancer Research Centre, University College London, 67 Riding House Street, London, UK, aamir.ahmed@ucl.ac.uk

Takayuki Asahara Department of Regenerative Medicine, Tokai University School of Medicine, Isehara, Kanagawa 259-1193, Japan, asa777@aol.com

K. T. Brouillette Division of Surgery and Interventional Sciences, Charles Bell House Laboratories, Prostate Cancer Research Centre, University College London, 67 Riding House Street, London, UK, k.brouillette@ucl.ac.uk

P. Cammareri Department of GENURTO, University of Palermo, Palermo, Italy, patrizia.cammareri@gmail.com

G. Cocorullo Department of GENURTO, University of Palermo, Palermo, Italy, gianfranco.cocorullo@unipa.it

Julie T. Daniels UCL Institute of Ophthalmology, 11-43 Bath Street, EC1V 9EL, London, UK, j.daniels@ucl.ac.uk

Yiqin Du Department of Ophthalmology, School of Medicine, UPMC Eye Center, University of Pittsburgh, Pittsburgh, PA 15213, USA, yiqindu@pitt.edu

V. Eterno Cellular and Molecular Pathophysiology Laboratory, Department of Surgical and Oncological Sciences, University of Palermo, Palermo, Italy, eternovincenzo@libero.it

C. Foley Division of Surgery and Interventional Sciences, Charles Bell House Laboratories, Prostate Cancer Research Centre, University College London, 67 Riding House Street, London, UK, charlotte.foley@hotmail.com

James L. Funderburgh Department of Ophthalmology, School of Medicine, UPMC Eye Center, University of Pittsburgh, Pittsburgh, PA 15213, USA, jlfunder@pitt.edu

Robert M. Hoffman Department of Surgery, University of California, AntiCancer, Inc., 7917 Ostrow Street, San Diego, CA 92111, USA, all@anticancer.com

Martin R. Hofmann The Burnham Institute for Medical Research, La Jolla, CA 92037, USA

F. Iovino Cellular and Molecular Pathophysiology Laboratory, Department of Surgical and Oncological Sciences, University of Palermo, Palermo, Italy, flora.iovino@gmail.com

Fang-Xu Jiang Western Australian Institute for Medical Research Centre for Diabetes Research and Centre for Medical Research, The University of Western Australia, 50 Murray St (Rear), Perth, WA 6000, Australia, jiang@waimr.uwa.edu.au

C. Kane Division of Surgery and Interventional Sciences, Charles Bell House Laboratories, Prostate Cancer Research Centre, University College London, 67 Riding House Street, London, UK, c.kane@ucl.ac.uk

Sangmo Kwon Department of Regenerative Medicine, Tokai University School of Medicine, Isehara, Kanagawa 259-1193, Japan

G. Astrid Limb UCL Institute of Ophthalmology, 11-43 Bath Street, EC1V 9EL, London, UK, g.limb@ucl.ac.uk

Y. Lombardo Cellular and Molecular Pathophysiology Laboratory, Department of Surgical and Oncological Sciences, University of Palermo, Palermo, Italy, ylela@hotmail.com

Megha Makam Department of Pediatrics, Stanford University School of Medicine, Stanford, CA 94305-5318, USA, meghasmakam@gmail.com

Grant Morahan Western Australian Institute for Medical Research, and Centre for Medical Research, Centre for Diabetes Research, The University of Western Australia, Perth 6000, Australia, gem@wairmr.uwa.edu.au

Makoto C. Nagano Department of Obstetrics and Gynecology, Royal Victoria Hospital, McGill University, Montreal, Quebec H3A 1A1, Canada, makoto.nagano@muhc.mcgill.ca

Maria Notara UCL Institute of Ophthalmology, 11-43 Bath street, EC1V 9EL, London, UK, m.notara@ucl.ac.uk

H. Patel Division of Surgery and Interventional Sciences, Charles Bell House Laboratories, Prostate Cancer Research Centre, University College London, 67 Riding House Street, London, UK, hrhpatel@hotmail.com

Bruno Péault Departments of Pediatrics and Cell Biology, Stem Cell Research Center, Children's Hospital of Pittsburgh, Pittsburgh, PA 15213, USA, bruno.peault@chp.edu

Darwin J. Prockop Institute for Regenerative Medicine at Scott and White, Texas A&M Health Sciences Center, Temple, TX, 76502, USA

Roxanne L. Reger Institute for Regenerative Medicine at Scott and White, Texas A&M Health Sciences Center, Temple, TX, 76502, USA

Evan Y. Snyder The Burnham Institute for Medical Research, University of California at San Diego, Graduate Program in Biomedical Sciences, 9500 Gilman Dr., La Jolla, CA 92093, USA, esnyder@burnham.org

G. Stassi Cellular and Molecular Pathophysiology Laboratory, Department of Surgical and Oncological Sciences, University of Palermo, Palermo, Italy, gstassi@tiscali.it

Yang D. Teng Departments of Neurosurgery, and Physical Medicine and Rehabilitation, Harvard Medical School, Brigham and Women's Hospital and Spaulding Rehabilitation Hospital; Division of Spinal Cord Injury Research, Veterans Affairs Boston Healthcare System, Boston, MA 02130, USA

Rabindra Tirouvanziam Department of Pediatrics, Stanford University School of Medicine, Stanford, CA 94305-5318, USA, tirouvan@stanford.edu

M. Todaro Cellular and Molecular Pathophysiology Laboratory, Department of Surgical and Oncological Sciences, University of Palermo, Palermo, Italy, matilde.todaro@tiscali.it

Alan Tucker Center for Gene Therapy, Tulane University Health Sciences, New Orleans, LA, 70112, USA, atucker@tulane.edu

Dustin R. Wakeman The Burnham Institute for Medical Research, University of California at San Diego, Graduate Program in Biomedical Sciences, 9500 Gilman Dr., La Jolla, CA 92093, USA, dwakeman@burnham.org

Margaret Wolfe Center for Gene Therapy, Tulane University Health Sciences, New Orleans, LA, 70112, USA, peggiwolfe@bellsouth.net

H. Yamamoto Division of Surgery and Interventional Sciences, Charles Bell House Laboratories, Prostate Cancer Research Centre, University College London, 67 Riding House Street, London, UK, h.yamamoto@ucl.ac.uk

Jonathan R. Yeh Department of Obstetrics and Gynecology, Royal Victoria Hospital, McGill University, Montreal, Quebec H3A 1A1, Canada

Khaled Zohni Department of Obstetrics and Gynecology, Royal Victoria Hospital, McGill University, Montreal, Quebec H3A 1A1, Canada

Chapter 1

Neural Progenitors

Dustin R. Wakeman, Martin R. Hofmann, Yang D. Teng
and Evan Y. Snyder

Abstract Several derivation techniques have been published [1–11] describing both free floating aggregate and adherent human NSC/NPC cultures under a variety of growth factor regimes [3, 12–45]. We describe here, a detailed reproducible methodology for the successful isolation, expansion, and preservation of bona fide human fetal (10–24 weeks) NPC that relies on a specific temporal combination of mitogenic growth factors (EGF, bFGF, and LIF) and is independent of whether cells are cultured adherent or as aggregates. We have implemented strict selection and expansion criteria to further exclude more restricted cellular phenotypes from the stem/progenitor pool during the initial derivation procedure. Selection criteria ensure that cells fulfill both an operational definition of a stem cell as well as retain engraftability in multiple experimental models. For simplicity sake, we will refrain from the stem vs. progenitor debate [46–51] and simply refer to both neural stem and progenitor cells as NPCs from here forward.

1.1 Primary Derivation and Selection of hNPC

In general, the primary goal while culturing hNPC is to minimize signals that promote maturation and maximize signals that promote maintenance of the cell-cycle and active proliferation, while holding differentiation in abeyance. In a practical sense, this means providing mitogens and minimizing extensively prolonged cell–cell contact or unchecked adherence to surfaces. Throughout all hNPC derivation and maintenance procedures, it is *EXTREMELY* important to adhere to the following recommendations to ensure maximum cellular recovery. Excessive mechanical force will shear fragile hNPC, therefore, they should always be triturated gently and centrifuged at low speeds for short periods of time to minimize overall cell death,

E.Y. Snyder (✉)

Burnham Institute for Medical Research, 10901 North Torrey Pines Road, La Jolla,
CA 92037, USA

e-mail: esnyder@burnham.org

The authors declare no conflicting or competing financial interest.

maximize recovery, and increase the overall viability of hNPC cultures. In addition, anytime hNPC are centrifuged, the supernatant should be carefully removed so as not to dislodge the cell pellet. The process is easily achieved by slowly tilting the 15 mL conical tube and removing all but the lower 50–100 μ l of supernatant directly above and adjacent to the cell pellet (approximately 1 mm below meniscus of supernatant).

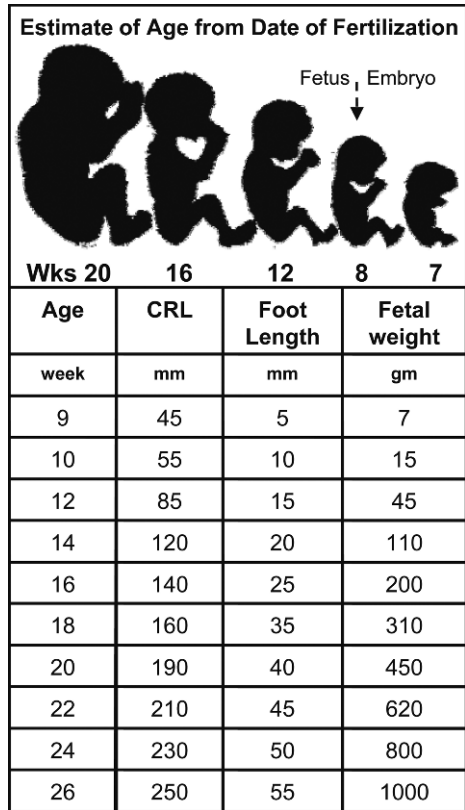
Derivation and expansion of hNPC is a multifaceted, highly dynamic process with many underappreciated intricacies. Although the procedures described here may appear fairly clear-cut, hNPC cultures can be highly variable and often deviate from the prototypical “normality” of standard tissue culture. As a result, it is often necessary to adjust standard protocols “impromptu” to ensure the health and stability of progenitor cultures over time. Understanding how to cope with and adapt to specific hNPC culture disparities will ultimately be learned through hands-on experience in the tissue culture hood. The following procedures should be used as the backbone upon which to learn the basic techniques of hNPC culture and more importantly should be adapted to best accommodate the properties of each specific hNPC line.

1.1.1 Determination of Fetal Age and Developmental Stage

The investigator typically comes into possession of fetal tissue post-mortem as cadaveric material (Prior to 23 weeks of gestation, a fetus is non-viable outside of the womb). Between the eighth and ninth week of development, the embryo undergoes several distinct developmental transitions [52–67]. Both the feet and hands lose their webbing and become separated into distinct digits, and the stubby tail disappears. At 9 weeks post-fertilization, by convention, the embryo is called a fetus. Estimation of fetal age can be extremely tricky without prior knowledge of the last normal menstrual period or day of fertilization (which is rarely known by clinicians); however there are a few decent methods to gauge estimated fetal age and developmental stage. Fetal entities are most accurately staged using pre-term ultrasound measurements [66, 68–70], however, these vital records are rarely granted to the investigator, therefore, we must rely on post-mortem methods including crown to rump length (CRL) [71–77], foot length, head to trunk, cheek to cheek, and fetal weight for quantitative analysis (Table 1.1). When utilized individually, these methods are often inaccurate, as fetal specimens are affected by stretching. A combination of strategies, however, can be used to accurately determine fetal age within several days of fertilization.

The most common and useful parameter for aging and developmental analysis has remained CRL due to its high correlation with definitive gestational changes. Starting at week 9 (from date of fertilization), the head contributes to almost half of the CRL, which more than doubles by the end of week 12. From weeks 12 to 16, fetal growth is rapid, albeit the head remains relatively stable, contributing less to the total CRL than during weeks 9–12. Importantly, skull and long bone ossification

Table 1.1 Fetal developmental staging. Determining the relative fetal developmental age is crucial for proper anatomical assessment prior to dissection of the brain. Specifically, Crown Rump Length (CRL) is used as an appropriate measure for staging post-mortem fetuses. All measurements are averages based on deviations from Streeter’s original tables from fixed fetuses based on the *time from fertilization* and intended as general reference points to gauge developmental staging of the brain. Gestational age begins 2 weeks after fertilization age. Fetuses born prematurely after 22 weeks may survive with artificial support but have limited capacity due to underdevelopment of both the respiratory and nervous systems



begins to set in and should be considered when deriving hNPC from fetuses of this developmental period. By the end of the 16th week, the eyes are repositioned anteriorly from anterolateral and overall fetal growth slows down considerably.

As development proceeds over the next four weeks, the CRL continues to increase by about 50 mm, and the lower limbs reach their final proportions. By 20 weeks, hair and genitalia begin to develop and the mother will start to experience fetal movements, or *quickenings*. It is at this time that the fetal entity begins to fully develop and take on substantial weight. Furthermore, between weeks 21 and 25, the fetus develops blood filled capillaries, fingernails, and rapid eye movements reminiscent of newborns. Several diagrams [78] and animations [79] of human development [80] can be found online. A thorough and accurate assessment should be made to properly identify the age of the fetus before dissection. All procedures must be carried out in strict accordance with federal regulations. For example, in the United States, federal law mandates that the latest time a woman may legally terminate pregnancy to be roughly 24 weeks. Typically, cadavers become available to the investigator at 9–15 weeks of age, a time at which landmarks are admittedly hard to identify.

1.1.2 Dissection and Digestion of Human Fetal Periventricular Zone

Specific CNS anatomical features and their respective stereotactic coordinates highly depend on the precise stage of development and age of the fetal cadaver (Fig. 1.1). Therefore, the exact methodology and localization for initial surgical dissection will largely depend on both the specific CNS region of interest as well as the overall quality of the donor brain, which can be sub-optimal, especially when dealing with pre-term aborted fetuses. In addition, careful tissue resection requires precise surgical coordination coupled with an extensive knowledge of basic developmental neuroanatomy to accurately delineate and specify defined anatomical boundaries.

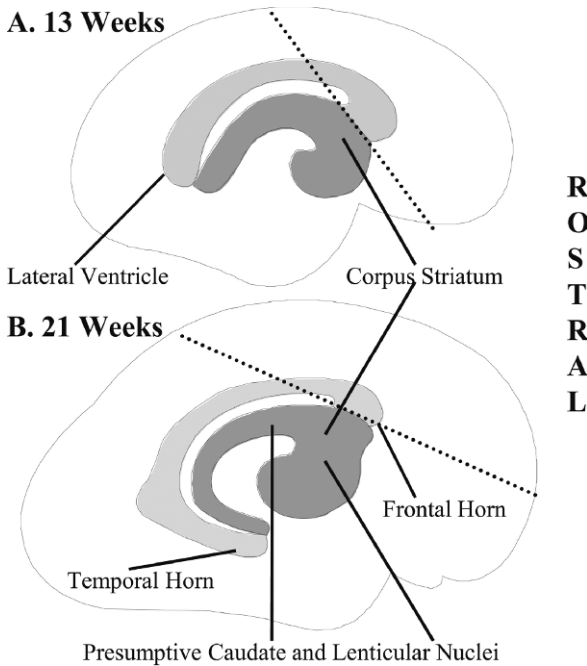


Fig. 1.1 Fetal cerebral hemispheres and ventricular zone development

Sagittal anatomical rendering of the medial surface of the fetal brain at 13 and 21 weeks after fertilization. As the brain develops, the cerebral hemispheres expand and meet at the midline, giving rise to the corpus striatum and shaping the cerebrospinal fluid filled, C-shaped cavities known as the lateral ventricles (A, B). As the cerebral cortex begins to differentiate, the corpus striatum eventually divides into the horseshoe shaped caudate nucleus and the bulbous lentiform nucleus, which houses the putamen and globus pallidus (B). At 13 weeks, the surface of the cerebral hemispheres are smooth and underdeveloped, highly resembling lower order mammals, however by 21 weeks, patterned convolutions (gyri) and grooves or furrows (sulci) form complex folds increasing the total surface area with little change in cranial parameters. In addition, the lateral sulcus begins to narrow as the insula becomes buried (not pictured). We generally dissect along the dashed line and remove the periventricular zone adjacent to the head of the caudate nucleus

A quality detailed description for the basic autopsy of post-mortem fetal brain has been detailed previously [37] and is suggested as a preliminary anatomical outline for primary dissection. Specifically, we refer the reader to anatomical coordinates for the isolation of periventricular zone [61] telencephalic forebrain hNPC for which culturing techniques will be described in detail here.

The following procedures are to be performed aseptically in a sterile, level-2 biosafety hood. Surgical tools are sterilized in a hot bead sterilizer, autoclave (250°F, 2 h), or by gas sterilization prior to surgical resection of the brain. Tools are placed in fresh 70% Et-OH when not in use throughout the procedure and briefly rinsed two times in fresh sterile dPBS immediately following removal from Et-OH, just prior to tissue exposure. The most frequently utilized basal medium for serum-free rodent NPC culture has traditionally been DMEM/F-12 supplemented with N2, however, we have adapted the recipe to best suit human NPC by utilizing specially formulated Neurobasal medium [81–83] with B-27 supplement (without vitamin A) [84–88] to enhance the long-term proliferative potential of hNPC in vitro. In addition, heparin has been shown beneficial in stabilizing the binding of the heparin-sulfate proteoglycan, basic fibroblast growth factor (bFGF), to its FGFR-1 receptor [89, 90], potentiating cell–cell attachments that favor adherent hNPC growth [91, 92]. On the day of derivation, prepare fresh *NB-B27 growth medium* (see Section 1.7.3) + (20 ng/mL) Epidermal Growth Factor (EGF), (20 ng/mL) basic Fibroblast Growth Factor (bFGF) and (4 μ l/mL) (2X) Normocin as an anti-pathogenic agent (replaces pen/strep/amphoB to deter mycoplasma, gram (+) and (–) bacteria, and fungal contamination).

Upon removal of the fetus, a quick examination for overall integrity should be undertaken. Specifically, freshly expelled normal healthy fetuses will display a “shiny translucent appearance [93]” in contrast to their deceased counterparts that generally take on a “tanned appearance and lack normal resilience [93]”. Only normal healthy intact forebrain should be utilized for proper anatomical assessment. Following anatomical measurement and developmental staging, open the head cavity and carefully remove the intact brain. Separate the cerebral hemispheres with one midline sagittal cut, followed by region specific 1 cm coronal cuts from frontal to occipital poles. Select and set aside the desired brain tissue slice and block for subsequent dissociation. The remaining tissue should be fixed in Formalin (10%) for a more extensive neuropathological examination to ensure no gross abnormalities exist. A standard pathogen testing program for hepatitis B and C, HTLV-1/2, syphilis RPR, HIV-1/2, cytomegalovirus, Hantaviruses (Hantaan, Seoul, Sin Nombre), West Nile virus, *Trypanosoma cruzi*, and mycoplasma should also be performed before autopsy and *throughout* the entire natural history of the NPC culture to ensure proper safety. In addition, we recommend the h-IMPACT Profile pathogen test in conjunction with the IMPACT Profile VIII– Comprehensive Murine Panel from the University of Missouri Research Animal Diagnostic Laboratory (RADIL) to thoroughly check hNPC population throughout long-term expansion.

With a fine surgical scalpel, carefully scrape or cut the ventricular wall and adjacent subventricular zone region from the forebrain block of interest. Delicately mince the dissected tissue into small pieces with the scalpel blade, and gently

transfer to a 15 mL sterile conical tube containing 6 mL **cold** NB-B27 growth medium + (20 ng/mL) EGF, (20 ng/mL) basic bFGF, and (4 μ l/mL) (2X) Normocin. Allow the minced tissue to settle by gravity (1–2 min), rinse three times with 8 mL **cold** medium, and resuspend the tissue into 8 mL total medium. Primary dissection should be performed as sterile as possible, but contamination is possible and thus Normocin should be supplemented regularly (48-h half-life) to deter pathogens during the initial derivation process. Normocin and any other antibiotics employed may be weaned from the culture after an adequate period of time. We do not recommend primary derivation without a pathogen control agent. In our hands, Normocin is the most gentle yet potent and comprehensive single treatment application on the market.

Gently triturate the fetal tissue suspension (10–15 times) with a fire polished glass pipette or 5 mL pipette on medium speed (without introducing air bubbles) against the wall of the 15 mL conical tube to dissociate the culture into a “milky” solution of mainly single cells and a lesser portion of small cellular clumps that may not completely dissociate. Earlier term CNS tissue is much softer than its fully developed myelinated adult counterpart [1, 2, 9], therefore, later stage preparations may need to be catalytically enhanced by the addition of an enzymatic agent such as Accutase, Trypsin-EDTA, Papain-Protease-DNase I (PPD), Dispase, or any of the other new commercially available agents to fully dissociate primary cultures for initial plating. It is important that the primary tissue is not overzealously digested into single cell suspensions due to the excessive period of time required and subsequent damage to the progenitor fraction within the culture. Any large undissociated “brain bits” present after initial trituration can be removed by allowing them to settle by gravity (2–3 min) followed by collecting the suspension of cells in the top supernatant. The remaining undissociated cell clumps can then be subjected to a second round of dissociation and pooled together with the originally dissociated cell suspension. In general, fetal tissue dissociation averages around 5–10 min, while adult tissue can take upwards to 45–90 min to generate the desired breakdown of brain tissue. Enzymatic preparations are inactivated and centrifuged for 5 min at 400 rcf, followed by plating in 8 mL pre-warmed medium as described below.

1.1.3 Establishing Primary hNPC Cultures

Upon thorough dissociation, the primary cell suspension is brought to working volume with pre-warmed NB-B27 growth medium + (20 ng/mL) EGF, (20 ng/mL) bFGF, (10 ng/mL) LIF, and (4 μ l/mL) Normocin (2X) for a final density of approximately (1×10^5 cells/cm²) and transferred to either non-TC treated culture flasks for three dimensional (3D) mixed aggregate/adherent parameters or to fibronectin coated TC-treated flasks for monolayer-like (2D) adherent growth (discussed further [94]) and placed in a humidified 5% CO₂ incubator at 37°C. Cell viability counts can be made utilizing either the propidium iodide or trypan blue exclusion assay and hemacytometer to estimate the number of live cells for reconstitution, however this can often be difficult due to the presence of sticky cellular debris and small undissociated neural clumps.

Although the majority of cells will either die or differentiate, the addition of (0.1–1%) Fetal Bovine Serum (FBS) has been found to increase the initial NPC expansion success and efficiency as well as promote adhesion [2]. Serum components promote initial attachment of primary cultures at a relatively low cost to differentiation, but bring the added cost of unwanted variability. It is generally accepted that short periods of time in serum followed by replacement with serum-free defined medium will not potentiate any unwarranted long-term side effects on hNPC. Careful consideration should be made with regards to undefined serum formulations, as newly derived stem cell lines are often desired to be established using serum-free protocols.

Within 12–48 h, cultures containing serum are rinsed two times in dPBS and switched to serum-free conditions in NB-B27 growth medium + (20 ng/mL) EGF + (20 ng/mL) bFGF + (10 ng/mL) LIF + (4 μl/mL) Normocin (2X). Three to four days after the initial plating, primary cultures are supplemented by carefully removing the top half of the culture medium from each flask, termed “conditioned medium” (CM), and replacing with fresh NB-B27 growth medium + (40 ng/mL) EGF + (40 ng/mL) bFGF + (20 ng/mL) LIF + (8 μl/mL) Normocin (4X) to achieve a final working culture concentration of (20 ng/mL) EGF, (20 ng/mL) bFGF, (10 ng/mL) LIF, and (4 μl/mL) Normocin (2X). To enhance recovery, the removed CM (containing free-floating aggregates of remaining primary tissue) is then transferred to a new flask, triturated thoroughly to redissociate the neural clumps, and itself supplemented with fresh growth factors and antibiotics by the same procedure. Alternatively, you may centrifuge unattached floating aggregates and cellular debris for 3.5 min at 400 rcf, aspirate, and either replate into 8 mL fresh pre-warmed NB-B27 growth medium + (20 ng/mL) EGF, (20 ng/mL) bFGF, (10 ng/mL) LIF, and (4 μl/mL) Normocin (2X) or add the cells back to the original parent culture flask for further expansion (Fig. 1.2).

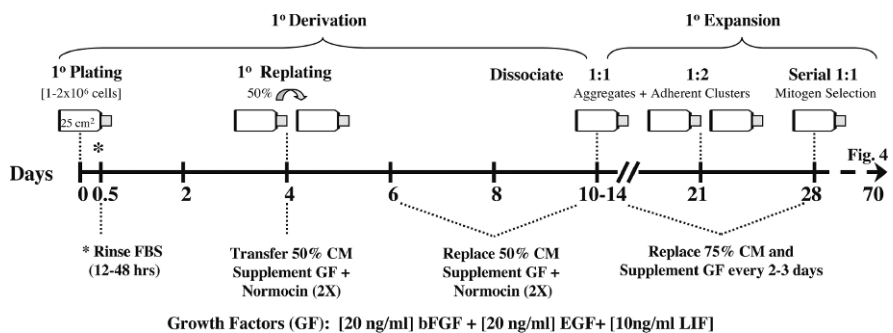


Fig. 1.2 Human neural progenitor cell primary derivation and expansion

Telencephalic forebrain tissue is dissociated and replated with(*) or without serum supplementation. Primary hNPC are then supplemented 3–4 days later with fresh NB-B27 and growth factors (GF) (bFGF, EGF, LIF), and every 2 days thereafter for around 10–14 days until cultures proliferate and expand throughout the flask. After approximately 2 weeks, hNPC cultures are lightly dissociated into single cells and small (4–8 cell) clusters

During the first few weeks a primary culture will begin to proliferate and expand throughout the flask. Initially, cultures are comprised of both free-floating and adherent aggregates that can be easily detached from the surface by simple trituration. *Adherent monolayer-like* hNPC will also actively proliferate within the primary cultures and *should be incorporated* with the suspension aggregates during the initial expansion. As cells continue to proliferate and overtake their differentiating post-mitotic counterparts, confluent adherent hNPC cultures spontaneously give rise to spherical blast like balls that break away from the initial culture and continue to expand and self-renew as aggregates. Promising hNPC cultures that grow well and continue to proliferate in a morphologically relevant manner are subsequently dissociated into small clumps (3–8 cells/clump) or single cell suspensions with Accutase or Cell Dissociation Buffer (CDB)/Cellstripper *when cellular clusters become greater than 12–15 cells in diameter and can no longer be mechanically separated by simple trituration or when adherent cultures become greater than 75% confluent* (Fig. 1.3) (see Section 1.2.5). Both free floating and adherent cells may be pooled together, however, cultures that cannot be readily dissociated are promptly excluded from the remaining pool of primary cells. The surviving hNPC are then replated at a 1:1 or 1:2 ratio and grown as either adherent monolayers (Fig. 1.3E,F) or as lightly adherent aggregates (Fig. 1.3A,B) (see Section 1.2.6) in NB-B27 growth medium + (20 ng/mL) EGF, (20 ng/mL) bFGF, and (10 ng/mL) LIF for two more weeks. During this period, 75% of the medium is exchanged every 2–3 days to replenish the growth factors [95] and antibiotics. Cultures are passaged (1:1 or 1:2) once per week or as necessary. After 2 weeks, LIF and EGF are excluded and hNPC are switched to NB-B27 growth medium + (20 ng/mL) bFGF for mitogen selection.

1.1.3.1 Mitogenic Signaling and Self-Renewal in hNPC

The successful expansion of hNPC requires optimal culture conditions and nutrient balance to support proliferation and survival of newly derived progenitors. Long-term in vitro self-renewal in serum-free defined medium requires addition of mitogens [96, 97], activating the mitogen-activated-protein-kinase (MAPK) signaling cascade to enhance hNPC division and offset the naturally occurring apoptotic process in the developing telencephalon [98–100]. Although originally described utilizing epidermal growth factor (EGF) alone [101–104], EGF was only half as effective in replacing serum, whereas basic fibroblast growth factor (bFGF) could entirely emulate the proliferative capacity of serum [105–125] in serum-free medium at low concentrations (<1 ng/mL) serving as a survival and elongation factor or at higher concentration (20 ng/mL) as a proliferative substitute [116, 126]. Both mitogens give rise to proliferative precursors, albeit at different efficiencies [101, 126, 127], suggesting that separate or overlapping subpopulations [128] may be mobilized by these growth factors. Developmentally, the most immature neural progenitors are said to be first bFGF responsive and then acquire EGF responsiveness [129], therefore, we began with the assumption that the most immature cells are responsive to both EGF and bFGF.

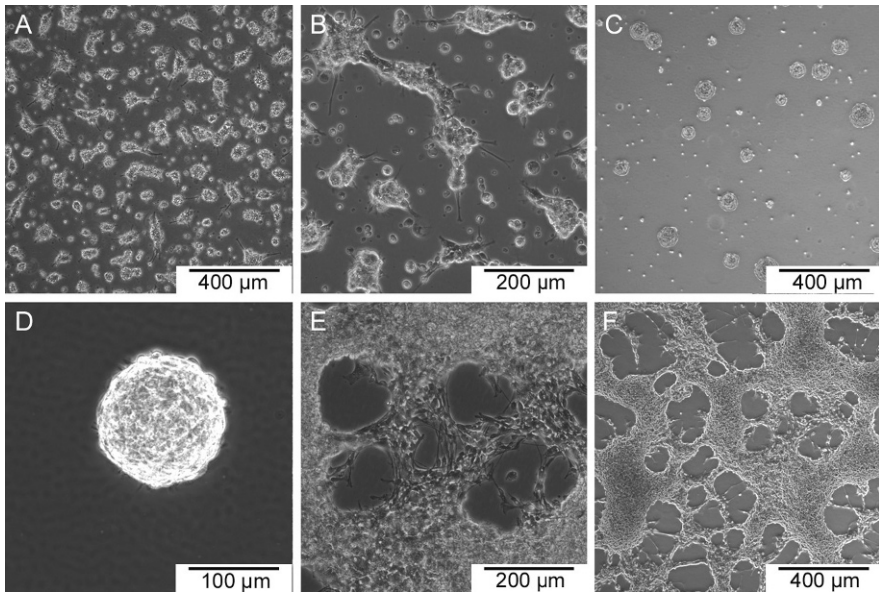


Fig. 1.3 Human neural stem/precursor cells (hNSC/NPC) are propagated in vitro by a variety of techniques

HNPC can be grown as loosely adherent aggregates (**A**, **B**), “neurosphere” aggregates (**C**, **D**), or as monolayer-like, multilayer adherent networks³ (**E**, **F**), displaying variable morphologies. Adherent aggregates typically display small neuritic extension processes (**B**) that are capable of sampling the local microenvironment and reorganize in relation to spatial signaling molecules (pictured here 48 hours post-dissociation, notice the heterogeneous presence that also includes single-cells, floating spheres, and dead floating phase-dark cells). Some labs have tried to grow NPC as large aggregated suspension spheres, or “neospheres” (**C**, **D**). These suspension cultures are heterogeneous in both their size and shape (**C**). In general, we dissociate aggregates when cells become larger than 12–15 cells in diameter (**D**) to avoid necrosis and differentiation. For example, we will typically not allow aggregates to grow past the size in panel (**D**). We have also developed a new culturing technique in our lab, termed the multilayer adherent network³ (**E**, **F**). Under these hybrid culturing parameters, hNPC display dynamic behavior and are able to maintain self-renewal and a replication capacity several fold higher than their neurosphere counterpart. Multilayer adherent networks are dissociated when cultures become greater than 75% confluent (**F**) to the surface of the culture flask. Notice the meandering neuritic processes that predominate and demarcate small boundaries between adherent networks. Time-lapse videomicroscopy (not shown here) confirms that hNPCs migrate extensively along these processes as they expand and retract within the dense network of precursors. Importantly, hNPC lines should maintain the capability to be propagated interchangeably using any of these culturing methods and retain an antigen profile consistent with stemness. In general we recommend growth as lightly adherent aggregates or multilayer adherent networks due to their elevated growth rate and ease of use. Importantly, adherent cells and floating aggregates are regarded as being equally valuable in containing neural stem-like cells

Results comparing NPC derived by similar conditions from different species demonstrate that the characteristic cell properties of NPC are inherently different depending on how they are manipulated in vitro [127]. Traditionally, bFGF and EGF have been utilized for adherent monolayer or neurosphere growth respectively, or utilized in combination to derive an overlapping population of hNPC from both

progenitor pools [126, 130–143]. In addition, the neurotrophic leukemia inhibitory factor (LIF) has been shown to regulate neurogenesis *in vivo* and generate GFAP+ progenitors with tri-potential morphology as well as NPC marker expression, cell-cycle dynamics, and behavior *in vitro* (see Section 1.5). Furthermore, LIF can improve viability, enhance telomerase expression, and extend the doubling capacity and time until terminal senescence of hNPC when used in combination with bFGF and/or EGF [144–149]. These cells have a greater neuronal differentiation potential suggesting interplay between bone morphogenic protein (BMP) and LIF signaling as a key regulator of stem cell fate [150, 151] and determination within the neurogenic niche [152]. LIF signaling appears to have different downstream effects on NPC from different species and has been shown by some laboratories to induce glial specific differentiation in rodent NPC [144]. However, in our hands, LIF not only enhances survival and doubling time of human NPC, it is absolutely essential and required for maintenance of symmetric cell divisions in *long-term* hNPC cultures. As a result, we have adopted a derivation regimen utilizing all three growth factors in a temporally regulated fashion to enact extensive proliferation. This process is followed by functional receptor selection, and finally, sustained proliferative expansion of karyotypically normal undifferentiated hNPC in basal growth medium consisting of bFGF and LIF.

1.1.3.2 Sequential Mitogen Selection of Primary hNPC

After several weeks of primary expansion, some hNPC colonies will proliferate and establish healthy populations of undifferentiated progenitors. Thriving hNPC cultures are then subjected to a 10-week sequential growth factor selection process (Fig. 1.4) based on parameters of growth rather than markers alone [138]. Successfully expanded primary cells are then grown as a mixed population of lightly adherent clusters and suspension aggregate in NB-B27 growth medium+(20 ng/mL] *bFGF alone* for 2 weeks with (1:1 or 1:2) dissociation approximately once per week

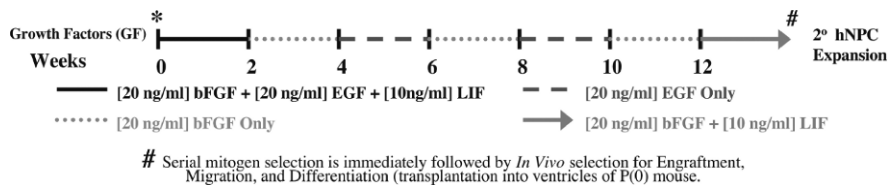


Fig. 1.4 Chronological order for primary hNPC sequential mitogen selection

The schematic represents the next series of steps after those depicted in Fig. 1. 2. Following expansion of proliferative primary tissue, successful cultures are subjected to 10 weeks of sequential growth factor selection to acquire hNPC responsive to both bFGF and EGF. Only a small percentage of the total primary population will ultimately survive and continue to proliferate for secondary expansion and long-term maintenance. (*) Fetal Bovine Serum can increase the derivation efficiency but should be removed with 48 hours to deter differentiation. LIF is added to successfully expanded cultures immediately following growth factor selection to protect telomeric integrity and provide additional trophic support

throughout the selection process as dictated by size exclusion and morphological parameters. *After 2 weeks*, mitogens are substituted, and bFGF is replaced with (20 ng/mL) *EGF alone for two additional weeks*. The bFGF-EGF two-week rotation schedule is maintained for 2–3 *sequential rounds* (10 weeks) and completed after the *final bFGF alone cycle*. Upon completion of the entire cycle, a few primary hNSC/hNPC cultures will successfully proliferate and display appropriate morphology of hNPC worthy of further expansion. These flasks are then dissociated (see Section 1.2.5) and pooled together *into NB-B27 growth medium*, including LIF, for a final *hNPC complete basal maintenance medium* comprised of *NB-B27 growth medium + (20 ng/mL) bFGF + (10 ng/mL) LIF for secondary hNPC expansion*.

1.2 Long Term Expansion and Maintenance of hNPC

Once a primary hNPC population has been successfully established, the next step is to carefully and meticulously expand cultures into a larger secondary set of daughter “sub-populations”. These cells can either be pooled together as one larger “mother” population at time of passaging or maintained as separate sub-lines to monitor for any phenotypic changes that exist or occur spontaneously during prolonged cell culture. We recommend maintaining many smaller sub-populations of hNPC to decrease the chance for contamination of the entire population. After five to ten passages, these cells can be re-pooled to ensure cultures remain similar in composition over time. Due to the relatively large “vault” of flasks that are likely to develop in the incubator over the future months of culture, it is imperative that primary hNPC expansions are appropriately documented for phenotypic change qualitatively through imaging and quantitatively for any future comparisons. Furthermore, genetic stability of these lines should be confirmed through periodic karyotyping and gene microarray fingerprinting to demonstrate a normal chromosomal complement and sustained expression of all classical stemness-associated genes [153–159].

During the expansion process, a careful “eye-ball” examination of NPC cultures at the phase-contrast microscope should be employed as a preliminary assay for undifferentiated cell growth. While long-term hNPC self-renewal is impossible to forecast, sustained multipotency can be assessed by a variety of *in vitro* and *in vivo* functional screens (see Section 1.6) to ensure long-term expanded cultures do not change phenotypically and become lineage restricted nulli- or uni-potent progenitors over time. As successfully derived cultures continue to proliferate over the first 12–15 weeks *in vitro*, it will become imperative to not only cryopreserve “batched” aliquots of cells for later reconstitution (see Section 1.2.1), but also to continually test these newly derived hNPC for the cardinal operational characteristics of NSC/NPC (long-term self-renewal and multipotency). We recommend freezing large “batches” of hNPC subpopulations, followed by thawing several vials for reconstitution to test for overall freeze-thaw success, cell viability and sustained multipotency. In order to efficiently manage time, resources, and money invested, it is best to begin testing primary hNPC lines as soon as possible to ensure the new cultures exhibit functional NPC properties.

1.2.1 Freezing hNPC Aliquots

Cryopreservation of hNPC is essential so that early passage “batched” cell populations can be easily thawed and expanded at a later time for experimental replication. We recommend freezing aliquots of hNPC, at minimum, every five population doublings to ensure low passage cells will be available in adequate numbers for extended studies. It is our opinion that freezing cells as small aggregates versus single cells results in the greatest recovery post-thaw. Although we have frozen hNPC both with and without enzymatic dissociation immediately prior to cryopreservation, we find that single cell dissociation of hNPC (see Section 1.2.5) 48–72 h before freezing, producing small (8–16 cells/aggregate) to medium (16–32 cells/aggregate) size aggregates, yields the best post-thaw recovery. While 10–30% of hNPC may actively divide in this period of time, active proliferation is offset by the cell death associated with freeze-thaw cycles. As a result, we generally assume the same number of cells will survive from a frozen vial that is later thawed and thus, the number of hNPC originally dissociated is generally equivalent to the number that survive the subsequent thawing process. Exact measurements can be made using the following equation:

$$\text{Viable hNPC originally plated} + [(10\text{--}30\%) \text{ active proliferation } 48\text{--}72 \text{ h post-dissociation} - (10\text{--}30\%) \text{ hNPC death (freeze+thaw)}] = \text{Viable hNPC post thaw}$$

Once the hNPC have been resuspended into freezing medium, the preparation process should be completed as quickly as possible to reduce the amount of time hNPC are exposed to the osmotic shock of DMSO. The ideal freezing duration occurs at a slow rate to reduce shock from crystallization and subsequent shearing. Freezing medium (see Section 1.7.3) is made fresh at time of use and cooled to 4°C on wet ice. Prior to cryopreservation, print labels for each cryovial, recording the date, passage number, and any other information pertinent for proper identification at later time of use. Inside the sterile TC hood (see Section 1.8), place each label around the cryovial, wipe thoroughly with 70% Et-OH, close the TC-hood, and turn the UV light on for 2 h to sterilize the working area. After 2 h, open the TC-hood and allow it to equilibrate with the blower on for 15 min. Loosely untighten the caps from the cryovials to allow for easy access when distributing cells.

Utilizing cultures that were dissociated 48–72 h earlier (see Section 1.2.5), gently dislodge any adherent aggregates from the flask by mechanical trituration of medium (assume the number of cells originally plated at time of passage still represents the number of cells frozen). Transfer the contents of the flask into a 15 mL conical tube, rinse the flask with 4 mL fresh pre-warmed NB-B27 growth medium, and transfer the contents to the previous 15 mL conical tube. Centrifuge the tube for 3.5–4 min at 400 rcf to pellet hNPC and aspirate the supernatant. Alternatively, transfer the conditioned medium (CM) supernatant to a 15 mL conical tube and process (see Section 1.3).

Gently resuspend the cell pellet by trituration with **cold** freezing medium (1mL cell suspension/1.8 mL cryovial). We generally freeze at a concentration of

($1-3 \times 10^6$ cells/mL) for medium to small aggregates respectively. In a timely manner, distribute the hNPC suspension equally among the sterile cryovials and transfer to a controlled-rate freezing device such that the cells are cooled at approximately ($1^\circ\text{C}/\text{min}$). Human NPC clusters will quickly begin to fall by gravity to the bottom of the cryovial, therefore it is best to freeze at maximum 10–15 vials at one time, minimizing time and subsequent clumping of cells at the bottom of the each vial which may lead to a decreased thaw efficiency. Immediately place the freezing chamber at -80°C for 18–24 h then transfer the cryovials to a liquid nitrogen tank or to a -140°C freezer where they may be maintained indefinitely (We have successfully thawed cells after 10 years [18] in storage without noticeable loss of stemness or viability).

1.2.2 Thawing Cryopreserved hNPC

Unfortunately, some hNPC will differentiate or die during the freeze-thaw process, yielding between 10–30 or 70–90% survival for single cells or small aggregates respectively. Extremely delicate handling and processing of hNPC during this process is essential for high efficiency thaws and sustained viability, as freshly thawed hNPC are extremely fragile and highly susceptible to mechanical shear forces. Furthermore, it can take several weeks after an initial thaw to expand and amass a usable numbers of cells for experimentation. To aid in this process, conditioned medium (CM) can be collected from previously growing cultures for future use (see Section 1.3). Similar to cryopreservation, great care should be taken to minimize the time hNPC are exposed to DMSO and the subsequent osmotic shock post-thaw. Careful dilution of DMSO, gentle handling, and minimization of time from freeze to thaw will ultimately determine the final freeze-thaw efficiency and overall expansion success of newly thawed cultures.

Wearing appropriate face and hand protection, carefully remove frozen hNPC vials from liquid nitrogen and place them onto dry ice. Thaw 1–2 vials (1–2 mL frozen hNPC) quickly with constant shaking (until ice cube is almost cleared; approximately 60–90 s) in a 37°C H_2O bath, rinse thoroughly with 70% Et-OH, and place the cryovials into a sterile tissue culture hood. Carefully open the vial to release built up pressure, gently triturate the cell suspension twice with a P1000 micro-pipette to resuspend, and immediately transfer the hNPC suspension to a 15 mL centrifuge tube (excessive trituration at this point will induce significant cell death). Dropwise, add approximately 7 mL **cold thaw** (see Section 1.7.3) medium (50% CM:50% fresh NB-B27 growth medium) to dilute DMSO from the freezing medium. It is essential to transfer cells gently but quickly into **cold thaw** medium, as extended incubation in DMSO will destroy hNPC by osmotic shock. Rinse the cryovial once with 1 mL **cold thaw** medium, transfer the contents to a 15 mL conical tube, and centrifuge for 3.5–4 min at 400 rcf. Alternatively, the tube is placed vertically in an incubator at 37°C for approximately 0.5–2 h. This step allows the cell clusters to settle by gravity but is not conducive to differentiation. Larger aggregates will require less time to equilibrate to the bottom of the tube. The mixture of

freezing and feeding media can then be centrifuged for 1–2 min at 400 rcf and safely aspirated (warning: attempting to aspirate the medium without centrifugation will result in the loss of many cells). Resuspend the hNPC pellet by gentle trituration with a 5 mL pipette in a mixture of 50% fresh NB-B27 growth medium and 50% CM + (10 ng/mL) LIF + (20 ng/mL) bFGF and replate onto non-coated TC treated flasks. After 1–2 weeks in culture, the percentage of CM may be reduced from 50 to 25% and eventually 0% CM when nicely expanded cultures are established (tip: always thaw small to medium size hNPC aggregates (dissociated 48–72 h before freezing) at a 2:1 or 1:1 ratio into the same or lesser volume/surface area from pre-freeze culture density).

1.2.3 Establishing Secondary hNPC Cultures

No less than $(1-2 \times 10^6)$ cells/mL should be thawed into a 25 cm² surface area for secondary hNPC expansion. In general, small aggregates will form then lightly adhere onto the plastic surface if left undisturbed. Aggregate cultures must be gently triturated each day to detach any adherent cell clusters and supplemented with (10 ng/mL) LIF + (20 ng/mL) bFGF every 2 days for 1 week past the initial thaw date to reconstitute the frozen cells. Initially, proliferation may be slow, taking 2–3 weeks to double the population, however, once the hNPC have equilibrated and recovered from the trauma of the initial thaw process, hNPC populations should maintain a steady (4–7 day) doubling rate. As cultures expand, cells are triturated routinely to deter extensive adherence and accumulation of large aggregates. These cultures can then be dissociated and maintained as 3-D cultures on uncoated flasks or subsequently induced into 2-D adherent cultures on ECM if desired [94].

1.2.4 General Feeding of hNPC

These instructions apply to hNPC grown without an extracellular matrix in tissue culture treated 25 cm² T-flasks with 6–10 mL of medium. We generally utilize uncoated tissue culture (TC) treated (0.22 μm) vented cap T-flasks for expansion of undifferentiated hNPC due to the low level risk for contamination in comparison to standard petri-dish style culture vessels. In addition, it is easier to evenly disperse the cells in rectangular T-flasks. Circular petri-style well dishes often lead to aggregation of cells to the center of the well, causing premature merging of small cellular clusters into large globular masses via integrins and self-secreted extracellular matrix proteins [160–165]. The result of such events leads to an uneven distribution of single cells, small NPC clusters, and large aggregates (Fig. 1.5A,B). Cultures that exhibit these features need to be dissociated once again, despite the fact that the smaller clusters of cells are still fragile and not in need of passaging. The result of this “premature dissociation” ultimately leads to loss of hNPC through the stresses involved with additional cycles of the enzymatic dissociation process and should be avoided if possible.

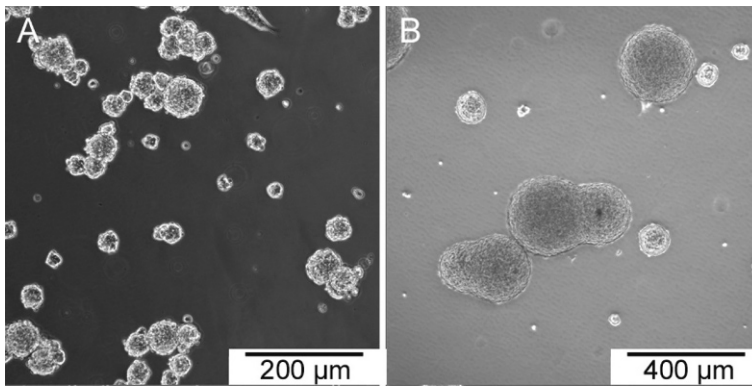


Fig. 1.5 Human NPC aggregate and merge

Human NPC cultures are disrupted and become unevenly distributed, following movement of the culture vessel. Upon contact with neighboring aggregates, cellular clusters will spontaneously merge into one large aggregate. This phenomena is most frequently encountered when culturing suspension aggregates at medium to high densities (**A**, **B**), or following mechanical movement of the culture vessel. hNPC have an incredible affinity for each other, and are quickly absorbed within their neighboring cellular environment (**A**). Unfortunately, spontaneous merging can be very hard to counteract, and often leads to a large pool of heterogeneous sized aggregates (**B**). Several large aggregates have made contact and are merging into one large irregular cluster. Within 6–12 hours the aggregate clusters will be completely merged into one very large aggregate. Furthermore, a dark necrotic center is apparent by phase-contrast microscopy indicating that essential nutrients and gas exchange are not available at the core of this aggregate (**B**). The dark central core is no longer proliferative (i.e. will not take up BrdU) and tends to differentiate quickly. A culture displaying these features is dissociated into single cells and any remaining aggregates discarded from culture

As hNPC colonies proliferate, the larger spherical aggregates will begin to differentiate at the periphery [17] and may start to become necrotic at the central core [166] (indicated by dark pigmentation in suspension aggregate masses under phase-contrast microscopy) (Fig. 1.5B). These cells are much more difficult to dissociate, do not continue to proliferate when isolated, and thus, should be discarded from culture when possible. Although these phase-dark centers were originally described as proliferative cores in neurosphere cultures [101], we believe they more accurately reflect overly packed hNPC that are not receiving adequate gas exchange and nutrients for normal metabolic activity and thus have begun to become necrotic. In our hands, dark cores only appear when aggregates become extremely large (>250 μm), such that the inner core cells are no longer bathing in extracellular medium. If it were true that phase-dark cells were true *bona-fide* neural stem cells, it would logically follow that cloned multipotent spheres would initially proliferate as phase-dark cells, which clearly does not occur. In fact, several groups have shown immature proliferative Nestin immunoreactive progenitors are dispersed throughout both rodent and human neurospheres and not exclusively localized to the central core of the sphere [20, 129, 167–169].

Ideally, hNPC are fed fresh medium 1–2 times per week depending on the density and metabolic capacity of the culture. Cellular debris commonly seen after intense

trituration, freeze-thaw, or enzymatic dissociation, as well as insoluble salt residues that may develop with prolonged culture should be removed by the described method as well. On occasions when medium is not exchanged, it is still necessary to supplement medium with additional growth factors. Every two days or when aggregates project processes adherent to the plastic surface, cells should be triturated gently with a 5 mL pipette and supplemented with growth factors for a final concentration of (20 ng/mL) bFGF and (10 ng/mL) LIF. The growth factors, bFGF and LIF, are only stable at 37°C for 2–3 days [95] and must be supplemented as needed, whereas, EGF should remain stable in solution for 4–6 days.

To supplement fresh medium, adjust the pipette to slow speed for intake and out-take, and slowly triturate the surface of the flask with a 5 mL pipette (repeat 5–10 times) thoroughly but gently (minimizing bubbles) to detach any aggregates that have attached and become adherent cell clusters. It is often helpful to tilt the flask to expose the bottom surface while expelling the medium onto the plastic. Try to triturate the entire surface by tilting the flask accordingly, paying careful attention to the corners where cells tend to congregate and adhere preferentially (this is just like triturating a flask of fibroblasts after trypsinization, but more gently). It is not necessary to detach every extremely adherent cell, as excessive trituration will ultimately lead to more significant cell loss from mechanical destruction of hNPC. When cells become detached, transfer 4–6 mL of the cell suspension into a 15 mL centrifuge tube, leaving 2–4 mL in the flask as conditioned medium (CM). Centrifuge the tube for 3–4 min at 400 rcf and vacuum aspirate the supernatant. Alternatively, filter the supernatant CM. It is recommended to leave 0.5 mL of supernatant in the conical tube, but stay clear of the bottom of the conical tube as the cell pellet can be easily dislodged and lost.

Resuspend the cell pellet in 2 mL fresh pre-warmed NB-B27 growth medium with a P1000 pipette and gently triturate at a 45-degree angle against the wall of the conical tube (6–8 times) until large clusters are no longer visible and the solution has a homogenous “milky” and “sandy” appearance (warning: do **not** hold the pipette tip firmly against the tube or triturate with excessive force to avoid shearing). It is important to thoroughly break up the cell pellet, again gently, but thoroughly before re-plating. To the cell suspension, add 2 mL of NB-B27 growth medium, evenly mix the cells by simple trituration, and return the entire contents of the tube to its original flask. Rinse the conical tube with 2–4 mL pre-warmed NB-B27 growth medium or CM to the desired ratio and transfer the cell suspension to the flask. Add growth factors to achieve the final concentrations of (10 μ g/mL) LIF + (20 μ g/mL) bFGF and place back into humidified incubator at 37°C, 5% CO₂.

1.2.5 Dissociation of hNPC

The most influential procedure involved during all facets of hNPC culture is the dissociation process involved during routine “passaging” of cells. Whether employed enzymatically or through modified salt solutions, specific emphasis should be placed on optimizing recovery of viable progenitors during this crucial procedure. We stress

this point because single-cell or small cluster dissociation is a major component of every *in vitro* handling technique employed utilizing hNPC, from basic derivation, expansion, and maintenance, to cloning, genetic manipulation, chemical labeling, and transplantation [94]. In fact, dissociation is truly the core procedural determinant of success with any application involving hNPC. The long-term future success of newly derived hNPC lines revolves around successful high viability primary expansion minimizing stress involved throughout the duration of this process.

Many “dissociation” techniques have been employed and described for expansion of hNSC including enzymatic treatments utilizing agents like Accutase or Trypsin-EDTA as well as non-cleaving, non-enzymatic agents such as the Hank’s based Cell Dissociation Buffer or Cell Stripper. In addition, Clive Svendsen’s group pioneered an alternative, non-enzymatic, mechanical chopping technique [17, 170], demonstrating an increase in hNPC viability and prolonged undifferentiated growth in comparison to traditional trypsin-EDTA based single cell dissociation standards. Each of these different techniques provides their own unique advantage, and the most reasonable method for large-scale, long-term expansion of viable proliferative undifferentiated hNPC should be determined based on the specific questions and assays relevant to the particular study.

We prefer enzymatic dissociation of hNPC with Accutase for most applications and Cell Dissociation Buffer (CDB) for special assays where surface receptor analysis is necessary (i.e. FACS). In addition, we agree that chopping large spheres into smaller cellular clusters is highly beneficial so as not to destroy integral cell–cell contacts crucial for continued proliferation, however, we can attain the same small size cellular clusters by decreasing Accutase incubation times and inactivating the suspension before clusters are fully dissociated into single cells. Furthermore, single cells can easily be counted with a hemacytometer and accurately replated at higher densities than conventionally employed for standard growth. High-density single cell cultures rapidly induce cell–cell contacts and early aggregate formation through premature merging, effectively resulting in small to medium size cell clusters within 6–24 h post-dissociation (Fig. 1.6A,B).

Human NPC are enzymatically passaged (approximately once a week) when aggregates become larger than 12–15 cells (100–200 μm) in diameter (Fig. 1.3C,D) and adherent clusters can no longer be readily dissociated by gentle trituration. Accutase is designed to be less harsh than Trypsin-EDTA, although the dissociation times are increased 1–2 min to achieve the same results. Similarly, non-enzymatic Hanks based agents like CDB require up to 2–3 times longer incubation times to achieve the same results. When using Accutase, the addition of serum or inhibitor for enzyme inactivation is not necessary and may be substituted by simply diluting the enzyme with basal medium. According to the Accutase product information sheet, centrifuging the suspension to eliminate residual Accutase is also not necessary, however, we have retained the final centrifugation step to remove cellular debris and trace enzymes. Other dissociation agents such as TrypLE, Accumax, and Collagenase are also acceptable, provided inactivation steps and incubation times are adapted into the protocol as necessary. The remainder of the procedure remains the same throughout.

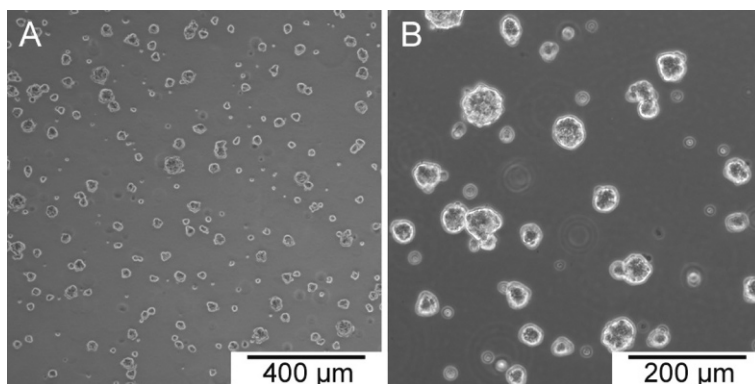


Fig. 1.6 High-density single-cell dissociation induces cellular aggregation and enhances viability of hNPC.

To promote cell-cell contact and enhance recovery of hNPC after dissociation into single cells, cultures are replated at medium to high density to quickly promote 4–8 cell clusters (A). Individual hNPC sample their environment with 1–2 forked processes and migrate to each other forming small evenly dispersed aggregates. After 12–24 hours the small individual clusters (B) are triturerated to induce suspended clusters or allowed to attach undisturbed to induce adherent aggregates and multilayer adherent networks. It is important to keep in mind that anytime cultures are disturbed, the clusters will adhere to each other, as can be seen in (B). These cells were imaged just two minutes after being removed from the incubator. They were evenly dispersed on the stage immediately following removal and allowed to settle by gravity, indicating how quickly and strong the interactions can form between neighboring cells. In addition, cell clusters also migrate on the culture surface towards each other via small microspike growth cones when maintained in the resting position

To dissociate hNPC, triturate the contents of a 25 cm² T-flask gently with a 5 mL pipette to detach any adherent colonies from the plastic surface (8–10 times), making sure to rinse the entire bottom surface of the flask. Transfer the contents of the flask to a 15 mL conical tube, rinse the flask with 2 mL fresh pre-warmed NB-B27 growth medium to collect any residual hNPC, and transfer the contents to the conical tube. Centrifuge the tube for 3–4 min at 400 rcf, remove the supernatant from the conical tube, and filter for conditioned medium (CM) (see Section 1.3) (tip: be careful not to dislodge the cell pellet). To the cell pellet, dropwise, add 750 μ l Accutase using an extended length P1000 pipette and carefully triturate the pellet 3–5 times lightly against the wall of the tube to dislodge the cells. Be very careful not to touch the pipette to the side of the conical tube while pulling the solution up and down into the tip (tip: extended length pipette tips allow for easier access into the conical tube and reduce the chance of contamination). Place the 15 mL conical tube into a 37°C H₂O bath and incubate with constant swirling to avoid settling and subsequent clumping of hNPC.

After 3–5 min, triturate the cell suspension gently at a 45-degree angle against the wall of the conical tube by sucking the plunger of a P1000 pipette up and down slowly (5–15 times) until large clumps are no longer visible and the dissociated solution has a homogenous “sandy” appearance (tip: set the P1000 to 750 μ l so

that the cells do not reach the filter in the tip). It is important to gently but thoroughly break the cell cluster up before replating, therefore it may be necessary to triturate a second time (5–10 times) with a P200 pipette until any large pellets are not visible (tip: do **not** hold the tip firmly against the tube or triturate with excessive mechanical force to avoid shearing, resulting in sticky DNA clumps and poor overall cell viability). Inactivate the enzymatic reaction by diluting Accutase with a total of 6 mL fresh NB-B27 growth medium, (tip: cell clusters will readily stick to the meniscus (approximately 750 μ L line) of the pipette tip throughout the dissociation process. To recover these cells, adjust the pipette plunger from 750 to 1000 μ l without removing the tip, rinse P1000 tip once with 1000 μ l NB-B27 growth medium to dislodge residual clusters, and the transfer contents to the original conical tube).

Large aggregates may not dissociate immediately and thus require a second round of enzymatic treatment. In this case, place the conical tube vertically for 2–3 min until the visible clusters have settled to the bottom of the tube. Carefully transfer the top portion of supernatant containing dissociated cells into 6 mL fresh NB-B27 growth medium in a new 15 mL conical tube. With the remainder of undissociated cells, add 1 mL pre-warmed Accutase, triturate twice, and incubate in a water bath at 37°C with constant swirling for an additional 2–4 min. Repeat the trituration process and transfer the appropriately dissociated cell suspension to the previous conical tube. Remaining clusters that have not dissociated efficiently after the second round are considered “abnormal” and subsequently discarded. Centrifuge the 15 mL conical tube for 4 min at 400 rcf, aspirate the supernatant, and resuspend the cell pellet with 900 μ l fresh NB-B27 growth medium using a P1000 pipette, gently triturating (5–10 times) to break up the cell pellet. Dilute hNPC in the conical tube with 6 mL fresh NB-B27 growth medium, repeat rinse of pipette tip as previously described, and count the cells for replating.

Typically, the growth parameters of hNPC culture dictates passaging once per week at a 1:2 dilution, however, accurate cell counts using a hemacytometer are recommended for proper documentation and to ensure normal growth parameters are maintained. As a general rule, more concentrated splits survive and proliferate more effectively than their diluted counterparts. In some assays, it can be beneficial to maintain cell–cell contacts, therefore, cells may be dissociated into 2–4 cell clusters by simply decreasing the incubation time and trituration frequency. The specific timing is slightly different for each cell line, but generally reducing incubation time by 30–45 s works well. In addition, inactivating the dissociation process early generally results in a greater recovery of healthy rounded phase bright hNPC, whereas extended single cell dissociation incubation times can lead to dramatic breakdown of the cell membrane and an increased susceptibility to mechanical shearing. Overall, single cell dissociation generally requires a 1–2 h re-equilibration phase before cells fully recover from the shock and stress of enzymatic dissociation. These variables may be overcome by efficient expansion and rigorous attention to detail throughout the dissociation process to minimize enzymatic incubation time and mechanical stress.

1.2.6 Replating Dissociated hNPC for General Expansion

We plate freshly dissociated hNPC at a minimum density ($1\text{--}2 \times 10^6$ cells/25 cm²) for standard expansion and maintenance, and a maximum density of ($3\text{--}4 \times 10^6$ cells/25 cm²) to induce small to medium size aggregates within 24–72 h for cryopreservation (see Section 1.2.1). After counting, add 7 mL conditioned medium (50% CM) to the conical tube and replate into new 25 cm² T-flasks. Alternatively, adjust the final fresh medium to CM ratio accordingly, bring cells to the desired density and appropriate volume, and replate into new flasks. As a guideline, a 25 cm² T-flask containing 1×10^6 cells is fed 50% CM, 2×10^6 cells fed 25% CM, and $3\text{--}4 \times 10^6$ cells do not necessitate CM as they quickly condition the medium due to the high density. Add growth factors to achieve a final concentration of (20 ng/mL) bFGF and (10 ng/mL) LIF, gently swirl contents of flask horizontally to evenly disperse cells, and place the flask in a humidified incubator at 37°C, 5% CO₂, without agitation, to allow cultures to equilibrate and return to homeostasis. Subsequent culturing methods will depend on the density of cells plated and method for further expansion.

Within 2–3 days, small to medium size (4–16 cell) clusters will form and may begin to adhere to the plastic surface. Simply triturate any adherent cells from the flask daily and feed every 2 days (see Section 1.2.4). Small cellular hNPC clusters are extremely fragile during the first 48 h post-plating, therefore extra care should be taken to minimize shear forces while triturating cells throughout the duration of this time. When expanding small populations of hNPC at low densities, we recommend utilizing these procedures, where cells generally fuse and form abundant cell–cell contacts necessary for rapid expansion, in contrast to low-density adherent growth parameters where cells will spread and migrate throughout the area provided.

1.3 Preservation of Conditioned Medium

It is often useful to have a stock of frozen “conditioned medium” (CM) to enhance survival of hNPC during various procedural manipulations. Addition of CM to valuable low-density cultures, freshly thawed NPC aliquots, or as an aid in problematic single-cell cloning can often be the key to a successful experiment. CM contains paracrine effector molecules, which act in concert with growth factors to enhance mitosis. We have applied a strict standard and limitations on the quality of cultures that can be utilized to produce this paracrine enriched basal medium supplement. Specifically, we only collect medium conditioned by healthy, highly proliferative cultures that have been grown in fresh NB-B27 growth medium + (10 ng/mL) LIF + (20 ng/mL) bFGF for 20–24 h. This timing allows the cells to adequately secrete paracrine molecules into the medium but not become toxic due to metabolite build up.

Approximately 20–24 h prior to collection of CM, replace 100% of the medium in a healthy high density hNPC culture with 10 mL fresh NB-B27 growth medium + (10 ng/mL) LIF + (20 ng/mL) bFGF. To harvest CM, carefully remove 10 mL CM from 25 cm² T-flask, centrifuge for 5 min at 500 rcf to pellet the cells, and transfer

the supernatant CM to a new conical tube. Immediately filter 10 mL CM through a sterile 0.22 μm filter into a 15 mL conical tube. Add (20 ng/mL) bFGF and (10 ng/mL) LIF, mix by inversion, and freeze immediately at -20°C to limit degradation of valuable signaling molecules. Prolonged exposure to environmental gas exchange, light, or room temperature conditions will rapidly degrade the CM, rendering it toxic or unbalanced as a salt solution and therefore useless as a supplement. To thaw CM, place the frozen tube at 4°C overnight to slowly melt the contents. If resultant thawed tube contains any insoluble particles, discard immediately and thaw a new tube from a different batch. Once the CM has thawed, pre-warm to 37°C , mix accordingly with fresh NB-B27 medium and supplement growth factors to a final concentration of (10 ng/mL) LIF + (20 ng/mL) bFGF.

1.4 “What About Neurospheres?”

For many years, some labs employed a technique known as “neurosphere” formation [101, 171, 172] for the derivation and expansion of murine [173–180] and human somatic stem cells (Fig. 1.3C,D) from various regions of the brain [181–186]. This entailed the expansion of neural tissue aggregates, termed “neurospheres,” in serum free medium to produce neural precursors in vitro. The basic technique relied on the inherent ability of proliferative, BrdU incorporating cells to expand and form cellular aggregates resembling spherical balls. Although each neurosphere was originally assumed to be a clonal population of *multipotent, self-renewing* NSC from the small ($< 0.1\%$) quiescent neural stem cell population, we now know that these “neurospheres” are actually heterogeneous mixtures of stem, progenitor, and differentiated cells that spontaneously migrate, merge and dynamically intermix with each other [10, 187]. As a result, neural aggregate expansion can be a useful tool to first select and expand proliferative primary cells, but it does not inherently assume the criteria for stemness have been met. The ability to proliferate is the first, though not the only criteria for a clonal self-renewing bona-fide NSC population. In fact, true proliferative hNPC with characteristic progenitor and stem-like qualities can be found within adherent monolayer populations as well, and may offer significant growth advantages to the “neurosphere” expansion technique.

1.5 Characterization of Undifferentiated hNPC

Throughout hNPC culture, it is important to assay individual sub-populations for expression of known stemness related genes to ensure normal undifferentiated growth is maintained long-term. Unlike the hematopoietic system, there remains no definitive lineage specific marker for NPC. Therefore, proper characterization of hNPC relies on identification of combinatorial subsets of genes known to be activated throughout the continuum of neural development [188, 189]. Unfortunately, characterization of undifferentiated cells based on antigenic profile reveals no direct information as to the cardinal features of stemness, self-renewal and multi-potency. The fact that neural stem cells have traditionally been characterized by their *lack* of

expression of mature neuronal markers has plagued the neurodevelopmental field for years and perhaps may be responsible for a variety of misleading results given that hNPC tend to accumulate non-physiological gene expression patterns *in vitro* [190, 191]. In addition, *in vitro* cell culture conditions can confer homogenizing effects on hNPC further complicating the distinction between cultured stem cells and their *in vivo* counterparts. As a whole, *in vitro* derived stem cells have different properties from their *in vivo* counterparts, therefore, direct comparisons cannot be made.

In our laboratory, proliferative (Ki-67+ [late G1, S, G2, and M] [192] or PCNA+ [G1, S] [193, 194]) hNPC must display an undifferentiated morphology and express classic NPC markers including the nuclear transcription factor sox-2 [195, 196], musashi-1/2 [197], as well as the filamentous cytoplasmic proteins Nestin and Vimentin [198–204] in cellularly appropriate locations. Furthermore, in our hands, fetal hNPC also express the glial fibrillar associated protein (GFAP) in morphologically appropriate (non-protoplasmic) locations, consistent with rodent data [205–208], suggesting that GFAP may label hNPC or that astrocytes themselves, at a particular stage, may be hNPC. Although expression of any of these markers alone does not infer stemness, combinatorial multi-labeling techniques can be utilized to confirm co-expression of sets of standard phenotypic markers.

In addition to these classic NPC markers, a small percentage of the hNPC population (derived in our lab) may also express the radial glial (RG) associated brain lipid binding protein (BLBP) [209, 210], recently described as the *in vivo* unified lineage link between early neuroepithelial stem cells and quiescent adult astrocyte-like SVZ progenitors [208, 211–225]. Early reports demonstrated evidence that these multipotent progenitors resumed stem cell-like behaviors when propagated as monolayer cultures *in vitro*, retaining an immature radial glia phenotype similar to hNSC cells *in vivo*. Furthermore, some progenitor populations also markedly co-express the microtubule associated protein doublecortin (DCX) in the nucleus and cytoplasm and polysialylated neural cell adhesion molecule (PSA-NCAM) on the membrane surface of leading processes and growth cones of neurite extensions [185, 226–230]. These cells are highly reminiscent of transiently amplifying type-C cells and migratory type-A neuroblasts important for cell morphology and migration within the *in vivo* neurogenic niche [231]. In both of these cases, the phenotypically diverse cell types exhibit an altered morphology from their NPC counterparts as either highly branched, elongated, bipolar radial glia [232–234] or small bipolar type-A like cells that migrate by somal translocation (Data Not Shown), suggesting an *in vitro* developmental continuum reminiscent of the SVZ neurogenic niche *in vivo*. Moreover, as hNPC cultures mature and accumulate *in vitro* culture adaptations, we have noticed the highly congruent colocalization of GFAP [235–239] with the intermediate filament protein, beta-3-tubulin (Tuj-1) [240–244], that has been described as an early marker for immature neuronally restricted NPCs.

We have verified these findings by both standard immunocytochemistry as well as western blotting in three hNPC lines ranging from 10 to 22 weeks (from fertilization date) and independently derived by outside laboratories (to be published in a future research article) providing further evidence that hNPC cultures are not homogeneously composed of identical stem cells, but rather highly dynamic

heterogeneous populations [245] of neural progenitors that adapt and respond to local extracellular signaling cascades. In vitro, these morphological variants maintain the ability to self-renew either symmetrically or asymmetrically and differentiate into all three neuroectodermal lineages when provided with appropriate cues. Clonal analysis and in vivo functional screens will be necessary to determine how these highly coupled cell types interact, adapt, and regulate NPC survival.

It is still unknown if these individual phenotypes represent functionally distinct, restricted sub-populations or highly plastic interchangeable progenitors capable of prolonged self-renewal and multi-potential “trans/re-differentiation” or “reprogramming” in response to the local cellular composition and complementary signaling cues accrued during in vitro cell culture [205, 246, 247]. Further, the new wave of research on induced pluripotent stem (IPS) cells [248–270] raises the notion that any cell has the genetic capacity to serve as a functional stem cell within the correct genetic context. The incongruent gap between the “possible versus actual [48]” further demonstrates the problematic divergence between in vitro and in vivo stem cell dynamics when introduced to artificial culture conditions. Although there is currently no precise definition sufficient to fully define hNSC, Morrison, Shah, and Anderson’s borrowed phrase, “It’s hard to define, but I know it when I see it [271],” has been appropriately adapted to the stem cell field as we forge forward in search of better objective indicators of stemness.

1.6 Functional Diagnostics for Multipotency

Human NPC fate-determination is a multi-step process tightly regulated by cell-cycle dynamics [35, 272–274] as undifferentiated neuroepithelial cells form and develop into mature functionally competent CNS tissue, in vivo. Specific fate-choice decisions are influenced by extracellular ligands, their receptors, and the cumulative interplay of all extrinsic and intrinsic signaling inputs impinging on the cell. This continuous process is highly dynamic and context dependent, exerting differential effects on hNPC at different stages of development. As hNPC progressively mature, they undergo nuclear reorganization, resulting in alterations in gene expression patterns and morphology. Changes incurred over time are hypothesized to then be measured and stored by the cells “biological sensor,” that in turn regulates the cells functional properties [275, 276].

In much the same way, we can regulate stemness in vitro, by careful manipulation of the cellular environment and critical molecular signaling pathways involved in hNPC maintenance. What little we know about intrinsic maintenance of hNPC and their differentiated counterparts in vitro, have produced variable results between species and among the plethora of experimental paradigms and chemical regimes employed. What is certain is that hNPC can be directed into all three neuroectodermal lineages in vitro by a variety of techniques. The most simple differentiation assay that can be employed on a relatively small population of NPC employs addition of a variety of chemical cues such as serum, forskolin [127], retinoic acid

(RA) [277], valproic acid [278], PDGF [230, 279], IGF-1/2 [280], BMPs [281], noggin, NGF, BDNF, GDNF, and CTNF [279, 282], or exclusion of mitogenic signaling molecules (bFGF, EGF, and LIF) to trigger spontaneous or lineage directed neural differentiation into mainly neurons and astrocytes, and a small number of oligodendrocytes.

1.6.1 In Vitro Differentiation

The earliest “stemness” assay employed should assess in vitro multipotency before expensive, time consuming in vivo assays are undertaken. Many newly derived hNPC lines will ultimately fail to fulfill their operational NPC definition at this early stage despite their apparent morphological relevance. In general, differentiation times for human cells are much longer than their rodent counterparts. As a result, it may be necessary to extend the following time periods to accommodate for the species differences. Briefly, plate freshly dissociated hNPC (see Section 1.2.5) onto an adherent substrate such as Matrigel or Collagen at low density ($1-3 \times 10^4$ cells/well) on round glass-bottom coverslips (24 well-plate) in 0.75 mL differentiation medium for 6–12 h to induce attachment. Upon adherence, add 1 mL differentiation medium (see below) slowly to the top of each well so as not to disturb the fragile cellular attachments. Replace 50–75% differentiation medium every 3–4 days or as cellular metabolism dictates. Medium with phenol red should be utilized to determine appropriate time for medium change.

Prolonged exposure to acidic culture conditions can promote gliogenesis over neurogenesis. Even short-term exposure can induce an initial commitment down the astroglial lineage. Furthermore, we can utilize these conditions to preferentially promote fate restriction of astrocytes and oligodendrocytes in vitro (Araceli Espinosa, unpublished personal communication). Initial differentiation will occur within 1–2 weeks, while mature differentiation can take up to 3–6 months to achieve synaptically active mature CNS cell subtypes. In addition, Studer et al. have shown that lowered oxygen levels, more closely resembling the in vivo microenvironment, can enhance the proliferative capacity and differentiation potential of CNS precursors [283]. In concert with these findings, we have seen enhanced differentiation of hNPC in 3–5% oxygen (Unpublished Data), suggesting a similar effect could be attained for human cells.

1.6.1.1 Differentiation Medium

Add the following components to NB-B27 growth medium without growth factors unless specified otherwise.

1. Neuronal differentiation:

Method 1: Add 5 μ M forskolin + 1% Fetal Bovine Serum (FBS) + 1 μ M RA (optional) for 4–6 days [127]. To fully mature hNPC, replace medium with NB-B27 + (20 ng/mL) BDNF + 1% FBS for 6 days [277] then increase to 100 ng/mL BDNF + 2% FBS for 7–8 days [284].

Method 2: Add 1 mM valproic acid for 4 days [285].

Method 3: Add (10 ng/mL) PDGF-AA, AB, or BB isoforms for 2 days with bFGF followed by 6 days without bFGF [279].

2. Astrocyte differentiation:

Method 1: Add 50 ng/mL LIF + 50 ng/mL BMP-2 for 6 days [285].

Method 2: Add 5–10% FBS for 6 days

Method 3: Add (10 ng/mL) CNTF for 6 days [279].

3. Oligodendrocyte differentiation:

Method 1: Add (500 ng/mL) IGF-1, IGF-2, or insulin in insulin-free N2 supplemented Neurobasal medium [285].

Method 2: Add 10 mM T3 thyroid hormone for 6 days [279].

1.6.2 In Vivo Differentiation

Of the few NPC subpopulations that pass the initial in vitro differentiation screen, many will fail the ultimate in vivo functional screen that includes the ability to engraft, migrate, and differentiate following implantation into the developing lateral ventricles and cerebella of newborn (P0) wild-type or immunodeficient mice. Techniques for preparation and transplantation of hNPC into neonatal and adult mice are covered elsewhere [94, 286, 287]. After 2–6 weeks, transplanted mice are sacrificed and assayed histopathologically for donor hNPC derived neuronal integration and differentiation yielding cytoarchitecturally appropriate glia in the cortex, olfactory bulb neurons or cerebellar granule neurons, respectively. Upon completion of this extensive in vivo screen, a very small portion of original NPC primary cultures, such as those we and our colleagues have published including (H1, HFT-13, and HFB-2050) [18, 31, 42, 45, 288, 289] are ultimately expanded, frozen, and stored as multiple aliquot early passage “batches” for future developmental and large animal transplantation studies [290].

In general, it is best to establish multipotency of hNPC populations from undifferentiated clonal populations. However, pre-differentiation of cells into restricted progenitors in vitro is often helpful in testing hNPC for in vivo multipotency and assaying the functionality of specifically derived neural cell types of interest. Furthermore, the in vivo adult environment may not be suitable or adequate for differentiation of undifferentiated hNPC into specialized cell types, generating a limited subset of mature neuronal phenotypes. As a result, the global cell fate potential of newly derived lines must often be supplemented with lineage specific in vitro differentiation assays. It should be noted that in vitro potential often surpasses that seen in vivo when transplanted into the developing CNS, suggesting either in vivo assays are not sensitive enough to fully detect multipotentiality or that the environmental differences between the two systems have different inductive potentials on stem and progenitor cells. Furthermore, in vivo survival and engraftment success of progenitors transplanted into *pathologically relevant models* has

been reported to improve following specified in vitro pre-differentiation of undifferentiated hNPC prior to transplantation. These cells do not migrate as extensively into non-pathological areas as their undifferentiated counterparts and have been suggested to improve functional output in relevant disease paradigms [291].

1.7 Equipment, Supplies, Chemicals, Reagents, and Media

1.7.1 Equipment and Consumable Supplies

Item	Supplier	Catalog number
Aspiration pipette, 2 mL	BD Falcon	357558
Centrifuge tubes, 15 mL	Corning Life Sciences	430790
Centrifuge tubes, 50 mL	Corning Life Sciences	430828
Cryovial, 1.8 mL	Nunc	377267
DMSO-Safe acrodisc sterile syringe filter (0.2 μ m)	Pall Corporation	4433
Freezing device	Fisher Scientific	15-350-50
Kimwipe, 11.8 in \times 11.8 in	Fisher Scientific	06-666-1A
Pipettes, serological 2 mL	BD Falcon	356507
Pipettes, serological 5 mL	BD Falcon	357543
Pipettes, serological 10 mL	BD Falcon	357551
Pipettes, serological 25 mL	BD Falcon	357525
Syringe (10 ml)	Normject	53548-006
Tissue culture flask, 25 cm ²	BD Falcon	353109
Tissue culture flask, 75 cm ²	Corning Life Sciences	430641
Tissue culture flask, 225 cm ²	Corning Life Sciences	431082
6-Well TC microplates, costar	Corning Life Sciences	3516
Vacuum filter/storage bottle system, 500 mL (0.22 μ m)	Corning Life Sciences	431097

1.7.2 Chemicals and Reagents

Item	Supplier	Catalog number
Accumax	Millipore	SCR006
Accutase	Millipore	SCR005
B-27, Vitamin A-free, 10 mL	Gibco	12587-010
BDNF, human recombinant	Millipore	GF029
Cell dissociation buffer, 100 mL	Gibco	13150-016
Cellstripper, 100 mL	Cellgro	25-056-CI
CNTF, human recombinant	Millipore	GF109
D-MEM/F12, 500 mL	Gibco	10565-018
Dispase II, 5g	Roche	165859
DMSO, 100 mL	Sigma-Aldrich	D2650
DNase, 25 mg	Worthington	2138
dPBS, w/o Ca ⁺⁺ Mg ⁺⁺	Mediatech	21-031-CM

Item	Supplier	Catalog number
Epidermal growth factor (EGF), human recombinant; (100 μ g)	Invitrogen	13247-051
Fetal Bovine Serum	Gibco	16140-071
Fibroblast growth factor-basic (bFGF), human recombinant; (50 μ g)	Chemicon	GF003
Fibronectin, human plasma (0.1%)	Sigma-Aldrich	F0895
Forskolin	Sigma-Aldrich	F6886
GlutaMAX	Gibco	35050-061
Heparin	Sigma-Aldrich	H-3149
IGF-I	Sigma-Aldrich	I3769
Insulin	Sigma-Aldrich	91077C
Laminin, murine	Sigma-Aldrich	L2020
Laminin, human	Sigma-Aldrich	L6274
Leukemia inhibitory factor (LIF), human recombinant; (10 μ g)	Millipore	LIF1010
Matrigel (growth factor reduced)	BD Bioscience	354230
N2 supplement	Gibco	17502-048
Neurobasal, 500 mL	Gibco	21103-049
Normocin	Invivogen	ANT-NR-1
Papain, 100 mg	Worthington	3126
PDGF-AA	Sigma-Aldrich	P3076
Poly-D-lysine	Sigma-Aldrich	P6407
Poly-L-ornithine	Sigma-Aldrich	P4957
Retinoic acid	Sigma-Aldrich	R2625
3,3',5-Triiodo-L-thyronine sodium salt (T3 Thyroid hormone)	Sigma-Aldrich	T5516
TrypLE	Invitrogen	12605-036
Valproic acid	Sigma-Aldrich	P4543

1.7.3 Media

Medium name	Item	Concentration	Amount in 50 mL
<i>NB-B27 growth medium</i>	Neurobasal	97%	48.4 mL
	B-27 w/o Vitamin A	2%	1 mL
	GlutaMAX	1%	0.5 mL
	Normocin (optional)	0.2%	0.1 mL
	Heparin	8 μ g/mL	400 μ g
<i>Freeze medium</i>	LIF (added <i>after</i> filtering)	10 ng/mL	500 ng
	NB-B27 growth medium	40%	20 mL
	Fetal Bovine Serum	50%	25 mL
<i>Thaw medium</i>	DMSO	10%	5 mL
	NB-B27 growth medium	50%	25 mL
	Conditioned medium	50%	25 mL

1.7.4 Preparation Notes

Media: Media and components should always be stored at 4°C and away from light until time of use. The formulations above are to be made as needed from

stock solutions. Due to the high molecular weight of LIF, it must be added to NB-B27 growth medium *after* filtering. We have found 50 mL to be a convenient working volume. Substitute any omitted Normocin volumes with Neurobasal. To aliquot stocks, thaw B-27 Supplement, Glutamax, Normocin, and FBS at 4°C overnight, aliquot 1 mL, 0.5 mL, 100 μ l, and 25 mL volumes respectively, and store at -20°C till use. Slow thaw aliquots overnight at 4°C on the night before use.

Leukemia Inhibitory Factor (LIF): Human recombinant. The working concentration for LIF is (10 ng/mL); as packaged it is in solution at 1000X the working concentration. We recommend generating 500 μ L aliquots in sterile cryovial tubes, remembering to spray the stock container with 70% Et-OH before drawing with a sterile insulin syringe. Store at 4°C.

Basic Fibroblast Growth Factor (bFGF): Human recombinant. The working concentration for bFGF is (20 ng/mL). Prior to opening the stock container, briefly centrifuge lyophilized bFGF to pool any residual powder sticking to the walls and spray with 70% Et-OH. Sterile filter dPBS (+ 0.1% BSA as a carrier protein optional) through a 0.2 μ m filter and reconstitute the lyophilized powder to (40 μ g/mL) (2000X) and store 100 μ l aliquots at -20°C for up to 6 months. Do not repeat freeze-thaw cycles. Stable at 4°C from thaw for 1–2 weeks.

Epidermal Growth Factor (EGF): Human recombinant. The working concentration for EGF is (20 ng/mL). Briefly, follow directions above for bFGF. Make (500X) stock solution in dPBS (+ 0.1% BSA optional) and store 100 μ l aliquots at -20°C. Do not repeat freeze-thaw cycles. Stable at 4°C from thaw for 1 to 2 weeks.

Heparin: Reconstitute lyophilized powder to (50 mg/mL) in sterile water and filter through a 0.2 μ m filter before using. The working concentration in medium is (8 μ g/mL). Store at 4°C for up to 2 years. Do not freeze.

Accutase: Slow thaw stock bottle at 4°C or on wet ice. Aliquot 2–5 mL aliquots in sterile conical tubes and store at -20°C. Thaw aliquot overnight at 4°C then place in 37°C water bath for 5 min before use.

1.7.5 Normal Plating Volumes

Dish	Area (cm ² /well)	Normal plating volume
20 mm	3	1 mL
25 mm	8	2.5 mL
60 mm	25	8 mL
100 mm	78.5	18 mL
Plate		
6 well	9.6	3.5 mL
12 well	3.8	2 mL
24 well	2	1 mL

Dish	Area (cm ² /well)	Normal plating volume
48 well	0.75	500 μ L
96 well	0.32	250 μ L
Slide		
1 well	9.4	3 mL
2 well	4.2	2 mL
4 well	1.8	1 mL
8 well	0.8	250 μ L
Flask		
T-25	25	8 mL
T-75	75	16 mL
T-225	225	40 mL

1.8 Introduction to the Tissue Culture (TC) Hood

The tissue culture (TC) hood serves as a sterile environment that protects both the cultures from contamination and the lab worker from harm or infection from chemicals, reagents, or biological material. In the pursuit of this goal, all tasks to be performed in the hood should be carefully planned with regards to the equipment, chemicals, and reagents needed. The first step in reducing the risk of contamination comes with foresight and deliberate action.

1.8.1 Preparation of the Tissue Culture (TC) Hood

Before undertaking any culture work, it is important to prepare the tissue culture hood so that it may be both sterile and clean, reducing the risk of contamination. The following steps are to be executed with standard personal protection equipment (including a lab coat, gloves, and goggles). Turn the UV light on for 12 h (turning it off prior to beginning work), open the hood, and turn the vent on. Just outside of the hood, soak one large Kimwipe by spraying it multiple times with a 70% ethanol solution. Starting from the back, wipe all surfaces of the tissue culture hood with the ethanol soaked Kimwipe (use new wipes as necessary). With a new ethanol soaked Kimwipe, wipe down all instruments that are in the tissue culture hood (pipettors, aspirators, etc.) (tip: micro-pipettors should be extensively wiped due to their propensity for use at close distances to working solutions). Allow all ethanol to evaporate and the ventilation system to run for 15 min before introducing any new materials into the tissue culture hood (tip: It is important to both start in the back and avoid reaching too far with your body to reduce the chance of introducing contaminants into the hood).

1.8.2 Notes on Sterility and Methods of Sterilization

The sterility of the tissue culture hood is an important aspect when undertaking any culture work. The goal should be to maintain a level of sterility through careful work

habits, cleanliness, and appropriate knowledge on how to counteract the introduction of possible contaminants to the TC hood. Below is a brief listing of the three most common methods to maintain sterility in the tissue culture hood. Refer to your facility's safety department for specific instructions.

1. *Liquid bleach (sodium hypochlorite solution)*: Used at a concentration of 10% liquid bleach is one of the most powerful sterilization agents used. After soaking the area with 10% liquid bleach, it must be left for 20 min before rinsing with water. Although 10% bleach has the advantage of killing a broad spectrum of microorganisms, it is also corrosive to metal and fairly toxic. Generally, it is only used when contamination is suspected.
2. *Ethanol*: A 70% ethanol solution is the most commonly used cleansing and sterilization agent in the tissue culture hood. Although its rapid evaporation eliminates the need for rinsing, it also reduces contact time and therefore sterilizing ability. Additionally, ethanol is flammable and has no effectiveness against bacterial spores.
3. *Ultra-violet light*: Most tissue culture hoods are equipped with ultra-violet lights to be turned on when the hood is not being used. Although ultra-violet light has been shown to be an effective sterilizing tool, it has no effect on microorganisms that are sheltered from light by dust particles or instruments. Therefore, the use of ultra-violet light should not be fully relied on to ensure sterility.

Acknowledgments DRW would like to thank Steven A. Wakeman, Pamela S. Burnett, and D. Eugene Redmond Jr. for constructive comments and support; Ilyas Singec, Scott R. McKercher, Michael Marconi, Phillip H. Schwartz, Jeanne F. Loring, Franz-Josef Mueller, Jean-Pyo Lee, Seung U. Kim, and Kook I. Park for technical advice and procedural training. Funding for DRW comes from (NIH/NIGMS T32 GM008666) UCSD Institutional Training Fellowship in Basic and Clinical Genetics, HHMI Med-Into-Grad Training Fellowship, American Society for Neural Therapy and Repair, and the American Parkinson's Disease Association. Additional support was provided by The Stem Cell Center at the Burnham Institute NIH P20 GM075059-03.

Abbreviations

BFGF	Basic Fibroblast Growth Factor
BLBP	Brain Lipid Binding Protein
BMP	Bone Morphogenic Protein
CDB	Cell Dissociation Buffer
CM	Conditioned Medium
CRL	Crown Rump Length
DCX	Doublecortin
ECM	Extracellular Matrix
EGF	Epidermal Growth Factor
FBS	Fetal Bovine Serum
GF	Growth Factor
GFAP	Glial Fibrillar Acidic Protein
iPS	Induced Pluripotent Stem (Cell)

LIF	Leukemia Inhibitory Factor
MAPK	Mitogen-Activated-Protein-Kinase
NPC	Neural Precursor Cell
NSC	Neural Stem Cell
PPD	Papain-Protease-DNase I
PSA-NCAM	Polysialylated Neural Cell Adhesion Molecule
RA	Retinoic Acid
RG	Radial Glia
SVZ	Subventricular Zone
TUJ1	Beta-3-Tubulin

References

1. Ray J, Raymon HK, Gage FH. Generation and culturing of precursor cells and neuroblasts from embryonic and adult central nervous system. *Methods Enzymol.* 1995;254:20–37.
2. Gage FH, Ray J, Fisher LJ. Isolation, characterization, and use of stem cells from the CNS. *Annu Rev Neurosci.* 1995;18:159–92.
3. Svendsen CN, Caldwell MA, Ostenfeld T. Human neural stem cells: isolation, expansion and transplantation. *Brain Pathol.* 1999 July;9(3):499–513.
4. Wu YY, Mujtaba T, Rao MS. Isolation of stem and precursor cells from fetal tissue. *Methods Mol Biol.* 2002;198:29–40.
5. Walsh K, Megyesi J, Hammond R. Human central nervous system tissue culture: a historical review and examination of recent advances. *Neurobiol Dis.* 2005 February;18(1):2–18.
6. Rajan P, Snyder E. Neural stem cells and their manipulation. *Methods Enzymol.* 2006;419:23–52.
7. Pollard SM, Benchoua A, Lowell S. Neural stem cells, neurons, and glia. *Methods Enzymol.* 2006;418:151–69.
8. De Filippis L, Lamorte G, Snyder EY, Malgaroli A, Vescovi AL. A novel, immortal, and multipotent human neural stem cell line generating functional neurons and oligodendrocytes. *Stem Cells.* 2007 September;25(9):2312–21.
9. Nethercott H, Maxwell H, Schwartz PH. Neural Progenitor Cell Culture. In: Loring JF, Weselschmidt RL, Schwartz PH (eds). *Human Stem Cell Manual: A Laboratory Guide.* 1st ed. New York: Elsevier Academic Press, 2007:309–31.
10. Singec I, Quinones-Hinojosa A. Neurospheres. In: Gage FH, Kempermann G, Song H (eds). *Adult Neurogenesis.* New York: Cold Spring Harbor Press, 2008:119–34.
11. Ray J. Monolayer Cultures of Neural Stem/Progenitor Cells. In: Gage FH, Kempermann G, Song H (eds). *Adult Neurogenesis.* New York: Cold Spring Harbor Press, 2008:135–57.
12. Kirschenbaum B, Nedergaard M, Preuss A, Barami K, Fraser RA, Goldman SA. In vitro neuronal production and differentiation by precursor cells derived from the adult human forebrain. *Cereb Cortex.* 1994 November–December;4(6):576–89.
13. Buc-Caron MH. Neuroepithelial progenitor cells explanted from human fetal brain proliferate and differentiate in vitro. *Neurobiol Dis.* 1995 February;2(1):37–47.
14. Chalmers-Redman RM, Priestley T, Kemp JA, Fine A. In vitro propagation and inducible differentiation of multipotential progenitor cells from human fetal brain. *Neuroscience.* 1997 February;76(4):1121–8.
15. Sah DW, Ray J, Gage FH. Bipotent progenitor cell lines from the human CNS. *Nat Biotechnol.* 1997 June;15(6):574–80.
16. Moyer MP, Johnson RA, Zompa EA, Cain L, Morshed T, Hulsebosch CE. Culture, expansion, and transplantation of human fetal neural progenitor cells. *Transplant Proc.* 1997 June;29(4):2040–1.

17. Svendsen CN, ter Borg MG, Armstrong RJ, et al. A new method for the rapid and long term growth of human neural precursor cells. *J Neurosci Methods*. 1998 December 1;85(2): 141–52.
18. Flax JD, Aurora S, Yang C, et al. Engraftable human neural stem cells respond to developmental cues, replace neurons, and express foreign genes. *Nat Biotechnol*. 1998 November;16(11):1033–9.
19. Carpenter MK, Cui X, Hu ZY, et al. In vitro expansion of a multipotent population of human neural progenitor cells. *Exp Neurol*. 1999 August;158(2):265–78.
20. Kukekov VG, Laywell ED, Suslov O, et al. Multipotent stem/progenitor cells with similar properties arise from two neurogenic regions of adult human brain. *Exp Neurol*. 1999 April;156(2):333–44.
21. Vescovi AL, Gritti A, Galli R, Parati EA. Isolation and intracerebral grafting of non-transformed multipotential embryonic human CNS stem cells. *J Neurotrauma*. 1999 August;16(8):689–93.
22. Vescovi AL, Parati EA, Gritti A, et al. Isolation and cloning of multipotential stem cells from the embryonic human CNS and establishment of transplantable human neural stem cell lines by epigenetic stimulation. *Exp Neurol*. 1999 March;156(1):71–83.
23. Villa A, Snyder EY, Vescovi A, Martinez-Serrano A. Establishment and properties of a growth factor-dependent, perpetual neural stem cell line from the human CNS. *Exp Neurol*. 2000 January;161(1):67–84.
24. Uchida N, Buck DW, He D, et al. Direct isolation of human central nervous system stem cells. *Proc Natl Acad Sci U S A*. 2000 December 19;97(26):14720–5.
25. Roy NS, Benraiss A, Wang S, et al. Promoter-targeted selection and isolation of neural progenitor cells from the adult human ventricular zone. *J Neurosci Res*. 2000 February 1;59(3):321–31.
26. Piper DR, Mujtaba T, Rao MS, Lucero MT. Immunocytochemical and physiological characterization of a population of cultured human neural precursors. *J Neurophysiol*. 2000 July;84(1):534–48.
27. Piper DR, Mujtaba T, Keyoung H, et al. Identification and characterization of neuronal precursors and their progeny from human fetal tissue. *J Neurosci Res*. 2001 November 1;66(3):356–68.
28. Keyoung HM, Roy NS, Benraiss A, et al. High-yield selection and extraction of two promoter-defined phenotypes of neural stem cells from the fetal human brain. *Nat Biotechnol*. 2001 September;19(9):843–50.
29. Arsenijevic Y, Villemure JG, Brunet JF, et al. Isolation of multipotent neural precursors residing in the cortex of the adult human brain. *Exp Neurol*. 2001 July;170(1):48–62.
30. Palmer TD, Schwartz PH, Taupin P, Kaspar B, Stein SA, Gage FH. Cell culture. Progenitor cells from human brain after death. *Nature*. 2001 May 3;411(6833):42–3.
31. Ourednik V, Ourednik J, Flax JD, et al. Segregation of human neural stem cells in the developing primate forebrain. *Science (New York)*. 2001 September 7;293(5536):1820–4.
32. Ostenfeld T, Joly E, Tai YT, et al. Regional specification of rodent and human neurospheres. *Brain Res Dev Brain Res*. 2002 March 31;134(1–2):43–55.
33. Laywell ED, Kukekov VG, Suslov O, Zheng T, Steindler DA. Production and analysis of neurospheres from acutely dissociated and postmortem CNS specimens. *Methods Mol Biol*. 2002;198:15–27.
34. Tamaki S, Eckert K, He D, et al. Engraftment of sorted/expanded human central nervous system stem cells from fetal brain. *J Neurosci Res*. 2002 September 15;69(6):976–86.
35. Cai J, Wu Y, Mirua T, et al. Properties of a fetal multipotent neural stem cell (NEP cell). *Dev Biol*. 2002 November 15;251(2):221–40.
36. Nunes MC, Roy NS, Keyoung HM, et al. Identification and isolation of multipotential neural progenitor cells from the subcortical white matter of the adult human brain. *Nat Med*. 2003 April;9(4):439–47.
37. Schwartz PH, Bryant PJ, Fujia TJ, Su H, O’Dowd DK, Klassen H. Isolation and characterization of neural progenitor cells from post-mortem human cortex. *J Neurosci Res*. 2003 December 15;74(6):838–51.

38. Zhang H, Zhao Y, Zhao C, Yu S, Duan D, Xu Q. Long-term expansion of human neural progenitor cells by epigenetic stimulation in vitro. *Neurosci Res.* 2005 February;51(2):157–65.
39. Li X, Xu J, Bai Y, et al. Isolation and characterization of neural stem cells from human fetal striatum. *Biochem Biophys Res Commun.* 2005 January 14;326(2):425–34.
40. Conti L, Pollard SM, Gorba T, et al. Niche-independent symmetrical self-renewal of a mammalian tissue stem cell. *PLoS Biol.* 2005 September;3(9):e283.
41. Yin XJ, Ju R, Feng ZC. Experimental study on growth, proliferation and differentiation of neural stem cell from subventricular zone of human fetal brain at different gestational age. *Zhonghua Er Ke Za Zhi.* 2006 July;44(7):500–4.
42. Kim HT, Kim IS, Lee IS, Lee JP, Snyder EY, Park KI. Human neurospheres derived from the fetal central nervous system are regionally and temporally specified but are not committed. *Exp Neurol.* 2006 May;199(1):222–35.
43. Pollard SM, Conti L, Sun Y, Goffredo D, Smith A. Adherent neural stem (NS) cells from fetal and adult forebrain. *Cereb Cortex.* 2006 July;16 Suppl 1:i112–20.
44. Kallur T, Darsalia V, Lindvall O, Kokaia Z. Human fetal cortical and striatal neural stem cells generate region-specific neurons in vitro and differentiate extensively to neurons after intrastriatal transplantation in neonatal rats. *J Neurosci Res.* 2006 December;84(8):1630–44.
45. Redmond DE, Jr., Bjugstad KB, Teng YD, et al. Behavioral improvement in a primate Parkinson's model is associated with multiple homeostatic effects of human neural stem cells. *Proc Natl Acad Sci U S A.* 2007 July 17;104(29):12175–80.
46. Vescovi AL, Snyder EY. Establishment and properties of neural stem cell clones: plasticity in vitro and in vivo. *Brain Pathol.* 1999 July;9(3):569–98.
47. Weissman IL, Anderson DJ, Gage F. Stem and progenitor cells: origins, phenotypes, lineage commitments, and transdifferentiations. *Annu Rev Cell Dev Biol.* 2001;17:387–403.
48. Anderson DJ. Stem cells and pattern formation in the nervous system: the possible versus the actual. *Neuron.* 2001 April;30(1):19–35.
49. Seaberg RM, van der Kooy D. Stem and progenitor cells: the premature desertion of rigorous definitions. *Trends Neurosci.* 2003 March;26(3):125–31.
50. Parker MA, Anderson JK, Corliss DA, et al. Expression profile of an operationally-defined neural stem cell clone. *Exp Neurol.* 2005 August;194(2):320–32.
51. Navarro-Galve B, Martinez-Serrano A. “Is there any need to argue...” about the nature and genetic signature of in vitro neural stem cells? *Exp Neurol.* 2006 May;199(1):20–5.
52. Streeter G. Carnegie Institution of Washington Publications. 1942;30:211–45.
53. Streeter G. Carnegie Institution of Washington Publications. 1948;32:133–203.
54. O'Rahilly R. Guide to the staging of human embryos. *Anat Anz.* 1972;130(5):556–9.
55. Muller F, O'Rahilly R. The first appearance of the major divisions of the human brain at stage 9. *Anat Embryol (Berl).* 1983;168(3):419–32.
56. O'Rahilly R, Muller F, Hutchins GM, Moore GW. Computer ranking of the sequence of appearance of 100 features of the brain and related structures in staged human embryos during the first 5 weeks of development. *Am J Anat.* 1984 November;171(3):243–57.
57. O'Rahilly R. Human embryo. *Nature.* 1987 October 1–7;329(6138):385.
58. Muller F, O'Rahilly R. The development of the human brain, the closure of the caudal neuropore, and the beginning of secondary neurulation at stage 12. *Anat Embryol (Berl).* 1987;176(4):413–30.
59. Muller F, O'Rahilly R. The development of the human brain from a closed neural tube at stage 13. *Anat Embryol (Berl).* 1988;177(3):203–24.
60. Muller F, O'Rahilly R. The human brain at stage 17, including the appearance of the future olfactory bulb and the first amygdaloid nuclei. *Anat Embryol (Berl).* 1989;180(4):353–69.
61. Hanaway J. *The Brain Atlas: A Visual Guide to the Human Central Nervous System.* Bethesda, MD: Fitzgerald Science Inc.; 1998.
62. Muller F, O'Rahilly R. The human brain at stages 21–23, with particular reference to the cerebral cortical plate and to the development of the cerebellum. *Anat Embryol (Berl).* 1990;182(4):375–400.

63. Muller F, O'Rahilly R. The human brain at stages 18–20, including the choroid plexuses and the amygdaloid and septal nuclei. *Anat Embryol (Berl)*. 1990;182(3):285–306.
64. O'Rahilly R, Muller F. Ventricular system and choroid plexuses of the human brain during the embryonic period proper. *Am J Anat*. 1990 December;189(4):285–302.
65. O'Rahilly R, Muller F. Minireview: summary of the initial development of the human nervous system. *Teratology*. 1999 July;60(1):39–41.
66. Degani S. Fetal biometry: clinical, pathological, and technical considerations. *Obstet Gynecol Surv*. 2001 March;56(3):159–67.
67. O'Rahilly R, Muller F. Significant features in the early prenatal development of the human brain. *Ann Anat*. 2008;190(2):105–18.
68. Nazarian LN, Halpern EJ, Kurtz AB, Hauck WW, Needleman L. Normal interval fetal growth rates based on obstetrical ultrasonographic measurements. *J Ultrasound Med*. 1995 November;14(11):829–36.
69. Doubilet PM, Benson CB, Nadel AS, Ringer SA. Improved birth weight table for neonates developed from gestations dated by early ultrasonography. *J Ultrasound Med*. 1997 April;16(4):241–9.
70. Sherer DM. First trimester ultrasonography of multiple gestations: a review. *Obstet Gynecol Surv*. 1998 November;53(11):715–26.
71. Usher R, McLean F, Scott KE. Judgment of fetal age. II. Clinical significance of gestational age and an objective method for its assessment. *Pediatr Clin North Am*. 1966 August;13(3):835–62 contd.
72. Iffy L, Shepard TH, Jakobovits A, Lemire RJ, Kerner P. The rate of growth in young human embryos of Streeter's horizons. 13 to 23. *Acta Anat (Basel)*. 1967;66(2):178–86.
73. Usher R, McLean F. Intrauterine growth of live-born Caucasian infants at sea level: standards obtained from measurements in 7 dimensions of infants born between 25 and 44 weeks of gestation. *J Pediatr*. 1969 June;74(6):901–10.
74. Drumm JE, O'Rahilly R. The assessment of prenatal age from the crown-rump length determined ultrasonically. *Am J Anat*. 1977 April;148(4):555–60.
75. Englund M. *A Color Atlas of Life Before Birth: Normal Fetal Development*. Chicago, IL: Year Book Medical Publishers Inc.; 1990.
76. Schats R, Van Os HC, Jansen CA, Wladimiroff JW. The crown-rump length in early human pregnancy: a reappraisal. *Br J Obstet Gynaecol*. 1991 May;98(5):460–2.
77. Hadlock FP, Shah YP, Kanon DJ, Lindsey JV. Fetal crown-rump length: reevaluation of relation to menstrual age (5–18 weeks) with high-resolution real-time US. *Radiology*. 1992 February;182(2):501–5.
78. Medline Plus T. *Medical Encyclopedia: Fetal Development* <<http://www.nlm.nih.gov/medlineplus/ency/article/002398.htm>>. Accessed.
79. my3dvideos. *Development of Fetus* <http://www.youtube.com/watch?v=aR-Qa_LD2m4&feature=related>. Accessed January 17, 2007.
80. makana116. *Fetal Development* <<http://www.youtube.com/watch?v=RS1ti23SUSw&feature=related>>. Accessed July 28, 2007.
81. Brewer GJ. Serum-free B27/neurobasal medium supports differentiated growth of neurons from the striatum, substantia nigra, septum, cerebral cortex, cerebellum, and dentate gyrus. *J Neurosci Res*. 1995 December;42(5):674–83.
82. Brewer GJ. Isolation and culture of adult rat hippocampal neurons. *J Neurosci Methods*. 1997 February;71(2):143–55.
83. Hazel T. Culture of Neuroepithelial Stem Cells. In: McKay R, Gerfen C (eds). *Current Protocols in Neuroscience*. New York: John Wiley & Sons, 1997.
84. Brewer GJ, Torricelli JR, Evege EK, Price PJ. Optimized survival of hippocampal neurons in B27-supplemented Neurobasal, a new serum-free medium combination. *J Neurosci Res*. 1993 August 1;35(5):567–76.
85. Svendsen CN, Fawcett JW, Bentlage C, Dunnett SB. Increased survival of rat EGF-generated CNS precursor cells using B27 supplemented medium. *Exp Brain Res*. 1995;102(3):407–14.

86. Gritti A, Galli R, Vescovi AL. Cultures of Stem Cells in the Central Nervous System. In: A FSaR (ed). *Protocols for Neural Cell Culture*. 3rd ed. Totowa, NJ: Humana Press, 2001: 173–97.
87. Price PJ, Brewer GJ. Serum-Free Medium for Neural Cell Culture. In: Federaff S, Richardson A (eds). *Protocols for Neural Cell Culture*. 3rd ed. Totowa, NJ: Humana Press, 2001:255–64.
88. Brewer GJ, Torricelli JR. Isolation and culture of adult neurons and neurospheres. *Nat Protoc*. 2007 06//print;2(6):1490–8.
89. Caldwell MA, Garcion E, terBorg MG, He X, Svendsen CN. Heparin stabilizes FGF-2 and modulates striatal precursor cell behavior in response to EGF. *Exp Neurol*. 2004 August;188(2):408–20.
90. Balaci L, Presta M, Ennas MG, et al. Differential expression of fibroblast growth factor receptors by human neurones, astrocytes and microglia. *Neuroreport*. 1994 December 30;6(1):197–200.
91. Richard C, Liuzzo JP, Moscatelli D. Fibroblast growth factor-2 can mediate cell attachment by linking receptors and heparan sulfate proteoglycans on neighboring cells. *J Biol Chem*. 1995 October 13;270(41):24188–96.
92. Richard C, Roghani M, Moscatelli D. Fibroblast growth factor (FGF)-2 mediates cell attachment through interactions with two FGF receptor-1 isoforms and extracellular matrix or cell-associated heparan sulfate proteoglycans. *Biochem Biophys Res Commun*. 2000;276:399–405.
93. Moore KL, Persaud TVN. The Fetal Period: The Ninth Week to Birth. In: Persaud Ma (ed). *The Developing Human: Clinically Oriented Embryology*. 5th ed. Philadelphia, PA: WB Saunders, 1993:93–112.
94. Wakeman DR, Hofmann MR, Redmond Jr. DE, Snyder EY. Preparation, Manipulation, and Transplantation of Human Fetal Neural Stem Cells (Unit 2.D) *Current Protocols in Stem Cell Biology*. New York: Wiley, 2009.
95. Kanemura Y, Mori H, Nakagawa A, et al. In vitro screening of exogenous factors for human neural stem/progenitor cell proliferation using measurement of total ATP content in viable cells. *Cell Transplant*. 2005;14(9):673–82.
96. Temple S. The development of neural stem cells. *Nature*. 2001 November;414(6859):112–7.
97. Kitchens DL, Snyder EY, Gottlieb DI. FGF and EGF are mitogens for immortalized neural progenitors. *J Neurobiol*. 1994 July;25(7):797–807.
98. Oppenheim RW. Cell death during development of the nervous system. *Annu Rev Neurosci*. 1991 (03/60);14(1):453–501.
99. Biebl M, Cooper CM, Winkler J, Kuhn HG. Analysis of neurogenesis and programmed cell death reveals a self-renewing capacity in the adult rat brain. *Neurosci Lett*. 2000 September 8;291(1):17–20.
100. Rakic S, Zecevic N. Programmed cell death in the developing human telencephalon. *Eur J Neurosci*. 2000 August;12(8):2721–34.
101. Reynolds BA, Tetzlaff W, Weiss S. A multipotent EGF-responsive striatal embryonic progenitor cell produces neurons and astrocytes. *J Neurosci*. 1992 November;12(11):4565–74.
102. Svendsen CN, Clarke DJ, Rosser AE, Dunnett SB. Survival and differentiation of rat and human epidermal growth factor-responsive precursor cells following grafting into the lesioned adult central nervous system. *Exp Neurol*. 1996 February;137(2): 376–88.
103. Reynolds BA, Weiss S. Clonal and population analyses demonstrate that an EGF-responsive mammalian embryonic CNS precursor is a stem cell. *Dev Biol*. 1996 April 10;175(1):1–13.
104. Rosser AE, Tyers P, ter Borg M, Dunnett SB, Svendsen CN. Co-expression of MAP-2 and GFAP in cells developing from rat EGF responsive precursor cells. *Brain Res Dev Brain Res*. 1997 February 20;98(2):291–5.
105. Morrison RS, Sharma A, de Vellis J, Bradshaw RA. Basic fibroblast growth factor supports the survival of cerebral cortical neurons in primary culture. *Proc Natl Acad Sci U S A*. 1986 October;83(19):7537–41.

106. Walicke P, Cowan WM, Ueno N, Baird A, Guillemin R. Fibroblast growth factor promotes survival of dissociated hippocampal neurons and enhances neurite extension. *Proc Natl Acad Sci U S A*. 1986 May;83(9):3012–6.
107. Gensburger C, Labourdette G, Sensenbrenner M. Brain basic fibroblast growth factor stimulates the proliferation of rat neuronal precursor cells in vitro. *FEBS Lett*. 1987 June 8;217(1):1–5.
108. Perraud F, Besnard F, Pettmann B, Sensenbrenner M, Labourdette G. Effects of acidic and basic fibroblast growth factors (aFGF and bFGF) on the proliferation and the glutamine synthetase expression of rat astroblasts in culture. *Glia*. 1988;1(2):124–31.
109. Walicke PA. Basic and acidic fibroblast growth factors have trophic effects on neurons from multiple CNS regions. *J Neurosci*. 1988 July;8(7):2618–27.
110. Walicke PA, Baird A. Trophic effects of fibroblast growth factor on neural tissue. *Prog Brain Res*. 1988;78:333–8.
111. Murphy M, Drago J, Bartlett PF. Fibroblast growth factor stimulates the proliferation and differentiation of neural precursor cells in vitro. *J Neurosci Res*. 1990 April;25(4):463–75.
112. Deloulme JC, Baudier J, Sensenbrenner M. Establishment of pure neuronal cultures from fetal rat spinal cord and proliferation of the neuronal precursor cells in the presence of fibroblast growth factor. *J Neurosci Res*. 1991 August;29(4):499–509.
113. Drago J, Murphy M, Carroll SM, Harvey RP, Bartlett PF. Fibroblast growth factor-mediated proliferation of central nervous system precursors depends on endogenous production of insulin-like growth factor I. *Proc Natl Acad Sci U S A*. 1991 March 15;88(6):2199–203.
114. Drago J, Nurcombe V, Pearse MJ, Murphy M, Bartlett PF. Basic fibroblast growth factor upregulates steady-state levels of laminin B1 and B2 chain mRNA in cultured neuroepithelial cells. *Exp Cell Res*. 1991 October;196(2):246–54.
115. Bernfield M, Kokenyesi R, Kato M, et al. Biology of the syndecans: a family of transmembrane heparan sulfate proteoglycans. *Annu Rev Cell Biol*. 1992;8:365–93.
116. Ray J, Gage FH. Spinal cord neuroblasts proliferate in response to basic fibroblast growth factor. *J Neurosci*. 1994 June;14(6):3548–64.
117. Palmer TD, Ray J, Gage FH. FGF-2-responsive neuronal progenitors reside in proliferative and quiescent regions of the adult rodent brain. *Mol Cell Neurosci*. 1995 October;6(5):474–86.
118. Vicario-Abejon C, Johe KK, Hazel TG, Collazo D, McKay RDG. Functions of basic fibroblast growth factor and neurotrophins in the differentiation of hippocampal neurons. *Neuron*. 1995;15:105–14.
119. Ghosh A, Greenberg ME. Distinct roles for bFGF and NT-3 in the regulation of cortical neurogenesis. *Neuron*. 1995 July;15(1):89–103.
120. Gritti A, Parati EA, Cova L, et al. Multipotential stem cells from the adult mouse brain proliferate and self-renew in response to basic fibroblast growth factor. *J Neurosci*. 1996 February 1;16(3):1091–100.
121. Shihabuddin LS, Ray J, Gage FH. FGF-2 is sufficient to isolate progenitors found in the adult mammalian spinal cord. *Exp Neurol*. 1997 December;148(2):577–86.
122. Qian X, Davis AA, Goderie SK, Temple S. FGF2 concentration regulates the generation of neurons and glia from multipotent cortical stem cells. *Neuron*. 1997 January;18(1):81–93.
123. Daadi M, Arcellana-Panlilio M, Weiss S. Activin co-operates with fibroblast growth factor 2 to regulate tyrosine hydroxylase expression in the basal forebrain ventricular zone progenitors. *Neuroscience*. 1998;86:867–80.
124. Caldwell MA, Svendsen CN. Heparin, but not other proteoglycans potentiates the mitogenic effects of FGF-2 on mesencephalic precursor cells. *Exp Neurol*. 1998 July;152(1):1–10.
125. Palmer TD, Markakis EA, Willhoite AR, Safar F, Gage FH. Fibroblast Growth Factor-2 Activates a Latent Neurogenic Program in Neural Stem Cells from Diverse Regions of the Adult CNS. *J Neurosci*. 1999 October 1;19(19):8487–97.
126. Ray J, Peterson DA, Schinstine M, Gage FH. Proliferation, differentiation, and long-term culture of primary hippocampal neurons. *Proc Natl Acad Sci U S A*. 1993 April 15;90(8):3602–6.

127. Ray J, Gage FH. Differential properties of adult rat and mouse brain-derived neural stem/progenitor cells. *Mol Cell Neurosci*. 2006 March;31(3):560–73.
128. Kornblum HI, Raymon HK, Morrison RS, Cavanaugh KP, Bradshaw RA, Leslie FM. Epidermal growth factor and basic fibroblast growth factor: effects on an overlapping population of neocortical neurons in vitro. *Brain Res*. 1990 December 10;535(2):255–63.
129. Tropepe V, Sibilia M, Ciruna BG, Rossant J, Wagner EF, van der Kooy D. Distinct neural stem cells proliferate in response to EGF and FGF in the developing mouse telencephalon. *Dev Biol*. 1999 April 1;208(1):166–88.
130. Kilpatrick TJ, Bartlett PF. Cloning and growth of multipotential neural precursors: requirements for proliferation and differentiation. *Neuron*. 1993 February;10(2):255–65.
131. Vescovi AL, Reynolds BA, Fraser DD, Weiss S. bFGF regulates the proliferative fate of unipotent (neuronal) and bipotent (neuronal/astroglial) EGF-generated CNS progenitor cells. *Neuron*. 1993 November;11(5):951–66.
132. Bartlett PF, Kilpatrick TJ, Richards LJ, Talman PS, Murphy M. Regulation of the early development of the nervous system by growth factors. *Pharmacol Ther*. 1994;64(3):371–93.
133. Kilpatrick TJ, Richards LJ, Bartlett PF. The regulation of neural precursor cells within the mammalian brain. *Mol Cell Neurosci*. 1995 February;6(1):2–15.
134. Gritti A, Cova L, Parati EA, Galli R, Vescovi AL. Basic fibroblast growth factor supports the proliferation of epidermal growth factor-generated neuronal precursor cells of the adult mouse CNS. *Neurosci Lett*. 1995 February 13;185(3):151–4.
135. Kuhn HG, Winkler J, Kempermann G, Thal LJ, Gage FH. Epidermal growth factor and fibroblast growth factor-2 have different effects on neural progenitors in the adult rat brain. *J Neurosci*. 1997 August 1;17(15):5820–9.
136. Ciccolini F, Svendsen CN. Fibroblast growth factor 2 (FGF-2) promotes acquisition of epidermal growth factor (EGF) responsiveness in mouse striatal precursor cells: identification of neural precursors responding to both EGF and FGF-2. *J Neurosci*. 1998 October 1;18(19):7869–80.
137. Gritti A, Frolichsthal-Schoeller P, Galli R, et al. Epidermal and fibroblast growth factors behave as mitogenic regulators for a single multipotent stem cell-like population from the subventricular region of the adult mouse forebrain. *J Neurosci*. 1999 May 1;19(9):3287–97.
138. Kalyani AJ, Mujtaba T, Rao MS. Expression of EGF receptor and FGF receptor isoforms during neuroepithelial stem cell differentiation. *J Neurobiol*. 1999 February 5;38(2):207–24.
139. Caldwell MA, He X, Wilkie N, et al. Growth factors regulate the survival and fate of cells derived from human neurospheres. *Nat Biotechnol*. 2001 May;19(5):475–9.
140. Arsenijevic Y, Weiss S, Schneider B, Aebischer P. Insulin-like growth factor-i is necessary for neural stem cell proliferation and demonstrates distinct actions of epidermal growth factor and fibroblast growth factor-2. *J Neurosci*. 2001 September 15;21(18):7194–202.
141. Ostefeld T, Svendsen CN. Requirement for neurogenesis to proceed through the division of neuronal progenitors following differentiation of epidermal growth factor and fibroblast growth factor-2-responsive human neural stem cells. *Stem Cells*. 2004 September 1;22(5):798–811.
142. Tarasenko YI, Yu Y, Jordan PM, Bottenstein J, Wu P. Effect of growth factors on proliferation and phenotypic differentiation of human fetal neural stem cells. *J Neurosci Res*. 2004 December 1;78(5):625–36.
143. Kelly CM, Tyers P, Borg Mt, Svendsen CN, Dunnett SB, Rosser AE. EGF and FGF-2 responsiveness of rat and mouse neural precursors derived from the embryonic CNS. Proceedings of the 14th and 15th Meetings of the European Network for CNS Transplantation and Repair (NECTAR). 2005 12/15;68(1–2):83–94.
144. Galli R, Pagano SF, Gritti A, Vescovi AL. Regulation of neuronal differentiation in human CNS stem cell progeny by leukemia inhibitory factor. *Dev Neurosci*. 2000;22(1–2):86–95.
145. Molne M, Studer L, Tabar V, Ting YT, Eiden MV, McKay RD. Early cortical precursors do not undergo LIF-mediated astrocytic differentiation. *J Neurosci Res*. 2000 February 1;59(3):301–11.

146. Shimazaki T, Shingo T, Weiss S. The ciliary neurotrophic factor/leukemia inhibitory factor/gp130 receptor complex operates in the maintenance of mammalian forebrain neural stem cells. *J Neurosci*. 2001 October 1;21(19):7642–53.
147. Wright LS, Li J, Caldwell MA, Wallace K, Johnson JA, Svendsen CN. Gene expression in human neural stem cells: effects of leukemia inhibitory factor. *J Neurochem*. 2003 July;86(1):179–95.
148. Chojnacki A, Weiss S. Isolation of a novel platelet-derived growth factor-responsive precursor from the embryonic ventral forebrain. *J Neurosci*. 2004 December 1;24(48):10888–99.
149. Gregg C, Weiss S. CNTF/LIF/gp130 receptor complex signaling maintains a VZ precursor differentiation gradient in the developing ventral forebrain. *Development*. 2005 February 1;132(3):565–78.
150. Ying QL, Nichols J, Chambers I, Smith A. BMP induction of Id proteins suppresses differentiation and sustains embryonic stem cell self-renewal in collaboration with STAT3. *Cell*. 2003 October 31;115(3):281–92.
151. Bonaguidi MA, McGuire T, Hu M, Kan L, Samanta J, Kessler JA. LIF and BMP signaling generate separate and discrete types of GFAP-expressing cells. *Development*. 2005 December 15;132(24):5503–14.
152. Lim DA, Huang YC, Alvarez-Buylla A. Adult Subventricular Zone and Olfactory Bulb Neurogenesis. In: Gage FH, Kempermann G, Song H (eds). *Adult Neurogenesis*. 52nd ed. New York: Cold Spring Harbor Press, 2008:159–74.
153. Perez-Iratxeta C, Palidwor G, Porter CJ, et al. Study of stem cell function using microarray experiments. *FEBS Lett*. 2005 March 21;579(8):1795–801.
154. Shin S, Rao MS. Large-scale analysis of neural stem cells and progenitor cells. *Neurodegener Dis*. 2006;3(1–2):106–11.
155. Luo Y, Bhattacharya B, Yang AX, Puri RK, Rao MS. Designing, testing, and validating a microarray for stem cell characterization. *Methods Mol Biol*. 2006;331:241–66.
156. Luo Y, Schwartz C, Shin S, et al. A focused microarray to assess dopaminergic and glial cell differentiation from fetal tissue or embryonic stem cells. *Stem Cells*. 2006 April;24(4):865–75.
157. Chang HY, Thomson JA, Chen X. Microarray analysis of stem cells and differentiation. *Methods Enzymol*. 2006;420:225–54.
158. Anisimov SV, Christophersen NS, Correia AS, Li JY, Brundin P. “NeuroStem Chip”: a novel highly specialized tool to study neural differentiation pathways in human stem cells. *BMC Genomics*. 2007;8:46.
159. Shin S, Sun Y, Liu Y, et al. Whole genome analysis of human neural stem cells derived from embryonic stem cells and stem and progenitor cells isolated from fetal tissue. *Stem Cells*. 2007 May;25(5):1298–306.
160. Jacques TS, Relvas JB, Nishimura S, et al. Neural precursor cell chain migration and division are regulated through different beta1 integrins. *Development*. 1998 August 1;125(16):3167–77.
161. Hynes RO. Integrins: bidirectional, allosteric signaling machines. *Cell*. 2002 September 20;110(6):673–87.
162. Campos LS, Leone DP, Relvas JB, et al. {beta}1 integrins activate a MAPK signalling pathway in neural stem cells that contributes to their maintenance. *Development*. 2004 July 15;131(14):3433–44.
163. Leone DP, Relvas JB, Campos LS, et al. Regulation of neural progenitor proliferation and survival by {beta}1 integrins. *J Cell Sci*. 2005 June 15;118(12):2589–99.
164. Mueller F-J, Seroby N, Schraufstatter IU, et al. Adhesive interactions between human neural stem cells and inflamed human vascular endothelium are mediated by integrins. *Stem Cells*. 2006 November 1;24(11):2367–72.
165. Flanagan LA, Rebaza LM, Derzic S, Schwartz PH, Monuki ES. Regulation of human neural precursor cells by laminin and integrins. *J Neurosci Res*. 2006 April;83(5):845–56.

166. Svendsen CN, Skepper J, Rosser AE, ter Borg MG, Tyres P, Ryken T. Restricted growth potential of rat neural precursors as compared to mouse. *Brain Res Dev Brain Res.* 1997 April 18;99(2):253–8.
167. Steindler DA, Scheffler B, Laywell ED, et al. Neural Stem/Progenitor Cell Clones or “neurospheres”: A Model for Understanding Neuromorphogenesis. In: Zigova T, Snyder EY, Sanberg PR (eds). *Neural Stem Cells for Brain and Spinal Cord Repair.* Totowa, NJ: Humana Press, 2003:183–202.
168. Lobo MV, Alonso FJ, Redondo C, et al. Cellular characterization of epidermal growth factor-expanded free-floating neurospheres. *J Histochem Cytochem.* 2003 January;51(1):89–103.
169. Bez A, Corsini E, Curti D, et al. Neurosphere and neurosphere-forming cells: morphological and ultrastructural characterization. *Brain Res.* 2003;993(1–2):18–29.
170. Anderson L, Burnstein RM, He X, et al. Gene expression changes in long term expanded human neural progenitor cells passaged by chopping lead to loss of neurogenic potential in vivo. *Exp Neurol.* 2007 April;204(2):512–24.
171. Reynolds BA, Weiss S. Generation of neurons and astrocytes from isolated cells of the adult mammalian central nervous system. *Science.* 1992 March 27;255(5052):1707–10.
172. Rietze RL, Reynolds BA. Neural stem cell isolation and characterization. *Methods Enzymol.* 2006;419:3–23.
173. Snyder EY, Deitcher DL, Walsh C, Arnold-Aldea S, Hartweg EA, Cepko CL. Multipotent neural cell lines can engraft and participate in development of mouse cerebellum. *Cell.* 1992 January 10;68(1):33–51.
174. Luskin MB. Restricted proliferation and migration of postnatally generated neurons derived from the forebrain subventricular zone. *Neuron.* 1993 July;11(1):173–89.
175. Levison SW, Goldman JE. Both oligodendrocytes and astrocytes develop from progenitors in the subventricular zone of postnatal rat forebrain. *Neuron.* 1993 February;10(2):201–12.
176. Lois C, Alvarez-Buylla A. Proliferating subventricular zone cells in the adult mammalian forebrain can differentiate into neurons and glia. *Proc Natl Acad Sci U S A.* 1993 March 1;90(5):2074–7.
177. Morshead CM, Reynolds BA, Craig CG, et al. Neural stem cells in the adult mammalian forebrain: a relatively quiescent subpopulation of subependymal cells. *Neuron.* 1994 November;13(5):1071–82.
178. Weiss S, Dunne C, Hewson J, et al. Multipotent CNS stem cells are present in the adult mammalian spinal cord and ventricular neuroaxis. *J Neurosci.* 1996 December 1;16(23):7599–609.
179. McKay R. Stem cells in the central nervous system. *Science.* 1997 April 4;276(5309):66–71.
180. Luskin MB, Zigova T, Soteres BJ, Stewart RR. Neuronal progenitor cells derived from the anterior subventricular zone of the neonatal rat forebrain continue to proliferate in vitro and express a neuronal phenotype. *Mol Cell Neurosci.* 1997;8(5):351–66.
181. Sanai N, Tramontin AD, Quinones-Hinojosa A, et al. Unique astrocyte ribbon in adult human brain contains neural stem cells but lacks chain migration. *Nature.* 2004 February 19;427(6976):740–4.
182. Howard B, Chen Y, Zecevic N. Cortical progenitor cells in the developing human telencephalon. *Glia.* 2006 January 1;53(1):57–66.
183. Quinones-Hinojosa A, Sanai N, Soriano-Navarro M, et al. Cellular composition and cytoarchitecture of the adult human subventricular zone: a niche of neural stem cells. *J Comp Neurol.* 2006 January 20;494(3):415–34.
184. Merkle FT, Mirzadeh Z, Alvarez-Buylla A. Mosaic organization of neural stem cells in the adult brain. *Science.* 2007 July 20;317(5836):381–4.
185. Curtis MA, Kam M, Nannmark U, et al. Human neuroblasts migrate to the olfactory bulb via a lateral ventricular extension. *Science.* 2007 March 2;315(5816):1243–9.
186. Quinones-Hinojosa A, Sanai N, Gonzalez-Perez O, Garcia-Verdugo JM. The human brain subventricular zone: stem cells in this niche and its organization. *Neurosurg Clin N Am.* 2007 January;18(1):15–20, vii.

187. Singec I, Knoth R, Meyer RP, et al. Defining the actual sensitivity and specificity of the neurosphere assay in stem cell biology. *Nat Methods*. 2006 October;3(10):801–6.
188. Potten CS, Loeffler M. Stem cells: attributes, cycles, spirals, pitfalls and uncertainties. Lessons for and from the crypt. *Development*. 1990 December 1;110(4):1001–20.
189. Loeffler M, Potten CS. Stem Cells and Cellular Pedigrees – A Conceptual Introduction. In: Potten CS (ed). *Stem Cells*. London: Academic, 1997:1–27.
190. Santa-Olalla J, Baizabal JM, Fregoso M, del Carmen Cardenas M, Covarrubias L. The in vivo positional identity gene expression code is not preserved in neural stem cells grown in culture. *Eur J Neurosci*. 2003 September;18(5):1073–84.
191. Hack MA, Sugimori M, Lundberg C, Nakafuku M, Gotz M. Regionalization and fate specification in neurospheres: the role of Olig2 and Pax6. *Mol Cell Neurosci*. 2004 April;25(4):664–78.
192. Scholzen T, Gerdes J. The Ki-67 protein: from the known and the unknown. *J Cell Physiol*. 2000 March;182(3):311–22.
193. Hall PA, Levison DA. Review: assessment of cell proliferation in histological material. *J Clin Pathol*. 1990 March;43(3):184–92.
194. Hall PA, Levison DA, Woods AL, et al. Proliferating cell nuclear antigen (PCNA) immunolocalization in paraffin sections: an index of cell proliferation with evidence of deregulated expression in some neoplasms. *J Pathol*. 1990 December;162(4):285–94.
195. D'Amour KA, Gage FH. Genetic and functional differences between multipotent neural and pluripotent embryonic stem cells. *Proc Natl Acad Sci U S A*. 2003 September 30;100 Suppl 1:11866–72.
196. Komitova M, Eriksson PS. Sox-2 is expressed by neural progenitors and astroglia in the adult rat brain. *Neurosci Lett*. 2004 October 7;369(1):24–7.
197. Chan C, Moore BE, Cotman CW, et al. Musashi1 antigen expression in human fetal germinal matrix development. *Exp Neurol*. 2006 October;201(2):515–8.
198. Pixley SK, de Vellis J. Transition between immature radial glia and mature astrocytes studied with a monoclonal antibody to vimentin. *Brain Res*. 1984 August;317(2):201–9.
199. Pixley SK, Kobayashi Y, de Vellis J. A monoclonal antibody against vimentin: characterization. *Brain Res*. 1984 August;317(2):185–99.
200. Pixley SK, Kobayashi Y, de Vellis J. Monoclonal antibody to intermediate filament proteins in astrocytes. *J Neurosci Res*. 1984;12(4):525–41.
201. Hockfield S, McKay RD. Identification of major cell classes in the developing mammalian nervous system. *J Neurosci*. 1985 December;5(12):3310–28.
202. Lendahl U, Zimmerman LB, McKay RD. CNS stem cells express a new class of intermediate filament protein. *Cell*. 1990 February 23;60(4):585–95.
203. Dahlstrand J, Zimmerman LB, McKay RD, Lendahl U. Characterization of the human nestin gene reveals a close evolutionary relationship to neurofilaments. *J Cell Sci*. 1992 October;103 (Pt 2):589–97.
204. Zimmerman L, Parr B, Lendahl U, et al. Independent regulatory elements in the nestin gene direct transgene expression to neural stem cells or muscle precursors. *Neuron*. 1994 January;12(1):11–24.
205. Doetsch F, Caille I, Lim DA, Garcia-Verdugo JM, Alvarez-Buylla A. Subventricular zone astrocytes are neural stem cells in the adult mammalian brain. *Cell*. 1999 June 11;97(6):703–16.
206. Laywell ED, Rakic P, Kukekov VG, Holland EC, Steindler DA. Identification of a multipotent astrocytic stem cell in the immature and adult mouse brain. *Proc Natl Acad Sci U S A*. 2000 December 5;97(25):13883–8.
207. Imura T, Kornblum HI, Sofroniew MV. The predominant neural stem cell isolated from postnatal and adult forebrain but not early embryonic forebrain expresses GFAP. *J Neurosci*. 2003 April 1;23(7):2824–32.
208. Garcia AD, Doan NB, Imura T, Bush TG, Sofroniew MV. GFAP-expressing progenitors are the principal source of constitutive neurogenesis in adult mouse forebrain. *Nat Neurosci*. 2004 November;7(11):1233–41.

209. Feng L, Hatten ME, Heintz N. Brain lipid-binding protein (BLBP): a novel signaling system in the developing mammalian CNS. *Neuron*. 1994 April;12(4):895–908.
210. Feng L, Heintz N. Differentiating neurons activate transcription of the brain lipid-binding protein gene in radial glia through a novel regulatory element. *Development* (Cambridge, England). 1995 June;121(6):1719–30.
211. Malatesta P, Hartfuss E, Gotz M. Isolation of radial glial cells by fluorescent-activated cell sorting reveals a neuronal lineage. *Development* (Cambridge, England). 2000 December;127(24):5253–63.
212. Hartfuss E, Galli R, Heins N, Gotz M. Characterization of CNS precursor subtypes and radial glia. *Dev Biol*. 2001 January 1;229(1):15–30.
213. Alvarez-Buylla A, Garcia-Verdugo JM, Tramontin AD. A unified hypothesis on the lineage of neural stem cells. *Nat Rev Neurosci*. 2001 April;2(4):287–93.
214. Miyata T, Kawaguchi A, Okano H, Ogawa M. Asymmetric inheritance of radial glial fibers by cortical neurons. *Neuron*. 2001 September 13;31(5):727–41.
215. Noctor SC, Flint AC, Weissman TA, Dammerman RS, Kriegstein AR. Neurons derived from radial glial cells establish radial units in neocortex. *Nature*. 2001 February 8;409(6821):714–20.
216. Noctor SC, Flint AC, Weissman TA, Wong WS, Clinton BK, Kriegstein AR. Dividing precursor cells of the embryonic cortical ventricular zone have morphological and molecular characteristics of radial glia. *J Neurosci*. 2002 April 15;22(8):3161–73.
217. Gotz M, Hartfuss E, Malatesta P. Radial glial cells as neuronal precursors: a new perspective on the correlation of morphology and lineage restriction in the developing cerebral cortex of mice. *Brain Res Bull*. 2002 April;57(6):777–88.
218. Gotz M. Glial cells generate neurons – master control within CNS regions: developmental perspectives on neural stem cells. *Neuroscientist*. 2003 October;9(5):379–97.
219. Malatesta P, Hack MA, Hartfuss E, et al. Neuronal or glial progeny: regional differences in radial glia fate. *Neuron*. 2003 March 6;37(5):751–64.
220. Doetsch F. The glial identity of neural stem cells. *Nat Neurosci*. 2003 November;6(11):1127–34.
221. Goldman S. Glia as neural progenitor cells. *Trends Neurosci*. 2003 November;26(11):590–6.
222. Noctor SC, Martinez-Cerdeno V, Ivic L, Kriegstein AR. Cortical neurons arise in symmetric and asymmetric division zones and migrate through specific phases. *Nat Neurosci*. 2004 February;7(2):136–44.
223. Merkle FT, Tramontin AD, Garcia-Verdugo JM, Alvarez-Buylla A. Radial glia give rise to adult neural stem cells in the subventricular zone. *Proc Natl Acad Sci U S A*. 2004 December 14;101(50):17528–32.
224. Gotz M, Barde YA. Radial glial cells defined and major intermediates between embryonic stem cells and CNS neurons. *Neuron*. 2005 May 5;46(3):369–72.
225. Noctor SC, Martinez-Cerdeno V, Kriegstein AR. Distinct behaviors of neural stem and progenitor cells underlie cortical neurogenesis. *J Comp Neurol*. 2008 May 1;508(1):28–44.
226. Gleeson JG, Lin PT, Flanagan LA, Walsh CA. Doublecortin is a microtubule-associated protein and is expressed widely by migrating neurons. *Neuron*. 1999 June;23(2):257–71.
227. Francis F, Koulakoff A, Boucher D, et al. Doublecortin is a developmentally regulated, microtubule-associated protein expressed in migrating and differentiating neurons. *Neuron*. 1999 June;23(2):247–56.
228. Friocourt G, Koulakoff A, Chafey P, et al. Doublecortin functions at the extremities of growing neuronal processes. *Cerebral Cortex* (New York 1991). 2003 June;13(6):620–6.
229. Hu H, Tomaszewicz H, Magnuson T, Rutishauser U. The role of polysialic acid in migration of olfactory bulb interneuron precursors in the subventricular zone. *Neuron*. 1996 April;16(4):735–43.
230. Merkle FT, Alvarez-Buylla A. Neural stem cells in mammalian development. *Curr Opin Cell Biol*. 2006 December;18(6):704–9.

231. Alvarez-Buylla A, Seri B, Doetsch F. Identification of neural stem cells in the adult vertebrate brain. *Brain Res Bull.* 2002 April;57(6):751–8.
232. Gregg CT, Chojnacki AK, Weiss S. Radial glial cells as neuronal precursors: the next generation? *J Neurosci Res.* 2002 September 15;69(6):708–13.
233. Gregg C, Weiss S. Generation of functional radial glial cells by embryonic and adult forebrain neural stem cells. *J Neurosci.* 2003 December 17;23(37):11587–601.
234. Pollard SM, Conti L. Investigating radial glia in vitro. *Prog Neurobiol.* 2007 September;83(1):53–67.
235. Rakic P. Mode of cell migration to the superficial layers of fetal monkey neocortex. *J Comp Neurol.* 1972 May;145(1):61–83.
236. Sidman RL, Rakic P. Neuronal migration, with special reference to developing human brain: a review. *Brain Res.* 1973 November 9;62(1):1–35.
237. Levitt P, Rakic P. Immunoperoxidase localization of glial fibrillary acidic protein in radial glial cells and astrocytes of the developing rhesus monkey brain. *J Comp Neurol.* 1980 October 1;193(3):815–40.
238. Levitt P, Cooper ML, Rakic P. Coexistence of neuronal and glial precursor cells in the cerebral ventricular zone of the fetal monkey: an ultrastructural immunoperoxidase analysis. *J Neurosci.* 1981 January;1(1):27–39.
239. Levitt P, Cooper ML, Rakic P. Early divergence and changing proportions of neuronal and glial precursor cells in the primate cerebral ventricular zone. *Dev Biol.* 1983 April;96(2):472–84.
240. Caccamo D, Katsetos CD, Herman MM, Frankfurter A, Collins VP, Rubinstein LJ. Immunohistochemistry of a spontaneous murine ovarian teratoma with neuroepithelial differentiation. Neuron-associated beta-tubulin as a marker for primitive neuroepithelium. *Lab Invest.* 1989 March;60(3):390–8.
241. Geisert EE, Jr., Frankfurter A. The neuronal response to injury as visualized by immunostaining of class III beta-tubulin in the rat. *Neurosci Lett.* 1989 July 31;102(2–3):137–41.
242. Lee MK, Tuttle JB, Rebhun LI, Cleveland DW, Frankfurter A. The expression and posttranslational modification of a neuron-specific beta-tubulin isotype during chick embryogenesis. *Cell Motil Cytoskeleton.* 1990;17(2):118–32.
243. Menezes JR, Luskin MB. Expression of neuron-specific tubulin defines a novel population in the proliferative layers of the developing telencephalon. *J Neurosci.* 1994 September;14(9):5399–416.
244. Menezes JR, Smith CM, Nelson KC, Luskin MB. The division of neuronal progenitor cells during migration in the neonatal mammalian forebrain. *Mol Cell Neurosci.* 1995 December;6(6):496–508.
245. Suslov ON, Kukekov VG, Ignatova TN, Steindler DA. Neural stem cell heterogeneity demonstrated by molecular phenotyping of clonal neurospheres. *Proc Natl Acad Sci U S A.* 2002 October 29;99(22):14506–11.
246. Kondo T, Raff M. Oligodendrocyte precursor cells reprogrammed to become multipotential CNS stem cells. *Science.* 2000 September 8;289(5485):1754–7.
247. Pollard SM, Wallbank R, Tomlinson S, Grotewold L, Smith A. Fibroblast growth factor induces a neural stem cell phenotype in foetal forebrain progenitors and during embryonic stem cell differentiation. *Mol Cell Neurosci.* 2008 July;38(3):393–403.
248. Takahashi K, Yamanaka S. Induction of pluripotent stem cells from mouse embryonic and adult fibroblast cultures by defined factors. *Cell.* 2006 August 25;126(4):663–76.
249. Yamanaka S. Strategies and new developments in the generation of patient-specific pluripotent stem cells. *Cell Stem Cell.* 2007 June 7;1(1):39–49.
250. Maherali N, Sridharan R, Xie W, et al. Directly reprogrammed fibroblasts show global epigenetic remodeling and widespread tissue contribution. *Cell Stem Cell.* 2007 June 7;1(1):55–70.
251. Wernig M, Meissner A, Foreman R, et al. In vitro reprogramming of fibroblasts into a pluripotent ES-cell-like state. *Nature.* 2007 July 19;448(7151):318–24.

252. Takahashi K, Okita K, Nakagawa M, Yamanaka S. Induction of pluripotent stem cells from fibroblast cultures. *Nat Protoc.* 2007;2(12):3081–9.
253. Takahashi K, Tanabe K, Ohnuki M, et al. Induction of pluripotent stem cells from adult human fibroblasts by defined factors. *Cell.* 2007 November 30;131(5):861–72.
254. Okita K, Ichisaka T, Yamanaka S. Generation of germline-competent induced pluripotent stem cells. *Nature.* 2007 July 19;448(7151):313–7.
255. Meissner A, Wernig M, Jaenisch R. Direct reprogramming of genetically unmodified fibroblasts into pluripotent stem cells. *Nat Biotechnol.* 2007 October;25(10):1177–81.
256. Hyun I, Hochedlinger K, Jaenisch R, Yamanaka S. New advances in iPS cell research do not obviate the need for human embryonic stem cells. *Cell Stem Cell.* 2007 October 11;1(4):367–8.
257. Lewitzky M, Yamanaka S. Reprogramming somatic cells towards pluripotency by defined factors. *Curr Opin Biotechnol.* 2007 October;18(5):467–73.
258. Yu J, Vodyanik MA, Smuga-Otto K, et al. Induced pluripotent stem cell lines derived from human somatic cells. *Science.* 2007 December 21;318(5858):1917–20.
259. Nakagawa M, Koyanagi M, Tanabe K, et al. Generation of induced pluripotent stem cells without Myc from mouse and human fibroblasts. *Nat Biotechnol.* 2008 January;26(1):101–6.
260. Wernig M, Meissner A, Cassady JP, Jaenisch R. c-Myc is dispensable for direct reprogramming of mouse fibroblasts. *Cell Stem Cell.* 2008 January 10;2(1):10–2.
261. Park IH, Zhao R, West JA, et al. Reprogramming of human somatic cells to pluripotency with defined factors. *Nature.* 2008 January 10;451(7175):141–6.
262. Brambrink T, Foreman R, Welstead GG, et al. Sequential expression of pluripotency markers during direct reprogramming of mouse somatic cells. *Cell Stem Cell.* 2008 February 7;2(2):151–9.
263. Stadtfeld M, Maherali N, Breault DT, Hochedlinger K. Defining molecular cornerstones during fibroblast to iPS cell reprogramming in mouse. *Cell Stem Cell.* 2008 March 6;2(3):230–40.
264. Yamanaka S. Induction of pluripotent stem cells from mouse fibroblasts by four transcription factors. *Cell Prolif.* 2008 February;41 Suppl 1:51–6.
265. Liu SV. iPS cells: a more critical review. *Stem Cells Dev.* 2008 June;17(3):391–7.
266. Xu Y, Shi Y, Ding S. A chemical approach to stem-cell biology and regenerative medicine. *Nature.* 2008 May 15;453(7193):338–44.
267. Shi Y, Do JT, Despons C, Hahm HS, Scholer HR, Ding S. A combined chemical and genetic approach for the generation of induced pluripotent stem cells. *Cell Stem Cell.* 2008 June 5;2(6):525–8.
268. Kim JB, Zaehres H, Wu G, et al. Pluripotent stem cells induced from adult neural stem cells by reprogramming with two factors. *Nature.* 2008 July 31;454(7204):646–50.
269. Yamanaka S. Pluripotency and nuclear reprogramming. *Philos Trans R Soc Lond B Biol Sci.* 2008 June 27;363(1500):2079–87.
270. Egli D, Birkhoff G, Eggan K. Mediators of reprogramming: transcription factors and transitions through mitosis. *Nat Rev Mol Cell Biol.* 2008 July;9(7):505–16.
271. Morrison SJ, Shah NM, Anderson DJ. Regulatory mechanisms in stem cell biology. *Cell.* 1997 February 7;88(3):287–98.
272. Nowakowski RS, Caviness VS, Jr., Takahashi T, Hayes NL. Population dynamics during cell proliferation and neurogenesis in the developing murine neocortex. *Results Probl Cell Differ.* 2002;39:1–25.
273. Calegari F, Huttner WB. An inhibition of cyclin-dependent kinases that lengthens, but does not arrest, neuroepithelial cell cycle induces premature neurogenesis. *J Cell Sci.* 2003 December 15;116(Pt 24):4947–55.
274. Calegari F, Haubensak W, Haffner C, Huttner WB. Selective lengthening of the cell cycle in the neurogenic subpopulation of neural progenitor cells during mouse brain development. *J Neurosci.* 2005 July 13;25(28):6533–8.

275. Qian X, Goderie SK, Shen Q, Stern JH, Temple S. Intrinsic programs of patterned cell lineages in isolated vertebrate CNS ventricular zone cells. *Development*. 1998 August;125(16):3143–52.
276. Qian X, Shen Q, Goderie SK, et al. Timing of CNS cell generation: a programmed sequence of neuron and glial cell production from isolated murine cortical stem cells. *Neuron*. 2000 October;28(1):69–80.
277. Takahashi J, Palmer TD, Gage FH. Retinoic acid and neurotrophins collaborate to regulate neurogenesis in adult-derived neural stem cell cultures. *J Neurobiol*. 1999 January;38(1):65–81.
278. Watterson JM, Watson DG, Meyer EM, Lenox RH. A role for protein kinase C and its substrates in the action of valproic acid in the brain: implications for neural plasticity. *Brain Res*. 2002 April 26;934(1):69–80.
279. Johe KK, Hazel TG, Muller T, Dugich-Djordjevic MM, McKay RD. Single factors direct the differentiation of stem cells from the fetal and adult central nervous system. *Genes Dev*. 1996 December 15;10(24):3129–40.
280. Aberg MA, Aberg ND, Palmer TD, et al. IGF-I has a direct proliferative effect in adult hippocampal progenitor cells. *Mol Cell Neurosci*. 2003 September;24(1):23–40.
281. Gross RE, Mehler MF, Mabie PC, Zang Z, Santschi L, Kessler JA. Bone morphogenetic proteins promote astroglial lineage commitment by mammalian subventricular zone progenitor cells. *Neuron*. 1996 October;17(4):595–606.
282. Bonni A, Sun Y, Nadal-Vicens M, et al. Regulation of gliogenesis in the central nervous system by the JAK-STAT signaling pathway. *Science*. 1997 October 17;278(5337):477–83.
283. Studer L, Csete M, Lee SH, et al. Enhanced proliferation, survival, and dopaminergic differentiation of CNS precursors in lowered oxygen. *J Neurosci*. 2000 October 1;20(19):7377–83.
284. Bull ND, Bartlett PF. The adult mouse hippocampal progenitor is neurogenic but not a stem cell. *J Neurosci*. 2005 November 23;25(47):10815–21.
285. Hsieh J, Gage FH. Epigenetic control of neural stem cell fate. *Curr Opin Genet Dev*. 2004 October;14(5):461–9.
286. Lee J-P, Schmidt NO, Baier PC. Stem Cell Transplantation in the Brain. In: Loring J, Weselschmidt R, Schwartz P (eds). *Human Stem Cell Manual: A Laboratory Guide*. 1st ed. New York: Elsevier Inc., 2007:332–50.
287. Lee JP, McKercher S, Muller FJ, Snyder EY. Neural stem cell transplantation in mouse brain. *Curr Protoc Neurosci*. 2008 January;Chapter 3:Unit 3 10.
288. Bjugstad KB, Redmond DE, Jr., Teng YD, et al. Neural stem cells implanted into MPTP-treated monkeys increase the size of endogenous tyrosine hydroxylase-positive cells found in the striatum: a return to control measures. *Cell Transplant*. 2005;14(4):183–92.
289. Bjugstad KB, Teng YD, Redmond DE, Jr., et al. Human neural stem cells migrate along the nigrostriatal pathway in a primate model of Parkinson's disease. *Exp Neurol*. 2008 June;211(2):362–9.
290. Wakeman DR, Crain AM, Snyder EY. Large animal models are critical for rationally advancing regenerative therapies. *Regen Med*. 2006 July;1(4):405–13.
291. Le Belle JE, Caldwell MA, Svendsen CN. Improving the survival of human CNS precursor-derived neurons after transplantation. *J Neurosci Res*. 2004 April 15;76(2):174–83.

Chapter 2

Multipotent Stromal Cells (hMSCs)

Margaret Wolfe, Alan Tucker, Roxanne L. Reger and Darwin J. Prockop

Abstract The existence of the non-hematopoietic stem/progenitor cells from bone marrow known as mesenchymal stem cells, marrow stromal cells, or multipotent mesenchymal stromal cells (MSCs), was first suggested over a hundred years ago. Definitive evidence that bone marrow contains cells that can differentiate into fibroblasts as well as other mesenchymal cells has been available since the mid-1970s. Over the last three decades, a great deal of research has been conducted on MSCs in laboratories worldwide. It has been found that these cells are easily isolated from small volumes of bone marrow, can be expanded to large numbers in a relatively short period of time with basic tissue culture techniques and can undergo differentiation into several different tissue types. In addition, it has been shown that MSCs are a part of the body's natural repair mechanism and, thus, there has been great interest in using MSCs for treatment of various diseases and injuries, such as diabetes, chronic heart failure, Parkinson's disease, Alzheimer's disease, and spinal cord injury, to name just a few. Although the knowledge of these cells has grown exponentially and interest in MSCs has increased proportionally, each lab has developed their own protocols and methods of isolation, culture and characterization, thus, making it difficult to compare the results from experiments with MSCs from different labs. In spite of the ease with which these cells are isolated and cultured, there are some important criteria for the culture of these cells which must be observed in order to produce MSCs which have the capability to expand, multidifferentiate, form colonies and also to perform well when used for in vitro and in vivo studies and in clinical therapies. This chapter will cover human MSC isolation, expansion, characterization and potential therapeutic uses.

2.1 Introduction

The existence of stem/progenitor cells from bone marrow known as mesenchymal stem cells, marrow stromal cells, or multipotent mesenchymal stromal stem/progenitor cells (MSCs) was first suspected in 1867 when Cohnheim, a German pathologist, studied inflammation and wound repair by injecting an insoluble aniline

M. Wolfe (✉)

Center for Gene Therapy, Tulane University Health Sciences, New Orleans, LA, 70112, USA
e-mail: peggiwolfe@bellsouth.net

dye into the veins of animals and then looking for the appearance of dye-containing cells in wounds he created at a distal site [1]. He concluded that most, if not all, of the cells appearing in the wounds came from the bloodstream, and, by implication, from bone marrow. The stained cells included not only inflammatory cells, but also cells that had a fibroblast-like morphology and were associated with thin fibrils. Therefore, Cohnheim's work raised the possibility that bone marrow may be the source of fibroblasts that deposit collagen fibers as part of the normal process of wound repair. Although Cohnheim's thesis was initially controversial, definitive evidence that bone marrow contains cells that can differentiate into fibroblasts, as well as other mesenchymal cells, has been available since the pioneering work of Alexander Friedenstein, beginning in the mid-1970s [2]. Friedenstein placed samples of whole bone marrow in plastic culture dishes, and, after several hours, poured off the cells that did not adhere to the plastic. In essence, he discarded most of the hematopoietic stem cells (HSCs) and their hematopoietic progeny that are important in the field of bone marrow transplantation. He reported that the small number of adherent cells were heterogeneous in appearance, but the most tightly adherent cells were spindle-shaped and formed foci of two to four cells. The cells in the foci remained dormant for 2–4 days and then began to multiply rapidly. After passage several times in culture, the adherent cells became more uniformly spindle-shaped in appearance. The most striking feature of the cells, however, was that they had the ability to differentiate into colonies that resembled small deposits of bone or cartilage. These cells were initially referred to as colony forming unit fibroblasts (CFU-F).

Originally, MSCs were primarily identified by their ability to: (1) adhere to tissue culture plasticware; (2) form colonies; and (3) differentiate into several different tissue types, such as adipocytes, osteoblasts, chondrocytes and rarely into other cell types [3–8]. Also, although there is no single cell surface epitope that can specifically identify MSCs, there is a pattern of markers that can help distinguish MSCs from other bone marrow cell populations, such as hematopoietic stem cells. Over the years since their initial discovery, many research laboratories have studied MSCs. However, each lab has developed their own protocols for isolation, expansion in culture, and characterization, making it difficult to compare experimental results among laboratories, leading to confusion in the field. The need for standardization of terminology and defining attributes, including surface epitopes and differentiation capacity, of MSCs has become quite clear in recent years and has led to the publication by the International Society for Cell Therapy of two position papers: "Clarification of the nomenclature for MSC: The International Society for Cellular Therapy position statement" [9] and "Minimal criteria for defining multipotent mesenchymal stromal cells. The International Society for Cellular Therapy position statement." [10]. The nomenclature position statement recommended the term "multipotent mesenchymal stromal cells" in order to move away from the term "stem" cell. The main criteria that have been established in order for stem/progenitor cells from bone marrow to be classified as MSCs are the following: (1) must be plastic-adherent when maintained in standard culture conditions; (2) must express CD105, CD73 and CD90; (3) must lack expression of CD45, CD34, CD14 or CD11b, CD79a or CD19 and HLA-DR, a HLA Class II antigen; and (4) must differentiate into osteoblasts, adipocytes and chondroblasts *in vitro*.

MSCs have become a focus of interest for use in clinical therapies for various diseases and injuries. They are considered good candidates for clinical treatments because: (1) they are easily obtained and isolated from bone marrow aspirates, either from the patient for autologous use or from normal donors for allogeneic use; (2) they are easily grown and expanded under normal culture conditions; (3) they can be genetically altered *ex vivo* to provide therapeutic proteins or correct genetic defects [11, 12]; (4) they are non-tumorigenic when grown under normal, unstressed culture conditions [13]; (5) they are part of the body's natural repair mechanism and thus home to damaged tissues to achieve repair [14–16]. Although, the exact mechanism of their repair ability is not clear, it appears they can accomplish this by several different means. These include: (1) secretion of cytokines to enhance repair [17–19]; (2) modulation of immune [20–23] and inflammatory responses [24, 25]; (3) stimulation of the proliferation of tissue endogenous stem cells [26, 27]; and (4) rescue of damaged cells, by fusion or possibly mitochondrial transfer [28, 29]. Although it is tempting to believe that because MSCs have the ability to differentiate into several different tissues types, engraftment and subsequent differentiation into tissue specific phenotypes may be a mode of rescue and repair *in vivo*, functional improvements do not correlate with transplanted MSC engraftment and differentiation in most animal models of disease [30–32].

Our laboratory has developed standardized protocols that can generate $120\text{--}200 \times 10^6$ MSCs in multilevel cell culture chambers (CCC) within approximately 2 weeks from just 1–4 ml of bone marrow aspirate. We have established procedures for CFU and multidifferentiation capabilities and have also developed panels of flow cytometry antibodies to determine surface cell markers. Also, through a National Institutes of Health/National Center for Research Resources grant (Grant # P40RR017447), we have created a center for distribution of frozen vials of standardized early passage MSCs to researchers worldwide. In addition to distributing the cells, we also provide detailed protocols and Product Specification Sheets with characterization data to the requesting scientists. This resource allows researchers from many different laboratories to study MSCs that are prepared the same way and, thus, makes data, results, and conclusions easier to compare. The protocols for MSC isolation and expansion [33], freezing and recovery [34], colony forming unit (CFU) assay [35], osteogenic, adipogenic and chondrogenic differentiation [36], and surface epitope analysis by flow cytometry [36], are presented here with slight modifications from previous publications [33–36].

2.2 Bone Marrow Procurement and Processing

2.2.1 Biohazard Safety and Universal Precautions

Although all donors are pre-screened for infectious diseases (ID) before aspirates are taken, there is always a possibility that: (1) an ID is either present in early stage and does not yet show up as positive on the screen or (2) it is an ID for which there are no tests available. Therefore, researchers should acquaint themselves with the FDA Code of Federal Regulation 29 CFR, Subsection 1910.1030 (US Department

of Labor, Occupational Health and Safety Administration, Bloodborne Pathogens). It is imperative to follow universal precautions whenever dealing with human samples, whether the samples are body fluids, cells or tissues. This includes gloves, preferably double gloves, disposable lab gowns, face shields or safety glasses and face mask. Also, there should be no eating, drinking or mouth pipetting in laboratories where processing of samples of human origin is performed. Samples should be processed aseptically in a Class II biosafety cabinet (BSC). Careful and regular cleaning with appropriate disinfecting agents should be done on all equipment used in the processing of human samples.

2.2.2 Bone Marrow Aspiration Procedure

Bone marrow aspirates are obtained from normal healthy male and female volunteer donors with informed consent under a protocol approved by the Institutional Review Board. All donors are screened using a basic panel for IDs before bone marrow aspirates are taken. The ID screen includes testing for presence of HIV, Hepatitis B, Hepatitis C, Cytomegalovirus, HTLV I/II, Syphilis and Mycoplasma. Potential donors must be negative on all tests before bone marrow aspirates are obtained. Our donors range in age from 18 to 66 years and several have donated multiple times. The eligibility criteria are normal body mass index (BMI), no physical disabilities or health problems and not pregnant. There must be 8 weeks between either a previous bone marrow donation or other medical donation before another aspirate can be taken. Labeled sterile blood drawing tubes, one per aspirate, containing heparin are sterilely preloaded with 2 ml of phenol red-free Alpha Minimum Essential Medium (α -MEM). Under local anesthesia, aspirates of 1–4 ml each of bone marrow are withdrawn from the right and left iliac crests, using a stylet-fixed sterile 16-gauge needle and a sterile syringe, rinsed prior to use with Heparin Sodium (1,000 units/ml). Each bone marrow aspirate is transferred to one of the pre-labeled, pre-filled sterile heparinized blood collection tubes. The aspirates are transported to the laboratory on cold packs and processed. The bone marrow aspirates obtained under these conditions can be held at 4°C for up to 24 h.

We have found that we can obtain just as many MSCs from a small volume (< 5 ml) of bone marrow as we can from a larger volume (\geq 5 ml). We compared the yields of the primary cultures of hMSCs (passage 0; P0) obtained from small and larger volume aspirates taken from the same donor at the same time (unpublished data). In some instances, the cultures were discarded because of slow or no growth in 7 days. This happened with both categories of aspirate, but of 23 small volume aspirates, only four were discarded, whereas of 23 large volume samples, 13 were discarded due to slow growth. The results are shown in Table 2.1.

Regardless of how discarded samples were analyzed, there is no statistical difference between small versus large volumes of aspirates. Since there is no difference in cell yields, and because bone marrow aspiration is a rather uncomfortable procedure, we decided to take the smaller volume (1–4 ml) of aspirate. The smaller volume takes less time to draw and causes less discomfort for the donor.

Table 2.1 P0 hMSCs from <5 cc and ≥ 5 cc bone marrow aspirates

Including discarded samples recorded as " 0.00×10^6 " P0 hMSCs:				
Aspirate vol	Average P0 hMSCs	SD of P0 hMSCs	N	T value, df
<5 cc	1.28×10^6	0.797	23	0.036, 44
≥ 5 cc	0.71×10^6	0.995	23	
With discarded samples left out of analysis:				
Aspirate vol	Average P0 hMSCs	SD of P0 hMSCs	N	T value, df
<5 cc	1.56×10^6	0.576	19	0.769, 27
≥ 5 cc	1.63×10^6	0.861	10	

2.2.3 Isolation and Initial Expansion of MSCs

Because of sampling variability in obtaining aspirates of bone marrow, we have found that about two-thirds of bone marrow aspirates are adequately enriched for stem/progenitor cells. The protocol, in brief, consists of isolating the mononuclear cells (MNCs) on a density gradient, plating them at high density for incubation for 4–12 days, harvesting them and then re-plating them at low density for incubation for 6–14 days. The procedures for isolation and expansion of MSCs have been developed in the Tulane Center for Gene Therapy over the last seven years. All procedures are carried out under sterile conditions in a Class 100 BSC following Universal Precautions. All media should be pre-warmed to room temperature (RT) or 37°C before use.

Fetal Bovine Serum (FBS) is an essential ingredient of culture medium for MSCs. FBS is lot-selected by requesting several lots of premium FBS from various vendors. The first stage of testing involves doing low density culture of frozen vials of P1 cells from a well-characterized MSC preparation from a single donor using the different test lots and the current lot of FBS concurrently. We use MSCs from a single donor preparation in order to remove differences in results due to donor variability. After the completion of the first stage of testing, cell counts, viability, morphology and surface epitopes by flow cytometry of the cells cultured in the different lots are compared. Only those lots of FBS which give comparable results to the current lot of FBS are selected for second stage of testing. We then do Colony Forming Unit (CFU) assay, osteogenic and adipogenic differentiation using the lots chosen from the first stage and the current lot of FBS. We then compare the second stage of testing results and pick the FBS which gives results as good as or better than the current lot we are using. If none are as good as the current lot, we see what the difference(s) are and make a determination whether to purchase one of the lots we tested or to request new lots for testing.

Preparations enriched for mononuclear cells (MNCs) are isolated by density gradient centrifugation of the bone marrow aspirates. Each bone marrow aspirate is transferred to a sterile 50 ml conical tube and then diluted to approximately 20 ml with sterile Hank's Balanced Salt Solution (HBSS) at RT and gently mixed by inversion. In a fresh 50 ml conical tube, each of the diluted bone marrow aspirates is overlaid onto 16.5 ml sterile Ficoll-Paque density gradient solution (at RT). Take

care not to disturb the interface between the Ficoll and the HBSS-MNC suspension. If the Ficoll and HBSS-cell suspension layers are admixed, the mononuclear cells will not completely separate out during centrifugation. The samples are centrifuged in a swinging bucket rotor at 450–480g for 30 min with the Brake set to “Off”. This decreases the chance of the interface layer getting mixed by the braking effect. After centrifugation, each MNC-rich “buffy coat” layer (interface between the HBSS and Ficoll layers) is collected by using a sterile transfer pipet. Remove the cells in as small a volume as possible. This enhances the removal of Ficoll by dilution. The MNC-rich buffy coat is transferred to a fresh 50 ml conical tube and resuspended in approximately 25 ml sterile HBSS (the volume ratio of diluent to sample should be at least 3:1). Gently mix by inverting the tube 3–5 times. The MNCs are then centrifuged, 1,000g for 10 min. Remove the supernatant by aspiration and resuspend the cells with 5 ml of pre-warmed Complete Culture Medium (CCM), which consists of α MEM, 16.5% FBS, and additional glutamine, 2 mM final. Although the α MEM that we use already contains L-glutamine, we add additional L-glutamine because of its instability. Antibiotics (100 units/ml of penicillin; 100 μ g/ml of streptomycin) can be added to the medium, if desired. We do not usually add antibiotics to our CCM because the presence of antibiotics can mask a low level contamination. Remove an aliquot for cell count and viability for each MNC pellet.

Before performing cell count and viability, add approximately 25 ml CCM to each 5 ml MNC suspension to give a final volume of 30 ml. Add the 30 ml of each MNC suspension to a T-175 flask with filter cap. Incubate the cells at 37°C with 5% humidified CO₂ for 24 h to allow the adherent cells to attach.

Cell count and viability can be done by flow cytometry using propidium iodide (PI) and Annexin V. Using PI and Annexin V will not only give viability, but will also indicate those cells undergoing apoptosis. We consider viable cells to be those that are both PI and Annexin V negative. Viability of the cells can also be checked using 0.4% Trypan Blue and a hemacytometer. To 250 μ l of trypan blue, add 150 μ l HBSS and 100 μ l cell suspension (dilution factor = 5). Wait 5–15 min. (If cells are exposed to trypan blue for extended periods of time, viable cells, as well as non-viable cells, may begin to take up the dye). Non-viable cells will stain blue and live cells will be unstained. Count both the blue and clear cells. Count cells in at least 5 large squares on each side of the hemacytometer and calculate number of cells per ml using the formula:

$$\frac{(\text{Total cells counted}) \times (\text{Dilution factor}) \times (10^4)}{(\text{Number of large squares counted})} = \text{Number of cells/ml}$$

$$\text{Total number of cells: } (\text{Number of cells/ml}) \times (\text{Total mls of cell suspension})$$

$$\text{Viability (\%)} : \left(\frac{\text{Total viable cells (unstained)}}{\text{Total cells (stained and unstained)}} \right) \times 100$$

Approximately 24 h later, remove the plate or flask from the incubator and remove the media and non-adherent cells by aspiration. If the non-adherent cells are not removed, hematopoietic cells may become attached and contaminate the

hMSC culture. Add 10 ml of pre-warmed 1X PBS (without Ca^{++} or Mg^{++} , pH 7.4) to the culture, rock gently to cover the entire surface area, and then remove the 1X PBS. Repeat the wash two additional times. Add 30 ml of fresh CCM to the flask and return to the incubator. Incubate the cells at 37°C with 5% humidified CO_2 for 5–12 days. Examine daily by phase microscopy to assess confluence and morphology of the cells. Every third day, remove the media, rinse the cells with 10 ml of pre-warmed 1X PBS, remove the PBS, and feed with a fresh 30 ml of CCM. Continue until the cells are between 60 and 80% confluent.

It is critical to harvest the cultures before they become confluent. We have observed decreased growth, decreased CFU, and decreased multidifferentiation on harvested confluent cultures. Levels of confluence can be difficult to estimate. MSCs can tend to grow in colonies and, even though the overall culture may not be confluent, the colonies can become quite dense and thus may start down the default differentiation pathway (bone) [11, 12], grow slowly on subsequent passage, change surface epitopes, and/or develop the flat morphology associated with older MSCs. Thus, cultures should be harvested before the colonies become too dense. In MSC cultures, it is often a balance between generating a large number of cells and keeping the stem/progenitor aspect of the cells, which could be lost if the cells become confluent in culture. In addition, it is shown that human MSCs cannot be passaged indefinitely because they lose their ability to make CFUs, multidifferentiation, and expansion.

Once the cells have reached 60–80% confluence, they should be harvested for either freezing or for further expansion. It is recommended that the cells be expanded for another passage to generate a large number of cells to develop a seed bank of early passage MSCs. The cells can be expanded in flasks, dishes or multilevel cell culture chambers (CCC), such as Nunc Cell Factories or Corning Cell Stacks. The method of expansion in flasks and CCCs will be discussed below.

At harvest, remove the media and rinse the cells gently but quickly with 30 ml PBS twice. Remove the PBS after each wash. Add 5 ml of pre-warmed sterile 0.25% Trypsin-1 mM EDTA-4 Na solution to the flask. Distribute the trypsin across the surface area of the flask and monitor the trypsinization on a microscope at room temperature. After about 2–3 min, 80–90% of the cells will have become detached. Gently tap the sides of the flask to dislodge any remaining attached cells, and add 10 ml CCM to the flask. Rock the flask back and forth to swirl the media around flask, and transfer the cell suspension into a clean 50 ml conical tube. Rinse the flask with 30 ml of CCM and combine with the cell suspension.

Centrifuge at 450–480g for 10 min at room temperature in a swinging bucket rotor with the BRAKE ON. Remove the supernatant and resuspend the cells with 1–2 ml of PBS or HBSS. Count the cells and determine viability using a hemacytometer and trypan blue or flow cytometry using Propidium Iodide (PI) and Annexin V. These cells are considered Passage 0 (P0) MSCs, the initial isolation from the bone marrow aspirate.

These cells can either be frozen or can be passaged immediately at low density (60–100 viable cells/cm²) into dishes, flasks or multilevel cell culture chambers

(CCCs) in CCM. hMSCs can usually be successfully expanded through Passage 4–5 without significant loss of stem cell phenotype.

2.3 Freezing and Recovery of MSCs

Since human MSCs are not immortal cells and can not be passaged for more than about 6 passages, it is important to maximize the use of early passage cells by freezing them down for future culture and expansion. It is a good idea to freeze down harvested P0 and/or P1–P2 MSCs and create a cell bank of as many vials of low passage MSCs as possible. We have kept hMSCs in vapor phase LN2 storage for over 4 years without loss of viability and defining characteristics.

2.3.1 Freezing Harvested MSCs for Long Term Storage

Before processing cells for freezing, prepare Freezing Medium (FM) and label appropriate number of sterile 2.0 ml cryovials. Depending on number of cells/vials to be frozen and how many vials can be aliquoted within 15–20 min, prepare either 1X FM for just a few vials (α MEM, 30% FBS, 5% DMSO, tissue culture tested, no additional L-glutamine) or, if freezing a large number vials of MSCs, prepare 2X FM (α MEM, 60% FBS, 10% DMSO, no additional L-glutamine). Filter the FM in a 0.2 μ m unit that is filter-safe for DMSO.

After the cell count and viability have been determined for the harvested cells, pellet the cells at 450–480g for 10 min. Aspirate the supernatant and gently resuspend the cell pellet up to a concentration of 1×10^6 MSCs/ml in either 1X FM (small number of cells) or in α MEM to a concentration of 2×10^6 MSCs/ml (large number of cells). Ensure that cells are resuspended completely before aliquoting into the cryovials. It is also important that the cells are not left in FM at room temperature for longer than about 20 min. DMSO can be detrimental to the cells if left in FM longer than this (Table 2.2).

If cells are in 1X Freezing Medium, pipet 1 ml of cell suspension into each cryovial. If a large of number of cells are to be frozen, pipet 0.5 ml 2X Freezing Medium into each of the cryovials first, then pipet 0.5 ml of cell suspension in α MEM into each vial. Cap vials tightly and give each vial a slight shake to mix. The cells can be frozen using either a 5,100 1°C Freezing Container (“Mr. Frosty”);

Table 2.2 Scheme for freezing vials of MSCs

Time to aliquot cells	Bring cells up in/cell conc	Add to cryovials
<15–20 min	1X FM (α MEM, 30% FBS, 5% DMSO, no additional L-glutamine)/ 1×10^6 /ml	1 ml 1×10^6 MSCs in 1X FM
≥ 15 –20 min	α MEM/ 2×10^6 /ml	0.5 ml 2X FM, 2×10^6 MSCs in 0.5 ml α MEM

Nalge) or in a controlled rate freezing apparatus. The 1°C Freezing Container uses 100% isopropyl alcohol, has space for 18 vials and freezes at a rate of approximately $-1^{\circ}\text{C}/\text{min}$ when placed in a -80°C freezer overnight.

Place the 1°C Freezing Container containing the vials of MSCs in FM in a -80°C freezer overnight and then transfer vials to the vapor phase of a liquid nitrogen (LN2) storage unit.

If using a controlled rate freezing apparatus, freeze using the following freezing profile:

- Step 1 Wait at 4.0°C
- Step 2 -1.0 C/m Sample Temperature to -40°C
- Step 3 -10.0 C/m Chamber Temperature to -90°C
- Step 4 End

Once the freezing process has halted, transfer the vials to the vapor phase of an LN2 storage unit.

2.3.2 Recovery of Frozen MSCs

Before removing vials of MSCs from LN2 storage for recovery, for each vial to be recovered, add 30 ml CCM to a 15 cm diameter plate. It is best to label each plate with the date, sample number and “Passage # Recovery”. For instance, if recovering P0 cells, label the plate “P0 Recovery”. To recover MSCs that have been frozen in vials and stored in LN2, remove vial(s) from LN2 storage unit, spray well with 70% ethanol, and immediately place in a 37°C waterbath. If the LN2 unit is some distance away from the waterbath, transfer the vial(s) onto dry ice to transport to the waterbath. Leave the vial(s) in the waterbath until there is just a small piece of ice remaining in the vial. Using a 5 ml sterile pipet, immediately add the thawed cells to the plate by dripping the cell suspension in a spiral over the surface of the dish to evenly distribute the cells. Do not be too forceful with the pipetting in order not to shear the cells or cause bubbles. Using the same 5 ml pipet, remove 1.0 ml of media from the plate and add it to the vial to wash out any remaining cells and then transfer that 1.0 ml back into the 15 cm plate.

Place the plate(s) into the incubator at 37°C with 5% humidified CO_2 at least overnight and preferably for 24 h. At the end of the incubation time, remove CCM with aspiration. Add 20 ml 1X PBS (without Ca^{++} and Mg^{++}) to plate to wash off any residual CCM containing FBS. (Since FBS can neutralize trypsin, it should be removed before the addition of trypsin). Remove PBS with aspiration. Add 3 ml 0.25% Trypsin-1 mM EDTA·4 Na solution to the plate. Start monitoring cell detachment immediately using an inverted microscope. When cells are about 90% detached, add 5 ml CCM to inactivate the trypsin. Do not let trypsin go beyond 5 min. If cells are still not detached within 5 min, trypsin may be old or has lost activity.

Transfer cell-trypsin-CCM solution to a sterile 50 ml conical tube. Add 10 ml CCM to 15 cm plate to wash off any remaining cells and transfer that to the 50 ml conical tube containing the neutralized trypsin-cell suspension. Centrifuge at 450–480g for 10 min.

Remove the supernatant and gently resuspend the cells with 1–2 ml of CCM. Count the cells with a hemacytometer and trypan blue or other method, such as Annexin V and PI using a flow cytometer.

2.4 Expansion of Harvested MSCs in Flasks or Cell Culture Chambers (CCCs)

After harvest of either P0 MSCs (initial isolation), early passage (P1 or P2) low density MSCs cultures or the recovery plate of early passage MSCs from frozen vials, the cells can then be expanded to fairly large numbers in flasks, plates or multilevel cell culture chambers (CCCs). This can be done by plating many tissue culture flasks or plates at low density (60–100 cells/cm²).

The procedure for expansion in plates or flasks is similar to the isolation culture to obtain hMSCs. However, instead of starting with the MNC fraction from Ficoll, harvested cultured or recovered cells are plated at low density in flasks or dishes.

2.4.1 Low Density (LD) Expansion of hMSCs in Plates or Flasks

To expand the cells by plating at an initial density of about 60–100 cells/cm² in a 15 cm dish or T175 flask, dilute 0.1 ml of harvested cell suspension to a concentration of about 10,000 viable cells per ml. For example, if the cell count and viability indicates concentration is 500,000 viable cells/ml, dilute 0.2 ml in 9.8 ml of CCM = 10,000 cells/ml. Add 24 ml fresh CCM to the 15 cm dish (or 29 ml to T175 flask), and then about 9,000 (10,500 for T175 flask) of the diluted viable cells. For example, if the diluted sample contains 10,000 viable cells/ml, add 0.9 ml of the cell suspension (1.05 ml for T175 flask). Every 3 days, remove spent media with gentle aspiration and replace with fresh CCM (25 ml for 15 cm² plate, 30 ml for T175 flask).

Monitor cells by phase microscopy. When they have reached 60–80% confluence, usually in 7–10 days, remove medium, wash cells with 10 ml PBS twice, aspirate and discard the PBS after each wash. Add 3–4 ml for a 15 cm² plate, 5 ml for a T175 plate of 0.25% trypsin/1 mM EDTA·4 Na solution that was pre-warmed to 37°C and incubate for 2–5 min at RT. Immediately monitor lifting of the cells carefully by phase microscopy on an inverted microscope. Stop the incubation in trypsin/EDTA when about 90% of the cells have been lifted. The time needed can vary with the lot of trypsin/EDTA, so monitor detachment closely. Tap sides of dish/flask to help loosen the cells.

Stop the incubation with trypsin/EDTA by adding 6–8 ml (10 ml for T175 flask) CCM. Gently swirl the media around plate, aspirate detached cells and transfer them

to a sterile 50 ml plastic conical centrifuge tube. The FBS in the CCM stops action of trypsin. Wash the plate with 15 ml CCM (30 ml for T175 flask), aspirate and add this wash to the tube containing the detached cells.

Centrifuge for 10 min at 450–480g at room temperature with BRAKE ON. Aspirate and discard the supernatant. Add 1.0 ml CCM to cell pellet. Resuspend cells by gently drawing cells up and down in a 5 ml pipette to disperse clumps. These cells are then counted and viability determined. These cells can be either used for in vitro or in vivo experiments, frozen for future use, or passaged into new plates/flasks, if they are early passage cells (P1–P4).

2.4.2 Low Density Expansion in Multilevel Cell Culture Chambers (CCCs)

Another way to generate large numbers of cells is to expand P0 MSCs in large cell growth surface vessels, such as multilevel cell culture chambers (CCCs). CCCs are used for large-scale cell culture and production of biomaterials such as vaccines, monoclonal antibodies and interferon. CCCs provide a large amount of growth surface in a small footprint with easy handling and low risk of contamination. They are designed for static cultures and can be used for anchorage dependent cells or cell suspensions. There are two major types of CCCs – Nunc Cell Factories (1, 2, 4, and 10 levels) and Corning CellSTACK[®] (1, 2, 5 and 10 levels) CCCs with multiple levels, assembled by sonic or electronic welding, that are treated to produce a surface for enhanced cell attachment. The chambers are connected by two port tubes for input and output of reagents, etc. The tubes have openings located in the upper half of each chamber. By having these openings high in the chamber, they are above media level during incubation. Turning the CCC on its side puts the Fill/Drain port tube at the lowest point of the unit. In this position, the unit can be filled or drained. See Fig. 2.1.

There are websites for both of these products that have a great deal of information and instructions about the CCCs. For Nunc Cell Factories, the website is: <http://www.nuncbrand.com/en/page.aspx?ID=304>. For Corning CellSTACKS[®],

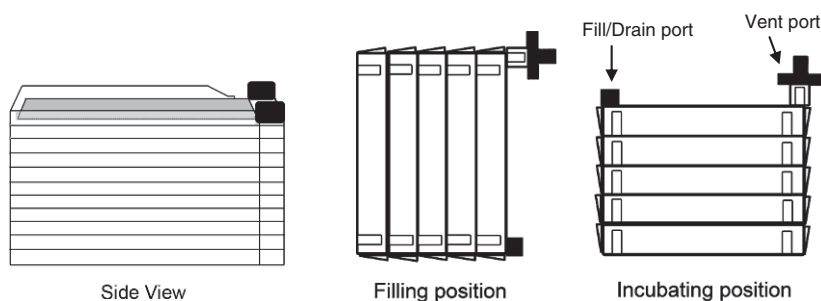


Fig. 2.1 Generic diagram of a 10 level cell culture chamber (CCC)

Table 2.3 Culture growth surface area for CCCs

Number of levels	Nunc cell factory	Corning CellSTACK
1	632	636
2	1,264	1,272
4	2,528	NA
5	NA	3,180
10	6,320	6,360

the website is: http://www.corning.com/lifesciences/products_services/features/cstackportal.asp

See Table 2.3 for the different culture growth areas of the Nunc and Corning multilevel CCCs:

There are two basic methods for loading, feeding and harvesting the CCCs – an Open System and a Closed System. Because the Closed System is more expensive and involves specialized equipment (tube welders and sealers) and special consumable supplies (transfer bags, couplers, spikes, plasma transfer sets, septum caps, welding wafers, etc.), this chapter will not cover this particular method of culture in CCCs. The less expensive, but more hands-on method is the Open System, which involves filling and draining the CCC using either a large sterile glass aspirator bottle for CCCs with 10 levels or a pipet or reagent bottles for CCCs with 1–5 levels. The large glass aspirator bottle has a bottom opening port that accepts tubing that then connects to the CCC. In addition, we have found that we can increase the cell growth by either pre-incubating the CCC for 48 h in the culture incubator or by actively gassing the multilevel (4, 5, and 10) CCCs for 20 min right before they are seeded with MSCs. See Fig. 2.2.

There are CCCs that are specially made for active gassing. This requires a variable air flow pump, that can be purchased from various scientific product vendors

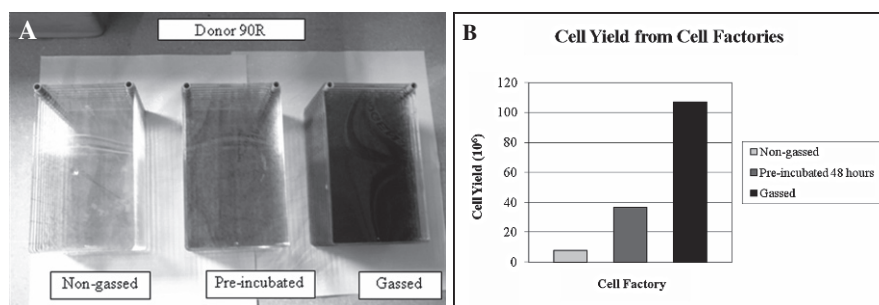


Fig. 2.2 Yield of MSCs from CCCs under Different Aeration Conditions. (A) CCCs that were cultured under different aeration conditions: not gassed, not pre-incubated (Non-gassed), pre-incubated in incubator for 48 h (Pre-incubated), and gassed for 20 min at 0.5 L/min (Gassed) and then cultured until the first CCC reached 60–80% confluence. When the first CCC was ready for harvest, all three CCCs were washed with PBS and then stained using Crystal Violet and then photographed. (B) Indicates cell counts from another three CCCs that were cultured with the same cell preparation under identical conditions and at the same time as the stained CCCs

Table 2.4 Volume of media for CCCs

Number of levels	α MEM (ml)	FBS (ml)	200 mM L-glutamine (ml)
1	100	20	1.2
2	200	40	2.4
4	400	80	4.8
5	500	100	6
10	1,000	200	12

or, instead, a variable flow aquarium pump can be used, that can deliver between 0.5 L and 2 L/min of air. This can be fitted with a flow meter to monitor rate of air flow into the CCC. This section describes how to perform cell culture in multilevel CCCs using the Open System. This is a description for 10 level CCCs, which can be supplemented by using the instructions provided by the manufacturer, and can be downloaded from the product website. Only minor modifications are needed to culture in 1, 2, 4, or 5 level CCCs.

If active gassing of the CCCs is not possible, 48 h before seeding CCCs, place them in the cell culture incubator with 0.2 μ m air vent filters or vented caps on both ports of the CCC. Before seeding a 10 level CCC, be sure 2 L glass aspirator bottle with tubing, connector and clamp have been autoclaved and are sterile. Be sure tubing end with connector and bottle mouth are covered with foil when autoclaving.

In order to monitor growth in a CCC with more than 1 level, an inverted phase microscope fitted with a Super Long Working Distance Condenser (SLWDC) is necessary. If microscope with a SLWDC is available, the growth on the bottom level of a multilevel CCC can be monitored directly without the preparation of a control plate or control CCC. If there is no phase microscope with a SLWDC available, a control plate or flask must be made in order to monitor the approximate cell growth in the CCC, using a plate or flask from the same manufacturer with the same culture surface as the multilevel CCC. The other option, which may be preferable, is to prepare a control single layer CCC, from the same manufacturer with the same culture surface and plated at the same density as the multilevel CCC. This control plate/flask or CCC is used to monitor the MSC culture microscopically to estimate MSC growth in the CCC.

Depending on the number of levels of CCC used, determine volume of CCM and number of cells needed for each CCC. See Tables 2.4 and 2.5. Before beginning culture, prepare media.

Table 2.5 Number of cells needed for seeding CCCs

Number of levels	Nunc cell factory		Corning CellSTACK	
	60 cells/cm ²	100 cells/cm ²	60 cells/cm ²	100 cells/cm ²
1	37,920	63,200	38,160	63,600
2	75,840	126,400	76,320	127,200
4	151,680	252,800	NA	NA
5	NA	NA	190,800	318,000
10	379,200	632,000	381,600	636,000

Filter CCM using the appropriate size of 0.2 μm sterile filter unit. Place in 37°C waterbath until use. Before adding cells to CCCs, hook the variable air flow pump to the port on the CCC using tubing fitted with an in-line 0.2 μm air-vent filter (accessory for CCC) filter. Be sure to thoroughly wipe the CCC, the pump and the outside of the tubing and flush the inside of the tubing with 70% alcohol before placing them into the incubator. Place the CCC and the pump and tubing inside the incubator and turn the pump on. Actively gas for 20 min at the appropriate rate (0.5 L/min for 10 level Nunc Cell Factories and 0.1 L/min for 10 level Corning CellSTACKs).

From harvested cell suspension, withdraw the necessary volume to give the appropriate number of cells needed to seed each CCC with a pipettor (i.e. 100–1,000 μL) at a density of 60–100 cells/ cm^2 culture surface area and dispense the cells directly into bottle of pre-warmed 1.2 L CCM. If a control culture needs to be prepared for CCC monitoring, be sure to leave enough cell suspension to prepare cells for the control plate, flask or single level CCC. Replace cap and mix by gently inverting, taking care to avoid bubbles.

To prepare a control plate or flask, to 10 ml (for 10 cm diameter plate, with a culture area of approximately 55 cm^2) or 15 ml (for T75 flask) CCM, add cells from harvested cell suspension to give a seeding density of 60–100 cells/ cm^2 (about 3,300–5,500 cells for 10 cm plate and 4,500–7,500 cells for T75 flask) and add this to the control plate or flask. To prepare a control single level CCC, to 100 ml CCM, add cells from the harvested cell suspension to seed at 60–100 cells/ cm^2 with a sterile pipette and carefully add to the single level CCC with a 100 ml pipette (See Table 2.5 for number of cells needed to seed a single level CCC).

Making sure the clamp on the tubing is closed, add the CCM containing the MSCs to the sterile glass aspirator bottle fitted with the tubing, tube connector and clamp. Mix thoroughly by swirling, taking care to avoid bubbles.

For a complete detailed description of procedure, please refer to the manufacturer's instructions for the specific CCC being utilized. In general, the procedure is as follows: To load the CCC, attach the tubing from the aspirator bottle via the connector to the Fill/Drain port on the left side of the CCC. Lay the CCC on its side and place the aspirator bottle of CCM containing the cells above the CCC. Open the clamp and let the cells drain into the CCC by gravity. Once filling is complete, rotate the CCC so that the filling and venting ports are up (stand on its end) The medium should be evenly dispersed throughout the CCC, but it is normal for the medium level in the bottom chamber to be slightly higher. Remove the tubing from the Fill port and replace with either a vented cap or a filter. Lower the CCC to horizontal position and, if necessary, rock it gently side-to-side and back-to-front to evenly wet all levels of the CCC. When transporting CCC, hold it slightly tilted with the ports up.

Carefully, place the CCC (and control vessel, if applicable) into the incubator, ensuring that the CCC is level with equal distribution of the media and that there is clearance for the filters. Incubate the CCC(s) (and control cultures, if applicable) at 37°C with 5% humidified CO_2 for 5–14 days. Examine the CCC(s) and the control culture, if applicable, daily by phase microscopy.

Every third day, remove the media from CCC by draining it through the Fill/Drain port using either the aspirator bottle with tubing and connector or by carefully pouring the spent CCM into a large beaker. Feed the CCC with 1.2 L of fresh, pre-warmed CCM, following CCC filling instructions mentioned above. Rotate CCC on end with ports up (as with initial filling) and then down to horizontal position and rock it gently side-to-side and back-to-front to evenly wash all levels of the CCC. Feed a 10 cm diameter control plate, the T75 flask or the control CCC with 12 ml fresh CCM, 15 ml fresh CCM or 100 ml fresh CCM, respectively. Continue incubation of CCC (and control plate/CCC) culture, feeding every third day, until the cells are between 60 and 80% confluent.

When cells have reached 60–80% confluence, either determined directly from examining the CCC itself or by using the “control” plate/CCC as an estimate, harvest the CCC (and the control plate/CCC). Be sure to have several aspirator bottles with tubing, tubing connectors and clamps sterilized.

To harvest the CCC, drain culture media from CCC into a 2 L waste beaker. (To harvest the control plate, remove culture media from plate by aspiration or by pipetting and discarding into the 2 L waste beaker or remove culture media from CCC by pouring off CCM into the waste beaker). Add 200 ml warmed PBS (without Ca^{++} and Mg^{++}) to CCC using the sterile aspirator bottle with tubing and connector. For the control plate, add 5 ml PBS to a 10 cm diameter dish (10 ml PBS to a T75 flask) or for control CCC, add 30 ml PBS, using a pipette. Rotate CCC to upright position and then lower it to horizontal position and rock it gently side-to-side and back-to-front to evenly wash all levels of the CCC.

Drain PBS from the CCC into the 2 L waste beaker. Remove PBS from control plate using aspiration or a pipette or remove PBS from control CCC by carefully pouring it into waste beaker.

Add 200 ml of pre-warmed 0.25% Trypsin in 1 mM EDTA to CCC using aspirator bottle and tubing. For control plate, add 3 ml trypsin/EDTA to 10 cm diameter dish (or T75 flask) or for the control CCC, add 15 ml trypsin using a pipette. Place CCC (and control plate/CCC) in 37°C CO₂ incubator for 3–5 min. After 2–3 min, monitor cell detachment microscopically either on the CCC itself or by using the control plate/CCC as a monitor. When about 90% of the cells are detached, stop the reaction.

Add 200 ml pre-warmed CCM to the CCC using the aspirator bottle and tubing. Rotate the CCC to stand-up position and then to horizontal and rock it gently side-to-side and back-to-front to evenly cover all levels of the CCC. For control plate, add 6 ml pre-warmed CCM to 10 cm diameter dish (or T75 flask) or add 15 ml CCM to control CCC.

Drain the contents of CCC (cells in CCM-neutralized trypsin) into a sterile container with a 1 L capacity. Transfer the contents of the control plate to a 15 ml plastic sterile conical tube or transfer contents of the control CCC to a 50 ml conical tube.

Add 200 ml CCM to CCC using aspirator bottle and tubing. Rotate the CCC to upright and then to horizontal position and rock it gently side-to-side and back-to-front to evenly cover all levels of the CCC. For control plate, add 3 ml CCM to a 10 cm diameter dish (or T75 flask) or add 15 ml CCM to a control CCC.

Drain CCM into the 1 L sterile container containing the neutralized trypsin-cell suspension. For control plate, add CCM wash to 15 ml conical tube containing harvested cells. For control CCC, add CCM wash to 50 ml conical tube containing harvested cells.

For cell suspension from harvested CCC, distribute equally into four 175–200 ml sterile plastic conical tubes. Centrifuge at 480g for 10 min at room temperature in a swinging bucket rotor with the BRAKE ON. For control plate, centrifuge the 15 ml conical tube containing the cell suspension with a balance tube or for control CCC, centrifuge 50 ml conical tube containing harvested cells with a balance tube at these parameters.

Remove and discard the supernatant and resuspend each pellet from the harvested CCC in 5 ml of HBSS without Ca^{++} and Mg^{++} . Resuspend the pellet by drawing the cell suspension gently into and out of the pipet 10–15 times. Repeat for the remaining tubes. For control plate, remove supernatant from 15 ml conical tube or for control CCC, remove supernatant from 50 ml conical tube. Add 1 ml HBSS and resuspend cell pellet by gently pipetting.

Combine the contents of the four 200 ml tubes into one. Rinse each tube with 25 ml of HBSS and combine with the cell suspension.

Centrifuge (with a balance tube) at 480g for 10 min at room temperature in a swinging bucket rotor with the BRAKE ON.

If a centrifuge with carriers that can hold the 200 ml tubes is not available, an alternative method is to distribute the cell suspension over 50 ml conical tubes.

- a. Pipet 50 ml aliquots of mixed cell suspension into twelve (12) 50 ml conical centrifuge tubes.
- d. Centrifuge (Brake ON) at 480g, RT for 10 min.
- c. Aspirate supernatant. Add 1 ml HBBS to each tube and resuspend cells. Combine all cell suspensions into one 50 ml conical tube.
- d. Wash each tube with 2 ml HBBS and add the washes to the 50 ml conical tube containing the cells.
- e. Centrifuge (with balance tube) at 480g, RT for 10 min with Brake ON.

Remove the supernatant. Resuspend the cells in a small volume (typically 2–5 ml) of CCM (if continuing to expand) or HBSS. Count the cells with a hemacytometer and Trypan Blue or other method as described above in Section 2.2.3. If the CCCs were seeded using P0 MSCs, then, on harvest, these are considered P1 MSCs. If CCCs were seeded using recovered (P#) MSCs, then, on harvest, the cells are considered (P#+1) MSCs. For example, if P1 cells were recovered and used to seed CCCs, on harvest from the CCCs, the cells would be considered P2 cells.

At this point the cells can be: (1) used for experimental purposes, (2) further expanded at a seeding density of 60–100 viable cells/cm², or (3) cryopreserved as described above in Section 2.3.1.

Assess hMSC characteristics and quality by: Colony Forming Units (CFU), FACs analysis of selected cell surface markers, and the ability of hMSCs to differentiate to osteoblasts, adipocytes, and chondroblasts *in vitro*.

2.5 Characterization of MSCs – Colony Forming Unit Assay and Differentiation

Two of the main hallmarks of MSCs are their ability to form colonies from a single cell [35] and to differentiate into multiple cell lineages, such as osteocytes [37–39], adipocytes [37, 40, 41], and chondrocytes [37, 42]. When cultured under defined conditions, the cells can be induced to differentiate into numerous other cell types. However, if hMSCs cultures are allowed to become over-confluent in CCM, some of the cells will progress down their default pathway and exhibit characteristics of osteocytes or adipocytes, as evidenced by production of mineral or presence of lipid containing vacuoles, respectively. The protocols given here are for the colony forming unit (CFU) assay and the basic differentiation procedures for inducing osteogenesis, adipogenesis and chondrogenesis in cultures of hMSCs.

2.5.1 Colony Forming Unit (CFU) Assay Procedure

Harvest low density culture plates when cells are between 60 and 80% confluent. Determine cell count and viability using a hemacytometer and trypan blue or using a flow cytometer with Annexin V and PI staining of the cell suspension.

Serially dilute the cell suspension to obtain 100 viable cells in about 500 μ l. Add 12 ml of sterile CCM to each of three 10 cm diameter dishes (about 60 cm^2 culture area). Add the 100 viable cells to each dish by dripping the cell suspension in a spiral over the surface of the dish to evenly distribute the cells. Place the cells in a 37°C incubator with humidified 5% CO_2 for 14 days without feeding. After 14 days, remove the media, wash the cells with 10 ml 1X PBS and discard the PBS. Add 5 ml 3.0% Crystal Violet in 100% methanol to each dish. Swirl the solution around to cover bottom of dish. Incubate for 5–10 min at room temperature. Gently flush the dish with tap water until background is clear. Examine dish under an inverted microscope to verify cell staining and, using the naked eye, count the number of colonies that are 2 mm or larger in diameter in each dish. Calculate % CFU for each plate:

$$\frac{\text{Total Number of Colonies (> 2 mm) Counted}}{\text{Total cells plated (100 in this case)}} \times 100 \text{ for each dish} = \% \text{ CFU}$$

To determine “average % CFU” for the preparation, add up the % CFU for each of the three dishes and divide by 3.

The % CFU is an important characteristic of these cells and should be recorded at each cell passage. The % CFUs for early passage hMSCs expanded at low density should be greater than 40%. However, the number of CFUs decreases as the cultures expand from low density cultures enriched for RS-MSCs to high density cultures enriched for SR-MSCs [43]. Plating only 100 cells per dish in this assay provides

enough cells for analysis and increases the probability that the colonies formed are derived from single cells.

2.5.2 Adipogenesis and Osteogenesis Differentiation Procedure

We perform osteogenic and adipogenic differentiation assays in 6 well tissue culture plates. The 6 well plates allow for 2 wells each for control, osteogenic and adipogenic cultures. See Fig. 2.3 for layout of plate.

Label the plates with sample number, passage, date and any other pertinent information. Add 2 ml CCM to each well. Add 100,000 cells in a volume of approximately 100–200 μl ($\sim 10,000$ cells/ cm^2). If you have an insufficient number of cells, a lower density can be substituted as long as each well receives the same number of cells. Incubate cells in humidified incubator at 37°C with 5% CO_2 . Every 3–4 days before the cells reach 100% confluency, aspirate media from each well, rinse with 2 ml of PBS, and add 2 ml of fresh CCM. Return to incubator. After the cells have reached between 70 and 80% confluency in 2–8 days, aspirate media from each well and rinse each well with 2 ml of PBS. Do not change to differentiation media before cells have reached 70% confluency or they will not differentiate and do not let the cultures attain greater than 85% confluency.

Add 2 ml CCM to the 2 control wells for no differentiation. To the 2 osteogenic differentiation wells, add 2 ml Osteogenic Differentiation Media (ODM), which

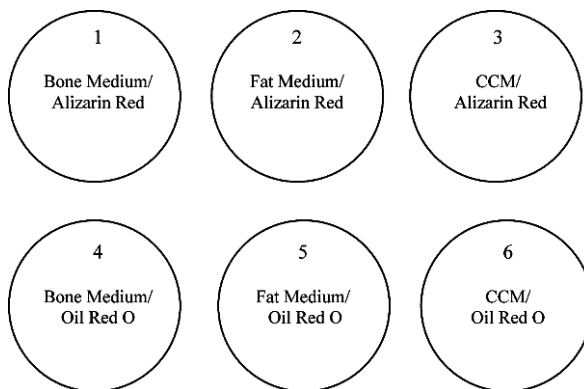


Fig. 2.3 Suggested Layout of 6 well plate for differentiation of MSCs. After MSCs become 60 and 80% confluent in CCM, induce differentiation with specific media. The first column of wells (1 and 4) gets MSCs + ODM (bone medium), second column of wells (2 and 5) get MSCs plus ADM (fat medium) and the third column of wells (3 and 6) gets MSCs plus CCM (control). The first row of wells (1, 2 and 3) gets rinsed with DI water, and then stained with Alizarin Red S. The second row of wells (4, 5 and 6) gets rinsed with PBS and then stained with Oil Red O. Alizarin Red staining for osteogenesis should be strong in Well 1 and absent to light in wells 2 and 3. Oil Red O staining for adipogenesis should be strong in Well 5 and absent to light in the wells 4 and 6. This arrangement allows for controls of media and staining specificity [36]

consists of 192 ml CCM with 10 nM dexamethasone, water soluble (200 μ l of 1:100 dilution of 1 mM stock solution in DI water); 20 mM β -glycerolphosphate (8 ml of 0.5 M stock in CCM); 50 μ M L-ascorbic acid 2-phosphate (200 μ l of 50 mM stock solution in DI water) to the 2 wells for osteogenic differentiation. To the 2 adipogenic differentiation wells, add 2 ml Adipogenic Differentiation Media (ADM) which consists of 200 ml CCM; 0.5 μ M dexamethasone (100 μ l of 1 mM stock in DI water); 0.5 μ M isobutylmethylxanthine (20 μ l of 5 mM stock in methanol); 50 μ M Indomethacin (333 μ l of 30 mM stock in methanol) to the 2 wells for adipogenic differentiation. All media should be filtered through a 0.2 μ m sterile filter unit and stored at 4°C for the duration of the differentiation culture period.

Continue to incubate cells in humidified incubator at 37°C with 5% CO₂. Every 3–4 days, for up to 21 days, wash each well gently with 2 ml PBS and replace the appropriate differentiation or control media. Monitor progress of differentiation using the inverted phase microscope. As the osteogenic cultures start to produce mineral, the cultures will appear cloudy or contaminated. It is just the presence of the externalized mineral that gives it that appearance. The mineral can be verified by focusing on the floating material in culture with the microscope on 20X power. If there is no Brownian movement noted, then this is probably not bacterial contamination.

2.5.3 Staining Osteogenic and Adipogenic Differentiation Plates

At the end of 21 days, or when definitive mineralization and fat deposition is evident, the wells should be stained with Alizarin Red S to visualize bone/mineral and Oil Red O to visualize fat. Alizarin Red S (1% solution) consists of 1 g Alizarin Red S (Sigma) in 100 ml DI water. Adjust pH of solution to 4.1–4.3 using 0.1% ammonium hydroxide. Filter stain through sterile filter unit and store tightly capped at room temperature (RT) protected from light for up to 3 months. Oil Red O working stain is made from a 0.5% stock solution which is 2.5 g Oil Red O (Sigma) in 500 ml isopropyl alcohol. Dissolve completely. Store in a tightly capped bottle at RT protected from light for up to 3 months. Oil Red-O Working Stain should be made fresh for each use. The Oil Red O working stain is three parts 0.5% Oil-Red-O Stock and two parts PBS. Mix and wait 10 min. Filter stain through sterile filter unit. Wait 10 min before use. Discard any unused stain.

Aspirate media and rinse each well with 2 ml PBS. Add 2 ml of neutral buffered formalin (NBF) to each well and incubate for 1 h at room temperature. Aspirate NBF from each well and discard. Rinse one control, bone and fat well (top row) to be stained with Alizarin Red S with 2 ml of DI water and aspirate. Rinse one control, bone and fat well (bottom row) to be stained with Oil Red O with 2 ml of PBS and aspirate.

Add 2 ml of Alizarin Red S to each the 3 wells across one row: 1 non-differentiated well (negative control), 1 fat well (specificity control) and 1 bone

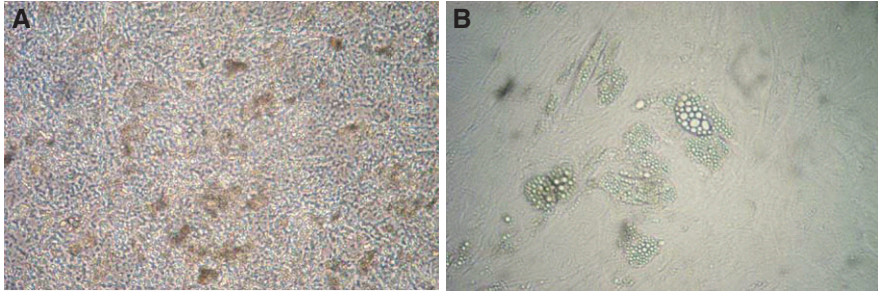


Fig. 2.4 Microscopy of Unstained Bone and Fat Differentiation Cultures. **(A)** Mineral deposition in MSCs in culture in osteogenic medium as seen under phase contrast. *Dark areas* indicate mineral that has been manufactured by the cells. Mag: 10X. **(B)** Evidence of fat formation in MSCs cultured in adipogenic medium as seen under phase contrast. *Bright round circles* are fat globules within the cell. Mag: 10X [36]

differentiated well for actual sample. Add 2 ml of Oil-Red-O to each of the 3 wells across one row: 1 non-differentiated well (negative control), 1 bone differentiated well (specificity control) and 1 fat well for actual sample. Incubate for 20 min at room temperature and then aspirate.

Rinse the wells stained with Alizarin Red S with 2 ml of DI water and aspirate. Repeat two times or until background is clear. Rinse the wells stained with Oil Red O with 2 ml of PBS and aspirate. Repeat two times or until background is clear. Add a final 2 ml of DI water to the Alizarin Red S stained wells (Wells 1–3). Add a final 2 ml of PBS to the Oil Red O stained wells (Wells 4–6).

Examine plate under inverted microscope for evidence of fat and/or bone differentiation. Negative control wells should not stain at all. Also, fat differentiated cells should not stain with Alizarin Red S and bone differentiated cells should not stain with Oil Red O. See Figs. 2.4 and 2.5 for illustration of osteogenic and adipogenic cultures, unstained and stained.

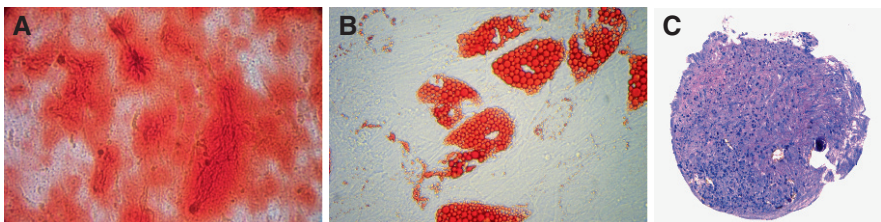


Fig. 2.5 Microscopy of Stained Bone, Fat and Cartilage Differentiation Cultures. **(A)** Mineral deposition by MSCs cultured in osteogenic medium indicating early stages of bone formation. Stained with Alizarin Red S. Mag: 20X. **(B)** Fat globules seen in MSC culture grown in adipogenic medium indicating differentiation into adipocytes. Stained with Oil Red O. Mag: 20X. **(C)** MSC micromass pellet, grown in chondrogenic medium and stained with Toluidine Blue Na Borate. Mag: 10X [36]

2.5.4 Chondrogenesis Differentiation

MSCs can be induced to differentiate into chondrocytes by utilizing micromass cultures [44]. There are two media needed: Chondrogenic Media without Cytokines (CMwoC) and Chondrogenesis Media with Cytokines (CMwC). CMwoC consists of 500 ml bottle of high-glucose DMEM (GIBCO) supplemented with: 50 $\mu\text{g/ml}$ L-ascorbic-2-phosphate (Sigma; 500 μl of 50 mg/ml stock in DI water); 40 $\mu\text{g/ml}$ L-proline (Sigma; 500 μl of 40 mg/ml stock in DI water); 100 $\mu\text{g/ml}$ sodium pyruvate (Sigma; 500 μl of 100 mg/ml stock in DI water); 5 ml ITS⁺ Culture Supplement (B&D Biosciences) which consists of 6.25 $\mu\text{g/ml}$ insulin, 6.25 $\mu\text{g/ml}$ transferrin, 6.25 ng/ml selenious acid, 1.25 mg/ml bovine serum albumin, 5.35 mg/ml linoleic acid. CMwoC can be stored for the duration of the chondrogenic culture at 2–8°C.

CMwC is made using the needed volume of CMwoC supplemented with 10 ng/ml rhTGF- β 3 (R&D Systems; from 10 $\mu\text{g/ml}$ stock in 4 mM HCl); 10^{-7} M dexamethasone (Sigma; from 1 mM stock in DI water); 500 ng/ml BMP-2 (rhBMP-2, CHO-derived, R&D Systems) OR BMP-6 (rhBMP-6, CHO-derived R&D Systems) from 10 $\mu\text{g/ml}$ stock in PBS.

Before harvesting the cells, place a clean, autoclaved test tube rack that is sufficiently large to hold all of the 15 ml conical tubes for chondrogenesis cultures and to allow an empty space on all four sides of each tube into the incubator. Never remove the rack from the incubator during the course of the assay. Use another clean rack to transport the tubes between the incubator and hood.

To begin chondrogenesis cultures, harvest low density MSC cultures when 70–80% confluent. Cells which are lifted during early to mid-log of growth or those that have reached 100% confluence will not differentiate as well, if at all.

Wash harvested MSCs in 10 ml PBS (centrifuge at 450–480g for 10 min at RT) and resuspend the cell pellet in 1.0 ml CMwC. Do cell count and viability. Adjust to a concentration to 400 viable cells/ μl with CMwC. For example, if cell count of 1 ml of cell suspension gives 1,000,000 cells/ml, add 1.5 ml CMwC to give 2.5 ml of 400 cells/ μl . Thus, 500 μl should contain 200,000 cells.

Transfer approximately 200,000 MSCs in 500 μl CMwC into a 15 ml conical polypropylene tube. Screw caps on tightly while in hood (sterility is of the utmost importance as no antibiotics are added to the media). Centrifuge the 15 ml conical tube at 450g for 10 min. DO NOT resuspend the pellet and DO NOT aspirate the medium.

Place the conical tubes into the cell culture incubator, which is humidified at 37°C with 5% CO₂. Loosen the caps on the tubes so that they are simply placed on the top of the tubes, without screwing on, allowing for full air exchange. Be sure to screw the caps on tightly before removing the conicals from the incubator.

Change media every 3–4 days by using a P-1000 pipette to remove the old media and add fresh CMwC, paying close attention to detach pellet from plastic with each media change. Take care not to aspirate the pellet when removing old medium. Pellets should be visible within 24 h.

At 21 days, chondrocyte pellet should be 2–4 mm in diameter with BMP-2 or 1–2 mm with BMP-6. The chondrocyte pellet may be fixed with NBF, embedded in

paraffin, cut into 5 μm sections onto slides, and stained with 1% toluidine blue/1% sodium borate.

2.5.5 Preparing and Staining Paraffin Sections of Chondrogenesis Pellets

Deparaffinize the pellet in Clear-rite 4 times for 5 min each at RT. Hydrate in descending grades of alcohol from 100, 95%, dH₂O, 2 \times 1 min each at RT. Incubate slides in 1% Toluidine Blue/1% Na Borate solution for 5 min at RT [**Working:** 1 g of Toluidine Blue (Richard-Allan Scientific); 1 g of Sodium (Na) borate (Sigma); 100 ml distilled H₂O (dH₂O). First, make 1% Na Borate solution (1 g/100 ml dH₂O). Dissolve completely until water is clear. Once clear, add 1 g Toluidine Blue, dissolve completely. Pre-filter using Whatman #1 filter paper and then filter using sterile filter unit. Store tightly capped in an amber bottle for up to 1 month at RT]. Rinse the slides in several changes of tap water, until water becomes clear. Rinse slides in dH₂O for 1 min at RT. Dehydrate sections in ascending grades of alcohol from 95 to 100%, 2 times for 1 min each at RT. Clear in four changes of Clear-rite, 1 min each, at RT. Coverslip in Permount mounting media. Examine by microscopy. To assess chondrogenesis staining, purple color indicates the presence of proteoglycans (cartilage) and the blue color indicates negative for proteoglycans. See Fig. 2.5C for stained chondrogenesis pellet.

2.6 hMSC Surface Epitope Analysis by Flow Cytometry

Although there is still no single specific antigen that will define hMSCs, a combination of surface epitopes can help define MSCs and distinguish them from hematopoietic stem cells. The “Minimum Criteria for Multipotent Mesenchymal Stromal Cells” position paper published in Cytotherapy in 2006 by the ISCT listed the following criteria for surface markers in order for cells to be classified as “MSCs”: Greater than 95% of the MSC population must express CD105, CD73 and CD90, as measured by flow cytometry. Additionally, these cells must lack expression (<2% positive) of CD45, CD34, CD14 or CD11b, CD79a or CD19 and HLA DR, an HLA Class II antigen.

The utility of flow cytometric analysis of hMSCs for surface proteins lies in determining the type of cells obtained and establishing continuity of results among cell preparations and over time in culture. Due to the large number of antibodies needed to evaluate hMSCs, a very large number of cells is needed to complete the procedure. This problem can be alleviated in part using a panel of antibodies in each analysis thus reducing the number of cells needed from 1 million to 500 thousand per panel. The number of antibodies that can be mixed is determined by the type of flow cytometer, the number of channels that instrument has available and the cross-reactivity of the antibodies with each other. The list of surface antigens that can be examined on hMSCs is extensive.

A protocol is presented for the flow cytometric analysis utilizing a series of antibody panels which we have developed in our lab over the last 8 years for surface epitope analysis of MSC preparations. The analysis of these surface epitope patterns can assist in the isolation and characterization of hMSCs.

Start up the flow cytometer and perform quality control (QC) checks. The instrument procedure for startup and quality control should be performed as described by the manufacturer. This should include the analysis of fluorescent beads to validate the function of the lasers, flow systems, and detection systems. Any problems encountered during this phase should be corrected before proceeding with the analysis of prepared samples.

Following the antibody manufacturer's recommendations, the appropriate volume of reagents should be dispensed into a series of nine (9) 1.5 ml microfuge tubes (one tube for each panel of antibodies) as follows:

- Tube 1: CD36 FITC, CD34 PE, CD19 ECD, CD11b PeCy5, CD45 PeCy7
- Tube 2: CD166 PE, CD90 PeCy5
- Tube 3: CD49b FITC, CD105 PE, CD184 APC, CD3 PeCy7
- Tube 4: CD147 FITC, CD49c PE, CD29 PeCy5
- Tube 5: CD59 FITC, CD146 PE, CD79a PeCy5
- Tube 6: HLA-Class I: ABC FITC, CD271 PE, CD49f PeCy5, CD117 PeCy7
- Tube 7: HLA-Class II (DR, DP, DQ) FITC, CD73a PE, CD106 PeCy5
- Tube 8: CD49d PE, CD14 ECD, CD44 APC
- Tube 9: Isotype controls: IgG1 FITC, IgG2a PE
- Tube 10: MSCs only (no antibodies, no isotype controls)

The tubes containing the antibody cocktails can be made ahead and stored at 4°C in the dark until needed.

Harvest cells at 60–80% confluence and count using Trypan Blue or other method to determine viability. In addition, the MSC only tube may be used to evaluate the viability of the cells after it is used to check for autofluorescence using Annexin-V FITC and Propidium Iodide (PI) (refer to AnnexinV-PI manufacturer's instructions for procedure). Resuspend cells in PBS at a final concentration of 1×10^6 viable cells/ml. Approximately $3\text{--}4 \times 10^6$ cells will be required to complete this protocol.

Aliquot between 2×10^5 and 5×10^5 cells per panel tube set up. Additionally, set up a 10th tube containing only cell suspension as a control for autofluorescence. Gently vortex to mix and incubate in the dark for 20 min at RT.

Wash the cells by adding PBS to the 1.5 ml mark on each tube. Pellet the cells at 110g for 3 min at RT in a microcentrifuge. Remove the supernatant, resuspend the pellet in 1.5 ml PBS and centrifuge again. Repeat one more time for a total of 3 washes. Resuspend the final pellet in 500 μ l PBS and gently vortex. Be sure no aggregates are present.

Using a transfer pipette, place the cell suspensions into the 12 \times 75 mm culture test tubes (or recommended device) and analyze on the flow cytometer. Analyze the unlabeled cells (Tube 10) first, followed by the isotype control (Tube 9). Use the results of these two control tubes to set the gates and analysis regions. Then read

Table 2.6 Flow cytometry MSC panels

Panel	Antibody	Tag	Ig type	Vendor	Catalog*	Expected / Required on MSCs†
1	CD36	FITC	IgG1	Coulter	IM0766	Negative
	CD34	PE	IgG1	Coulter	IM1871	≤ 2%
	CD45	PeCY7	IgG1	Coulter	IM3548	≤ 2%
	CD11b	PeCY5	IgG1	Coulter	IM3611	≤ 2%
	CD19	ECD‡	IgG1	Coulter	IM2708	≤ 2%
2	CD166	PE	IgG1	Coulter	A22361	Positive
	CD90	PeCY5	IgG1	Coulter	IM3703	≥ 95%
3	CD49b	FITC	IgG1	Coulter	IM1425	Positive
	CD105	PE	IgG1	Coulter	A07414	≥ 95%
	CD184	APC	IgG2a	BD	555976	Dim positive
	CD3	PeCY7	IgG1	Coulter	6607100	Negative
4	CD147	FITC	IgG1	BD	555962	Positive
	CD49c	PE	IgG1	BD	556025	Positive
	CD29	PeCY5	IgG1	BD	559882	Positive
5	CD59	FITC	IgG1	Coulter	IM3457	Positive
	CD79a	PeCY5	IgG1	Coulter	IM3456	≤ 2%
6	HLA-I	FITC	IgG1	BD	555552	Dim positive
	CD271	PE	IgG1	BD	557196	Negative
	CD49f	PeCY5	IgG1	BD	551129	Dim positive
	CD117	PeCy7	IgG1	Coulter	IM3698	Negative
7	HLA-II	FITC	IgG2a	BD	555558	≤ 2%
	CD73a	PE	IgG1	BD	550257	≥ 95%
	CD106	PeCY5	IgG1	BD	551148	Negative
8	CD49d	PE	IgG1	BD	555503	Positive
	CD14	ECD	IgG2a	Coulter	IM2707	≤ 2%
	CD44	APC	IgG2a	BD	559942	Positive
Controls	Isotype	FITC	IgG1	Coulter	A17599	Negative
		PE	IgG2a	Coulter	A17599	Negative

* Number of cells needed for 8 panels = $3-4 \times 10^6$ in 1 ml PBS

† Numbers in **bold** indicate required result for markers as per ISCT position paper. Unbolded text indicates the expected results on MSCs.

‡ ECD is equivalent to PE-Texas Red

each of the antibody cocktail-labeled cells. See Table 2.6 for expected expression levels of the panels of antibodies on MSCs.

2.7 Potential Therapeutic Applications

The stem cell-like ability of MSCs to differentiate into multiple cell types in vitro was thought to underlie their observed therapeutic effects when delivered to various animal models of diseases and injury. This may, in fact, be the case for treatment of bone and cartilage defects, because one of the defining characteristics of human

MSCs is their innate ability to differentiate into osteocytes and chondrocytes in culture. However, functional improvements do not correlate with transplanted MSC engraftment and differentiation in most other animal models of disease including Parkinsonism, spinal cord injury, stroke and myocardial infarction [reviewed in 30–32]. In fact, when delivered systemically in animal models, MSCs can no longer be detected by various assays of the host tissues after a few days, yet therapeutic effects of the cells are observed. Thus, there must be other mechanisms MSCs utilize to exert their therapeutic effects [see 31].

It is now believed that MSCs provide therapeutic effects unrelated to their ability to replace damaged cells and tissues through differentiation. The ability of MSCs to support hematopoietic cell growth in culture [45] is being revisited to explain some of these effects. MSCs secrete numerous cytokines and chemokines which can contribute to their ability to home to sites of injury when delivered systemically and also support recovery of the damaged/diseased cells [17–19]. MSCs can also stimulate the proliferation and differentiation of endogenous tissue-specific stem cells [26] and this stimulation may in part underlie the observed ability of human MSCs to stimulate production of mouse insulin in immunodeficient mice made diabetic with Streptozotocin [27].

The ability of MSCs to modulate immune responses has been demonstrated *in vitro* and *in vivo* in various animal models [20–22]. This property of MSCs is already being utilized clinically in the treatment of graft versus host disease and may also underlie their therapeutic efficacy in trials of Crohn's Disease patients. The mechanisms of immune suppression by MSCs have recently been determined [23].

There is also evidence that MSCs can exert therapeutic effects by suppression of acute and chronic excessive inflammatory responses. This mechanism can explain the improvements observed after MSC treatment in animal models of bleomycin-induced lung fibrosis [24] and LPS-induced lung inflammation [25]. In addition, suppression of both inflammatory and immune responses to transient global ischemia in mice may be the mechanisms by which human MSC therapy was found to reduce neuronal death and neurological deficits [46].

The mechanism(s) by which MSCs exert their therapeutic effect may well be disease/injury dependent and directed by the microenvironment at the deficit site. Human MSCs respond to the injured microenvironment with altered gene expression and subsequent production of injury appropriate proteins [46]. While there remains much to be discovered about the basic biology of MSCs and their interaction with other cell types *in vitro* and *in vivo*, the multiple demonstrated and still unknown mechanisms of reparative action of MSCs make these cells potential therapeutic candidates for a variety of diseases and injuries.

2.8 Summary

This chapter is intended to provide the basic methodology for the culture and characterization of human multipotent stromal cells or MSCs and to give a short overview of their possible therapeutic applications. The human MSC has become a

very important candidate in the search for possible clinical treatments of injury and disease because of many factors: (1) ease of obtaining, isolating and culturing; (2) ability to be generate large numbers of cells in a relatively short period of time; (3) ability to be genetically altered ex vivo to express necessary proteins or correct a genetic defect; (4) their apparent role in the body's natural repair mechanism; (5) ability to differentiate into multiple cell types; (6) secretion of cytokines to enhance repair; (7) modulation of immune and inflammatory responses; (8) stimulation of the proliferation of tissue endogenous stem cells; and (9) rescue of damaged cells, by fusion or possibly mitochondrial transfer. Although there is still much to be learned about the mysteries of the MSC, it is apparent that the possibility of using MSCs for successful treatment of a number of diseases and injuries, some of which are devastating and life-threatening, is on the horizon.

Acknowledgments Some of the materials and protocols employed in this work were provided by the Tulane Center for Gene Therapy through a grant from NCRR of the NIH, Grant # P40RR017447.

References

1. Cohnheim J. (1867) Ueber Ebtzuendung and Eiterung. *Arch. Path. Anat. Physiol. Klin. Med.* 40: 1–79.
2. Friedenstein AJ, Gorskaja U, Kulagina NN. (1976) Fibroblast precursors in normal and irradiated mouse hematopoietic organs. *Exp. Hematol.* 4: 267–274.
3. Prockop DJ, Sekiya I, Colter DC. (2001) Isolation and characterization of rapidly self-renewing stem cells from cultures of human marrow stromal cells. *Cytotherapy* 3: 393–396.
4. Sanchez-Ramos J, Song S, Cardozo-Pelaez F, Hazzi C, Stedeford T, Willing A, Freeman TB, Saporta S, Janssen W, Patel N, Cooper DR, Sanberg PR. (2000) Adult bone marrow stromal cells differentiate into neural cells in vitro. *Exp. Neurol.* 164: 247–256.
5. Woodbury D, Schwarz EJ, Prockop DJ, Black IB. (2000) Adult rat and human bone marrow stromal cells differentiate into neurons. *J. Neurosci. Res.* 61: 364–370.
6. Kotton DN, Ma BY, Cardoso WV, Sanderson EA, Summer RS, Williams MC, Fine A. (2001) Bone marrow-derived cells as progenitors of lung alveolar epithelium. *Development* 128: 5181–5188.
7. Wakitani S, Saito T, Caplan AI. (1995) Myogenic cells derived from rat bone marrow mesenchymal stem cells exposed to 5-azacytidine. *Muscle Nerve* 18: 1417–1426.
8. Fukuda K. (2002) Molecular characterization of regenerated cardiomyocytes derived from adult mesenchymal stem cells. *Congenit. Anom. Kyoto* 42: 1–9.
9. Horwitz EM, Le Blanc K, Dominici M, Mueller I, Slaper-Cortenbach I, Marini FC, Deans RJ, Krause DS, Keating A. (2005) Clarification of the nomenclature for MSC: The International Society for Cellular Therapy position statement. *Cytotherapy* 7: 393–395.
10. Dominici M, Le Blanc K, Mueller I, Slaper-Cortenbach I, Marini F, Krause D, Deans R, Keating A, Prockop DJ, Horwitz E. (2006) Minimal criteria for defining multipotent mesenchymal stromal cells. The International Society for Cellular Therapy position statement. *Cytotherapy* 8: 315–317.
11. Meyerrose TE, Roberts M, Ohlemiller KK, Vogler CA, Wirthlin L, Nolte JA, Sands MS. (2008) Lentiviral-transduced human mesenchymal stem cells persistently express therapeutic levels of enzyme in a xenotransplantation model of human disease. *Stem Cells* 26: 1713–1722.

12. Zhang XY, La Russa VF, Reiser J. (2004) Transduction of bone-marrow-derived mesenchymal stem cells by using lentivirus vectors pseudotyped with modified RD114 envelope glycoproteins. *J. Virol.* 78(3):1219–1229.
13. Rubio D, Garcia-Castro J, Martin MC, de la FR, Cigudosa JC, Lloyd AC, Bernad A. (2005) Spontaneous human adult stem cell transformation. *Cancer Res.* 65: 3035–3039.
14. Ferrari G, Cusella-De Angelis G, Coletta M, Paolucci E, Stornaiuolo A, Cossu G, Mavilio F. (1998) Muscle regeneration by bone marrow-derived myogenic progenitors. *Science* 279: 1528–1530.
15. Chopp M, Zhang XH, Li Y, Wang L, Chen J, Lu D, Lu M, Rosenblum M. (2000) Spinal cord injury in rat: treatment with bone marrow stromal cell transplantation. *Neuroreport* 11(13): 3001–3005.
16. Olson L, Widenfalk J, Josephson A, Greitz D, Klason T, Kiyotani T, Lipson A, Ebendal T, Cao Y, Hofstetter C, Schwartz E, Prockop D, Manson S, Jubran M, Lindqvist E, Lundströmer K, Nosrta I, Nosrat C, Brené S, Spenger C. (2001) Experimental spinal cord injury models: protective and repair strategies. In: *Tissue Engineering for Therapeutic Use* 5. Y. Ikada and N. Ohshima, Eds. pp 21–36.
17. Zacharek A, Chen J, Cui X, Li A, Li Y, Roberts C, Feng Y, Gao Q, Chopp M. (2007) Angiopoietin1/Tie2 and VEGF/Flk1 induced by MSC treatment amplifies angiogenesis and vascular stabilization after stroke. *J. Cereb. Blood Flow Metab.* 27(10): 1684–1691.
18. Schinköthe T, Bloch W, Schmidt A. (2008) In vitro secreting profile of human mesenchymal stem cells. *Stem Cells Dev.* 17(1): 199–206.
19. Penolazzi L, Lambertini E, Tavanti E, Torreggiani E, Vesce F, Gambari R, Piva R. (2008) Evaluation of chemokine and cytokine profiles in osteoblast progenitors from umbilical cord blood stem cells by BIO-PLEX technology. *Cell Biol. Int.* 32(2): 320–325.
20. Gerdoni E, Gallo B, Casazza S, Musio S, Bonanni I, Pedemonte E, Mantegazza R, Frassoni F, Mancardi G, Pedotti R, Uccelli A. (2007) Mesenchymal stem cells effectively modulate pathogenic immune response in experimental autoimmune encephalomyelitis. *Ann. Neurol.* 61(3): 219–227.
21. Aggarwal S, Pittenger MF. (2005) Human mesenchymal stem cells modulate allogeneic immune cell responses. *Blood* 105(4): 1815–1822.
22. Le Blanc K, Ringdén O. (2007) Immunomodulation by mesenchymal stem cells and clinical experience. *J. Intern. Med.* 262(5): 509–525.
23. Ren G, Zhang L, Zhao X, Xu G, Zhang Y, Roberts AI, Zhao RC, Shi Y. (2008) Mesenchymal stem cell-mediated immunosuppression occurs via concerted action of chemokines and nitric oxide. *Cell Stem Cell* 2(2):141–150.
24. Ortiz LA, Dutreil M, Fattman C, Pandey AC, Torres G, Go K, Phinney DG. (2007) Interleukin 1 receptor antagonist mediates the antiinflammatory and antifibrotic effect of mesenchymal stem cells during lung injury. *Proc. Natl. Acad. Sci. USA.* 104(26): 11002–11007.
25. Gupta N, Su X, Popov B, Lee JW, Serikov V, Matthay MA. (2007) Intrapulmonary delivery of bone marrow-derived mesenchymal stem cells improves survival and attenuates endotoxin-induced acute lung injury in mice. *J. Immunol.* 179(3): 1855–1863.
26. Munoz JR, Stoutenger BR, Robinson AP, Spees JL, Prockop DJ. (2005) Human stem/progenitor cells from bone marrow promote neurogenesis of endogenous neural stem cells in the hippocampus of mice. *Proc. Natl. Acad. Sci. USA.* 102(50):18171–18176.
27. Lee RH, Seo MJ, Reger RL, Spees JL, Pulin AA, Olson SD, Prockop DJ. (2006) Multipotent stromal cells from human marrow home to and promote repair of pancreatic islets and renal glomeruli in diabetic NOD/scid mice. *Proc. Natl. Acad. Sci. USA.* 103(46): 17438–17443.
28. Spees JL, Olson SD, Ylostalo J, Lynch PJ, Smith J, Perry A, Peister A, Wang MY, Prockop DJ. (2003) Differentiation, cell fusion, and nuclear fusion during ex vivo repair of epithelium by human adult stem cells from bone marrow stroma. *Proc. Natl. Acad. Sci. USA.* 100(5): 2397–2402.
29. Spees JL, Olson SD, Whitney MJ, Prockop DJ. (2006) Mitochondrial transfer between cells can rescue aerobic respiration. *Proc. Natl. Acad. Sci. USA.* 103(5): 1283–1288.

30. Prockop DJ, Gregory CA, Spees JL. (2003) One strategy for cell and gene therapy: harnessing the power of adult stem cells to repair tissues. *Proc. Natl. Acad. Sci. USA*. 100 Suppl 1: 11917–11923.
31. Prockop DJ. (2007) “Stemness” does not explain the repair of many tissues by mesenchymal stem/multipotent stromal cells (MSCs). *Clin. Pharmacol. Ther.* September;82(3): 241–243.
32. Caplan AI, Dennis JE. (2006) Mesenchymal stem cells as trophic mediators. *J. Cell. Biochem.* August 1;98(5): 1076–1084.
33. Wolfe M, Pochampally R, Swaney W, Reger RL. (2008) Isolation and culture of bone marrow-derived human multipotent stromal cells (hMSCs). *Methods Mol. Biol.* 449: 3–25.
34. Reger RL, Wolfe MR. (2008) Freezing harvested hMSCs and recovery of hMSCs from frozen vials for subsequent expansion, analysis, and experimentation. *Methods Mol. Biol.* 449: 109–116.
35. DiGirolamo CM, Stokes D, Colter D, Phinney DG, Class R and Prockop DJ. (1999) Propagation and senescence of human marrow stromal cells in culture: a simple colony forming assay identifies samples with the greatest potential to propagate and differentiate. *Br. J. Haematol.* 107: 275–281.
36. Reger RL, Tucker AH, Wolfe MR. (2008) Differentiation and characterization of human MSCs. *Methods Mol. Biol.* 449: 93–107.
37. Baksh D, Song L, Tuan RS. (2004). Adult mesenchymal stem cells: characterization, differentiation, and application in cell and gene therapy. *J. Cell. Mol. Med.* 8(3): 301–316.
38. Bruder SP, Jaiswal N, Haynesworth SE. (1997). Growth kinetics, self-renewal, and the osteogenic potential of purified human mesenchymal stem cells during extensive subcultivation and following cryopreservation. *J. Cell. Biochem.* 64: 278–294.
39. Bruder SP, Kurth AA, Shea M, Hayes WC, Jaiswal N, Kadiyala S. (1998). Bone regeneration by implantation of purified, culture-expanded human mesenchymal stem cells. *J. Orthop. Res.* 16: 155–162.
40. Prockop DJ. (1997) Marrow stromal cells as stem cells for nonhematopoietic tissues. *Science* 276: 71–74.
41. Sekiya I, Larson BL, Smith JR, Pochampally R, Cui JG, Prockop DJ. (2002) Expansion of human adult stem cells from bone marrow stroma: conditions that maximize the yields of early progenitors and evaluate their quality. *Stem Cells* 20: 530–541.
42. Sekiya I, Larson BL, Vuoristo JT, Reger RL, Prockop DJ. (2005) Comparison of effect of BMP-2, -4, and -6 on in vitro cartilage formation of human adult stem cells from bone marrow stroma. *Cell Tissue Res.* 320(2): 269–276.
43. Smith JR, Pochampally R, Perry A, Hsu S-C, Prockop DJ. (2004). Isolation of a highly clonogenic and multipotential subfraction of adult stem cells from bone marrow stroma. *Stem Cells* 22: 823–831.
44. Sekiya I, Colter DC, Prockop DJ. (2001) BMP-6 enhances chondrogenesis in a subpopulation of human marrow stromal cells. *Biochem. Biophys. Res. Commun.* 284: 411–418.
45. Eaves C, Glimm H, Eisterer W, Audet J, Maguer-Satta V, Piret J. (2001) Characterization of human hematopoietic cells with short-lived in vivo repopulating activity. *Ann. NY Acad. Sci.* 938: 63–70; discussion 70–71.
46. Ohtaki H, Ylostalo J, Foraker JE, Robinson AP, Reger RL, Shioda S, Prockop DJ. (2008). Stem/progenitor cells from bone marrow (hMSCs) decrease neural cell death in global ischemia by modulation of the inflammatory/immune responses. *Proc. Natl. Acad. Sci. USA.* 105(38): 14638–14643.

Chapter 3

Endothelium

Sangmo Kwon and Takayuki Asahara

Abstract Endothelial progenitor cells (EPCs) were first isolated by Asahara [1]. Since then, a new paradigm termed postnatal vascularization, has been proposed to explain the functional contribution of EPCs to vascular repair in various disorders including myocardial infarction, limb ischemia and diabetes. Although vascularization was thought to occur only in the developing fetus [2–4], the finding of circulating EPCs reset the concept of vascularization as *de novo* formation of vessels and remodeling of the circulatory system in the adult [1]. In vivo functional studies have demonstrated that the recruitment of bone marrow (BM) derived EPC dynamically contributes to neovascularization by two distinct pathways: (1) direct contribution by differentiation into endothelial cells, and (2) indirect contribution by secreting cytokines and modifying the extracellular space [5–15]. Accordingly, EPCs have been broadly accepted as one of the most likely candidate sources for stem cell therapy for vascular disease and as biomarkers to measure the severity of human vascular disorders [16–22].

EPCs have been isolated and identified by two methodologies. One method is EPC culture as originally established by Asahara et al. [1] with various modifications, including (1) Hill’s modified methods, (2) Dimmeler’s modified methods, (3) Ingram and Yoda’s method (Fig. 3.1). These cells are termed “tissue EPC” or “cultured EPCs”, because of their endothelial cell (EC) like spindle shape and their ability to differentiate into functional endothelium in ischemic sites. The second methodology is enrichment of circulating EPC by flow cytometry. This definition of EPCs originates from the concept of “circulating EPCs” in human peripheral blood (PB). In this chapter, we will review and describe the methodology for the isolation, growth, and differentiation of “tissue EPCs” and “circulating EPCs” and the assays for EPC characterization.

S. Kwon (✉)

Department of Regenerative Medicine, Tokai University School of Medicine,
Kanagawa 259-1193, Japan

3.1 Introduction and Methodology for Tissue EPC Culture

In vitro culture methods have been developed to purify and expand the minor sub-population of EPCs (less than 0.05%) in adult bone marrow (BMCs). Variations in culture methodology include replating time, culture period, percentage of serum and other culture conditions. Also there is variation in the cell types or cell numbers used, including peripheral blood (PB)- derived mononuclear cells MNCs, cord blood (CB)- derived MNCs and BM- derived MNCs. Figure 3.1 shows the three in vitro culture methods which are widely employed to isolate tissue or cultured EPCs.

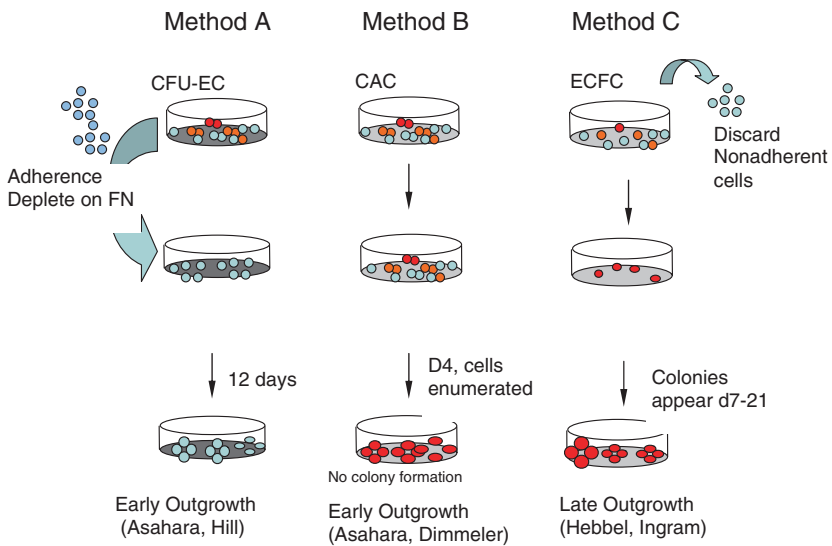


Fig. 3.1 Common methods of EPC culture (Prater et al. [23])

3.1.1 Isolation of MNCs

Adult PB or umbilical CB MNCs are plated on fibronectin-coated dishes. To isolate MNCs from human PB, we described a widely used method [6, 7]. Human PB samples (30 ml of PB in a 50 ml tube) are diluted 1:2 in 15 ml phosphate-buffered saline (PBS) supplemented with 5 mM EDTA (PBS-E). After mixing, the cells are pipetted on 15 ml of Histopaque 1077 very carefully and centrifuged at 2100 rpm, RT for 30 min. Monolayer cells are aspirated using an 18G syringe and collected in a fresh 50 ml conical tube containing 10–15 ml of PBS-EDTA. After centrifugation on low brake at 2400 rpm, 4°C for 10 min, the supernatant is removed and 5 ml of PBS-EDTA added to each tube. The cells are resuspended and transferred to a 50 ml conical tube and recentrifuged on low brake at 1100 rpm, 4°C for 10 min. After the supernatant is removed, 5 ml of PBD-EDTA is added, mixed and 15–20 ml of ammonium chloride added. After making up to 50 ml with PBS-E, the sample

is centrifuged on low brake at 1300 rpm, 4°C for 10 min. The resuspended cells are counted using a hemocytometer.

Isolation of MNCs from human umbilical CB MNCs is similar to that of human PB MNCs. First, 25 ml of human umbilical CB are transferred to 25 ml of 0.15 M DPBS (-), pH7.6 at ratio of 1:1, and then 35 ml of the mixed sample is pipetted onto 15 ml of Histopaque very carefully to isolate mononuclear cells. After centrifugation at 1500 rpm (470g), RT for 40 min, the plasma layer is aspirated. The upper MNC layer is transferred very carefully to a 50 ml tube containing 2 mM EDTA.PBS, and filled to 50 ml by 2 mM EDTA.PBS. After mixing gently, the sample is centrifuged at 2000 rpm (830g), 4°C for 20 min and the pellet resuspended in 5 ml of 2 mM EDTA.PBS. To deplete red blood cells, 15 ml of ammonium chloride solution is added, mixed gently and incubated at 37°C water bath for 5 min. After centrifugation at 1400 rpm, 4°C for 12 min the pellet is suspended in 50 ml of 2 mM EDTA.PBS. After centrifugation at 800–1000 rpm (130–200g) at 4°C for 15 min, the pellet is resuspended in 20 ml of 2 mM EDTA.PBS. The cells are centrifuged at 1000 rpm (200g) at 4°C for 15 min, the supernatant removed and 10 ml of EBM-2 complete medium added. The resuspended cells are counted by hemocytometer.

In the case of mouse BM MNCs, a modified methodology is employed. To obtain large numbers of BM MNCs, all bones including spinal cord are dissected, transferred to a mortar and minced with sterilized scissors. After carefully grinding the bones with 5 mM PBS-E, the supernatant is transferred using a 21G syringe to a 50 ml tube through a sterile 70 µm strainer. This process is repeated 3 times until the supernatant becomes clear. The cell solution (maximum volume of 20 ml) is pipetted on 4 ml of Histopaque 1083 (Sigma) and centrifuged at 2150 rpm (1100g) on low brake, RT for 20 min. After carefully collecting the MNC layer, transfer to 15 ml tubes with an 18G syringe and centrifuge at 2300 rpm (1150g) on low brake, 4°C for 5 min. After removing the supernatant, resuspend the cell pellet in 1 ml of PBS-E. Add a further 13 ml of PBS-E and centrifuge on low brake at 1100 rpm, 4°C for 5 min. After removing the supernatant, resuspend the cell pellet in 1 ml of PBS-E. Then 4 ml NH₄Cl can be added, incubate at 4°C for 10 min and centrifuge at 1400 rpm (350g) on low brake at 4°C for 15 min. Finally, after removing the supernatant, add 2 ml of complete EBM2 medium (Clonetics) and count cells.

3.1.2 Coating Protocol for Cell Culture

Fibronectin-coated (FN) dishes are used for human in vitro EPC culture. Make up the FN solution at 5 mg/5 ml in sterile DDW at 37°C for at least 30 min. Prior to use, dilute FN with sterile DDW at 1:1, and add to dish. After aspirating the FN solution with a pipette, dry the dishes for 15–30 min. In the case of 4 well slides, 35 mm dishes, or dishes that are made of glass, add 1.5% gelatin to the FN solution. For murine EPC culture, vitronectin (VN) coating is preferred. To prepare the VN solution, dilute to 50 µg/ml in sterile DDW, add to dish, aspirate with a pipette, and dry for 15 or 30 min. 4-well glass chamber slides should be coated with VN plus 0.1% gelatin.

3.1.3 Culture Method

In Hill's method of isolating tissue EPCs, purified MNCs are cultured on FN-coated dishes [24, 25]. This method is based on adherence depletion, because mature ECs and macrophages attach easily over a 48 h period. The non-attached cells including potential progenitors can be removed and re-plated on FN-coated dishes. After 4–9 days, colonies emerge with a characteristic morphology of round cells in the middle surrounded by spindle-shaped cells. These colonies are called colony-forming unit-ECs (CFU-ECs) or colony-forming unit-Hill (CFU-Hill) cells. The traditional tissue EPCs obtained by this culture method are enriched for either the human stem/progenitor marker CD34 or vascular endothelial growth factor receptor-2 (VEGFR-2, KDR, or Flk-1), although CD45 expressing cells are gradually lost. After 7 days culture, the expression of typical EPC markers, including CD34, Flk-1, CD31, Tie-2 and E-selectin can be observed. In the clinical setting using an animal hindlimb disease model, populations of MNCs enriched for CD34 and Flk-1 engraft into mouse capillaries at a rate of 13.4%. The number of CFU-EC colonies was significant lower in the PB of patients with hypertension, type I or II diabetes, high cholesterol, congestive heart failure, rheumatoid arthritis and chronic obstructive pulmonary disease. In acute cardiovascular disease, such as myocardial infarction, CFU-ECs increase, suggesting that EPC may contribute to postnatal vascularization as a protection against the development of cardiovascular disease.

The second methodology for the isolation of tissue EPCs is that of Asahara and Dimmeler (Fig. 3.2). The protocol is similar to Hill's modified method, except for the culture time and re-plating method. Freshly isolated MNCs are cultured in endothelial culture media (EGM-2 MV SingleQuots) supplemented with 5% fetal bovine serum (FBS), angiogenic growth factors (10 ng/ml FGF, 20 ng/ml VEGF, 10 ng/ml IGF, 10 ng/ml EGF) and other factors such as ascorbic acid. After 4 days culture, the non-adherent cells are removed, and the attached fraction of cells are replated and cultured for a further 3 days [26–29]. The resulting cells have endothelial characteristics, including binding the endothelial specific lectin Ulex Europaeus Agglutinin-1 (UEA-1), and uptake of acetylated low-density lipoprotein (acLDL) [26, 27]. The tissue EPC express various endothelial markers, including platelet-endothelial cell adhesion molecule (PECAM-1, or CD31), von Willebrand factor (vWF), vascular endothelial cadherin (VE-cadherin or CD144), VEGFR-2 and Tie2/TEK (angiopoietin-1 receptor precursor or tunica intima endothelial cell kinase), as well as binding *Andeiraea Simplicifolia* lectin (AS-1) [6, 26–28, 30]. These cells, comprising about 2% of the total MNC fraction, strongly promote post-natal angiogenesis in an animal model of limb ischemia [27, 31–33]. Hence they are referred to as circulating angiogenic cells (CACs). Using this method, a similar relationship of CFU-EC in patients with cardiovascular disease and risk has been reported by Vasa et al. [34]. They observed that CFU-EC concentration was markedly decreased in the PB in patients with risk factors for coronary artery disease (CAD), such as hypertension, low-density lipoprotein (LDL) cholesterol concentration, diabetes, age and family history. The migratory activity of these tissue EPCs also provided a parameter for clinical diagnosed CAD [34]. In a clinical

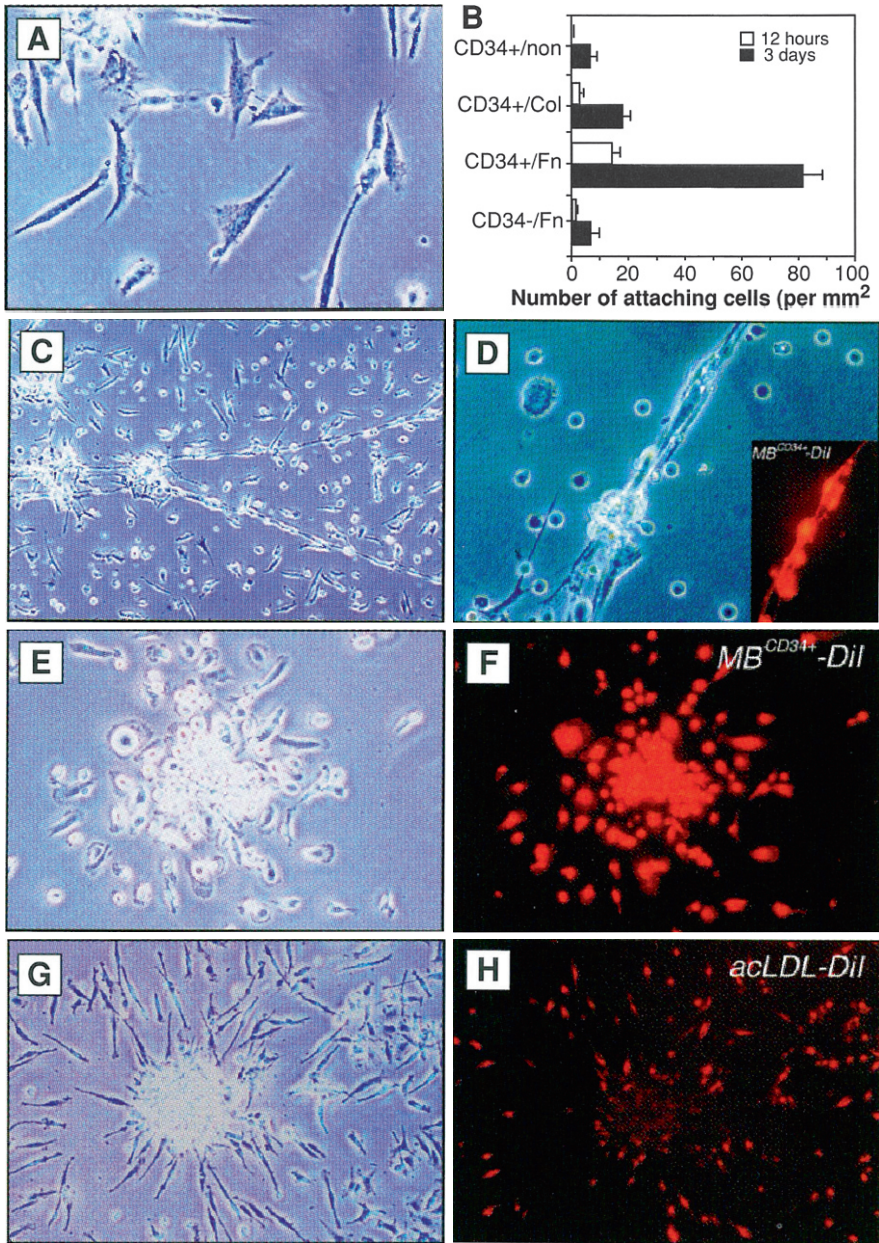


Fig. 3.2 Isolation of EPC in human peripheral blood by original EPC isolation method (Asahara et al. [1])

trial, Assmus et al. reported that the tissue EPCs isolated by Dimmeler’s modified method and infused into patients with acute MI have a limited efficacy in intracoronary cell fusion [35, 36]. In an animal model, these tissue EPC provided promise of therapeutic benefit for acute MI [37–40].

The third methodology to isolate tissue EPCs is that of Hebbel and Ingram, originally reported for endothelial outgrowth from human PB, termed as endothelial outgrowth cells (EOCs) [41]. Blood samples (50–100 mL) or human umbilical CB samples are collected in citrate phosphate dextrose (CPD) solution. Human MNCs are prepared as described above, with minor modifications. MNCs in 4 ml complete EGM-2 medium are plated on 6-well tissue culture dishes pre-coated with type I rat collagen (BD Biosciences) [42, 43]. Non-adherent cells or debris are removed by washing steps after 24 h of culture at 37°C in 5% CO₂ in a humidified incubator. Adherent cells are further washed with complete EGM-2 medium and cultured in same medium. In the case of human PB, endothelial colony-forming cells (ECFCs), also known as late outgrowth EPCs, emerge 10–21 days after plating and have a cobblestone appearance typical of ECs. If human umbilical CBs are seeded, ECFCs can be observed 5–7 days after plating. These tissue EPCs are indistinguishable from CFU-EC, but can be observed in the late stage of tissue EPC culture [44]. ECFCs are clonogenic, frequently forming colonies which can be serially replated. To examine the proliferative potential of EOCs, adult PB and CB-derived endothelial cells (at 1–2 passages) were transduced with retrovirus encoding enhanced fluorescent protein (EGFP) and plated into 96 well plates as single cells (Blood, Ingram et al., Fig. 3.2). After 14 days of culture, counts were made of wells that contained more than 1 cell and the total number of endothelial cells formed in each colony were examined [45]. To examine EPC differentiation in NOD/SCID mice, they established an *in vivo* EPC implantation method [42, 46, 47]. EPC cells were mixed with collagen type I gel and implanted into immunodeficient mice. 14 days later, vessel formation *in vivo* was examined histologically. Guven et al. reported the importance of Hebbel and Ingram's method as a parameter for clinical diagnosis, as the concentration of circulating PB-ECFCs appears to be correlated with the severity of disease [48].

3.2 Methodology for Isolation of Circulating EPCs

3.2.1 Introduction

Circulating EPCs are the accepted definition for the most primitive EPCs in the circulating MNCs, originating from the relationships between EPCs and vascular disorders. Many research groups have reported that circulating CD34+ cells, CD34+VEGFR2+ cells, or CD34+CD133+VEGFR2+ cells are associated with the risk of development of cardiovascular disease [49–53]. In addition, culture of fetal liver-derived CD34+ cells in the presence of VEGF and fibroblast growth factor-2 (FGF-2) appears to promote EC lineage differentiation [50]. The adherent cells take up acetylated LDL and have a spindle shaped EC morphology. Thus, human circulating EPCs have been identified as precursor cells expressing CD133, CD34 and/or VEGFR-2 (KDR). Using flow cytometry or MACS isolation human circulating EPCs can be isolated [54, 55] (Werner N, 2005). In this section, we summarize the isolation method of human PB-derived CD34+ cells, human CB-derived

CD133+ cells using autoMACS system and murine BM-derived KSL isolation using the FACSaria sorting system.

3.2.2 Isolation of Human PB-Derived CD34+ Cells or CB-Derived CD133+ Cells Using AutoMACS

The protocol for human MNC isolation was described in Section 3.1.1 Freshly isolated human PB-derived MNCs are centrifuged at 300g for 10 min and resuspended in 300 μ l of buffer solution with 1% FBS containing FACSFlo solution (10^8 cells). One hundred microlitre of FcR blocking reagents are added to the cell samples with 100 μ l of CD34 or CD133 microbeads. After mixing gently, the cells are incubated at 4°C for 30 min. To wash the cells, 5 ml of 1% FBS containing FACSFlo buffer is added and the cell pellet resuspended. After centrifugation at 300g, 4°C for 10 min, the resulting cell pellet is resuspended in 500 μ l of autoMACS running buffer (2 mM EDTA, 0.5% BSA/PBS, or 0.5% BSA/FACSFlo). To run autoMACS, prepare rinsing solution (2 mM EDTA in PBS, or FACSrinse, FACSFlo) and cleaning solution (70% EtOH in distilled water). To isolate cells with purity of greater than 97%, use either the POSSELD or POSSELD2 sorting program.

3.2.3 Isolation of Human PB-Derived CD34+ Cells or CB-Derived CD133+ Cells Using FACSaria System

To isolate human PB-derived CD34+ cells or CB-derived CD133+ cells with high purity (more than 99%), the FACSaria system can be utilized. Freshly isolated MNCs (less than 10^8 cells) are incubated with 100 μ l of FcR blocking reagents and 20 μ l of anti-CD34 antibodies in cell staining buffer (3% FBS in DPBS buffer) at 4°C for 30 min. After washing the cells 3 times with PBS-E buffer, a sample is applied to FACSaria system. To isolate CD34+/KDR+ (VEGFR-2) cells, the cells should be stained with antibodies against CD34 and KDR, and applied to the FACSaria.

3.2.4 Isolation of Mouse BM-KSL Cells Using the FACSaria

BM-derived MNCs ($1-2 \times 10^7$ /ml cells) are suspended in staining buffer consisting of 3% FBS in DPBS incubated with FCR block (5 μ l per 10^7 cells) at 4°C for 15 min. To deplete the lineage negative population of BM MNCs, add 50 μ l of biotinylated mouse lineage depletion cocktail per 10^7 cells and incubate at 4°C for 15 min. For cell washing, add IMag buffer (0.5% BSA, 2 mM EDTA/DPBS-2.5 g BSA, 2 ml EDTA, 500 ml DPBS) to the sample at 10 times the sample volume. After centrifugation at 300g, 4°C for 7 min, completely remove supernatant. Next, add 50 μ l of streptavidin particles plus DM per 10^7 cells, mix thoroughly and incubate at 4°C for 30 min. Suspend the cells in IMag buffer at ratio of $2-8 \times 10^7$ cells/ml

and incubate for 8 min for IMagnet. After collecting the negative fraction using a pasteur pipette, resuspend the positive fraction with IMag buffer by pipetting, and incubate for 8 min on IMagnet. Collect the negative fraction, centrifuge at 4°C at 500g for 5 min and resuspend the cells in 100 µl of 3% FBS in Hanks buffer. To stain the KSL subpopulation, add antibodies to streptavidin-APC Cy7, PE-Sca-1 and APC-cKit.

3.2.5 Other Putative EPC Subpopulation

Various BM progenitors or circulating EPCs have been identified. In BM, BM Sca-1+ progenitors appear to be enriched with EPC and include Sca-1+Flk-1+ cells, Sca-1+Lin- cells [56], and Kit+Sca-1+Lin-(KSL) cells. Other groups have evaluate c-Kit+ progenitors as PB or BM EPCs, because the c-Kit receptor is an early marker during development. c-Kit+/Flk-1+ cells, c-Kit+CD31+ cells, c-Kit+/Lin- cells [56–58] and KSL cells can be analyzed for in vivo and in vitro studies. As CD34 is a stem or progenitor marker, PB- or BM-CD34+Flk-1+ cells also can be used as EPC enriched cells [50]. Some groups have described the mobilization of CD45-CD34+Flk-1+ progenitors into the circulation in the presence of tumor [59]. Another group has studied in PB CD11b-Flk-1+ progenitors as circulating EPCs.

3.3 Protocols for Evaluating the Function of EPCs

3.3.1 In Vitro EPC Culture Assay

1×10^5 cells of BM MNCs, CB MNCs or PB MNCs were seeded onto fibronectin-coated 4 chamber slides (BD Falcon) to investigate in vitro differentiation of the target cells into the endothelial lineage. The attached spindle-shaped cells were assayed with DiI-conjugated Ac-LDL (DiI-Ac-LDL) (Biomedical Technologies Inc., Stoughton, MA) and FITC-conjugated isolectin B4 (Sigma Chemical Co., Milwaukee, WI), a marker of the endothelial lineage. EPCs identified as the double positive cells were randomly counted using fluorescence microscopy. Likewise, to determine the number of EPCs, the double positive cells for Flk-1 (e-Bio, San Diego, CA) and nitric oxide synthase (eNOS, Sigma) were randomly counted using fluorescence microscopy.

3.3.2 CFU-EPC Assay

To evaluate CFU-EPC capacity, Masuda et al. established a novel assay [60–62]. MNCs are isolated from PB by density-gradient centrifugation as previously described (Section 3.1.1). Lin-committed cells are depleted from the BM-MNCs using MACS™ system after incubating with a cocktail of biotin-conjugated antibodies against specific lineage markers, B220, CD3, Gr-1, Mac-1 and TER-119,

and streptavidin-coupled micro beads (Miltenyi Biotec, Bergisch Gladbach, Germany). KSLs can be isolated from the BM Lin⁻ cells using FACS Vantage sorting equipment (Becton Dickinson, Franklin Lakes, NJ). In the case of human CD34 or CD133 cells, the protocol of cell purification was described above. The number of EPC colonies is assessed after culturing 200–500 BM-KSLs, 500 hCD34 cells, 500 hCD133 cells or 200000 PB-MNCs for 7–10 days (mice) or 18–21 days (human) in methyl cellulose-containing medium M3236 (StemCell Technologies, Vancouver, Canada) with 50 ng/ml vascular endothelial growth factor (VEGF, R&D Systems, Minneapolis, Minn), 20 ng/ml stem cell factor (SCF, Kirin, Tokyo, Japan), 50 ng/ml epidermal growth factor receptor (EGF, Wako, Osaka, Japan), 20 ng/ml interleukin-3 (Kirin, Tokyo, Japan), 50 ng/ml insulin-like growth factor-1 (IGF-1, Wako, Osaka, Japan), 50 ng/ml basic fibroblast growth factor (bFGF, Wako, Osaka, Japan) and 2 U/ml heparin (Ajinomoto, Tokyo, Japan). An endothelial phenotype of the EPC colonies is confirmed by the analysis of both high uptake of acetyl LDL (Ac-LDL) and cytochemical positivity for isolectin B4 (Molecular Probes, Carlsbad, CA), Flk-1 (VEGFR2), VE-cadherin and eNOS.

3.3.3 Flow Cytometry Assay

Fluorescence-activated cell sorting (FACS) analysis can be performed to identify cell surface markers and endothelial lineage antigens on putative EPCs. Surface expression of mouse CD31 is determined with anti-mouse CD31 antibody directly conjugated to phycoerythrin (PE) (Becton Dickinson). Biotin-conjugated anti-mouse Flk-1 (VEGFR 2) antibody (e-Bio, San Diego, CA) and anti-streptavidin APC-conjugated secondary antibody (e-Bio, San Diego, CA) are used to determine the surface expression of Flk-1. Each staining procedure can be performed for 20 min at 4°C, and the stained cells are fixed with 2% paraformaldehyde (PFA) followed by quantitative analysis with FACSCalibur (Becton Dickinson) and Cell Quest software. To evaluate the frequency of CD31⁺/Flk-1⁺ cells in Sca-1⁺/Lin⁻ cells obtained from mice, Sca-1-FITC (Becton Dickinson), CD31-PE (Becton Dickinson) and Flk-1-APC (Becton Dickinson) antibodies can be used after isolating the Lin-depleted cells by the MACS system.

3.3.4 EPC Proliferation Assay

To evaluate EPC proliferation, a BrdU proliferation assay can be performed. BM or PB progenitor cells or cultured EPCs prepared as described above are pulsed with 10 μM BrdU (BrdU flow kit, BD pharmingen) for 45 min before immunostaining with PE-conjugated rat anti-mouse Sca-1 antibody. After fixation and permeabilization with Cytfix/Cytoperm buffer (BD pharmingen) according to the manufacturer's instructions, the cells are stained with APC-conjugated antibody against BrdU, and analyzed with FACSCalibur using CellQuest software (BD pharmingen).

The WST-1 assay provides another methodology for analyzing EPC proliferation [61]. In brief, 1×10^4 target cells are seeded in each well of fibronectin-coated

96-well plates and incubated for 48 h. For the evaluation of cell proliferation in response to various cytokines including VEGF, SCF, TPO and SDF-1, the cultured cells are starved in EBM-2 culture medium with 1% FBS without any growth factor. Thereafter, 10 μ l of the cell proliferation assay reagent WST-1 (Roche Applied Science, Indianapolis, IN), is added to each well and incubated for 3–5 h. Absorbance at 450 nm is measured for each well using an enzyme-linked immunosorbent assay reader.

3.3.5 EPC Adhesive Assay

Twenty four well culture plates are coated with human fibronectin (100 μ g/mL, Gibco, Carlsbad, CA). 2×10^4 EPCs/well are allowed to attach in EGM-2 (Cambrex BioScience Walkersville, Walkersville, MD) for 20 min at 37°C and the non-adherent cells are then removed. The attached cells are fixed with 1% PFA for 20 min and stored in PBS. The numbers of adherent cells can be quantified from counts in at least six random microscopic fields per well. AcLDL uptake positive cells can be measured in each well at the appropriate absorbance using an enzyme-linked immunosorbent assay reader.

3.3.6 EPC Apoptosis Assay

To analyze the apoptotic potential of EPCs, the TUNEL assay is available as a commercial in situ cell death detection kit (Roche, Penzberg, Germany). In brief, the EPC-enriched cells or cultured EPC can be preconditioned by specific signals, followed by serum starvation for 1–2 days in vitro, and the tissue samples obtained from hindlimb ischemia in vivo can be fixed with 4% PFA for 1 h at room temperature. After brief incubation in permeabilization solution containing 0.1% Triton X100 in 0.1% sodium citrate for 2 min, the samples are washed twice with PBS and incubated with 50 μ l of TUNEL reaction solution for 1 h in a humidified chamber at 37°C in the dark. After washing with PBS, apoptotic cells are quantified by flow cytometric analysis or fluorescence microscopy.

3.3.7 EPC Migration Assay

To examine EPC migratory capacity, an in vitro Boyden chamber assay (Costar, Cambridge, MA) can be used. In brief, 600 μ l of EBM-2 medium with 0.5% lipid-free FBS (Sigma Chemical Co.) and 4, 20 or 100 ng/ml of specific cytokines or vehicle can be placed in the lower compartment of the chamber. Target cells can be seeded in the upper compartment of the chamber. The in vitro migration potential of target cells are quantified by counting cells migrating from the upper to lower chamber in four randomly selected high-power fields.

To determine the invasive capacity of EPCs, the cells are seeded in the upper chamber coated with 0.2% methylcellulose (StemCell Technologies), while specific

cytokines or no growth factor is added in the lower compartment. In a similar fashion to the migration assay, the number of invading cells can be counted under each condition.

3.3.8 Tube Formation Assay

HUVECs or late types of cultured EPCs (EOCs) can be used for tube formation assay. These cells are confirmed to be ECs or EC like cells by tube formation and immunocytochemistry of KDR, VE-cadherin and eNOS. Each putative EPC can be labeled with acLDL-DiI for 1 h. After washing the labeled EPCs with PBS, the 1×10^3 putative EPCs are mixed with 1.2×10^4 ECs or EOCs in 50 μ L of 2% FBS/EBM-2 to evaluate the contribution of EPCs to EC-derived tube formation capacity. Fifty microlitre of cell suspension are applied to 50 μ L Matrigel (BD, Franklin Lakes, NJ) per well of a 96 well plate (BD Falcon, Franklin Lakes, NJ) and then incubated for 4–8 h. The number of tubular formations can be counted using photoshop software (Adobe, San Jose, CA) after taking one picture per well under light microscopy (Eclipse TE300, Nikon, Tokyo, Japan). The numbers of labeled cells incorporated into tubes can be counted on Photoshop software, after taking one picture per well under a fluorescence microscopy.

3.3.9 EPC Gene Induction Assay by Hypoxic Condition

The potential of putative EPCs to express endothelial surface markers is determined by semi-quantitative RT-PCR analysis or real time RT-PCR analysis. Following manufacturer's instructions, cellular mRNA can be extracted from each sample using RNeasy Micro Kit (QIAGEN, Valencia, CA). Reverse transcriptase-polymerase chain reaction (RT-PCR) is performed using 1 ng of mRNA. To investigate the expression of EPC-specific marker genes, PCR are performed for 25–30 cycles using the TITANIUM™ Taq RT-PCR kit system (BD Biosciences, San Jose, CA). Real-time PCR profiles in the expression of target cells can be analyzed using PrimeScript™ RT reagent Kit (TaKaRa, Shiga, Japan). To induce gene expression by hypoxia, a 1 or 5% oxygen concentration plus 5% CO₂ incubator can be used for 12 or 24 h.

3.3.10 In Vivo EPC Incorporation Assay

To determine the extent to which putative EPCs incorporate into sites of ischemia, 2.5×10^5 target EPCs (AcLDL-labelled-, DiI-labelled- cells or GFP mouse-derived cells) can be transplanted into the tail vein of nude mice with hindlimb ischemia, myocardial infarction or other disease. Ischemic muscle samples are embedded in OCT compound (Miles, Elkhart, IN), snap-frozen in liquid nitrogen, and cut into

6 μm -thick sections on day 4–7. Frozen sections of the ischemic hindlimb muscles can be stained with rat anti-mouse CD31 antibody (Becton Dickinson) overnight at 4°C, followed by staining with Alexa fluor-conjugated anti-rat antibody to identify capillaries in the ischemic tissue. The capacity of the transplanted cells to be incorporated can be evaluated by counting the number of double-positive cells for CD31. The frozen samples can also be stained with FITC-labeled isolectin B4 (Molecular Probes) to evaluate capillary density by counting capillaries.

3.3.11 In Vivo Functional Assay for Vascular Regeneration

Operative resection of the femoral artery is performed in C57BL6/J, Balb/C-nude mice or specific disease mice to generate the hindlimb ischemia model, as described previously. The 2.5×10^5 putative EPCs or cultured EPCs can be intravenously administered immediately after induction of ischemia. Laser Doppler perfusion imaging (LDPI) can be conducted to measure blood flow recovery ratio (ischemic/non-ischemic limb) for the evaluation of perfusion recovery from hindlimb ischemia.

3.3.12 In Vivo Matrigel Plug Assay

Athymic nude mice 8–9 weeks old are anesthetized with 50 mg/kg intraperitoneal pentobarbital for Matrigel plug injection or unilateral femoral artery resection. Four Matrigel plugs which contained four groups of 2×10^5 cells in 150 μL Matrigel can subcutaneously be injected into each quadrant of the abdominal wall of the mice for in vivo 3D Matrigel angiogenesis assay. To evaluate the therapeutic role of neovasculogenesis, surgery to induce hindlimb ischemia can be performed as described at Section 3.3.11.

3.3.13 In Vivo Capillary Density Measurement

Capillary density can be determined in tissue sections from the lower calf muscles of ischemic and healthy limbs as the number of CD31 positive cells as ECs per myocyte after 28 days after ischemia. For staining the capillary, rat-anti-mouse CD31 antibodies (BD Biosciences, Franklin Lakes, NJ) or Alexa-fluor 594 (Molecular probes, Carlsbad, CA) anti-iso-lectin B4 reagents (Sigma, St. Louis, MO) can be used.

3.4 Prospective of Development of EPC Culture System

Considering the clinical application of EPCs, one of the most promising strategies is administration of EPCs isolated from their own PB. To mobilize CD34+ progenitors, granulocyte (G)-CSF can be administered to patients. In our and other

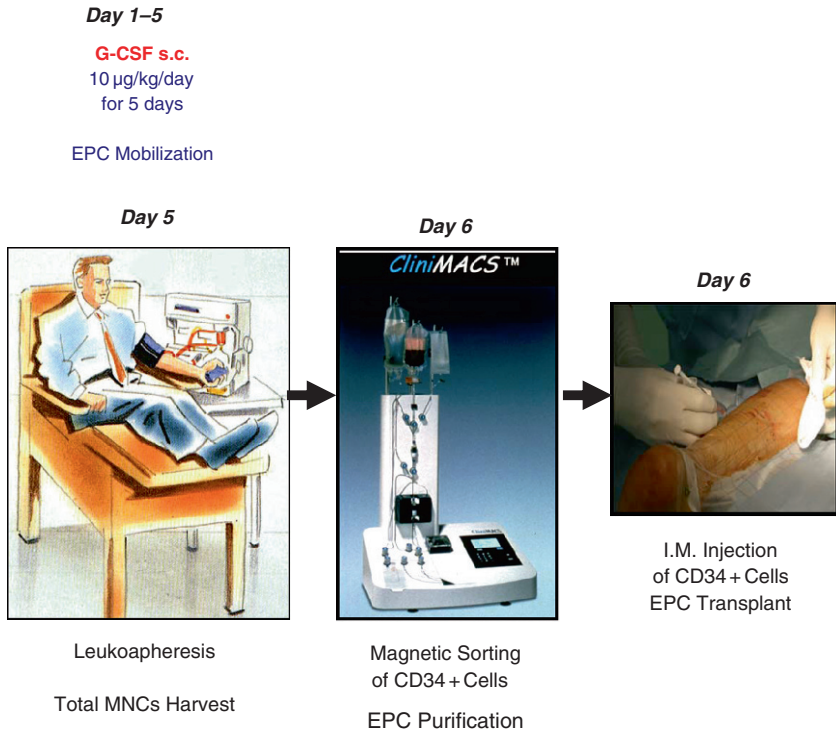


Fig. 3.3 EPC Transplantation for critical limb ischemia

laboratories, treatment of limb ischemic patients by direct injection of autologous CD34+ cells into the muscle of ischemic lower limb improves outcome (Fig. 3.3). But the CD34+ cells-derived EPC therapy has limitations. The patient's circulation contains only a small subpopulation of CD34+ cells (less than 0.3–0.5% in MNCs), which are inadequate for severe disease. Furthermore, aged patients have less EPCs function and fewer circulating EPCs. To overcome this obstacle, EPCs should be ex vivo expanded or should be activated to have enough efficacy for treatment of ischemic diseases. Some reports have demonstrated that EPC can be functionally activated through genetic modification of tissue EPCs by VEGF [63], eNOS [64], TERT (Telomere transcriptase) [65] or Shh (sonic hedgehog) [66] to obtain enhanced EPCs. Another promising strategy for EPC expansion is the serum-free based stem cell culture in the presence of specific cytokines, by which hemangioblastic stem cells can be committed into functional EPCs. To achieve this goal, the stem cell culture should (1) be bio-safe, (2) show significant expansion, (3) retain immaturity, (4) maintain commitment and (5) have regenerative function without senescence. To develop the best culture conditions for obtaining functional EPCs, some critical points need to be resolved. First, the molecular spectrum for EPC commitment in BM niche should be clarified by research including basic EPC cell biology. Second, the best cytokine cocktails should be determined to support the

function of cultured EPC in vitro or in vivo. Third, the number of purified heman-gioblastic stem cells should be determined at the outset. To achieve this goal, the origin of EPC needs to be intensively studied by sub-fractionation of stem cells.

3.5 Concluding Remarks

Interest in EPCs has been raised by the advent of EPC-based therapies for cardio-vascular disease, as well as understanding of the critical pathophysiological role of EPCs in the cardiovascular system. But there is no uniform definition of EPCs, because there are many experimental culture systems and assay methodologies to distinguish different types of EPCs in different EPC culture systems. Many research groups including our own have made great efforts to define EPC characteristics in both physiological and pathological settings. In this review, we classified two types of EPCs as “tissue EPCs” and “circulating EPCs”. Considering EPC cell biology during development, new definitions of EPC definition can be proposed, i.e. (1) primitive EPCs or early EPCs, (2) definitive EPCs or late EPCs.

References

1. Asahara T, Murohara T, Sullivan A, Silver M, van der Zee R, Li T, Witzenbichler B, Schatteman G, Isner JM. Isolation of putative progenitor endothelial cells for angiogenesis. *Science* 1997; 275:964–967.
2. Cleaver O, Melton DA. Endothelial signaling during development. *Nature Med* 2003; 9: 661–668
3. Risau W. Mechanism of angiogenesis. *Nature* 1997; 386:671–674
4. Conway EM, Collen D, Carmeliet P. Molecular mechanisms of blood vessel growth. *Cardio-vasc Res* 2001; 49:507–521
5. Aicher A, Zeiher AM, Dimmeler S. Mobilizing endothelial progenitor cells. *Hypertension* 2005; 45: 321–325.
6. Asahara T, Takahashi T, Masuda H, Kalka C, Chen D, Iwaguro H, Inai Y, Silver M, Isner JM. VEGF contributes to postnatal neovascularization by mobilizing bone marrow-derived endothelial progenitor cells. *EMBO J*. 1999; 18:3964–3972.
7. Takahashi T, Kalka C, Masuda H, Chen D, Silver M, Kearney M, Magner M, Isner JM, Asahara T. Ischemia- and cytokine-induced mobilization of bone marrow-derived endothelial progenitor cells for neovascularization. *Nat Med* 1999; 5:434–438.
8. Awad O, Dedkov EI, Jiao C, Bloomer S, Tomanek RJ, Schatteman GC. Differential healing activities of CD34+ and CD14+ endothelial cell progenitors. *Arterioscler Thromb Vasc Biol* 2006; 26:758–764.
9. Blann AD, Pretorius A. Circulating endothelial cells and endothelial progenitor cells: two sides of the same coin, or two different coins? *Atherosclerosis* 2006; 188:12–18.
10. Wassmann S, Werner N, Czech T, Nickenig G. Improvement of endothelial function by systemic transfusion of vascular progenitor cells. *Cir Res* 2006; 99:e74—e83.
11. Grunewald M, Avraham I, Dor Y, Bachar-Lustig E, Itin A, Jung S et al. VEGF-induced adult neovascularization: recruitment, retention, and role of accessory cells. *Cell* 2006; 124: 175–189.
12. Jin DK, Shido K, Kopp HG, Petit I, Shmelkov SV, Young LM et al. Cytokine-mediated deployment of SDF-1 induces neovascularization through recruitment of CXCR4+ hemangiocytes. *Nat Med* 2006; 12:557–567.

13. McCawley LJ, Matrisian LM. Matrix metalloproteinases: they're not just for matrix anymore. *Curr Opin Cell Biol* 2001; 13:534–540.
14. You D, Waeckel L, Ebrahimian TG, Blanc-Brude O, Foubert P, Barateau V et al. Increase in vascular permeability and vasodilation are critical for proangiogenic effects of stem cell therapy. *Circulation* 2006; 114:328–338.
15. Zentilin L, Tafuro S, Zacchigna S, Arsic N, Pattarini L, Sinigaglia M et al. Bone marrow mononuclear cells are recruited to the sites of VEGF-induced neovascularization but not incorporated into the newly formed vessel. *Blood* 2006; 107:3546–3554.
16. Urbich C, Dimmeler S. Endothelial progenitor cells: characterization and role in vascular biology. *Circ Res* 2004; 95:343–353.
17. Rafii S, Lyden D. Therapeutic stem and progenitor cell transplantation for organ vascularization and regeneration. *Nat Med* 2003; 9:702–712.
18. Shatteman GC. Adult bone marrow-derived hemangioblasts, endothelial progenitors, and EPCs. *Curr Top Dev Biol* 2004; 64:141–180.
19. Iwami Y, Masuda H, Asahara T. Endothelial progenitor cells: past, state of the art, and future. *J Cell Mol Med* 2004; 8:488–497.
20. Hristov M, Weber C. Endothelial progenitor cells: characterization, pathophysiology, and possible clinical relevance. *J Cell Mol Med* 2004; 8:498–508.
21. Blann AD. Assessment of endothelial dysfunction: focus on atherothrombotic disease. *Pathophysiol Haemost Thromb* 2003; 33:256–261.
22. Quilici J, Banzet N, Paule P et al. Circulating endothelial cell counting as a diagnostic marker for non-ST-elevation acute coronary syndromes. *Circulation* 2004; 110:1586–1591.
23. Prater DN, Case J, Ingram DA, Yoder MC. Working hypothesis to redefine endothelial progenitor cells. *Leukemia* 2007; 21:1141–1149.
24. Hill JM, Zalos G, Halcox JP, Schenke WH, Waclawiw MA, Quyyumi AA et al. Circulating endothelial progenitor cells, vascular function, and cardiovascular risk. *New Engl J Med* 2003; 348:593–600.
25. Ito H, Rovira II, Bloom ML, Takeda K, Ferrans VJ, Quyyumi AA et al. Endothelial progenitor cells as putative targets for angiostatin. *Cancer Res* 1999; 59:5875–5877.
26. Dimmeler S, Zeiher AM. Endothelial cell apoptosis in angiogenesis and vessel regression. *Circ Res* 2000; 87:434–439.
27. Kalka C, Masuda H, Takahashi T, Kalka-Moll WM, Silver M, Kearney M et al. Transplantation of ex vivo expanded endothelial progenitor cells for therapeutic neovascularization. *Proc Natl Acad Sci USA* 2000; 97:3422–3427.
28. Dimmeler S, Aicher A, Vasa M, Mildner-Rihm C, Adler K, Tiemann M et al. HMG-CoA reductase inhibitors (statins) increase endothelial progenitor cells via the PI 3-kinase/Akt pathway. *J Clin Invest* 2001; 108:391–397.
29. Ishikawa M, Asahara T. Endothelial progenitor cell culture for vascular regeneration. *Stem Cells Dev* 2004; 13:344–349.
30. Gehling UM, Ergun S, Schumacher U, Wägener C, Pantel K, Otte M et al. In vitro differentiation of endothelial cells from AC133-positive progenitor cells. *Blood* 2000; 95:3106–3112.
31. Kawamoto A, Gwon HC, Iwaguro H, Yamaguchi JI, Uchida S, Masuda H et al. Therapeutic potential of ex vivo expanded endothelial progenitor cells for myocardial ischemia. *Circulation* 2001; 103:634–637.
32. Rehman J, Li J, Orschell CM, March KL. Peripheral blood 'endothelial progenitor cells' are derived from monocyte/macrophage and secrete angiogenic growth factors. *Circulation* 2003; 107:1164–1169.
33. Rehman J, Li J, Parvathaneni L, Karlsson G, Panchal VR, Temm CJ et al. Exercise acutely increases circulating endothelial progenitor cells and monocyte-/macrophage-derived angiogenic cells. *J Am Coll Cardiol* 2004; 43:2314–2318.
34. Vasa M, Fichtlscherer S, Aicher A, Adler K, Urbich C, Martin H et al. Number and migratory activity of circulating endothelial progenitor cells inversely correlated with risk factors for coronary artery disease. *Circ Res* 2001; 89:E1–E7.

35. Assmus B, Schachinger V, Teupe C, Britten M, Lehmann R, Dobert N et al. Transplantation of progenitor cells and regeneration enhancement in acute myocardial infarction (TOPCARE-AMI). *Circulation* 2002; 106:3009–3017.
36. Assmus B, Honold J, Schachinger V, Britten MB, Fischer-Rasokat U, Lehmann R et al. Transcoronary transplantation of progenitor cells after myocardial infarction. *New Engl J Med* 2006; 355:1199–1209.
37. Rafii S, Lyden D. Therapeutic stem and progenitor cell transplantation for organ vascularization and regeneration. *Nat Med* 2003; 9:702–712.
38. Asahara T, Kawamoto A. Endothelial progenitor cells for postnatal neovascularization. *Am J Physiol Cell Physiol* 2004; 287:C572–C579.
39. Honold J, Assmus B, Lehman R, Zeiher AM, Dimmeler S. Stem cell therapy of cardiac disease: an update. *Nephrol Dial Transplant* 2004; 19:1673–1677.
40. Urbich C, Dimmeler S. Endothelial progenitor cells: characterization and role in vascular biology. *Circ Res* 2004; 95:343–353.
41. Lin Y, Weisdorf DJ, Solovey A, Heibel RP. Origins of circulating endothelial cells and endothelial outgrowth from blood. *J Clin Invest* 2000; 105:71–77.
42. Yoder MC, Mead LE, Prater D, Krier TR, Mroueh KN, Li F et al. Re-defining endothelial progenitor cells via clonal analysis and hematopoietic stem/progenitor cell principals. *Blood* 2007; 109:1801–1809.
43. Ingram DA, Mead LE, Tanaka H, Mead V, Fenoglio A, Mortell K et al. Identification of a novel hierarchy of endothelial progenitor cells using human peripheral and umbilical cord blood. *Blood* 2004; 104:2752–2760.
44. Ingram DA, Mead LE, Moore DB, Woodard W, Fenoglio A, Yoder MC. Vessel wall-derived endothelial cells rapidly proliferate because they contain a complete hierarchy of endothelial progenitor cells. *Blood* 2005; 105:2783–2786.
45. Stevens T, Rosenberg R, Aird W, Quertermous T, Johnson FL, Garcia JG et al. NHLBI workshop report: endothelial cell phenotypes in heart, lung, and blood diseases. *Am J Physiol Cell Physiol* 2001; 281:C1422–C1433.
46. Schechner JS, Nath AK, Zheng L, Kluger MS, Hughes CC, Sierra-Honigmann MR et al. In vivo formation of complex microvessels lined by human endothelial cells in an immunodeficient mouse. *Proc Natl Acad Sci USA* 2000; 97:9191–9196.
47. Enis DR, Shepherd BR, Wang Y, Qasim A, Shanahan CM, Weissberd PL et al. Induction, differentiation, and remodeling of blood vessels after transplantation of Bcl-2-transduced endothelial cells. *Proc Natl Acad Sci USA* 2005; 102:425–430.
48. Guven H, Shepherd RM, Bach RG, Capoccia BJ, Link DC. The number of endothelial progenitor cell colonies in the blood is increased in patients with angiographically significant coronary artery disease. *J Am Coll Cardiol* 2006; 48:1579–1587.
49. Gehling UM, Ergun S, Schumacher U, Wagener C, Pantel K, Otte M et al. In vitro differentiation of endothelial cells from AC133-positive progenitor cells. *Blood* 2000; 95:3106–3112.
50. Peichev M, Naiyer AJ, Pereira D, Zhu Z, Lane WJ, Williams M et al. Expression of VEGFR-2 and AC133 by circulating human CD34 (+) cells identifies a population of functional endothelial precursors. *Blood* 2000; 95:952–958.
51. Akashi K, Weissman IL. Stem cells and hematolymphoid development. In: Zon LI (ed). Oxford University Press: New York, 2001. pp 15–34.
52. Garmy-Susini B, Varner JA. Circulating endothelial progenitor cells. *Br J Cancer* 2005; 93:855–858.
53. Werner N, Kosiol S, Schiegl T, Ahlers P, Walenta K, Link A, Böhm M, Nickenig G. Circulating endothelial progenitor cells and cardiovascular outcomes. *N Engl J Med*. 2005; 353:999–1007.
54. Eizawa T, Ikeda U, Murakami Y, Matsui K, Yoshioka T, Takahashi M et al. Decrease in circulating endothelial progenitor cells in patients with stable coronary artery disease. *Heart* 2004; 90:685–686.

55. Schmidt-Lucke C, Rossig L, Fichtlscherer S, Vasa M, Britten M, Kamper U et al. Reduced number of circulating endothelial progenitor cells predicts future cardiovascular events: proof of concept for the clinical importance of endogenous vascular repair. *Circulation* 2005; 111:2981–2987.
56. Bailey AS, Willenbring H, Jiang S, Anderson DA, Schroeder DA, Wong MH, Grompe M, Fleming WH. Myeloid lineage progenitors give rise to vascular endothelium. *Proc Natl Acad Sci USA* 2006; 103(35):13156–13161.
57. Fazel S, Cimini M, Chen L, Li S, Angoulvant D, Fedak P, Verma S, Weisel RD, Keating A, Li RK. Cardioprotective c-Kit+ cells are from the bone marrow and regulate the myocardial balance of cytokines. *J Clin Invest* 2006; 116(7):1865–1877.
58. Balsam LB, Wager AJ, Christensen JL, Kofidis T, Weissman IL, Robbins RC. Hematopoietic stem cells adopt mature hematopoietic fates in ischemic myocardium. *Nature* 2004; 428(6983):668–673.
59. Chakraborty D, Chowdhury UR, Sarkar C, Baral R, Dasgupta PS, Basu S. Dopamine regulates endothelial progenitor cell mobilization from mouse bone marrow in tumor vascularization. *J Clin Invest* 2008; 118(4):1380–1389.
60. Tanaka R, Wada M, Kwon SM, Masuda H, Carr J, Ito R, Miyasaka M, Warren SM, Asahara T, Tepper OM. The effects of flap ischemia on normal and diabetic progenitor cell function. *Plast Reconstr Surg* 2008; 121(6):1929–1942.
61. Kwon SM, Eguchi M, Wada M, Iwami Y, Hozumi K, Iwaguro H, Masuda H, Kawamoto A, Asahara T. Specific Jagged-1 signal from bone marrow microenvironment is required for endothelial progenitor cell development for neovascularization. *Circulation* 2008; 118(2):157–165.
62. Kato M, Masuda K, Kakugawa K, Kawamoto H, Mugishima H, Katsura Y. Quantification of progenitors capable of generating T cells in human cord blood. *Eur J Haematol.* 2008; 80:151–159.
63. Iwaguro H, Yamaguchi J, Kalka C, Murasawa S, Masuda H, Hayashi S, Silver M, Li T, Isner JM, Asahara T. Endothelial progenitor cell vascular endothelial growth factor gene transfer for vascular regeneration. *Circulation* 2002; 105(6):732–738.
64. Kong D, Melo LG, Mangi AA, Zhang L, Lopez-Illasaca M, Perrella MA, Liew CC, Pratt RE, Dzau VJ. Enhanced inhibition of neointimal hyperplasia by genetically engineered endothelial progenitor cells. *Circulation* 2004; 109(14):1769–1775.
65. Murasawa S, Llevadot J, Silver M, Isner JM, Losordo DW, Asahara T. Constitutive human telomerase reverse transcriptase expression enhances regenerative properties of endothelial progenitor cells. *Circulation* 2002; 106(9):1133–1139.
66. Kusano KF, Pola R, Murayama T, Curry C, Kawamoto A, Iwakura A, Shintani S, Ii M, Asai J et al. Sonic hedgehog myocardial gene therapy: tissue repair through transient reconstitution of embryonic signaling. *Nat Med* 2005; 11(11):1197–1204.

Chapter 4

Lung

Rabindra Tirouvanziam, Megha Makam and Bruno Péault

Abstract Research on human stem and precursor cells (collectively dubbed “progenitor cells”) has undergone a major overhaul in the last few years, with pioneering discoveries on totipotent cells (e.g., embryonic stem cells) as well as multipotent adult progenitors (e.g., MAPC or mesenchymal stem cells, MSC) and committed downstream pluripotent precursors (e.g., hematopoietic stem cells, able to generate all lineages of blood cells). Here, we would like to propose a bottom-up approach for adult human lung progenitor cell research, rather than the conventional top-down approach. A thorough understanding of lung morphology and function in humans, as compared to other species, and the clinical reality of lung physiology in health and disease should come first. These, in turn, should not only instruct the choice of experimental and clinical approaches aimed at adult human lung progenitor cells but also constrain expectations thereof. We begin this review by providing a detailed description of the adult human lung, through a description of its ontogeny, morphological and spatial layers. Second, we assess how the concepts pertaining to progenitor cell biology apply to the lung, with particular emphasis on its (patho)physiological constraints during turnover and repair. Third, we present detailed protocols for the isolation, selection, in vitro culture and functional assessment of candidate adult human lung stem cells.

4.1 Foreword

Several groups have attempted to apply the theoretical and practical frameworks developed around canonical types of progenitor cells (embryonic stem cells, hematopoietic stem cells) to the particular context of the lung. For example, early experiments in mice suggested that certain bone marrow-derived progenitors participate in the normal epithelial cell turnover in the lung or/and to its repair upon injury [1], just as they might contribute to the cellular make-up of other organs. Further experiments

R. Tirouvanziam (✉)
Department of Pediatrics, Stanford University School of Medicine, Stanford,
CA 94305-5318, USA
e-mail: tirouvan@stanford.edu

have revealed a need for more caution in the interpretation of these early results, so far as to question the very ability of circulating progenitors to contribute to lung epithelial turnover/repair [2].

For this reason, we have chosen to emphasize in this review the idiosyncrasies of lung morphology and function in humans, as compared to other species, and the clinical reality of lung physiology in health and disease. This is a significant departure from conventional approaches that focus first on common notions related to stem cells, as gained mostly in animal models, and attempt to make them fit into the particular context of the human lung. Readers interested in gaining additional insight into such conventional approaches of the question are encouraged to refer to other recent reviews [3–6].

To begin this review, we will provide a detailed description of the adult human lung, through a description of its ontogeny, morphological and spatial layers. Second, we will assess how the concepts of progenitor cells may apply to the lung, with particular emphasis on its (patho) physiological complexity and constraints. Third, we will present detailed protocols for the isolation of candidate lung progenitor cells and for two *ex vivo* approaches aiming at testing the developmental and functional potential of such candidate cells.

4.2 Ontogeny, Morphological and Spatial Layers of the Human Lung

4.2.1 Ontogeny of the Human Lung

The lung emerges as an endodermal outpouching from the oesophagus, during the 4th week of gestation. It will take several months to turn this simple structure into a functional organ comprising 40+ differentiated cell types. The endoderm gives rise to the tracheobronchial, bronchiolar and alveolar surface epithelium, as well as the submucosal glands of the upper airways (see Fig. 4.1). The mesoderm gives rise to the interstitium, cartilage (in conducting airways), smooth muscle, resident hematopoietic cells and vascular network. The ectoderm gives rise to the networks of afferent and efferent neurons associated with the lung.

Lung development occurs in 5 slightly overlapping phases [7, 8]:

1. Embryonic phase (22–50 gestational days): arising at the 22nd day of gestation from the primitive gut, the respiratory anlage branches out between the 26th and 28th days of gestation into 2 buds, that will later form the right and left lungs. At the end of this phase, the 2nd and 3rd division of bronchi are formed. At this time, the lung is a mesenchymal pouch, lined internally by a simple, monostratified epithelium.
2. Pseudo-glandular phase (5–17 weeks of gestation): during this phase, all pre-acinar airways (i.e., upstream of the terminal bronchioles, see Fig. 4.1), including their associated vascular network are formed. The tracheobronchial epithelium becomes pseudostratified and invaginates into the mesenchyme to form

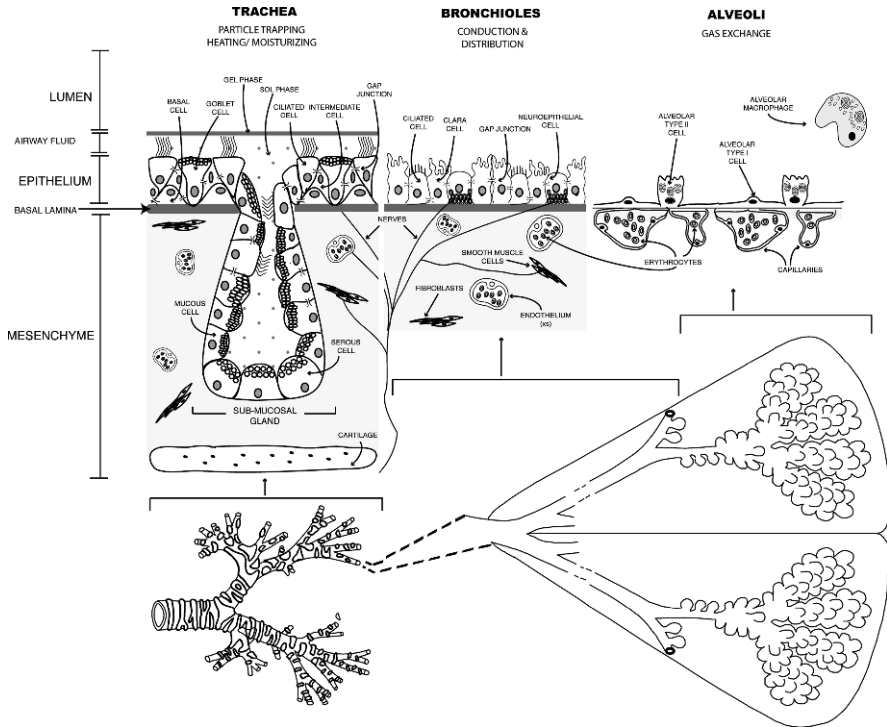


Fig. 4.1 Overview of the adult human lung anatomical and cellular architecture. *In the trachea and other gland-bearing large airways (left section of the figure)*, a prominent layer of mucus (to capture particles and bacteria) lies at the base of the lumen, pushed upwards to the glottis by the beating of cilia, present on cells residing in the epithelial layer. Co-occurring cells include basal cells (progenitor cells acting through intermediate cells which are intercalated throughout the epithelium). These cells can differentiate into all the epithelial cell types represented in the figure. Mucous cells (which, at baseline and upon injury, release granules containing mucins) are also present. The epithelium is anchored in a basal lamina, under which lies a large layer of mesenchyme. In this tissue, there are submucosal glands (containing mucous and serous cells) and scattered contractile patches of myofibroblasts and smooth muscle cells. The endothelium weaves throughout this layer, transporting erythrocytes through the tissue. This layer is rich in resident immune cells (plasmacytes, T lymphocytes, mast cells, macrophages). Intercellular gap junctions between adjacent cells facilitate transfer of cytosolic signaling molecules (horizontally) to synchronize ciliary movement and salt balance. *In the bronchioles (mid-section of the figure)*, the epithelium is composed of Clara cells, ciliated cells and neuroepithelial cells, which respond to environmental cues and communicate with the brain and neighboring tissues via nerve fibers. The mesenchyme continues (but as a thinner layer) in the bronchioles with scattered immune cells, but without submucosal glands. *In the alveolar region (right section of the figure)*, the epithelial layer is composed of long, flat type I pneumocytes (optimized for gas exchange) and type II pneumocytes (surfactant-producing). It is specialized for minimizing travel distance for gas exchange by sharing a fused basal lamina with the capillaries, which carry erythrocytes returning to the heart after accepting fresh oxygen from alveoli

submucosal glands. The first waves of hematopoietic cells arise in the mesenchyme, featuring resident mast cells and macrophages [9].

3. Canalicular phase (16–26 weeks of gestation): during this phase, acini are developed through formation of the terminal bronchioles and downstream of these,

of 2–4 sets of respiratory bronchioles and terminal buds. Capillaries branch out from pre-acinar arteries while epithelial differentiation starts to occur in the small airways with the appearance of Clara cells. In the most distal areas, type I and II pneumocytes arise, leading to surfactant secretion. Alveolar macrophages start to appear in the distal lung lumen [9].

4. Saccular phase (24 weeks of gestation to term): during this phase, terminal buds open up, thus forming tubular sacs. The apposition of capillaries induces the functional differentiation of the acini, thus enabling gas exchange across the distal epithelium for the first time. Other key developments occurring during that phase include those of the lymphatic plexus and neuroepithelial bodies of the small airways.
5. Alveolar and postnatal growth phases (beyond 36 weeks of gestation): Alveoli appear at the distal end of terminal sacs, just before term. Their number then increases exponentially. At about 3–4 years of age, the multiplication of alveoli stops and the double capillaries present in the interalveolar septa become single capillaries. From then on and until the end of the growth phase for the thoracic cage (end of puberty), the surface area for gas exchange continues to grow through an increase in the mean diameter of alveoli.

4.2.2 Morphological Layers in the Lung

The complexity of the adult human lung can be approached through investigation of its morphological layers [10]. The lumen of the lung differs in its content, according to the blocks outlined above. In large airways, it contains a mucus made of a very dilute sol phase (originating from serous cells) allowing ciliary beating and a gel phase (originating from mucous and goblet cells) placed above, the high mucin content of which enables particle trapping. The cooperation between mucus-secreting cells and surface ciliated cells, beating in rhythm to move the gel phase towards the glottis is a first line of defense against inhaled particulates. Small airways feature a non-continuous layer of liquid which does not completely block access of airborne particles to the underlying epithelium. Finally, in the alveolar region, the lumen is bathed with surfactant (a tenso-active fluid preventing collapse of the alveolar lumen) but also features a resident cell, the alveolar macrophage. The alveolar macrophage is a key sentinel in the lumen of alveoli, participating in surfactant recycling and ingesting particles that have escaped initial trapping by mucus (e.g., asbestos fibers, nanofibers), while exerting a largely anti-inflammatory action towards unwanted inflammatory cells, like neutrophils.

The “noble” part of the lung, the epithelium, is often depicted as a simple layer, mediating exchanges between the outside environment and the mucosa. Figure 4.1 depicts the complexity of the lung epithelium, not only as a horizontal barrier, but also with regards to its vertical structure. In large airways, the surface epithelium is anchored to the basal lamina by basal cells, with intermediate cells and differentiated ciliated and goblet cells touching the gel phase. The invagination of this

surface epithelium into glands provides an enormous additional surface area for mucus production. At the level of their basal membrane, submucosal glands feature an important interaction with plasmacytes, importing immunoglobulin A molecules to which they add a secretory piece that confers resistance to proteases in the mucus. In transition from large to small airways, the epithelium becomes monostratified, yet it maintains an important functional diversity, featuring ciliated, neuroendocrine and Clara cells. The latter are rich in detoxifying enzymes, antimicrobial molecules and surface receptors and serve as the main protective cell type in this area. Finally, in the alveolar region, most of the surface (95%) is covered by elongated and flattened type I pneumocytes, optimized for gas exchange. Type II pneumocytes bulge into the lumen and bear visible cytoplasmic inclusions of surfactant, of which they are the prime source.

One would be mistaken however to limit one's focus to the epithelial layer, without considering its intimate relationship with the underlying mesenchyme (in large and small airways) and endothelium (in the alveolar region). Indeed, during development as well as repair, the mesenchyme and endothelium of the airways are cooperating with the epithelium both structurally, via cell-cell-contact, and via the exchange of morphogens and growth factors. The mesenchyme (fibroblasts, smooth muscle cells and myofibroblasts) of the lung is not uniform across discrete areas of the lung [11]. The endothelium features two distinct circulatory systems that irrigate the lung. The bronchial network brings oxygen to the lung as one of the organs in the body, while the pulmonary network, allows venous blood to return from the lungs to the heart rid of its carbon dioxide and reloaded with oxygen.

4.2.3 Spatial Layers in the Lung

The adult human lung exists as a continuous organ spanning a large surface. Schematically, one can refer to the overall surface as equivalent to that of a tennis court (depending on the individual's size, between 100 and 200 m²), with conducting airways represented by a racket laid on the court. Three blocks emerge when considering the spatial make-up of the lung (Fig. 4.1): (i) large (tracheobronchial) airways, featuring a biphasic mucus blanket, a ciliated and secretory pseudostratified surface epithelium and submucosal glands, a multilayered mesenchyme and a cartilaginous structural support; (ii) small (bronchiolar) airways, featuring a complex monostratified epithelium and a thinner mesenchyme; and (iii) the alveolar region, featuring a simple epithelium sharing a basal lamina with the underlying endothelium, thereby minimizing the traveling distance needed for gas exchange between the lung lumen and the blood flow.

Several notions emerge from the study of this spatial structure. First, within the epithelium itself, adjacent cells communicate via gap junctions, which provide a privileged route for the intercellular passage of small molecules. In the pseudostratified large airway epithelium, gap junctions exist between basal, intermediate and differentiated cells at the surface. The functional importance of gap junctions is often overlooked, yet remains considerable [12]. Take, for example, the pathological

context of cystic fibrosis (CF), the main autosomal recessive disease in Caucasians. CF is caused by mutations of the CF transmembrane conductance regulator (CFTR), an epithelial channel involved in apical ion transport and other functions. Thanks to intercellular gap junctions, it was demonstrated that as little as 5–20% of the mutated epithelium needs to be “replaced” (either by gene transfer or potentially, stem cell transfer, or both, see below) by wild-type CFTR-expressing cells to generate 50% or more of the normal transepithelial chloride current [13]. Of course, what is true for chloride ions in the case of CFTR is true for calcium ions (waves of which can bear an organizational role [14]) or for other small molecules with developmental roles, such as cytokines and morphogens [15].

Second, biological information can travel via the lung fluid. A variable range of molecular cues (pollutants, growth factors, morphogens) may be exchanged between different areas of the lung to drive development or repair at the organ level. The movement of such molecular cues depends on airflow, as well as on the coordinated movement of cilia. In large airways, cilia control the mucociliary escalator, directing the flow of the mucus, trapped particulates and chelated molecules towards the glottis. In small airways, cilia are sparse and may at most generate local flows and counterflows. Other molecular cues may be secreted and impregnate the extracellular matrix and instruct incoming/migrating epithelial cells, as during the initial stage of epithelial establishment (see above).

Third, there is evidence that functional feedback regulation can occur between these distant blocks via central and peripheral nervous systems, as instructed by a dense network of fibers. Such high-level functional integration is seen, for example in the adaptive reaction to allergens, featuring changes in airflow, mucus secretion, ciliary function, contractility, breathing rate, etc [16]. This example clearly illustrates how lung function depends on this complex spatial structure housing several cooperating systems (epithelial, endothelial, mesenchymal, nervous, hematopoietic). In that regard, it is important to consider the large differences that exist between this spatial structure and that of the lung in common *in vivo* models [17], notably rodents, pigs and even certain primates (at least those that are not bipedal and therefore feature different airflow, vascular dynamics and structural constraints than in humans).

4.3 “Stemness” and the Adult Human Lung

4.3.1 *Turnover and Repair in the Adult Human Lung*

The concept of “stemness” and how it relates to the adult human lung should be judged in the context of turnover and repair processes taking place in this organ. In health, as opposed to other entities with a high turnover rate (granulocytes, hepatocytes, epidermis, intestinal epithelium), the lung is a very stable structure. Its mesenchymal and endothelial elements undergo little turnover and epithelial subsets, across the organ, are believed to last for several weeks, if not months [10]. Normal function exposes the lung constantly to pollutants that may get past the

continuous mucus blanket covering large airways and deposit in the lumen of small airways. Clara cells within bronchioles are believed to play a major role in the detoxification of such inhaled pollutants, and as such, are considered the epithelial subset with the highest propensity for functional exhaustion, turnover and/or repair. Clara cells express various proteins with immunoregulatory and detoxifying roles, including Clara cell protein 10 kDa (CC10), as well as enzymes of the glutathione-S-transferase and cytochrome P450 families. In normal turnover/repair, senescent Clara cells or other subsets of epithelial cells undergo an orderly apoptotic demise. Neighboring cells literally squeeze out the apoptotic cell, temporarily extending their cytoplasmic footprint to fill the gap, thereby preserving the junctional integrity of the epithelial layer.

In pathological settings, several types of changes can occur to hematopoietic, endothelial, mesenchymal and/or epithelial compartments. With regards to hematopoietic and mesenchymal compartments, increased proliferation can occur for resident mast cells and fibroblasts in asthma. In chronic and acute lung transplant rejection and in idiopathic pulmonary fibrosis (IPF), mesenchymal cells are recruited, not to the submucosa, but to the lumen of the lung, thereby hampering gas exchange. Surface epithelial cells in large and small airways can also be subjected to abrasion in acute pollution/infection and reorganize into a pluristratified layer of poorly differentiated cells or mucous cells, the purpose of which is mainly to ensure the reconstitution of a physical barrier. In CF, where chronic infections with drug-resistant bacteria such as mucoid *Pseudomonas aeruginosa* are pervasive, such pluristratified accumulations can be found as high as in epithelial pockets lining the nasal conduits and sinuses. CF submucosal glands in large airways undergo a typical hyperplasia of mucous cells.

To better understand the dynamics of turnover and repair in the adult human lung, numerous attempts have been made to model these processes in specialized culture models and in animal models, with the limitations that we outlined above. Research in patients is necessarily limited to indirect assessments using lung fluid sampling and imaging, while biopsies are not always easy to justify ethically. In this difficult experimental context, the etiology of evolvable disease of abnormal turnover/repair such as IPF remains unknown. It has to be noted that aging in human adults (i.e., above 50 and older) is associated with an increase in lung disorders associated with an abnormal turnover/repair. These disorders include IPF and chronic obstructive pulmonary disease (COPD), a fatal chronic disease typically affecting long-time smokers, and which also features a significant inflammatory component. Cancer is also a prominent example of an age-related disease of the lung, which may feature disorders in the turnover/repair of epithelial, mesenchymal and secondarily, endothelial, compartments. While some forms of lung cancer are clearly linked to smoking (e.g., non-small cell lung adenocarcinoma), others (e.g., mesothelioma) are linked to exposure to asbestos and other types of inorganic fibers, triggering abnormal lung repair. Hence, the question of precursor cells as seen through the prism of normal and pathological turnover and repair has to be approached with attention given to age and life history, including the potential exposure to toxicants and carcinogens.

4.3.2 Progenitor Cells of the Adult Human Lung

In Fig. 4.2, we provide a synthesis of the current information available on the relationships between candidate precursor subsets and differentiated subsets in the adult human lung. Endogenous epithelial precursors are the basal and intermediate cells of the bronchi, the mucous cells of the glands, the Clara cells of the bronchioles and the type II pneumocytes of the alveoli. These cells seem particularly well suited to fulfill the roles of progenitors in the context of turnover and repair of the adult human lung epithelium, for a number of functional reasons.

Basal and intermediate cells of the bronchi are not in contact with the lumen but sense changes in neighboring, senescent ciliated and mucous cells via intercellular junctions and anchor the epithelium to the basement membrane. In bronchial

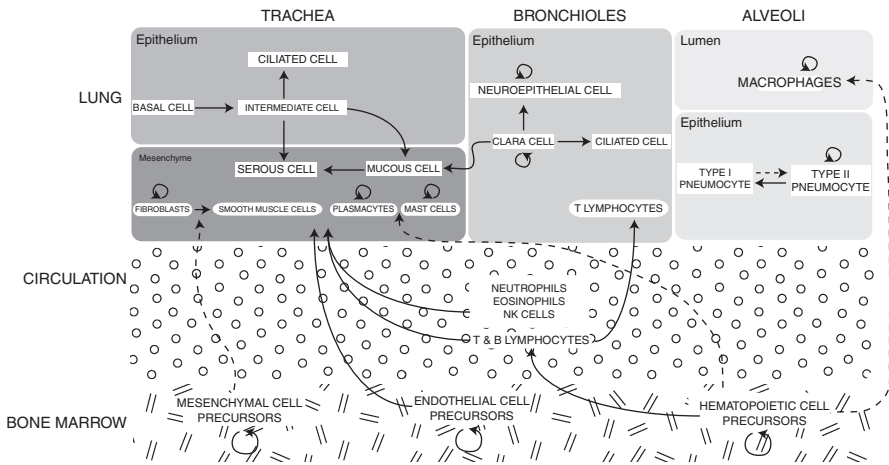


Fig. 4.2 Progenitor cells of the adult human lung. In humans, auto-renewing mesenchymal, endothelial, and hematopoietic precursor cells originating from the bone marrow are released into the circulation, later to reach the lung tissue. Some precursor cells are only transiently present in the circulation (indicated by *dashed lines*) and some travel through the peripheral vasculature and eventually reach the lung (indicated by *solid lines*). In the lung (divided into 3 distinct regions – trachea, bronchioles, alveoli), the tissue is stratified with different morphological layers (epithelium, mesenchyme, endothelium). The tracheal epithelium contains basal cells which give rise to intermediate cells, thereby able to differentiate into either ciliated cells, serous cells, and mucous cells (which can also give rise to serous cells). The mucous and serous cells reside in the tracheal mesenchyme, where a significant population of auto-renewing fibroblasts (which can differentiate into smooth muscle cells) and renewed hematopoietic cells (plasmacytes and mast cells) and other immune cells (neutrophils, eosinophils, NK cells, T and B lymphocytes) are found. The bronchiolar epithelium is composed of auto-renewing Clara cells, which can differentiate into ciliated cells and auto-renewing neuroepithelial cells, and even mucous cells. Alongside these cells in the terminal bronchiolar epithelium, Th2 lymphocytes circulate. In the alveolar epithelium, auto-renewing type II pneumocytes give rise to type I pneumocytes, and there may be evidence for type I pneumocytes having the ability to differentiate to type II pneumocytes (*dashed line arrow*). Renewable alveolar macrophages circulate within the lumen

glands, bronchioles and alveoli, mucous cells, Clara cells and type II pneumocytes, respectively, are the most metabolically active of all subsets and therefore may undergo the most ongoing damage, which requires the ability to sustain facilitated turnover/repair. As shown, mesenchymal, endothelial and hematopoietic compartments rely for their turnover and repair in the adult human lung on both resident and possibly, to a lesser extent, on precursors from remote areas in the body (e.g., bone marrow), transitioning via the circulation to home in the lungs.

As far as we know in humans, turnover and repair within the epithelial layer lining the adult lung occurs only via the proliferation and differentiation of resident precursors, to the exclusion of exogenous precursors. In natural cases of biological chimerism, i.e., pregnancies and transplantation, various degrees of lung colonization by exogenous precursors can be observed. Women with lung injury after male pregnancies were found to harbor significant numbers of male epithelial cells, mostly located to areas of injury [18]. In bone marrow transplant recipients, studies showed variable chimerism within the bronchial, bronchiolar and/or alveolar epithelium [19–21]. The degree of chimerism may be linked, in part, to the degree of damage sustained by the host lung during the myeloablative process [22]. Conversely, in lung transplant recipients, host cells are not systematically found within the donor lung epithelium [23], and if present, they cluster in areas of damage/repair [24] or cancer [25]. Hence, the contribution of exogenous precursors to the make-up of the human lung is greatly limited.

How then can we harness the power of either endogenous or exogenous precursors to contribute to the fabric of the organ? While this issue is readily tackled for other tissues, it remains a major unknown in lung research. Which properties are to be sought, that would qualify a precursor for efficient lung targeting? Which routes are to be pursued for such an *in vivo* targeting: systemic (via the endothelial system) or topical (deposition via a bronchoscope in discrete areas)? How to control the integration and subsequent differentiation of such precursors into the lung fabric? Does such control require significant conditioning of mesenchymal and/or endothelial cell layers that cooperate with the lung epithelium *in vivo*? These are some of the outstanding questions that currently limit the use of precursor cells in the context of the adult human lung.

Even if obstacles to the orderly insertion of therapeutic stem cells in the diseased human lung can be lifted, are candidate stem cells already at disposal? Mouse embryonic stem cells can be induced in culture to develop into airway cells [26], but related investigations on human ES cells are limited by ethical and technical considerations, and simply barred in some countries. The more accessible and ethically neutral bone marrow derived mesenchymal stem cells (MSC) cultured in the presence of human airway epithelial cells express airway cell markers, including cytokeratin, occludin and CFTR [27]. Native MSC-like stem cells have been recently, for the first time, prospectively identified and purified by some of us from multiple human tissues, including lung [28, 29]. Authors of the present review have also previously identified, by aquaporin 3 expression, and purified a population of basal cells in the human airway mucosa that can regenerate the proximal airway epithelium [30]. Considerable work still needs to be performed, though,

in order to document the full developmental potential, sustained activity and, as mentioned above, transplantability of such putative progenitors, as well as those identified by other groups [31], in the human lung. Arguably, direct stimulation in the patient, with exogenous growth factors, of discrete progenitor cell subsets (on the model of the routine activation of hematopoiesis) would alleviate the hurdle of stem cell engraftment in the lung. Stimulating factors for respiratory tissue progenitors remain, however, obviously unknown in the absence of a clear identification of these cells.

Collectively, these questions make the advent of precursor cell-based therapies for outstanding lung diseases such as CF, IPF, COPD, highly unlikely in the near future. Recent progress in stem cell research has nevertheless taught us to be optimistic about the occurrence of uncommon breakthroughs that can suddenly open up a field of endeavor. More realistically, much groundwork will need to be performed to understand the biology of human precursor cells in the adult human lung and to test their ability to promote normal function when targeted to a diseased area before we can envision this as a viable therapeutic option. It is important that this groundwork be thoroughly done before raising too much hope. Relevant to this issue is the once greatly overhyped idea, that stem cell based therapies were just around the corner for CF, leaving families of patients with a lot of resentment and unfulfilled expectations.

4.4 Protocols

As stated above, the field of lung stem cells is still in its infancy, with various limitations inherent to the organ and its physiology. While different approaches may be taken towards the study of adult human lung stem cells, we chose to highlight here a practical approach for isolating candidate progenitors from the adult human lung itself (Section 4.4.1) and selecting these cells further using cell sorting (Section 4.1.4). Upon differentiation *in vitro* (Section 4.4.2) and testing for various phenotypical and functional properties (Section 4.4.3), cells can be isolated and selected again, thereby allowing for another differentiation cycle to be performed.

4.4.1 Isolation of Endogenous Candidate Progenitors for the Adult Human Lung

We will not elaborate here on the question of exogenous precursors for the adult human lung. As argued earlier, there is no current notion that exogenous precursors may play more than a negligible role in the make-up of the normal adult lung, or that they could participate in the regeneration of an injured lung to a significant level. Our focus here will therefore be on endogenous precursors, *i.e.*, basal cells for bronchi, Clara cells for bronchioles and type II pneumocytes for alveoli. Hence, the protocol described below involves the collection of primary lung tissue from

adult donors, followed by the proteolytic dissociation of dissected airways to isolate candidate progenitors, among other cell subsets.

4.4.1.1 Dissection of Airway Segments from Lung Transplant Donor Tissue

This step describes a simple protocol for optimizing cell yield from adult human lung tissue. The best source is tissue that has been harvested surgically for transplantation but has been resected or rejected, yet has remained in excellent condition, i.e., is collected by the laboratory in the original sterile physiological solution less than 12 h after recovery. While our previous experiments with fetal tissue have demonstrated that such tissues can retain high proliferative activity in certain areas even 24 h after dissection, postnatal and adult tissue are much less resistant in that regard. Hence, it is important to obtain adult human lung tissue as fresh as possible. See also ref [32] for useful details.

Material

- Laboratories interested in collecting cells from adult human lung tissue must be current in their institutional approval and health and safety certificates for human tissue handling and bloodborne pathogens.
- Dissection is performed in a laminar flow hood that must be thoroughly decontaminated before and after the dissection using bleach and ethanol 70%.
- Personnel must wear sterile gloves and use autoclaved surgical instruments (scalpel with interchangeable sterile blades, two pairs of large forceps, two pairs of fine forceps, one pair of large scissors, one pair of fine scissors).
- Medium used in this step is phosphate buffered saline (Sigma), 2.5 mM ethylene diamine tetra acetic acid (EDTA, also from Sigma), a cation chelator that traps calcium and magnesium ions and prevents cell clumping.

Preparation of Airways for Proteolytic Dissociation

- Primary tissue is transferred to a large dissection plate, ice-cold PBS-EDTA is added and the tissue is methodically trimmed in the following manner.
- First, extrapulmonary tissue is dissected out, leaving the cartilage bare.
- Second, trachea, primary and secondary bronchi are dissected out and cut into cylinders of 2–3 cm of length.
- Third, bronchioles are dissected as part of the surrounding tissue, and cleaned on the outside as much as possible, keeping in mind that these are not rigid as cartilage-bearing airways and therefore are more fragile.
- Fourth, whole intact alveolar acini are dissected to enable type II pneumocyte isolation.
- After being dissected, tissues are rinsed four consecutive times with ice-cold PBS-EDTA (10 min incubation each, with gentle vortexing), to remove residual fragments, mucus and debris.

4.4.1.2 Proteolytic Dissociation of Dissected Airways

Material

- Medium in this step is Dulbecco Modified Eagle's Medium -DMEM- (Invitrogen), 2.5 mM EDTA.
- Proteolytic dissociation uses pronase (Sigma), a gentle yet efficient enzyme that does not damage surface antigens as trypsin does.
- Hematocytometer and microscope for cell counting.

Method

- Dissected tissues are placed in a 50 ml Falcon tube (BD Biosciences) and incubated with 0.1% pronase dissolved in DMEM for 36 h at 37°C in a 5% CO₂ incubator.
- After 12 and 24 h, vortex the 50 ml Falcon tube for 5 min at moderate speed and replace in the incubator.
- After 36 h, vortex the 50 ml Falcon tube for 5 min at moderate speed and collect the supernatant.
- Centrifuge at 800g for 10 min at 4°C, remove the supernatant.
- Resuspend the cells in DMEM-EDTA and wash three times (10-min incubation between washes, followed by 800g, 10-min centrifugation).
- Count a 10- μ l aliquot in a hematocytometer and keep on ice until further use.

Note: Access to transplant tissue can be very difficult to secure. Alternatively, laboratories may purchase bronchial or bronchiolar primary cells (alveolar cells are not available) from commercial sources such as Lonza (Basel, Switzerland).

4.4.1.3 FACS Staining Strategies

Cells are prepared for sorting by FACS using staining cocktails of fluorescent markers for viability, positive and negative selection [33]. It is important that viability markers are used to prevent contamination of sorted fractions with cells that have been damaged by the isolation protocol (Section 4.4.1). Also, one should stress the importance of negative markers (excluding viable cells that are not desired), to complement positive markers (expressed by the candidate cells). The choice of fluorochromes is also very important since many cells harvested from lungs are characterized by a high autofluorescence in certain wavelengths and hence, fluorescence channels have to be chosen appropriately to enable optimal cell sorting.

Reagents

- Reagents for FACS staining are available through various sources. BD Biosciences (San Jose, CA, USA) and Invitrogen (Carlsbad, CA, USA) are excellent sources for antibodies and probes, as well as conjugation kits for customizing antibody/fluorochrome conjugates.
- Viability markers are classically based on the staining of nucleic acids (e.g., propidium iodide) by cell-impermeant probes, which therefore label only cells with

a compromised membrane. However, these probes are sometimes toxic. Besides, in the lung, there can be significant binding of such probes to extracellular DNA present on the surface of cells (notably in the case of proteolytic dissociation), as well as in apoptotic bodies that are scavenged by cells, thereby creating false positives (viable cells that appear compromised or dead). The Live/Dead series of markers, from Invitrogen, is amino-based and does not suffer from these limitations. Live/Dead markers are stable, non-toxic, and provide 2–3 Log separation of live vs. compromised and dead cells. Live/Dead markers are available as violet-, blue-, green- and red-laser excited probes and can be easily multiplexed with positive and negative markers.

- Negative markers are necessary to exclude unwanted cells from candidate populations. For the sorting of candidate epithelial progenitors, one would want to exclude cells of hematopoietic, endothelial and mesenchymal lineages. These can be taken care of by staining with the CD14/34/45, CD31/von Willebrand Factor and CD29/73/90/105 cocktails, respectively. Importantly, since these markers are all used for negative selection, they can all be conjugated to the same fluorochrome and used in a so-called “dump” gate [33].
- Positive markers are used to zoom in on the candidate population of choice. Although the search for markers is very active and constantly yielding new candidates, the best candidates are currently as follows. For basal cells of the bronchi, these include CD142 (tissue factor), the CD151 tetraspanin, as well as the aquaporin-3 [34, 35]. Beware that these markers are not specific and therefore require the use of negative markers to exclude unwanted true positives (e.g., CD151 can be co-expressed by certain endothelial and mesenchymal cells). For Clara cells of the bronchioles, the surface protein CC10 is the best bet and the same is true of the surfactant protein A receptor (SPAR) for the type II pneumocytes in alveoli. Here again, it is highly advisable to use negative markers to clean up the positive gate.

Staining Strategy

- To optimize signal-to-noise properties, it is generally recommended to use viability markers in a green-excited channel (e.g., phycoerythrin channel excited by the 532 nm laser line) or blue-excited channel (e.g., fluorescein channel excited by the 488 nm laser line), where the autofluorescence of dissociated cells is maximal, yet will not perturb the readout from efficient viability markers such as the Live/Dead series.
- Negative markers can be all put in one color, e.g., in blue- or green-excited channels, depending on the channel chosen for the viability marker above.
- Positive marker(s) can be chosen for excitation by the third, and if available fourth laser line. Ideally one can use two markers excited respectively by the ultraviolet/violet line (356 or 407 nm), such as Cascade Blue/Pacific Blue, and the red line (632 nm), such as allophycocyanin or Alexa 647.
- Before performing FACS sorts, always run several experiments with one or several staining controls (fluorescence-minus one controls omitting one marker and

leaving all other constant) to assess the feasibility and quality of the staining strategy on the cells of interest.

Staining Protocol

- Cells are kept at 4°C, on melting ice, throughout the staining procedure and are stained and washed in PBS-EDTA, as described in Section 4.1.2. These measures prevent cell clumping.
- Cells are resuspended at 5×10^6 per ml in PBS-EDTA. They are mixed with a staining cocktail made in PBS-EDTA, comprising a viability marker, as well as negative and positive antibodies, according to the titers defined by the manufacturer or the laboratory (some antibodies may require titration).
- Cells are incubated with the staining cocktail for 30 min in the dark, at 4°C, with occasional vortexing (every 5 min).
- Cells are washed with excess PBS-EDTA (generally 50 times the staining volume, e.g., 5 ml if the final staining volume was 100 μ l) and centrifuged at 800g for 5 min, at 4°C.
- The supernatant is aspirated and cells are resuspended gently in PBS-EDTA to a concentration of 5×10^6 per ml, for FACS sorting.

4.4.1.4 FACS Sorting

FACS sorting is the most efficient, rapid and repeatable way to select candidate progenitors for downstream applications, such as in vitro differentiation (Section 4.4.2). Sorting is best performed on 3- or 4-laser sorters, such as the FACS Aria (BD Biosciences) or the MoFlo (Dako Cytomation, Carpinteria, CA, USA).

Cell Sorting

- Sorting should be performed according to the guidelines relevant for the machine used, as they will differ between a FACS Aria and a MoFlo, for example.
- The sorters should be calibrated every day using sets of fluorescent beads, so as to maintain similar signal output from lasers (see details in [33]).
- Prior to running the sample of interest, the cell sorter should be sterilized by running bleach through the fluidics for at least 15 min, followed by 15 min of sterile water.
- These above sorters are capable of single-cell (clonal) sorting using 96-well plates and may sort up to $10\text{--}20 \times 10^3$ cells per second, in conservative sorts. It is advisable not to push the performance of these sorters up to their maximal advertised sorting speeds (several tens of thousands per second), which are usually attained using homogeneous sets of non-biological beads.
- Positive sorted fractions are defined analytically as “low” for the Live/Dead marker, “low or negative” for the negative marker set and “positive or high” for the positive marker set.

- Negative sorted fractions should also be obtained at the same time, for control purposes, and are defined analytically as “low” for the Live/Dead marker, “positive or high” for the negative marker set and “low or negative” for the positive marker set.
- Both positive and negative sorting gates should be stored in analytical files during the session on the FACS machine, for purposes of documentation.
- Sorted fractions should be retrieved in sterile Falcon tubes, filled halfway with sterile PBS-EDTA and maintained on ice.
- After sorting, the harvested fractions (positive and negative) are counted and part of these fractions is run through the sorter again for reanalysis [33], so as to ascertain the quality of the sort and for purposes of documentation.

4.4.2 Differentiation of Candidate Progenitors in Air–Liquid Interface Filter Cultures

This step involves the seeding of candidate progenitors onto permeable filters and the establishment of a differentiated culture at the air–liquid interface. These culture models enable the establishment of a polarized epithelium and have proven useful for assessing bronchial, bronchiolar, and more rarely, alveolar progenitors. After a first period of serum-supported proliferation, cells are switched to a serum-free medium that is conducive to differentiation. This leads to the establishment of an air–liquid interface at their apical surface, which is reminiscent of their physiological conditions, *in vivo*. Permeable filter culture has the additional advantage of allowing routine microscopic inspections, as well as enabling separate access to the basal and apical aspects of the culture. For example, one can sample the two separate compartments to try and identify secreted factors that may regulate progenitor growth and differentiation in autocrine/paracrine fashion [36]. This model may also be amenable to coculture with endothelial cells, to study the interaction between endothelial and epithelial layers in turnover and repair [37].

4.4.2.1 Seeding and Proliferation onto Permeable Filters

Permeable filters offer a customizable platform for growing candidate progenitors on a chosen matrix (a key element in epithelial differentiation, as argued in Section 4.2), and in chosen conditions for the basal and apical medium, once the culture is confluent and polarized (i.e., excluding basal medium from the apical surface, thanks to tight junctions).

Material

- Permeable filters are available commercially from Millipore (Billerica, MA, USA) and Corning/Costar (sold through Sigma). We prefer the Corning/Costar set dubbed snapwells, which correspond to permeable polycarbonate filter that

snap onto a holder, itself placed in culture wells to hold the filter suspended in the well.

- Snapwells come in different sizes (corresponding to 6 and 24-well plates) and in three pore sizes: 0.4, 3.0 and 5.0 μm of pore diameter. Pore size influences the speed of layer establishment: it is faster with 0.4 μm pores than with 3.0 and 5.0 pores. However, in case where one wants to study the potential transmigration of immune cells through a developed layer, the 3.0 or 5.0 pore sizes are more appropriate.
- It is imperative to coat the filter surface with a matrix substrate, to enable adhesion of candidate progenitors. In our experience, human placental collagen (Sigma) is the best all-around substrate for this purpose, surpassing rat tail collagen or other substrates.
- The serum-containing M1 medium used for the seeding and growth phases consists in 88% of a 1:1 mix of DMEM and Ham's F12, 10% (v/v) fetal bovine serum, 1% (v/v) L-glutamine and 1% (v/v) penicillin-streptomycin. Alternatively, one can use commercial media from Lonza optimized for airway epithelial cultures.

Seeding and Growth Phases

- Cells are seeded on HPC-coated filters at $2\text{--}5 \times 10^5$ cells/cm². This density prevents under-/over-crowding and also allows cells to establish paracrine and cell-cell communications during the first couple of days in culture.
- Cells are fed with M1 medium basally (in the well) and apically (on top of the filter).
- Cells are grown at 37°C in a 20% O₂ incubator, with 5% CO₂.
- On day 2, and every other day from then on, M1 medium is removed and the culture is rinsed basally with PBS-EDTA.
- Under an inverted microscope, the filter culture is checked for confluence and for the appearance of PBS-EDTA in the apical surface.
- If the filter is less than 90% confluent and/or if PBS-EDTA appears apically, the PBS-EDTA is removed and replaced by M1 medium basally and apically.
- If the culture is more than 90% confluent, the PBS-EDTA is removed and the culture is treated as described below (Section 4.4.2.2).

4.4.2.2 Establishment of a Differentiated Culture at Air-Liquid Interface

Material

- The M2 medium here uses the Ultrosor G (BioSeptra, Cergy, France) serum substitute, available in the USA through Pall Life Science (Ann Arbor, MI). M2 medium consists in 96% of a 1:1 mix of DMEM and Ham's F12, 2% (v/v) Ultrosor G, 1% (v/v) L-glutamine and 1% (v/v) penicillin-streptomycin.

Differentiation Phase

- Filter cultures are exposed to M2 medium on their basal surface only, leaving the apical surface exposed to air.
- Every other day, the basal medium is replaced and the apical aspect of the filter culture is checked for the presence of colored medium, to assess the tightness of the epithelium.
- Cells are continuously grown at 37°C in a 20% O₂ incubator, with 5% CO₂.
- By day 8–12, and for at least 12–24 days from then on, the culture should be tight, polarized and should gradually acquire properties of a differentiated epithelial layer, as assayed through various means, including procedures described in Section 4.4.3.

Note: Besides this air–liquid interface filter culture model, other models may be conducive to studies of adult human lung progenitor cells, such as the tridimensional spheroid culture model [34]. Also, since this series is dedicated to Human Cell Culture, we did not present protocols for the development of candidate progenitors in ex vivo xenograft models, be they in nude or severe combined immunodeficiency mice. Such models are detailed in publications by some of the present authors [34, 35], as well as by other groups [4] and collectively enable the differentiation of bronchial surface epithelium as well as submucosal glands, but not bronchiolar or alveolar epithelia.

4.4.3 Functional Characterization of Developed Epithelial Layers

This step involves the characterization of epithelial layers developed on filters by electrophysiological assays using Ussing chambers, as well as by morphological assays using electron microscopy.

4.4.3.1 Electrophysiological Assessment in the Ussing Chamber

Ussing chambers are made of two hemi-chambers that can be used to mount the air interface culture filters without edge damage. Ussing chambers are connected to a voltage clamp that can measure ion transport across the two hemi-chambers, i.e., across the epithelial layer that is mounted in-between. Different buffers (complete or depleted in certain ions), as well as drugs (agonists or antagonists of ion transport) can be added independently to one or both hemi-chambers, i.e., to the basal and/or apical sides of the epithelial layer, thereby allowing to dissect out the contribution of various basally or apically expressed channels to the transepithelial current. In the particular case of progenitor cell-derived lung epithelial layers, it is of great interest to correlate the degree of epithelial differentiation within the developed layer to the presence of channels expressed in vivo, notably the CFTR and the epithelial sodium channel (ENaC). Readers are encouraged to check reference [32]

for additional details and picture description of the Ussing chamber apparatus. Note that this method is non-destructive and filter cultures that have been tested in an Ussing chamber can be subsequently submitted to proteolytic dissociation to isolate cells of interest.

Buffers and Drugs

- All chemicals used for buffer preparation or as drugs in Ussing chamber experiments can be purchased from Sigma, St Louis, MO, USA.
- Regular buffer (Krebs Henseleit or KH) composition is: 117 mM NaCl, 25 mM NaHCO₃, 1.2 mM MgSO₄(H₂O)₇, 2.5 mM CaCl₂, 1.2 mM KH₂PO₄, 4.7 mM KCl. For ion depletion studies, Cl⁻ can be replaced with isethionate, HCO₃⁻ with HEPES, and Na⁺ with N-methyl-D-glucamine (NMDG).
- The Cl⁻-free solution is: 117 mM Na-isethionate, 25 mM NaHCO₃, 1.2 mM MgSO₄ (H₂O)₇, 2.5 mM Ca(NO₃)₂, 1.2 mM KH₂PO₄, and 4.7 mM KNO₃.
- The Cl⁻/HCO₃⁻-free solution is: 132 mM Na-isethionate, 10 mM HEPES, 1.2 mM MgSO₄(H₂O)₇, 2.5 mM Ca(NO₃)₂, 1.2 mM KH₂PO₄, 4.7 mM KNO₃.
- The Na⁺-free solution is: 132 mM NMDG, 10 mM HEPES, 1.2 mM MgSO₄ (H₂O)₇, 2.5 mM CaCl₂, 1.2 mM KH₂PO₄, 4.7 mM KCl.
- Drugs are added in small volumes from concentrated stocks.
- Typical drugs for the assessment of ion transport properties in airway epithelium include the cyclic AMP agonist and CFTR activator forskolin (10 μM from 10 mM stock in DMSO), the ENaC blocker amiloride (10 μM from 10 mM stock in double distilled water), the chloride and bicarbonate channel blockers (acting more or less specifically on CFTR and other channels) CFTRinh-172 (100 μM from 100 mM stock in DMSO), diphenylamine-2-carboxylate (1.5 mM from 500 mM stock in dimethyl sulfoxide -DMSO), glibenclamide (600 μM from 200 mM stock in DMSO) and nitro-phenylpropyl-amino-benzoate (100 μM from 100 mM stock in DMSO).
- In typical experiments, both sides of the filters are bathed with 12 ml of either regular KH buffer or ion depletion buffer with an osmolarity of 320 and pH of 7.4 at 37°C, containing 10 mM glucose.

Typical Ussing Chamber Experiment

- Commercial Ussing chambers fitted for filter cultures, as well as attached high-impedance electrometer can be purchased from WPI, Sarasota, FL, USA.
- Voltage is clamped to 0 and the current recorded. Pulses of 2 mV are applied every 2 s to determine conductance. Transepithelial potential difference is measured with agar bridges connected to a high-impedance electrometer. The amount of current needed to maintain this voltage clamp is measured continuously on a chart recorder and on a computer equipped with an Ussing chamber interface and software (ADInstruments, Grand Junction, CO, USA).
- Agar bridges are 0.4%, 3 M KCl for regular KH, 1 M Na-isethionate bridges is used for Cl⁻- and Cl⁻/HCO₃⁻-free experiments to prevent Cl⁻ contamination of the buffer.

- Solutions are gassed at the rate of one bubble/second with 95% O₂–5% CO₂ for regular and Cl⁻- and Na⁺-free conditions, and with 100% O₂ for HCO₃⁻- and Cl⁻/HCO₃⁻-free experiments to maintain pH.
- Mounting of filter cultures: the Ussing chamber apparatus is left to equilibrate in running conditions for at least 5 min before the liquid columns connected to each hemi-chamber are clamped, disconnected from the hemi-chambers, and the hemi-chambers removed from the apparatus. The filter is mounted by snapping it into place between the two hemi-chambers (one hemi-chamber contains a fitted hole for the filter). The hemi-chambers are gently placed back in the apparatus, reconnected to the liquid columns and the clamps removed to allow circulation of the liquid and gas back into the chamber.
- It is important to check for the presence of air bubbles during the unmounting/mounting procedure and remove them through gentle tapping of the tubes, otherwise the free flow of current is hampered.
- Once the filter is properly in place between the two hemi-chambers, measures of current intensity, and transepithelial conductance to ions are obtained through the computer interface, thereby documenting the presence/absence of certain channels, the response to drugs and the relative contribution of these channels to transepithelial current in the developed layer.

4.4.3.2 Morphological Assays Using Electron Microscopy

Electron microscopy is the method of choice for documenting the structural aspects of developed lung epithelial layers deriving from candidate progenitors. This technique is well-suited to the analysis of air-interface culture filters. Scanning electron microscopy (SEM) is performed on filters fixed en-masse and provides an assessment of the apical surface of the culture, allowing notably for the identification of cilia or membrane protrusions, typical of ciliated cells, Clara cells and type II pneumocytes. Transmission electron microscopy (TEM) is performed on ultrathin sections of fixed/dried air-interface culture filters. TEM provides information enabling the submicroscopic analysis of the layer's architecture and substructure, including intercellular junctions, intracellular granules, cilia and protrusions and membrane anchorage. TEM provides much higher spatial resolution than SEM but is more cumbersome to implement (sample preparation for TEM includes embedding and sectioning). As opposed to the Ussing chamber, SEM and TEM procedures are destructive techniques that prevent any subsequent use of the filter cultures.

Material

- Material for SEM/TEM protocols includes chemicals and specialized items such as specimen holders and equipment such as a critical-point dryer. All of these can be purchased commercially through specialized vendors such as Tousimis (Rockville, MD, USA) and JB EM Services (Dorval, QC, Canada).
- SEM and TEM machines are extremely onerous and these assays are best performed through institutional facilities, with the help of trained personnel.

Main commercial sources for electron microscopes are Philips (Eindhoven, The Netherlands) and Amray (Bedford, MA, USA) and Philips and JEOL (Tokyo, Japan), for SEM and TEM, respectively.

Sample Preparation: Fixation, Post-Fixation and Drying

- Filter cultures are fixed en-masse, overnight, at 4°C in 2 ml fixative (2.5% glutaraldehyde in 0.1 M Na cacodylate buffer).
- Filters are rinsed 3 times with 2 ml buffer for 3 min and post-fixed for 2 h at 4°C in 2 ml 1% OsO₄ solution in 0.1 M Na cacodylate buffer (prepared just before use).
- Filters are then rinsed 3 times with buffer and dehydrated in sequential baths of 35, 50, 70, 95 and 100% ethanol (10 min each) at room temperature.
- Filters are then either air-dried from hexamethyldisilazane or critical-point dried from liquid carbon dioxide, according to standard protocols.
- Filters are then cut out from the holders using a scalpel blade, by following the circular boundary between the filter membrane and the surrounding plastic.

SEM Protocol

- For SEM, fixed, post-fixed and dried filters are glued in a flat position onto aluminium specimen holders with a silver conductive adhesive paste.
- Approximately 150 Å of platinum is applied in a cooled triode sputter coater (Polaron, Newhaven, UK).
- Samples are viewed in the secondary electron mode, 20 kV accelerating voltage in the SEM and images are collected using an imaging hardware/software combination such as the DigiScan hardware with Digital Micrograph software (Gatan, Pleasanton, CA).

TEM Protocol

- For TEM, fixed, post-fixed and dried filters are embedded in Araldite and sectioned into ultra-thin (40–100 nm) sections.
- Ultra-thin sections are mounted on copper grids and stained with uranyl acetate and lead citrate.
- Samples are viewed in the TEM and images are collected using an imaging hardware/software combination such as the DigiScan hardware with TEM AutoTune software (Gatan).

Note: As mentioned in the introductory paragraph to this Protocols section, the procedure described in Section 4.4.1.2 can be used on filters covered with developed epithelial layers to harvest cell suspensions by proteolysis and to process the suspensions through flow cytometric staining and sorting, as described in Sections 4.4.1.3 and 4.4.1.4. This will lead to the isolation of candidate progenitors and will enable the whole cycle to be restarted. This recursive protocol can be depicted as: isolation

-> selection -> differentiation -> testing -> isolation -> etc. This variant of the protocol enables the expansion of putative stem cells (i.e., basal cells, Clara cells, which can both generate their likes upon differentiation in vitro) from an initial pool which is necessary limited in number because of the low yield inherent to resected tissues.

The derivation of disease-specific induced pluripotent stem cells obtained through reprogramming of adult epithelial cells (from skin), as published in late 2008 (Park IH, Arora N, Huo H et al. (2008) Disease-specific induced pluripotent stem cells. *Cell* 134:877–886) opens new possibilities for progenitor-cell based therapies for epithelial disease. Careful validation of this approach in the context of therapeutic transfer to the human lung remains an essential, and difficult, hurdle to clear.

References

1. Krause DS, Theise ND, Collector MI et al. (2001) Multi-organ, multi-lineage engraftment by a single bone marrow-derived stem cell. *Cell* 105:369–77
2. Kotton DN, Fabian AJ, Mulligan RC (2005) Failure of bone marrow to reconstitute lung epithelium. *Am J Respir Cell Mol Biol* 33:328–34
3. Kim CF (2007) Paving the road for lung stem cell biology: bronchioalveolar stem cells and other putative distal lung stem cells. *Am J Physiol Lung Cell Mol Physiol* 293:L1092–8
4. Liu X, Driskell RR, Engelhardt JF (2006) Stem cells in the lung. *Methods Enzymol* 419: 285–321
5. Randell SH (2006) Airway epithelial stem cells and the pathophysiology of chronic obstructive pulmonary disease. *Proc Am Thorac Soc* 3:718–25
6. Rawlins EL, Hogan BL (2006) Epithelial stem cells of the lung: privileged few or opportunities for many? *Development* 133:2455–65
7. Hilfer SR (1996) Morphogenesis of the lung: control of embryonic and fetal branching. *Annu Rev Physiol* 58:93–113
8. Jeffery PK (1998) The development of large and small airways. *Am J Respir Crit Care Med* 157:S174–80
9. Tirouvanziam R, Khazaal I, N'Sonde V et al. (2002) Ex vivo development of functional human lymph node and bronchus-associated lymphoid tissue. *Blood* 99:2483–9
10. Mason RJ, Murray JF, Broaddus VC et al. (2005) Textbook in respiratory medicine. Elsevier-Saunders, Philadelphia
11. Kotaru C, Schoonover KJ, Trudeau JB et al. (2006) Regional fibroblast heterogeneity in the lung: implications for remodeling. *Am J Respir Crit Care Med* 173:1208–15
12. Boitano S, Dirksen ER, Sanderson MJ (1992) Intercellular propagation of calcium waves mediated by inositol trisphosphate. *Science* 258:292–5
13. Farnen SL, Karp PH, Ng P et al. (2005) Gene transfer of CFTR to airway epithelia: low levels of expression are sufficient to correct Cl⁻ transport and overexpression can generate basolateral CFTR. *Am J Physiol Lung Cell Mol Physiol* 289:L1123–30
14. Rabito CA, Jarrell JA, Scott JA (1987) Gap junctions and synchronization of polarization process during epithelial reorganization. *Am J Physiol* 253:C329–36
15. Lechner H, Josten F, Fuss B et al. (2007) Cross regulation of intercellular gap junction communication and paracrine signaling pathways during organogenesis in *Drosophila*. *Dev Biol* 310:23–34
16. Bleecker ER (1986) Cholinergic and neurogenic mechanisms in obstructive airways disease. *Am J Med* 81:93–102
17. Tsujino I, Kawakami Y, Kaneko A (2005) Comparative simulation of gas transport in airway models of rat, dog, and human. *Inhal Toxicol* 17:475–85

18. O'Donoghue K, Sultan HA, Al-Allaf FA et al. (2008) Microchimeric fetal cells cluster at sites of tissue injury in lung decades after pregnancy. *Reprod Biomed Online* 16:382–90
19. Mattsson J, Jansson M, Wernerson A et al. (2004) Lung epithelial cells and type II pneumocytes of donor origin after allogeneic hematopoietic stem cell transplantation. *Transplantation* 78:154–7
20. Suratt BT, Cool CD, Serls AE et al. (2003) Human pulmonary chimerism after hematopoietic stem cell transplantation. *Am J Respir Crit Care Med* 168:318–22
21. Zander DS, Baz MA, Cogle CR et al. (2005) Bone marrow-derived stem-cell repopulation contributes minimally to the Type II pneumocyte pool in transplanted human lungs. *Transplantation* 80:206–12
22. Herzog EL, Van Arnem J, Hu B et al. (2006) Threshold of lung injury required for the appearance of marrow-derived lung epithelia. *Stem Cells* 24:1986–92
23. Bittmann I, Dose T, Baretton GB et al. (2001) Cellular chimerism of the lung after transplantation. An interphase cytogenetic study. *Am J Clin Pathol* 115:525–33
24. Kleeburger W, Versmold A, Rothamel T et al. (2003) Increased chimerism of bronchial and alveolar epithelium in human lung allografts undergoing chronic injury. *Am J Pathol* 162:1487–94
25. Picard C, Grenet D, Copie-Bergman C et al. (2006) Small-cell lung carcinoma of recipient origin after bilateral lung transplantation for cystic fibrosis. *J Heart Lung Transplant* 25:981–4
26. Denham M, Cole TJ, Mollard R (2006) Embryonic stem cells form glandular structures and express surfactant protein C following culture with dissociated fetal respiratory tissue. *Am J Physiol Lung Cell Mol Physiol* 290:L1210–5
27. Wang G, Bunnell BA, Painter RG et al. (2005) Adult stem cells from bone marrow stroma differentiate into airway epithelial cells: potential therapy for cystic fibrosis. *Proc Natl Acad Sci U S A* 102:186–91
28. Crisan M, Yap S, Casteilla L et al. (2008) A perivascular origin for mesenchymal stem cells in multiple human organs. *Cell Stem Cell* 3:301–13
29. Crisan M, Deasy B, Gavina M et al. (2008) Purification and long-term culture of multipotent progenitor cells affiliated with the walls of human blood vessels: myoendothelial cells and pericytes. *Methods Cell Biol* 86:295–309
30. Giangreco A, Reynolds SD, Stripp BR (2002) Terminal bronchioles harbor a unique airway stem cell population that localizes to the bronchoalveolar duct junction. *Am J Pathol* 161:173–82
31. Avril-Delplanque A, Casal I, Castillon N et al. (2005) Aquaporin-3 expression in human fetal airway epithelial progenitor cells. *Stem Cells* 23:992–1001
32. Karp PH, Moninger TO, Weber SP et al. (2002) An in vitro model of differentiated human airway epithelia. Methods for establishing primary cultures. *Methods Mol Biol* 188:115–37
33. Tung JW, Heydari K, Tirouvanziam R et al. (2007) Modern flow cytometry: a practical approach. *Clin Lab Med* 27:453–68
34. Castillon N, Avril-Delplanque A, Coraux C et al. (2004) Regeneration of a well-differentiated human airway surface epithelium by spheroid and lentivirus vector-transduced airway cells. *J Gene Med* 6:846–56
35. Delplanque A, Coraux C, Tirouvanziam R et al. (2000) Epithelial stem cell-mediated development of the human respiratory mucosa in SCID mice. *J Cell Sci* 113 (Pt 5):767–78
36. Ding S, Schultz PG (2004) A role for chemistry in stem cell biology. *Nat Biotechnol* 22:833–40
37. Zani BG, Kojima K, Vacanti CA et al. (2008) Tissue-engineered endothelial and epithelial implants differentially and synergistically regulate airway repair. *Proc Natl Acad Sci U S A* 105:7046–51

Chapter 5

Eye

**Maria Notara, Yiqin Du, G. Astrid Limb, James L. Funderburgh
and Julie T. Daniels**

Abstract Various ocular compartments host populations of stem cells which are active throughout the life of the adult human eye. This chapter describes culture methods for the corneal limbal epithelial stem cells, the corneal stromal stem cells and the Müller glia stem cells of the retina.

5.1 Limbal Epithelial Stem Cells

Maria Notara, Julie T Daniels

5.1.1 Introduction

In this section, limbal epithelial stem cells (LESC), a population believed to reside in the vascularised corneoscleral junction (i.e. the limbus) and which are responsible for the maintenance and repair of the corneal epithelium, will be described. Partial or total failure of the LES C population can have devastating effects including vision loss, pain and eventually blindness. LES Cs therapy is already established in the clinic for the treatment of blinding conditions of the cornea such as chemical burns, Stevens Johnson syndrome and aniridia. The functional properties, the isolation and characterisation of LES Cs and their potential therapeutic uses will be reviewed.

5.1.1.1 The Cornea

The integrity and functionality of the five-layer outer corneal epithelium is essential for vision. A population of limbal epithelial stem cells is responsible for the maintenance of the epithelium throughout life by constantly supplying daughter cells which can replenish the cells constantly lost from the outer ocular surface during

M. Notara (✉)

UCL Institute of Ophthalmology, 11-43 Bath street, EC1V 9EL, London, UK
e-mail: m.notara@ucl.ac.uk

regular wear and tear or following injury. LESC deficiency leads to severe inflammation, opacification, vascularisation and discomfort [14, 15]. Cultured LESC delivery is one of several examples of a successful adult stem cell therapy used in patients. The clinical precedence for use of stem cell therapy as well as the easy accessibility of a transparent stem cell niche make the cornea a unique model for the study of adult stem cells in health and disease.

5.1.1.2 The Limbus and the Limbal Epithelial Stem Cells

The Limbal Stem Cell Niche Concept

The limbus, or corneoscleral junction, measures 1.5–2 mm in width and is the intersection at which the cornea becomes continuous with the sclera (Fig. 5.1).

LESC are believed to reside in the basal layer of the limbal area, at the vascularised junction between the corneal and conjunctival epithelium.

Davanger and Evensen [16] were the first to suggest that the corneal epithelium is maintained and renewed by a cell population residing in the limbus [16]. In the last 35 years, further proof confirming that the corneal stem cells reside in the limbal region has been presented. For example, limbal epithelial basal cells can retain tritiated thymidine label for prolonged periods, thus suggesting that they have long cell cycle, a stem cell characteristic [13]. Limbal basal cells have been shown to have higher proliferative capability *in vitro* than cells originating from the central and paracentral corneal epithelium [78]. Finally, wounding or surgical removal of the limbus in a rabbit model was shown to delay corneal wound healing and to cause conjunctivalisation of the corneal surface [9, 46].

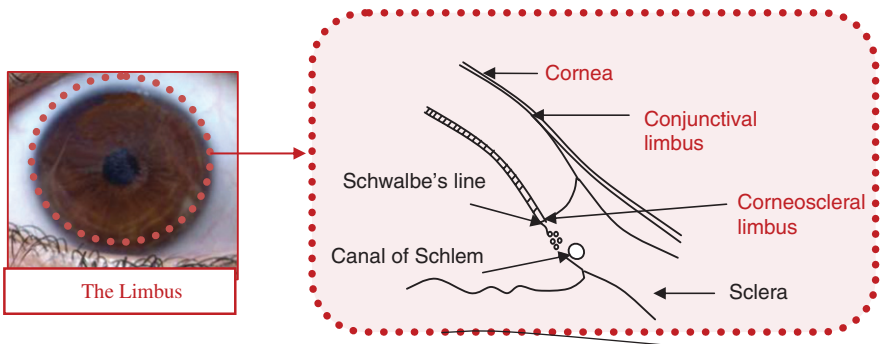


Fig. 5.1 The corneoscleral limbus and associated structures

Limbal Anatomy and Structure

Within the limbus, the LESC are believed to live in a stem cell niche, which preserves them in their undifferentiated status (Fig. 5.2). This stem cell niche has been identified as the palisades of Vogt, which are thrown into folds in the sub-epithelial connective tissue. These structures are thought to provide a protective environment

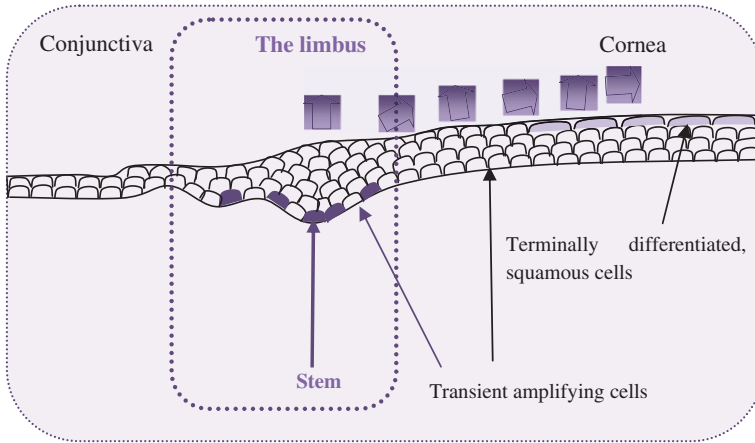


Fig. 5.2 Schematic representation of the function of the limbus: the stem cells (normally residing in the basal layers of the limbus) give rise to transit amplifying cells which migrate towards the anterior layers of the corneal area eventually developing into the terminally differentiated epithelium

for the LESC. Putative stem cells have been identified at the bottom of the epithelial papillae forming the limbal palisades of Vogt [91]. This irregular junction between the limbal epithelium and stroma provides protection to the cells from potentially damaging mechanical stress, while the adjacent vascular network provides a supply of nutrients for the resident cells [4]. It has been shown in histological tissue sections that LESC are discretely located in the basal layer of the corneal limbal epithelium, at the junction between the transparent cornea and the opaque sclera [10, 13, 90]. However, the total number and distribution of LESC remain elusive. The limbal palisades of Vogt have been proposed as the site of the LESC niche [16]. Photomicrographic, angiographic and histological studies have demonstrated the fibrovascular nature of the palisades and the presence of “ridges of thickened epithelium” in the interpalisade zone [34, 100].

Dua et al. [27] discovered a novel anatomical structure extending from the palisades of Vogt which the authors put forward as a putative LESC stem cell niche, the Limbal Epithelial Crypt (LEC). CK14 staining demonstrated that all the cells in this LEC were of epithelial nature, and the levels of ABCG2 expression, a putative LESC marker, suggested that the cells within these crypts may be stem cells although no functional evidence was shown [27]. In a recent follow-up study, the same research group further studied the frequency and distribution of LEC, investigated the immunophenotype of the cells within the LEC and studied their ultra-structural features. Cells within the crypt were shown to express cytokeratins CK32 and CK19 as well as CD34 vimentin, p63 and connexin 43, whereas they did not express the proliferation marker Ki67, an indication of slow cell cycle. Moreover, these cells had a high nuclear to cytoplasmic ratio and were adherent to the underlying basement membrane by multiple cytoplasmic projections. These

data suggested that LEC contain a unique sub-population of cells expressing several characteristics that are consistent with it representing a LESC niche [93].

Our group has recently identified two distinct candidate LESC niche structures; namely limbal crypts and focal stromal projections (FSP). These two structures could also be imaged *in vivo* in healthy human individuals. Biopsies targeted to limbal regions rich in FSP structures yielded significantly higher numbers of LESC in culture suggesting that targeted biopsy of adult stem cell niches can improve stem cell yield and may prove to be essential for the successful development of novel adult stem cell therapies [95].

The cornea possesses two unique characteristics that make it ideally suited as a model system for studying adult stem cells and their niche in humans. Firstly, LESC are found at the corneal limbus (the peripheral extent of the cornea) and are anatomically segregated from their transit amplifying cell progeny which migrate centrally to cover the paracentral and central cornea [78]. Secondly, it is optically transparent tissue and therefore non-invasive imaging of LESC in humans is possible [95].

The evidence that LESC reside within the corneal limbus is strong. It is therefore presumed that the corneal limbus constitutes a specialized adult stem cell niche. There is some functional evidence to support this.

5.1.2 Limbal Epithelial Isolation and Maintenance Stem Cell Protocols

Maintenance of 3T3 Mouse Fibroblasts for Use as a Feeder Layer: 3T3/J2 mouse fibroblasts were maintained in Dulbecco's Modified Eagle Medium (DMEM Gibco) supplemented with 10% Adult Bovine Serum (Gibco) and 1% penicillin/streptomycin (Gibco). Culture medium was changed three times a week and the cultures were passaged upon reaching 60–70% confluence at a ratio of 1:8. The cultures were kept at 37°C and 5% CO₂. The fibroblasts were growth arrested by the addition of mitomycin C (Sigma) at 4 µg/ml for 5 h.

5.1.2.1 Primary Human Limbal Epithelial Cell Isolation and Culture

Human limbal epithelial (HLE) cells were cultured in Corneal Epithelial Culture Medium (CECM) consisting of DMEM F12 (1:1) (Invitrogen) supplemented with 10% Fetal Bovine Serum (FBS), 1% penicillin/streptomycin (Gibco), 0.1 nM cholera toxin (Sigma), 5 µg/ml human recombinant insulin (Sigma), 0.05 mM hydrocortisone (Sigma) and 10 ng/ml epidermal growth factor (Invitrogen). Culture medium was changed three times a week and the cultures were passaged upon reaching 70–80% confluence at a ratio of 1:3.

HLE cells were isolated from research consented corneas supplied by the Moorfields Eye Bank, London. Corneas or limbal rims were cut into four segments and immersed in a 1.2 U/ml dispase II solution (Roche) for 2 h at 37°C or overnight at

4°C. After dispase treatment, the tissue pieces were transferred into a 35 mm Petri dish. With the epithelial side uppermost, the epithelial cells were gently scraped from the limbus area using a pair of fine pointed forceps. The cells were collected using 5 ml CECM. The cell suspension was pipetted up and down on the tissue segments to disperse the cells. The cell suspension was then placed with another 5 ml CECM into a T-75 tissue culture flask (Nunc) containing growth arrested 3T3 mouse fibroblasts plated at cell density of 2.4×10^4 cells/cm². Viable epithelial cells developed colonies in 2–3 days. The cultures were incubated at 37°C and 5% CO₂ in air.

5.1.3 Identification of Limbal Epithelial Stem Cells

There is no single marker that can be used to definitively identify a LESC. However there are stem cell associated markers that can be used in combination with the absence of differentiation markers to identify putative LESC.

ABCG2: The ATP binding cassette transporter protein ABCG2 has been proposed as a possible LESC marker [107], and may in fact be a universal marker for stem cells [110]. Zhou et al. [110] have found that ABCG2 is expressed in stem cells from bone marrow and skeletal muscle, and also embryonic stem cells. ABCG2 is also known as the breast cancer resistance protein 1 (BCRP1) [110], and mediates drug resistance [21]. ABCG2 expression is responsible for the efflux of many different anticancer drugs from a stem cell, and is able to exclude Hoechst 33342 dye [110]. ABCG2 is expressed in some of the limbal basal cell population but not in corneal epithelial cells; thus suggesting that it is a possible marker for LESC [10, 107].

p63: The transcription factor p63 is a putative LESC marker [77]. p63 is structurally similar to the tumour suppressor protein p53 [64], and is involved in morphogenesis [69]. p63 knockout mice (p63^{-/-}) have major defects in epithelial development and lack stratified epithelium [109]. These observations suggest that p63 may be involved in maintaining the stem cell population [109]. Pellegrini et al. [77] showed that p63 is expressed in the nuclei of human limbal epithelial basal cells but not in TA cells on the surface of the cornea. However, several groups have since found that p63 is also expressed by most of the basal cells in the central human cornea [8, 25]. Therefore although p63 is useful for identifying putative LESC, it is a specific marker for these cells.

The alpha isoform of p63 ($\Delta Np63\alpha$) has been shown to be more specific for LESC than other isoforms of this transcription factor [20]. Holoclones derived from the limbus express high levels of p63 α , meroclones express low levels, and paraclones exhibit no expression. The alpha isoform of p63 is therefore a putative marker for LESC. Expression of p63 α varies depending on the state of the corneal tissue post mortem and this may explain the discrepancy in p63 staining found between different research groups. Defects or abrasions on the central cornea, often caused by incomplete closure of the eyelids after death, can result in the cornea becoming “activated”. In these activated corneas p63 α expressing cells from the limbus migrate towards the central cornea and are found in the basal layer. ΔNp

beta and gamma isoforms of p63 appear in the suprabasal layers of the cornea and limbus in response to this wounding and therefore indicate more differentiated cells.

5.1.3.1 Other Markers

Other putative limbal stem cell associated markers include vimentin, integrin $\alpha 9$ [91] and cytokeratin 19 [40, 53]. Differentiation markers which can be used to identify which cells are not limbal stem cells include involucrin, connexin 43, and the cytokeratins K3 and K12 [10, 91].

5.1.3.2 Immunocytochemistry Protocols

Eight-well permanox chambered slides (Labtek, Nunk) were used for immunocytochemical analysis. The cells were washed three times with PBS, fixed for 10 min at room temperature in 2% (wt/vol) paraformaldehyde, and treated with 20% (wt/vol) sucrose before storage at -20°C . The cultures were blocked for 1 h in PBS supplemented with 5% goat serum (Jackson) and 0.5% Triton X followed by the primary antibody (mouse monoclonal antibody for ABCG2 and mouse monoclonal antibody for cytokeratin 3 from Chemicon International; rabbit polyclonal antibody for p63 α from Cell Signaling; mouse monoclonal antibody for integrin $\beta 1$ and chicken monoclonal antibody for integrin alpha 9 from Abcam and rabbit polyclonal antibody for PAX 6 from Santa Cruz) or blocking reagent only (negative control) overnight at 4°C .

Subsequently, the cells were incubated with their respective secondary antibody (goat anti-mouse FITC, goat anti-mouse TRITC or goat anti rabbit TRITC antibodies from Jackson), washed and counterstained with FITC or TRITC conjugated phalloidin (Sigma).

Finally, the chamber slide wells were removed and the slides were mounted using Vectashield media with DAPI (Vector Labs). All incubations apart from the primary antibody incubation were performed at room temperature, and each step was interspersed with three 5 min rinses with PBS containing 0.1% Tween-20 (Sigma).

5.1.3.3 Colony Forming Efficiency

For the colony forming efficiency (CFE) assay, HCE-S cells were plated at a cell density of 1000 cells / flask in three T12.5 flasks. The medium was changed every other day. The cultures were fixed on day 12. Plates were fixed with cold methanol for 30 min at -20°C . Subsequently, the cells were re-hydrated with PBS and stained with a 0.4% hematoxylin solution (Fisher). Finally, the flasks were photographed using a lightbox. Colonies that fit the description of a holoclone as defined by Barrandon and Green [2] were counted and the colony forming efficiency was calculated as the percentage of holoclonal colonies to the total number of seeded cells.

5.1.4 Methods for the Purification of Limbal Epithelial Stem Cell Population In Vitro

5.1.4.1 Side Population (SP) Cells

The cells which have the ability to efflux Hoechst 33342 dye are known as the “side population” (SP) and represent a population enriched for stem cells. SP cells have been found in human limbal epithelium but not in the peripheral and central corneal epithelium, thus suggesting that Hoechst dye can be utilised to partially distinguish and purify LESC [104, 106, 107]. SP cells make up 0.3–0.4% of the limbal epithelial cell population and have been found to have stem cell-like properties such as quiescence, slow cycling state, high levels of expression of putative stem cell markers e.g. ABCG2, and no expression of markers for differentiated corneal epithelial cells such as cytokeratin 3 [104, 107].

5.1.4.2 Rapid Adhesion to Collagen IV

Collagen IV can also be used to partially purify limbal epithelial cells with stem cell like properties [61]. This selectivity is founded on the interaction of type β_1 integrins which are highly expressed on the surface of putative LESC, with collagen IV. β_1 integrin intensity of expression has therefore been proposed as a marker for putative stem cells [61, 105]. Li et al. [61] showed that cells from the limbal region which adhere to collagen IV within 20 min exhibit greater stem cell-like properties than cells that adhere to collagen IV more slowly. Cells that did not adhere to collagen IV within 2 h were classed as “non-adherent”, and those that adhered between 20 min and 2 h were termed “slowly adherent cells” (Fig. 5.3). Rapidly

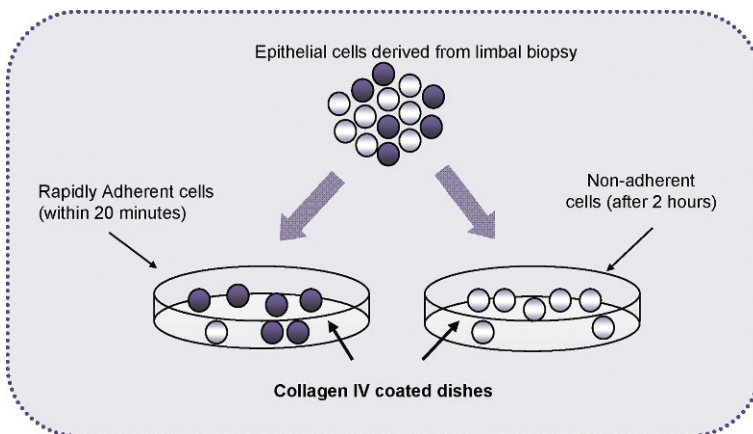


Fig. 5.3 Use of rapid adhesion on collagen IV to partially purify LESC. Cells which adhere to collagen IV within 20 min exhibit stem cell-like properties to a greater extent than cells that adhere more slowly

adherent cells were found to have higher proliferative capacity, greater colony forming efficiency, expressed higher levels of integrin β_1 , p63 and ABCG2 putative stem cell markers, and retained 5-fold the level of BrdU label retained by non-adherent cells indicating slow cycle. This population of rapidly adherent cells also did not express the differentiation markers involucrin and cytokeratin 12. It was calculated that 10% of the cells isolated from the limbal region rapidly adhered to collagen IV. This method of enrichment by attachment to collagen IV was based on a method developed by Jones and Watt [52] for putative epidermal keratinocyte stem cell selection [52].

Rapid adhesion assay protocol: 0.5 mg/ml BSA solution (in PBS), heat denatured at 60°C for 30 min.

Six-well plates are coated with 2 ml per well of Collagen IV solution (100 μ g/ml) overnight at 4°C or for 2 h at 37°C. Subsequently the plates are washed three times with PBS and 2 mls of BSA solution (0.5 mg/ml, heat denatured at 60°C for 30 min) are added for 1 h at 37°C.

The cornea is cut into quarters and placed into Dispase II solution for 2 h at 37°C. The epithelium is scraped off as above and pipetted up and down to make a single cell suspension. Cells are spun down to form a pellet and resuspended in 2 mls of medium. The suspension is plated in a coated well and incubated at 37°C in 5% CO₂ for 20 min. The cells are removed from the initial well and the cell suspension is added to another coated well. The first well is rinsed first well with 1 ml of medium to remove any non adhered cells and added to the second well. Three millilitres of medium to are added to the first well to keep the rapidly adherent cells alive. The plate is incubated at 37°C in 5% CO₂ for 24 h. Next, the cells from the first well (rapid adhering cells) are removed from collagen IV using 10X trypsin (Gibco) for 3–5 mins at 37°C and the cells are centrifuged cells at 1000 rpm for 5 mins. The pellet is resuspended in 5 mls of medium and plate onto a growth arrested 3T3 feeder layer (culture medium and 3T3 feeder layer growth arrest as above).

5.1.5 LESC Protocols in the Clinical Practice

5.1.5.1 Basics of Limbal Epithelial Stem Cell Failure

LESC deficiency can result from primary aetiologies such as the heritable genetic disorder, aniridia [44, 75]. More commonly LESL deficiency occurs as a result of causes such as thermal or chemical injury, Stevens Johnson Syndrome, contact lens wear and multiple surgeries [11, 26, 35, 43, 45]. The result is persistent epithelial breakdown, corneal vascularization and opacification, chronic discomfort and impaired vision caused by the migration of neighbouring conjunctival epithelial cells and blood vessels onto the corneal superficial layers [46, 80]. LESL failure may be partial or total [24]. Partial LESL deficiency can occur in a localised region of the limbus leaving an intact and functional population of LESCs in other areas. This results in sectoral ingrowth of conjunctival epithelium in the areas of LESL deficiency [45]. In total LESL deficiency there is dysfunction or destruction of the entire LESL population resulting in conjunctivalization of the entire cornea [45].

5.1.5.2 Limbal Epithelial Stem Cell Therapy Techniques for Graft Preparation

Two culture systems, explant and the single cell suspension, have been used to produce epithelial sheets containing LESC for delivery to the eye. During explant culture human amniotic membrane is often used as both a substrate and carrier for cultured LESCs. Limbal biopsy tissue is allowed to adhere to the amnion prior to being submerged in culture medium which stimulates the limbal epithelial cells to migrate out of the biopsy and proliferate on the amnion [39, 56, 57, 71, 88, 94, 103]. Once a confluent epithelial sheet has been formed, air lifting can be introduced to promote stratification of multi-layered epithelium. The method of amniotic membrane preparation may have an effect on the phenotype of the culture. Grueterich et al. showed that culturing limbal epithelial cells on amnion with an intact amniotic epithelium may result in a more stem cell like phenotype than de-epithelialised (denuded) amnion [40]. In the authors experience, the use of amniotic membrane has disadvantages, including unpredictable biological variability between donor tissues, often restricted tissue availability and the inherent semi-opaque nature if the membrane obstructs post-operative visual clarity until the tissue is remodeled (a process that depending on the patient can occur over a period of few days to several months).

The single cell suspension culture system requires first separating the epithelial cells from the stroma using dispase and then dissociating the epithelial cells from one another using trypsin prior to seeding [17, 72, 79, 92] either straight onto amniotic membrane or onto a plastic tissue culture dish containing a feeder layer of growth arrested 3T3 fibroblasts if more extensive in vitro cell expansion is desired. The cultures can be incubated for up to three weeks. When a confluent epithelial sheet is formed, it can be transferred to the ocular surface using either a contact lens, [79, 92], collagen shield, [92] or fibrin gel [82]. Usually, the suspensions of single limbal epithelial cells seeded onto amniotic membrane are co-cultured with a layer of growth arrested 3T3 fibroblasts in the bottom of the dish [16].

5.2 Culture of Human Corneal Stromal Stem Cells **Yiqin Du, James L. Funderburgh**

5.2.1 Introduction

The cornea is the outermost layer of the eye and it serves as a barrier and provides the essential optical function of transmitting light to the retina. The cornea also provides 70–75% of the refractive power required to focus the light into an image [111]. In structure, the cornea is a relatively simple organ, composed of three distinct tissue layers, epithelium, stroma and endothelium. The stroma, a collagenous connective tissue, makes up 90% of the cornea. It is populated with keratocytes, neural crest-derived mesenchymal cells that secrete the unique transparent tissue of the corneal stroma. In early gestation, neural crest cells migrate to form the corneal

stroma [51, 108]. They undergo rapid cell division after localization in the cornea in late embryogenesis, but after birth the keratocyte cell number stabilizes and little or no mitosis can be detected throughout the lifetime. In the case of inflammation or wounding, however, the stromal keratocytes become activated and mitotic. The phenotype of the activated keratocytes changes to that of fibroblasts and myofibroblasts, and connective tissue secreted by these cells during wound-healing becomes opaque scars. After healing the cells become quiescent, but human corneal scars are very slow to resolve and it is not clear if the resident cells return to a fully keratocytic phenotype. These properties suggest only a limited means of tissue renewal in the corneal stroma. So recently the research on the corneal wound healing and tissue bioengineering has focused on stem cells.

One method to isolate stem cells is side population cell sorting. Stem cells have the ability to efflux fluorescent dye Hoechst 33342, leading to reduced red and blue fluorescence in fluorescence-activated cell sorting (FACS) [36]. These cells are referred to as “side population” (SP) cells because in the two dimensional display of red and blue fluorescence, cells having reduced Hoechst dye appear as a small tail to the left side of the mass representing live somatic cells. SP cells from a number of adult tissues have been shown to exhibit many characteristics of stem cells. The SP cells are lost after treatment with verapamil, a drug that blocks action of the ATP-binding cassette transporter G family member ABCG2. This transporter protein has been identified as the Hoechst efflux pump [55, 89, 110] and as a specific marker for many kinds of stem cells such as hematopoietic, mesenchymal, muscle [110], neural [6, 47], cardiac [67], islet [59], and keratinocyte [99, 101] stem cells. Recent studies have shown the presence of side population cells present in corneal epithelial and stromal tissue. In these cells, ABCG2 protein and mRNA expression are correlated with the SP phenotype and with stem cell characteristics [5, 18, 91, 107].

During development the cornea stroma is produced by mesenchymal neural crest cells as they differentiate into keratocytes and begin to synthesize and secrete an extracellular matrix composed of collagens I, V and VI and proteoglycans [29, 30, 41, 42, 63]. As maturation proceeds, the stroma dehydrates, becomes thin and transparent, and contains flattened and interconnected keratocytes [48]. In adult mammals, however, numerous *in vitro* experiments show that keratocytes rapidly lose their characteristic phenotype after several population doublings. This loss of phenotype also occurs in healing wounds *in vivo*. In response to acute injury, keratocytes become mitotic, adopt a fibroblastic phenotype, and move to the injured area [7, 50]. In fact, primary keratocytes can be maintained *in vitro* in serum-free or low mitogen serum-containing culture medium in a quiescent state, exhibiting a morphology and matrix secretion similar to keratocytes *in vivo* [3, 49]. Fetal bovine serum can induce keratocytes to proliferate but also causes keratocytes to become fibroblasts and myofibroblasts [68]. The isolation and culture of stromal stem cells provides an important source of keratocytes for *in vitro* and *in vivo* research. Recently, the authors found that the stroma of bovine and human corneas contain small populations of cells exhibiting self-renewal ability

for an extended number of population doublings in culture [22, 31]. Immunostaining shows that in the human corneal stroma, most of the ABCG2 and PAX6 positive cells are in the anterior part of the peripheral cornea [22]. These stromal progenitor cells demonstrated potential for differentiation into several non-corneal cell types, a characteristic similar to that of adult stem cells from other mesenchymal tissues. These corneal stromal stem cells can be cloned and proliferate in vitro for more than 100 doublings. Like quiescent primary keratocytes, the cells secrete the keratan sulfate proteoglycans, lumican, keratocan, and mimecan, identified as molecular markers for keratocytes [32, 33]. They can organize cornea-like tissue in vitro by forming aligned collagen fibrils and secreting stroma specific extracellular matrix and connecting to each other by forming cellular junctions when the passaged stromal stem cells are cultured as cell pellets without any scaffolding [23].

Currently the function of the stromal stem cells in vivo, especially during wound healing is unclear. Some researchers have suggested that in corneal stroma there are stem cells derived from bone marrow [97] which are CD34 positive. Nakamura et al. [73] found that lethally irradiated mice, rescued by tail-vein injection of bone marrow cells from GFP expressing mice, exhibited a resident population of green cells in the cornea. The function of bone marrow derived stem cells in cornea and the relationship between bone marrow-derived cells and keratocytes remain unknown.

In this section, we describe methods to isolate and culture human stromal stem cells as well as to identify their characteristics and discuss the possible usage in cell based therapy and tissue bioengineering.

5.2.2 Isolation and Culture of Primary Human Stromal Cells

5.2.2.1 Reagents and Materials

Starting Material

- Whole human cornea. Note: Human tissue for research must be obtained with informed consent of the donor using a protocol approved by the Institutional Review Board. Deidentification of donor, procedures in accordance with the Declaration of Helsinki, and biosafety concerns will need to be addressed.

Sterile Supplies

- Stem cell culture medium (SCCM): Low-glucose-DMEM with MCDB-201, 2% fetal bovine serum (FBS), 10 ng/ml epidermal growth factor (EGF), 10 ng/ml platelet-derived growth factor (PDGF-BB), 1×10^{-8} ITS, 1 mg/ml AlbuMax (Lipid-Rich bovine serum albumin), 0.1 mM ascorbic acid-2-phosphate (A2P), 10^{-8} M dexamethasone, GASP antibiotics (Gentamicin, 50 μ g/ml; Amphotericin B, 1.25 μ g/ml; Streptomycin, 100 μ g/ml; Penicillin, 100 U/ml)

- CMF-Saline G with GASP antibiotics: 8 g/l NaCl; 0.4 g/l KCl; Na₂HPO₄·7H₂O, 0.29 g/l; KH₂PO₄, 0.15 g/l; glucose 1.1 g/l; pH 7.2, GASP.
- Dispase II
- TrypLE Express or 0.2% trypsin in CMF-Saline G
- DMEM/F-12 with GASP antibiotics
- Cell Strainer-70 μm nylon mesh
- Plastic spatula- “Cell Lifter”
- Curved Iris Scissors 4 3/8”
- 4” jeweler’s forceps
- Corneal scissors, 19 mm blades, sharp tip (Wescott #55541S)
- Colibri Suturing Forceps 0.1 mm (WPI #555063FT)

Non-Sterile

- Variable-speed tilting mixer; e.g. Barnstead/Thermolyne #M48725
- Centrifuge, low speed, refrigerated
- SDS sample buffer (6x): 7 ml 0.5 M Tris HCl (pH6.8), 3 ml glycerol, 1 g SDS, 1.2 mg Bromophenol Blue (Final: 0.35 M Tris, 33% glycerol, 10% SDS).

5.2.2.2 Protocol

- a) Wash the cornea 5 min × 3 in CMF-Saline G
- b) Trim off the residual sclera, conjunctiva and iris.
- c) Add 2 ml of 1.2 U Dispase II (2.4 U Dispase II diluted in DMEM/F-12 with GASP antibiotics) 4°C, overnight on a tilting mixer.
- d) Rotate the cornea in Dispase II for 30 min at 4°C.
- e) Wash the cornea once in DMEM/F-12 with GASP.
- f) Under dissection microscope, carefully peel off the epithelium and endothelium.
- g) Use a plastic spatula to scrape both epithelial side and endothelial side of the stroma. Observe through microscope to make sure all of these cellular layers are removed.
- h) Wash the corneal stroma in new medium once.
 - i) Cut the stroma into quarters using scalpel, or fine scissors.
 - j) Digest up to 20 h at 4°C with 0.5 mg/ml collagenase type L in DMEM/F-12+A2P+GlutaMax containing GASP antibiotics, until most of the tissues disappear.
- k) Centrifuge at 400g, 10 min and discard the supernatant.
 - l) Resuspend the cells in fresh DMEM/F-12 with GASP antibiotics, filter the digest through a 70 μm Cell-Strainer and repeat the centrifugation.
- m) Repeat this wash a second time. Count the cell number after each spin.
- n) Resuspend the primary stromal cells in SCCM and seed into tissue-culture coated plastic dishes at a density of 1 × 10⁴ cells per cm².
- o) Change the medium every 3 days.
- p) Passage: When the cells are 80~90% confluent, passage by trypsinization. Aspirate the medium, wash in CMF-Saline G and add trypsin or TrypLE to barely cover cells for 10 min at 37°C. Add DMEM/F-12 with 2%FBS to

terminate the digestion, count the cell number. Centrifuge resuspended cells and discard the supernatant. Resuspend in fresh SCCM and seed cultures at a density of 1×10^4 cells/cm².

5.2.3 Isolation of Stromal Side Population Cells Using FACS

5.2.3.1 Reagents and Materials

Sterile

- HBSS with 2% FBS
- Hoechst 33342 dye 1 mg/ml in water.
- Propidium Iodide 2 mg/ml in water.
- Verapamil 500 μ g/ml in water.
- DMEM with 2% FBS
- TrypLE or trypsin
- MoFlo (or similar) high-speed cell sorter, with 350 nm excitation.

5.2.3.2 Protocol

- a) Trypsinize passage 2–4 stromal cells.
- b) After digestion, filter the cells through a 70 μ m Cell-Strainer before counting.
- c) Count the cell number and dilute to 1.0×10^6 cells per ml in DMEM with 2% FBS.
- d) Add 5 μ g/ml Hoechst 33342 dye, incubate in 37°C water bath for 90 min, avoid light, agitate every 20 min.
- e) As a control, some cells, at the same concentration, are pre-incubated for 20 min with 50 μ g/ml verapamil before Hoechst 33342 incubation.
- f) After staining, wash the cells twice by centrifugation in Hanks' balanced salt solution (HBSS) with 2% FBS at 4°C and then resuspend and store them in cold HBSS with 2% FBS on ice.
- g) Immediately before sorting, add 2 μ g/ml propidium iodide to identify nonviable cells.
- h) Sort cells on a sterile, high-speed cell sorter, using 350 nm excitation. Collect the cells showing reduced fluorescence of both blue (670 nm) and red (450 nm). This "side population" is collected separately from dead cells and from fully-labeled cells. As a control, confirm that the side population is eliminated by verapamil preincubation.

Alternative Procedure: Cells can be sorted according to expression of ABCG2 protein, although this procedure may not yield a population with the same level of "stemness" as Side Population cells.

- a) For passage 2–4 cells, trypsinize the cells. Count the cell number.
- b) Spin down at 400g, 10 min.

- c) Wash once with PBS + 0.5% BSA.
- d) Block in 50 μ l block buffer (PBS+0.5%BSA+2% Normal Goat Serum), 10 min, on ice.
- e) Add 10 μ l Antibody (MAB 4155F, Clone 5D3 anti-ABCG2-FITC, or Isotype-FITC), 30 min, on ice, avoid light.
- f) Wash once by centrifugation in PBS-BSA
- g) Gently resuspend the cells in 1 ml PBS +2%FBS. Keep the cells on ice until flow cytometry is performed.
- h) Fluorescence-activated cell sorting (FACS) is performed using a high-pressure, high-speed cell sorter. A 488 nm argon laser excited fluorescein isothiocyanate, and a band-pass filter of 525/20 is used to measure emitted light. Gates in the right angle scatter versus forward scatter diagrams are used to exclude debris. Collect at least 100,000 events for analysis.
- i) The sorted ABCG2-positive and -negative cell populations can be used to evaluate their colony-forming efficiency and gene expression of stem cell markers and to passage for further investigation and in vivo transplantation.

5.2.4 Stem Cell Characterization and Differentiation

5.2.4.1 Stem Cell Characterization

Stromal stem cells in SCCM will exhibit expression of PAX6 and ABCG2, genes not expressed by differentiated keratocytes.

PAX6: Stem cells in sparse conditions in SCCM will express high levels of nuclear PAX6. Cells seeded at $1 \times 10^4/\text{cm}^2$ and cultured in SCCM to about 80–90% confluence are fixed in 3.2% PFA in PBS for 10 min, permeabilized in 0.1% Triton X-100 for 10 min and blocked in 10% goat serum for 30 min. The cells are stained with Anti-PAX6 (Covance) diluted 1:100 and counterstained with cytoplasmic myosin (CMII25, Developmental Hybridoma Bank) followed by secondary antibodies of Alexa 488-anti-rabbit and Alexa anti-mouse 546 for 1 h. The samples are washed two more times in PBS and mounted in a minimal volume of antifade mounting medium under a number 1 coverslip. The samples are photographed with an epifluorescence or Confocal microscope.

ABCG2: ABCG2 can be detected by immune precipitation after cell surface biotinylation. Cell layers are rinsed in PBS and incubated with Sulfo-NHS-LC-Biotin (Pierce, Rockford, IL,) at 1 mg/ml in PBS for 15 min on ice. Cell layers are washed again in PBS, the cells are scraped with a cell lifter and pelleted. Cells are lysed in 0.5 ml M-PER (Pierce) and cleared with 10 μ l of Protein G magnetic beads (DynaL Biotech). ABCG2 antibody (clone BXP-21; Chemicon International) is preincubated with Protein G Beads and then the loaded beads are incubated with samples overnight. The beads are collected, rinsed in PBS, and the bound protein is eluted by heating in SDS sample buffer. Proteins are separated on 4–20% SDS-PAGE gel, transferred to polyvinylidene difluoride (PVDF) membranes, and biotinylated protein is detected with streptavidin-horseradish peroxidase (BD Biosciences Pharmingen) using a luminescent substrate.

5.2.5 Keratocyte Differentiation

As the stem cells differentiate to keratocytes they will lose expression of PAX6 and ABCG2 and express molecular markers unique to keratocytes. The most reliable of these markers are the proteoglycan keratocan and the glycosaminoglycan keratan sulfate. These both can be detected by immunostaining and western blot. Keratocan mRNA can be quantified as well.

Procedure: Passage the stem cells at 1×10^4 cells/cm² in keratocyte differentiation medium, Advanced MEM (Invitrogen) with 10 ng/ml basic fibroblast growth factor (FGF2) and 0.1 mM ascorbic acid-2-phosphate (A2P). Change the medium every 2–3 days. After 1–2 weeks, the cells will be induced into keratocytes.

5.2.6 Immunodetection of Proteoglycans

Proteoglycans are recovered from culture media by passage over ion exchange columns (SPEC-NH2 microcolumns). These are rinsed in 0.2 M NaCl, 6 M urea, 0.02 M Tris, pH 7.4, and eluted in 0.5 ml 4 M guanidine-HCl, 0.02 M Tris, pH 7.4. The samples are dialyzed against water, and lyophilized. Samples are resuspended in 100 μ l 0.1 M ammonium acetate, pH 6.5, and divided into half. One half is digested overnight at 37°C with 2 mU/ml Keratanase II and 2 mU/ml endo-beta-galactosidase. Digested and undigested samples, normalized for cell number, are run on a 4–20% SDS-PAGE gel, transferred to PVDF membrane, and subjected to immunoblotting with Kera-C polyclonal antibody against keratocan and monoclonal antibody J36 against keratan sulfate. The digested samples will not react with J19 but will show a sharp band of 55 kDa for the keratocan.

5.2.7 Quantitative Reverse Transcription–Polymerase Chain Reaction (RT-PCR)

Quantitative RT-PCR is performed using SYBR Green RT-PCR Reagents according to the manufacturer's instructions. The reaction is carried out for 40 cycles of 15 s at 95°C and 1 min at 60°C after initial incubation at 95°C for 10 min. Reaction volume is 50 μ l, containing 1x SYBR Green PCR buffer, 3 mM Mg²⁺, 200 μ M dATP, dCTP, dGTP and 400 μ M dUTP, 0.025 units per ml AmpliTaq Gold polymerase, 5 μ l cDNA, and forward and reverse primers at optimized concentrations. A dissociation curve for each reaction is generated on the Gene-Amp ABI Prism 7700 Sequence Detection System to confirm the absence of nonspecific amplification. Amplification of 18S rRNA is performed for each cDNA (in triplicate) for normalization of RNA content. Threshold cycle number (Ct) of amplification in each sample is determined by ABI Prism Sequence Detection System software (Applied Biosystems). Relative mRNA abundance is calculated as the Ct for amplification of a gene-specific cDNA minus the average Ct for 18S expressed as a power of 2,

that is, $2^{-\Delta Ct}$. Three individual gene-specific values thus calculated are averaged to obtain mean \pm SD.

Human primers:

Keratocan	Forward: ATCTGCAGCACCTTCACCTT Reverse: CATTGGAATTGGTGGTTTGA
ABCG2	Forward: TGCAACATGTACTGGCGAAGA Reverse: TCTTCCACAAGCCCCAGG
Pax6	Forward: CAATCAAAACGTGTCCAACG Reverse: TAGCCAGGTTGCGAAGAAGT
18s	Forward: CAATCAAAACGTGTCCAACG Reverse: TAGCCAGGTTGCGAAGAAGT

5.2.8 Immunostaining

Primary antibodies:

ABCG2	Mouse Monoclonal BXP-21	1:100
Anti-PAX6	Rabbit Polyclonal	1:100
Kera C	Goat Polyclonal	1:100

Wash the cells with CMF-Saline G once, then fix in freshly made 3.2% paraformaldehyde (PFA) in PBS for 15 min at room temperature. Wash with PBS once, then permeabilize with 0.1% Triton X-100 in PBS for 10 min. Block nonspecific binding with 10% heat-inactivated goat serum in PBS. Incubate the samples for 1 h at room temperature with primary antibodies. After two washes with PBS, add secondary antibodies followed by incubation for 1 h at room temperature. Wash two more times in PBS and mount in a minimal volume of antifade mounting medium with coverslip. The samples are photographed with an epifluorescence or Confocal microscope using an 40 x oil objective.

The cells will have lost ABCG2 and PAX6 expression but will become positive for keratocan when stained with Kera C antibody.

5.2.9 Scaffolding-Free Pellet Culture

The stromal stem cells can differentiate into keratocytes and secrete and organize a cornea-like tissue in vitro by scaffolding-free pellet culture. The cells cultured as pellets secrete stromal specific extracellular matrix keratocan and keratan sulfate; partly form aligned collagen fibrils with collagen V and VI expression; the cells in the pellets form cell-cell junctions with connexin43 and cadherin11 expression.

Procedure: Trypsinize the cells, collect 2×10^5 cells in a 15 ml tube, centrifuge the cells at 400g for 5 min, culture the centrifuged cells in Advanced MEM + A2P + FGF2 for 3 weeks with medium changed every 3 days.

5.2.9.1 Cryopreservation

Trypsinize cells, count, pellet by centrifugation and resuspend the cells in freezing medium at $2-5 \times 10^6$ cells/ml with 1 ml per vial. Chill at a controlled rate of $1^\circ\text{C}/\text{h}$ using a commercial freezing box filled with isopropanol in a -80°C freezer overnight. On the next day, transfer the vials to liquid nitrogen. Freezing medium: 70% culture medium (DMEM/F-12), 20% FBS, 10% DMSO. Make fresh each time before freezing cells.

5.2.9.2 Variations and Applications of the Method

The corneal stromal stem cells have clonogenic and multipotent differentiation potential. These properties can be used to confirm the stem cell character of isolated cells.

1. *Clonal Growth*: Stromal stem cells grow clonally in SCCM. Trypsinized cells are counted and diluted in SCCM to a concentration of 0.3 cells/ml. In 96 well culture plates, 0.1 ml is plated per well. The ratio of 0.3 cells/well provides very low chance that any well will have two cells. After 2 weeks, wells with colonies are marked and medium changed. When confluent, the cells are trypsinized and expanded at 1×10^4 cells/cm². Cloning is recommended before differentiation.

2. *Chondrogenic potential*: Chondrocytes are never observed in mammalian eyes. The ability of cells to express cartilage-specific genes and gene products is therefore a strong marker for their multi-differentiation potential (and hence stem cell character). Chondrocyte differentiation medium (CDM) contains DMEM/MCDB-201, 2% FBS, 0.1 mM ascorbic acid-2-phosphate, 10^{-7} M dexamethasone, 10 ng/ml TGF β 1, and 100 $\mu\text{g}/\text{ml}$ sodium pyruvate. Cells (10^5) are resuspended in CDM and are pelleted in a 15 ml conical centrifuge tube. The medium is changed every 3 days. Pellets are cultured for 2–3 weeks. Messenger RNA for collagen II, aggrecan, and cartilage oligomatrix protein (COMP) can be detected under the chondrogenic conditions by stem cells but not by fibroblasts or keratocytes. Collagen II and COMP protein expression can also be detected using immunoblotting of pellet extracts.

Human primers:

Collagen II	Forward: CCGGGCAGAGGGCAATAGCAGGTT
	Reverse: CAATGATGGGGAGGCGTGAG
COMP	Forward: ACAATGACGGAGTCCCTGAC
	Reverse: AAGCTGGAGCTGTCCTGGTA
Aggrecan	Forward: TGAGGAGGGCTGGAACAAGTACC
	Reverse: GGAGGTGGTAATTGCAGGGAACA

5.3 Neural Differentiation

Stem cells are incubated under conditions that induce neural differentiation in Advanced MEM with 10 ng/ml epithelial growth factor (EGF), 10 ng/ml FGF2 and $1 \mu\text{M}$ all-trans retinoic acid. Retinoic acid is added every 3 days and the cells

are kept 2–3 weeks to induce neurogenesis. RT-PCR from these cells will detect mRNA upregulation of both GFAP and neurofilament protein. Increases in GFAP and neurofilament proteins can also be detected by western blotting. Immunofluorescent staining shows cells positive for neurofilament, GFAP, and beta-tubulin III. Procedures are similar to those discussed above.

Human primers:

Neurofilament protein	Forward: GAGGAACACCAAGTGGGAGA
	Reverse: CTCCTCCTCTTTGGCCTCTT
GFAP	Forward: ACTACATCGCCCTCCACATC
	Reverse: CAAAGGCACAGTCCCCAGAT

5.3.1 Conclusions

Keratoplasty is currently the only effective method providing recovery of vision after corneal blindness. Although donated corneal tissue currently meets the needs of most recipients in the US, worldwide, 8–10 million individuals suffer from corneal blindness without access to therapy. Additionally, numerous individuals reject allogeneic corneal tissue, and the supply of donated corneas may soon be reduced by the increasing number of refractive surgeries which render the corneas non-suitable for transplant. Because of these problems, there is significant interest in development of artificial and bioengineered corneas. Griffith et al. have demonstrated that corneal equivalents generated from the three corneal cell layers mimic human corneas in key physical and physiological functions. These studies used immortalized cell lines transformed with retrovirus, making them less suitable for transplantation. Focus has therefore turned to stem cells as a source of tissues for use in cell-based therapy and corneal tissue engineering. The stromal stem cells can differentiate into keratocytes and secrete stromal specific extracellular matrix, so they might be used as cell based therapy in corneal wound to decrease corneal scars. The stromal stem cells can also form cornea-like tissue *in vivo* with aligned collagen fibrils, so they might be used to make artificial corneas. In this way, millions of patients suffering from corneal blindness could benefit.

5.4 Isolation and Culture of Müller Stem Cells from the Adult Neural Retina of the Human Eye

G. Astrid Limb

5.4.1 Introduction

The vertebrate retina develops from a population of progenitor cells in the embryonic primordium of the diencephalon. These cells undergo multiple divisions to generate all the neurons and Müller glia of the adult retina, and in most vertebrates, a small group of retinal stem cells can be found in the adult eye at the retinal margin [70]. Pigmented cells from the ciliary epithelium exhibiting neural progenitor characteristics have been also reported in the adult murine and human eyes [12, 102].

These cells can be isolated and grown *in vitro* for extended periods, and can be made to differentiate into most types of retinal neurons by addition of growth and differentiation factors in culture [12, 102]. Fish and amphibians have been known for a long time to be able to regenerate retina throughout life [83, 84] and studies have shown that Müller glia form the retinal stem cell niche that generate retinal stem cells in the adult zebra fish after injury [84]. Müller cells have also been shown to regenerate chick [28] and rat retina [76], and more recent findings demonstrated that a population of Müller cells with neural stem cell characteristics is present in the adult human eye [58, 96].

Recent developments in the stem cell field have widened the prospects of applying cell-based therapies to regenerate ocular tissues that have been irreversibly damaged by disease or injury. In the clinical setting, stem cell transplantation to repair and regenerate neural retina constitutes a major challenge and many problems to establish such therapies remain to be solved. Transplantation of neural stem cells and retinal progenitors to regenerate retinal function has been extensively performed in various experimental models of retinal disease, yielded mixed results [1, 65, 66, 81, 98]. In order to develop practical methods for stem cell transplantation to regenerate retina, extensive research is still needed and requires reliable methods to isolate and grow retinal stem cells for transplantation.

Müller cells are radial glial cells which extend across the whole width of the retina, although their soma is normally found in the middle of the inner nuclear layer [85]. The distal border of Müller cells is marked by the outer limiting membrane, which consists of junctional processes of Müller cells and photoreceptors, while the proximal border of the cells is marked by the inner limiting membrane, consisting of the Müller cell membrane and a basement membrane [74]. Müller cells constitute the principal glial cells of the retina, capable of performing the functions that astrocytes, oligodendrocytes and ependymal cells do in other regions of the central nervous system [19]. Müller glia stabilize the retinal architecture, provide an orientation scaffold to neurons, give metabolic support to retinal neurons and blood vessels, and prevent aberrant photoreceptor migration into the subretinal space [86]. *In vitro*, Müller stem cells exhibit the morphological and physiological characteristics of all Müller glia [58] and stain for all the markers characteristic of these cells [58]. Müller stem cells can only be distinguished from terminally differentiated Müller glia by the expression of nestin, an intermediate filament protein that is expressed by neural progenitors in the central nervous system [58]. In general, Müller cells can be identified by their expression of glutamine synthetase, an enzyme involved in detoxification of ammonia and glutamate that operates in concert with the L-glutamate/L-aspartate transporter (GLAST), to terminate the neurotransmitter action of glutamate, and which is responsible for the supply of glutamine [86]. The cells also express cellular retinaldehyde binding protein (CRALPB), a protein that binds with high affinity to 11-cis-retinal and 11-cis-retinol, which are important components of the rod and cone visual cycle [59]. During isolation, Müller cells may be contaminated with retinal astrocytes. Because Müller cells share several characteristics *in vitro* with these cells, including morphology, expression of GFAP, and glutamine synthetase [87], Müller glia can be differentiated from astrocytes by their expression of CRALPB and its absence in

astrocytes [62]. Other markers characteristically expressed by Müller glia include epidermal growth factor receptors (EGF-R), alpha smooth muscle actin (α -SMA) and vimentin [54].

Since Müller stem cells isolated from the neural retina exhibit the characteristics of Müller glia in general [58, 62], they can be isolated and maintained *in vitro* under the conditions normally used to culture Müller cells. Their growth is however promoted by initial addition of EGF in the primary cultures. After the first colonies are established, it is not necessary to add this factor. They can be frozen and thawed without losing their characteristics for more than 100 passages (approximately 500 divisions) [58]. When cultured under specific conditions in the presence of growth factors, Müller stem cells are able to form neurospheres, to acquire neural morphology and to express markers of retinal neurons [58]. Differentiation of Müller stem cells can be achieved using conditions known to promote neural retinal differentiation [54, 58].

Müller stem cells can be isolated from the neural retina of human cadaveric donor eyes of both sexes and all ages. They have been successfully isolated from human eyes of ages ranging between 18 months and 83 years old and can be easily grown from eyes stored between 24 and 72 h post-mortem in Eye Banks, under conditions used to retrieve corneas for transplantation.

5.4.2 Protocol for Isolation of Müller Stem Cells from the Neural Human Retina

1. Remove cornea and lens by holding the optic nerve in the upright position.
2. Gently dislodge the vitreous and retina from the eye cup with a pair of small forceps, leaving behind the RPE and choroid.
3. Carefully cut the retina from the optic nerve and place in a Petri dish containing Phosphate-Buffered Saline 7.2 (1X) (Invitrogen, UK).

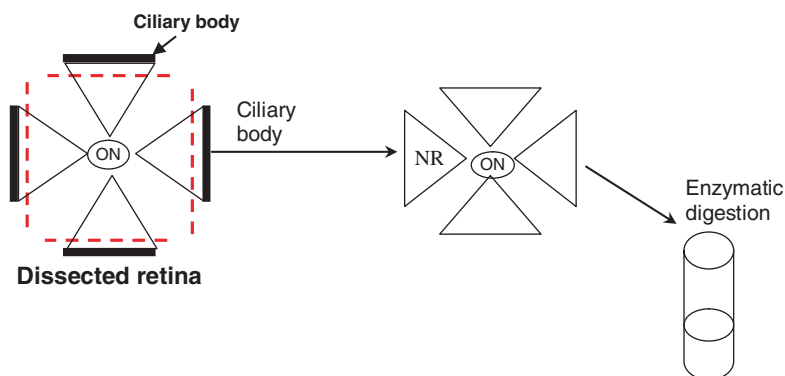


Fig. 5.4 Isolation of Müller stem cells from dissected neural retina. *Dotted lines* indicate the sites where neural retina needs to be excised from the ciliary body before enzymatic digestion to isolate the retinal Müller stem cells. (ON) optic nerve, (NR) neural retina (Figure from [58])

4. Using a surgical blade, excise the neural retina at approximately 4 mm away from the ciliary body (Fig. 5.4). To avoid contamination with retinal stem cells reported in this region (6), or with retinal pigment epithelium (RPE), special care should be taken when dislodging the neural retina from the vitreous.
5. Carefully remove any loose pigmented cells contaminating the neural retina by rinsing with PBS before enzymatic dissociation of retinal cells.
6. Place neural retina into a 12 ml tube containing 3 ml Trypsin-EDTA (5% trypsin, 2% EDTA- Gibco BRL, UK) and incubate tube for 20 min at 37°C.
7. Homogenize tissue by vigorous pipetting and incubate for a further 10 min at 37°C.
8. Repeat vigorous pipetting, add 9 ml of DMEM medium (Gibco BRL, UK) containing 10% foetal bovine serum (Gibco BRL, UK).
9. Remove large tissue debris by filtration through a stainless steel sieve pore size 200 μm (Sigma, UK). Stainless steel sieves can be replaced by sterile gauze 4-folded, which is placed over a 50 ml tube or a small Petri dish.
10. Alternatively, cells can also be dissociated from retinal fragments by incubating the tissue in 1 ml dispase (2.4 U/ml in PBS- Invitrogen, UK.) at 37°C for 20 min, followed by vigorous pipetting and addition of 1 ml of Trypsin-EDTA (5% trypsin, 2% EDTA) containing 0.67 mg hyaluronidase (Sigma, UK). Tissue is incubated for a further 20 min at 37°C before separating cells by filtration through a sieve (as above).
11. Pellet dissociated cells by centrifugation at 350g for 10 min.
12. Wash cells twice in the above medium.
13. Re-suspend cells in 5 ml of DMEM medium containing L-glutamax I (Gibco BRL, UK), 10% FBS and epidermal growth factor (EGF, Sigma, UK) at a final concentration of 40 ng/ml.
14. Prior to cell isolation, coat tissue culture flasks with fibronectin as follows: Dissolve fibronectin (from human plasma- Sigma, UK) in bicarbonate buffer (15 mM Na_2CO_3 , 35 mM NaHCO_3 , pH 9.6). Place 5 ml of this solution into a 12.5 cm^2 tissue culture flask (Becton-Dickinson, USA) and incubate overnight at 4°C or at room temperature for 2 h. Remove fibronectin and rinse flask with DMEM medium before plating the cells.
15. Plate isolated cells in a fibronectin coated flask and incubate at 37°C. Adhering Müller stem cells display a characteristic bipolar morphology (Fig. 5.5), which is observed after 5–7 days in culture. Original medium is maintained until the first colonies are formed (approx. 2 weeks). At this point, medium containing EGF is replaced until large colonies are formed. To expand the cells, large colonies are detached by incubation with Trypsin-EDTA (5.0 g/L trypsin, 2.0 g/L EDTA) (Sigma, UK) for 3 min at 37°C. Cells are then expanded in culture by plating them at a concentration of $2 \times 10^4 / \text{cm}^2$ in DMEM containing 10% FCS only and allowed to become confluent before dissociating them again.
16. Müller stem cells in culture can be identified by their characteristic morphology, electron-microscopic features and expression of cellular retinaldehyde binding protein (CRALBP) (Abcam, UK), vimentin (Dako, UK), glial fibrillary acidic protein (GFAP), epidermal growth factor receptor and glutamine

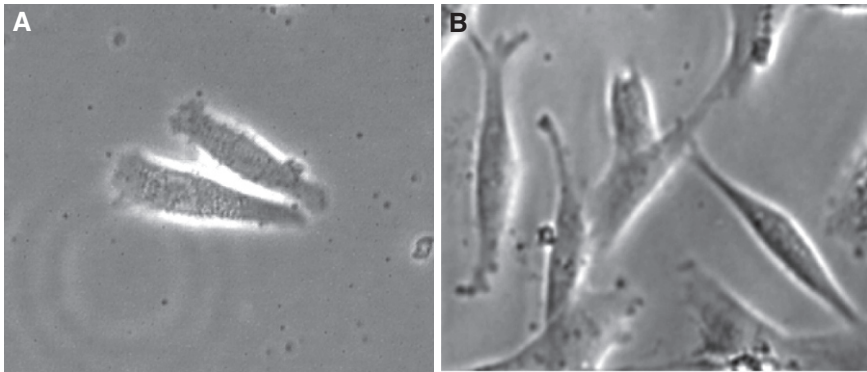


Fig. 5.5 Müller stem cell morphology in vitro. (A) Müller stem cells exhibit a granular appearance following 7 days in primary culture. (B) Following 3–4 weeks in culture, Müller cells spread and exhibit a characteristic bipolar morphology

synthetase (Santa Cruz Biotech, USA), using standard immunocytochemical methods previously described [58, 96] and indicated below. Negative staining for cytokeratin 8/18, using the antibody CAM 5.2 (Becton Dickinson, USA), can further help to identify Müller cells, as retinal pigment and ciliary epithelium, the main contaminants of Müller preparations, stain with CAM 5.2.

5.4.3 Protocol for Immunocytochemical Staining of Müller Stem Cells

1. Seed cells on glass microcoverslips coated with fibronectin (as indicated above) and culture until desired confluence. Remove culture medium and fix cells with 4% paraformaldehyde dissolved in PBS (pH 7.4).
2. Block cells in PBS + 0.3% Triton + 5% donkey serum for 1 h.
3. Add primary antibodies diluted in PBS + 0.3% Triton + 5% donkey serum + 0.5% BSA – overnight incubation
4. Wash 3 times with PBS – 10 min each
5. Add Alexa-fluorochrome labelled secondary antibody (Molecular Probes, USA) prepared in different species from the primary antibody at a 1:500 dilution in PBS, in 2% Donkey serum for 2 h at RT.
6. Wash 3 times with PBS (10 min each)
7. Add DAPI (Sigma, UK), 1:2500–5000 in PBS for 1 min.
8. Rinse in PBS
9. Wash 4×5 min Tris buffer pH 7.5 (6.35 g Trizma HCl and 1.18 g Trizma base per litre).
10. Mount with Vectashield (Vector Laboratories, UK)
11. Observe under fluorescence microscope

5.4.4 Protocol for Neurosphere Formation and Neural Differentiation of Müller Stem Cells

1. Detach confluent cells using Trypsin/EDTA as above. Resuspend cells at a concentration of 1×10^4 /ml in DMEM containing 10% FBS.
2. Place 100 μ l of the cell suspension in 96 well plates coated with extracellular matrix (ECM). This volume yields a cell density of approximately 500–800 cells/cm². If a larger number of cells is required, cells can be plated on larger surfaces provided these are coated with ECM and the proportion of cells is adjusted to the area of the well or flask.
3. Various ECM proteins may be used to differentiate Müller stem cells. Laminin, vitronectin and fibronectin (Sigma, UK) are used at a concentration of 10 μ g/ml, whilst basement membrane protein from Engelbreth-Holm-Swarm murine sarcoma (Sigma, UK) is used at a concentration of 50 μ g/ml. These proteins are dissolved in 15 mM Na₂CO₃, 35 mM NaHCO₃ buffer and used to coat tissue culture flasks or culture slides as indicated above.
4. To induce differentiation, FGF2 (Sigma, UK) at a final concentration of 40 ng/ml or RA (Sigma, UK) at a final concentration of 5 μ m are added to the wells and the cells incubated at 37°C for 3–7 days. Cell culture differentiation medium should be replaced every two days with fresh medium containing growth factors.
5. Under these conditions, neurospheres are formed after 4–5 days, whilst cells displaying neural morphology can be observed after two days in culture (Fig. 5.6).

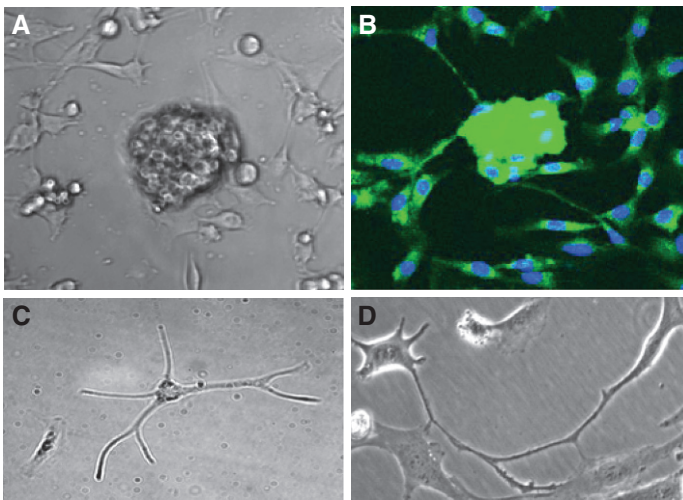


Fig. 5.6 Neural differentiation of Müller stem cells. (A) Following 5 days in culture at low cell density in the presence of basement membrane protein and FGF (40 ng/ml), Müller stem cells form neurospheres. (B) Neurospheres stain for various neural markers such as calbindin (*fluorescence* staining). (C,D) Müller stem cells cultured in the presence of FGF (40 ng/ml) acquire neural morphology

6. Acquisition of neural characteristics can be assessed by examination of morphology under phase contrast microscopy, and by confocal analysis of cells immunostained for various neural markers. These may include anti- β III tubulin (Chemicon Int, USA), protein kinase C (PKC) (Santa Cruz Biotech, USA), calcitonin (Swant, Switzerland); HuD and Brn3 (Santa Cruz Biotech, USA), 160 kDa neurofilament protein and calbindin (Chemicon, USA).

Acknowledgments The authors wish to acknowledge Martha L. Funderburgh for help in proof-reading the manuscript. The work was supported by National Institutes of Health Grants EY09368 and EY016415. JLF is a Jules and Doris Stein Research to Prevent Blindness Professor.

Abbreviations

LESC:	Limbal Epithelial Stem Cells
CK:	Cytokeratin
LEC:	Limbal Epithelial Crypt
FSP:	Focal Stromal Projections
HLE:	Human limbal epithelial
CECM:	Corneal Epithelial Culture Medium
FBS:	Fetal Bovine Serum
BCRP1:	Breast Cancer Resistance Protein 1
CFE:	Colony Forming Efficiency
SP:	Side Population
A2P:	Ascorbic acid-2-phosphate
DMEM:	Dulbecco's Modified Eagle's Medium
DMEM/F12:	Dulbecco's Modified Eagle's Medium/Nutrient Mixture F-12
FACS:	Fluorescence-Activated Cell Sorting
GASP:	50 μ g/mL gentamicin, 100 IU/ml penicillin, 100 μ g/ml streptomycin, 1.25 μ g/mL amphotericin B
PBS:	Phosphate-buffered saline
CMF-Saline G:	Calcium-Magnesium Free Hanks Saline G.: 8 g/l NaCl; 0.4 g/l KCl; Na ₂ HPO ₄ ·7H ₂ O, 0.29 g/l; KH ₂ PO ₄ , 0.15 g/l; glucose 1.1 g/l; pH 7.2
HBSS:	Hanks' balanced salt solution
FBS:	Fetal Bovine Serum
EDTA:	ethylene diamine tetraacetic acid
PFA:	Paraformaldehyde
DMSO:	Dimethyl sulfoxide
ABCG2:	ATP-Binding Cassette Transporter G family member
PI:	Propidium iodide
GLAST:	L-glutamate/L-aspartate transporter
CRALPB:	cellular retinaldehyde binding protein
EGF-R:	epidermal growth factor receptors
α -SMA:	alpha smooth muscle actin
RPE:	retinal pigment epithelium

References

1. Banin, E., A. Obolensky, et al. (2006). "Retinal incorporation and differentiation of neural precursors derived from human embryonic stem cells." *Stem Cells* **24**(2): 246–257.
2. Barrandon, Y. and H. Green (1987). "Three clonal types of keratinocyte with different capacities for multiplication." *Proceedings of the National Academy of Sciences of the United States of America* **84**(8): 2302–2306.
3. Beales, M. P., J. L. Funderburgh, J. V. Jester, and J. R. Hassell (1999). "Proteoglycan synthesis by bovine keratocytes and corneal fibroblasts: maintenance of the keratocyte phenotype in culture." *Investigative Ophthalmology & Visual Science* **40**(8): 1658–1663.
4. Boulton, M. and J. Albon (2004). "Stem cells in the eye." *International Journal of Biochemistry and Cell Biology* **36**(4): 643–657.
5. Budak, M. T., O. S. Alpdogan, M. Zhou, R. M. Lavker, M. A. Akinci, and J. M. Wolosin (2005). "Ocular surface epithelia contain ABCG2-dependent side population cells exhibiting features associated with stem cells." *Journal of Cell Science* **118**(Pt 8): 1715–1724.
6. Cai, J., A. Cheng, Y. Luo, C. Lu, M. P. Mattson, M. S. Rao, et al. (2004). "Membrane properties of rat embryonic multipotent neural stem cells." *Journal of Neurochemistry* **88**(1): 212–226.
7. Carlson, E. C., I. J. Wang, C. Y. Liu, P. Brannan, C. W. Kao, and W. W. Kao (2003). "Altered KSPG expression by keratocytes following corneal injury." *Molecular Vision* **9**: 615–623.
8. Chee, K. Y. H., A. Kicic and S. J. Wiffen (2006). "Limbal stem cells: the search for a marker." *Clinical and Experimental Ophthalmology* **34**(1): 64–73.
9. Chen, J. J. and S. C. Tseng (1991). "Abnormal corneal epithelial wound healing in partial-thickness removal of limbal epithelium." *Investigative Ophthalmology and Visual Science* **32**(8): 2219–2233.
10. Chen, Z., C. S. De Paiva, et al. (2004). "Characterization of putative stem cell phenotype in human limbal epithelia." *Stem Cells* **22**(3): 355–366.
11. Clinch, T. E., K. M. Goins, et al. (1992). "Treatment of contact lens-related ocular surface disorders with autologous conjunctival transplantation." *Ophthalmology* **99**: 634–638.
12. Coles, B. L. K., B. Angenieux, et al. (2004). "Facile isolation and the characterization of human retinal stem cells." *Proceedings of the National Academy of Sciences of the United States of America* **101**(44): 15772–15777.
13. Cotsarelis, G. and S. Z. Cheng, et al. (1989). "Existence of slow-cycling limbal epithelial basal cells that can be preferentially stimulated to proliferate: implications on epithelial stem cells." *Cell* **57**(2): 201–209.
14. Daniels, J. T., J. K. G. Dart, et al. (2001). "Corneal stem cells in review." *Wound Repair and Regeneration* **9**(6): 483–494.
15. Daniels, J. T., A. Harris, et al. (2006). "Corneal epithelial stem cells in health and disease." *Stem Cell Reviews* **2**(3): 247–254.
16. Davanger, M. and A. Evensen, (1971). "Role of the pericorneal papillary structure in renewal of corneal epithelium." *Nature* **229**(5286): 560–561.
17. Daya, S. M., A. Watson, et al. (2005). "Outcomes and DNA analysis of ex vivo expanded stem cell allograft for ocular surface reconstruction." *Ophthalmology* **112**(3): 470–477.
18. de Paiva, C. S., Z. Chen, R. M. Corrales, S. C. Pflugfelder, and D. Q. Li (2005). "ABCG2 transporter identifies a population of clonogenic human limbal epithelial cells." *Stem Cells* **23**(1): 63–73.
19. Derouiche, A. and T. Rauen, (1995). "Coincidence of L-glutamate L-aspartate transporter (Glast) and Glutamine-synthetase (Gs) immunoreactions in retinal glia – evidence for coupling of glast and gs in transmitter clearance." *Journal of Neuroscience Research* **42**(1): 131–143.
20. Di Iorio, E., V. Barbaro, et al. (2005). "Isoforms of Δ Np63 and the migration of ocular limbal cells in human corneal regeneration." *Proceedings of the National Academy of Sciences of the United States of America* **102**(27): 9523–9528.

21. Doyle, L. A. and D. D. Ross (2003). "Multidrug resistance mediated by the breast cancer resistance protein BCRP (ABCG2)." *Oncogene* **22**(47): 7340–7358.
22. Du, Y., M. L. Funderburgh, M. M. Mann, N. SundarRaj, and J. L. Funderburgh (2005). "Multipotent stem cells in human corneal stroma." *Stem Cells* **23**(9): 1266–1275.
23. Du, Y., N. Sundarraj, M. L. Funderburgh, S. A. Harvey, D. E. Birk, and J. L. Funderburgh (2007). "Secretion and organization of a cornea-like tissue in vitro by stem cells from human corneal stroma." *Investigative Ophthalmology & Visual Science* **48**(11): 5038–5045.
24. Dua, H. S. and A. Azuara-Blanco (2000). "Limbal stem cells of the corneal epithelium." *Survey of Ophthalmology* **44**(5): 415–425.
25. Dua, H. S., A. Joseph, V. A. Shanmuganathan and R. E. Jones, (2003). "Stem cell differentiation and the effects of deficiency." *Eye* **17**(8): 877–885.
26. Dua, H. S., J. S. Saini, et al. (2000). "Limbal stem cell deficiency: concept, aetiology, clinical presentation, diagnosis and management." *Indian Journal of Ophthalmology* **48**: 83–92.
27. Dua, H. S., V. A. Shanmuganathan, A. O. Powell-Richards, P. J. Tighe and A. Joseph, (2005). "Limbal epithelial crypts: a novel anatomical structure and a putative limbal stem cell niche." *British Journal of Ophthalmology* **89**(5): 529–532.
28. Fischer, A. J. and T. A. Reh (2001). "Muller glia are a potential source of neural regeneration in the postnatal chicken retina." *Nature Neuroscience* **4**(3): 247–252.
29. Funderburgh, J. L. (2000). "Keratan sulfate: structure, biosynthesis, and function." *Glycobiology* **10**(10): 951–958.
30. Funderburgh, J. L., B. Caterson, and G. W. Conrad (1986). "Keratan sulfate proteoglycan during embryonic development of the chicken cornea." *Developmental Biology* **116**(2): 267–277.
31. Funderburgh, M. L., Y. Du, M. M. Mann, N. SundarRaj, and J. L. Funderburgh (2005). "PAX6 expression identifies progenitor cells for corneal keratocytes." *Journal of the Federation of American Societies for Experimental Biology* **19**(10): 1371–1373.
32. Funderburgh, J. L., M. L. Funderburgh, M. M. Mann, L. Corpuz, and M. R. Roth (2001). "Proteoglycan expression during transforming growth factor beta-induced keratocyte-myofibroblast transdifferentiation." *Journal of Biological Chemistry* **276**(47): 44173–44178.
33. Funderburgh, J. L., M. M. Mann, and M. L. Funderburgh (2003). "Keratocyte phenotype mediates proteoglycan structure: a role for fibroblasts in corneal fibrosis." *Journal of Biological Chemistry* **278**(46): 45629–45637.
34. Goldberg, M. F. and A. J. Bron (1982). "Limbal palisades of Vogt." *Transactions of the American Ophthalmological Society* **80**: 155–171.
35. Gomes, J. A., M. S. Santos, et al. (2003). "Amniotic membrane with living related corneal limbal/conjunctival allograft for ocular surface reconstruction in Stevens-Johnson syndrome." *Archives of Ophthalmology* **121**: 1369–1374.
36. Goodell, M. A., K. Brose, G. Paradis, A. S. Conner, and R. C. Mulligan (1996). "Isolation and functional properties of murine hematopoietic stem cells that are replicating in vivo." *The Journal of Experimental Medicine* **183**(4): 1797–1806.
37. Griffith, M., R. Osborne, R. Munger, X. Xiong, C. J. Doillon, N. L. Laycock, et al. (1999). "Functional human corneal equivalents constructed from cell lines." *Science* **286**(5447): 2169–2172.
38. Grueterich, M., E. M. Espana, et al. (2002). "Phenotypic study of a case with successful transplantation of ex vivo expanded human limbal epithelium for unilateral total limbal stem cell deficiency." *Ophthalmology* **109**(8): 1547–1552.
39. Grueterich, M., E. M. Espana, et al. (2002). "Connexin 43 expression and proliferation of human limbal epithelium on intact and denuded amniotic membrane." *Investigative Ophthalmology and Visual Science* **43**: 63–71.
40. Harkin, D. G., Z. Barnard, et al. (2004). "Analysis of p63 and cytokeratin expression in a cultivated limbal autograft used in the treatment of limbal stem cell deficiency." *British Journal of Ophthalmology* **88**(9): 1154–1158.

41. Hart, G. W. (1976). "Biosynthesis of glycosaminoglycans during corneal development." *Journal of Biological Chemistry* **251**(21): 6513–6521.
42. Hay, E. D., T. F. Linsenmayer, R. L. Trelstad, and K. von der Mark (1979). "Origin and distribution of collagens in the developing avian cornea." *Current Topics in Eye Research* **1**: 1–35.
43. Holland, E. J. (1996). "Epithelial transplantation for severe ocular surface disease." *Transactions of the American Ophthalmological Society* **94**: 677–743.
44. Holland, E. J., A. R. Djalilian, et al. (2003). "Management of aniridic keratopathy with keratolimbal allograft: a limbal stem cell transplantation technique." *Ophthalmology* **110**(1): 125–130.
45. Holland, E. J. and G. S. Schwartz (1996). "The evolution of epithelial transplantation for severe ocular surface disease and a proposed classification system." *Cornea* **15**: 549–556.
46. Huang, A. J. and S. C. Tseng (1991). "Corneal epithelial wound healing in the absence of limbal epithelium." *Investigative Ophthalmology and Visual Science* **32**(1): 96–105.
47. Jang, Y. K., J. J. Park, M. C. Lee, B. H. Yoon, Y. S. Yang, S. E. Yang, et al. (2004). "Retinoic acid-mediated induction of neurons and glial cells from human umbilical cord-derived hematopoietic stem cells." *Journal of Neuroscience Research* **75**(4): 573–584.
48. Jester, J. V., P. A. Barry, G. J. Lind, W. M. Petroll, R. Garana, and H. D. Cavanagh (1994). "Corneal keratocytes: in situ and in vitro organization of cytoskeletal contractile proteins." *Investigative Ophthalmology & Visual Science* **35**(2): 730–743.
49. Jester, J. V., Barry-P. A. Lane, H. D. Cavanagh, and W. M. Petroll (1996). "Induction of alpha-smooth muscle actin expression and myofibroblast transformation in cultured corneal keratocytes." *Cornea* **15**(5): 505–516.
50. Jester, J. V., W. M. Petroll, and H. D. Cavanagh (1999). "Corneal stromal wound healing in refractive surgery: the role of myofibroblasts." *Progress in Retinal and Eye Research* **18**(3): 311–356.
51. Johnston, M. C., D. M. Noden, R. D. Hazelton, J. L. Coulombre, and A. J. Coulombre (1979). "Origins of avian ocular and periocular tissues." *Experimental Eye Research* **29**(1): 27–43.
52. Jones, P. and F. Watt (1993). "Separation of human epidermal stem cells from transit amplifying cells on the basis of differences in integrin function and expression." *Cell* **73**(4): 713–724.
53. Kasper, M. (1992). "Patterns of cytokeratins and vimentin in guinea-pig and mouse eye tissue – evidence for regional variations in intermediate filament expression in limbal epithelium." *Acta Histochemica* **93**(1): 319–332.
54. Kelley, M. W., J. K. Turner, et al. (1995). "Regulation of proliferation and photoreceptor differentiation in fetal human retinal cell-cultures." *Investigative Ophthalmology and Visual Science* **36**(7): 1280–1289.
55. Kim, M., H. Turnquist, J. Jackson, M. Sgagias, Y. Yan, M. Gong, et al. (2002). "The multidrug resistance transporter ABCG2 (breast cancer resistance protein 1) effluxes Hoechst 33342 and is overexpressed in hematopoietic stem cells." *Clinical Cancer Research* **8**(1): 22–28.
56. Koizumi, N., T. Inatomi, et al. (2001). "Cultivated corneal epithelial stem cell transplantation in ocular surface disorders." *Ophthalmology* **108**: 1569–1574.
57. Koizumi, N., T. Inatomi, et al. (2001). "Cultivated corneal epithelial transplantation for ocular surface reconstruction in acute phase of Stevens-Johnson syndrome." *Archives of Ophthalmology* **119**: 298–300.
58. Lawrence, J. M., S. Singhal, et al. (2007). "MIO-M1 cells and similar Muller glial cell lines derived from adult human retina exhibit neural stem cell characteristics." *Stem Cells* **25**(8): 2033–2043.
59. Lechner, A., C. A. Leech, E. J. Abraham, A. L. Nolan, and J. F. Habener (2002). "Nestin-positive progenitor cells derived from adult human pancreatic islets of Langerhans contain side population (SP) cells defined by expression of the ABCG2 (BCRP1) ATP-binding cassette transporter." *Biochemical and Biophysical Research Communications* **293**(2): 670–674.

60. Lewis, G. P., P. A. Erickson, et al. (1988). "An immunocytochemical comparison of muller cells and astrocytes in the cat retina." *Experimental Eye Research* **47**(6): 839–853.
61. Li, D. Q., Z. Chen, X. J. Song, de Paiva, C. S., H. S. Kim, and S. C. Pflugfelder (2005). "Partial enrichment of a population of human limbal epithelial cells with putative stem cell properties based on collagen type IV adhesiveness." *Experimental Eye Research* **80**(4): 581–590.
62. Limb, G. A., T. E. Salt, et al. (2002). "In vitro characterization of a spontaneously immortalized human Muller cell line (MIO-M1)." *Investigative Ophthalmology and Visual Science* **43**(3): 864–869.
63. Linsenmayer, T. F., J. M. Fitch, M. K. Gordon, C. X. Cai, F. Igoe, J. K. Marchant, et al. (1998). "Development and roles of collagenous matrices in the embryonic avian cornea." *Progress in Retinal and Eye Research* **17**(2): 231–265.
64. Lohrum, M. A. E., and K. H. Vousden (2000). "Regulation and function of the p53-related proteins: same family, different rules." *Trends in Cell Biology* **10**(5): 197–202.
65. Lund, R. D., P. Adamson, et al. (2001). "Subretinal transplantation of genetically modified human cell lines attenuates loss of visual function in dystrophic rats." *Proceedings of the National Academy of Sciences of the United States of America* **98**(17): 9942–9947.
66. Lund, R. D., S. M. Wang, et al. (2007). "Cells isolated from umbilical cord tissue rescue photoreceptors and visual functions in a rodent model of retinal disease." *Stem Cells* **25**(4): 602.
67. Martin, C. M., A. P. Meeson, S. M. Robertson, T. J. Hawke, J. A. Richardson, S. Bates, et al. (2004). "Persistent expression of the ATP-binding cassette transporter, *Abcg2*, identifies cardiac SP cells in the developing and adult heart." *Developmental Biology* **265**(1): 262–275.
68. Masur, S. K., H. S. Dewal, T. T. Dinh, I. Erenburg, and S. Petridou (1996). "Myofibroblasts differentiate from fibroblasts when plated at low density." *Proceedings of the National Academy of Sciences of the United States of America* **93**(9): 4219–4223.
69. Mills, A. A., B. Zheng, X. J. Wang, H. Vogel, D. R. Roop, and A. Bradley, (1999). "p63 is a p53 homologue required for limb and epidermal morphogenesis." *Nature* **398**(6729): 708–713.
70. Moshiri, A., J. Close, et al. (2004). "Retinal stem cells and regeneration." *International Journal of Developmental Biology* **48**(8–9): 1003–1014.
71. Nakamura, M., T. Inatomi, et al. (2004). "Successful primary culture and autologous transplantation of corneal limbal epithelial cells from minimal biopsy for unilateral severe ocular surface disorder." *Acta Ophthalmologica Scandinavica* **82**: 468–471.
72. Nakamura, M., T. Inatomi, et al. (2006). "Transplantation of autologous serum-derived cultivated corneal epithelial equivalents for the treatment of severe ocular surface disease." *Ophthalmology* **113**: 1756–1772.
73. Nakamura T., F. Ishikawa, K. H. Sonoda, T. Hisatomi, H. Qiao, J. Yamada, et al. (2005). "Characterization and distribution of bone marrow-derived cells in mouse cornea." *Investigative Ophthalmology & Visual Science* **46**(2): 497–503.
74. Newman, E. and A. Reichenbach (1996). "The Muller cell: a functional element of the retina." *Trends in Neurosciences* **19**(8): 307–312.
75. Nishida, K., S. Kinoshita, et al. (1995). "Ocular surface abnormalities in aniridia." *American Journal of Ophthalmology* **120**(3): 368–375.
76. Ooto, S., T. Akagi, et al. (2004). "Potential for neural regeneration after neurotoxic injury in the adult mammalian retina." *Proceedings of the National Academy of Sciences of the United States of America* **101**(37): 13654–13659.
77. Pellegrini, G., E. Dellambra, O. Golisano, E. Martinelli, I. Fantozzi, S. Bondanza, D. Ponzin, F. McKeon and M. De Luca (2001). "p63 identifies keratinocyte stem cells." *Proceedings of the National Academy of Sciences of the United States of America* **98**(6): 3156–3161.
78. Pellegrini, G., O. Golisano, et al. (1999). "Location and clonal analysis of stem cells and their differentiated progeny in the human ocular surface." *Journal of Cell Biology* **145**(4): 769–782.

79. Pellegrini, G., C. E. Traverso, et al. (1997). "Long-term restoration of damaged corneal surfaces with autologous cultivated human epithelium." *The Lancet* **349**: 990–993.
80. Puangsrichareon, V. and S. C. Tseng (1995). "Cytologic evidence of corneal diseases with limbal stem cell deficiency." *Ophthalmology* **102**(10): 1476–1485.
81. Qiu, G. T., M. J. Seiler, et al. (2005). "Photoreceptor differentiation and integration of retinal progenitor cells transplanted into transgenic rats." *Experimental Eye Research* **80**(4): 515–525.
82. Rama, P., S. Bonini, et al. (2001). "Autologous fibrin-cultured limbal stem cells permanently restore the corneal surface of patients with total limbal stem cell deficiency." *Transplantation* **72**(9): 1478–1485.
83. Raymond, P. A., L. K. Barthel, et al. (2006). "Molecular characterization of retinal stem cells and their niches in adult zebrafish." *BMC Developmental Biology* **6**.
84. Raymond, P. A. and P. F. Hitchcock (1997). "Retinal regeneration: common principles but a diversity of mechanisms." *Advances in Neurology* **72**: 171–184.
85. Rhodes, R. H. (1979). "Light microscopic study of the developing human neural retina." *American Journal of Anatomy* **154**(2): 195–209.
86. Saari, J. C. and J. W. Crabb (2005). "Focus on molecules: cellular retinaldehyde-binding protein (CRALBP)." *Experimental Eye Research* **81**(3): 245–246.
87. Saari, J. C., J. Huang, et al. (1997). "Cellular retinaldehyde-binding protein is expressed by oligodendrocytes in optic nerve and brain." *Glia* **21**(3): 259–268.
88. Sangwan, V. S., H. P. Matalia, et al. (2006). "Clinical outcome of autologous cultivated limbal epithelium transplantation." *Indian Journal of Ophthalmology* **54**: 29–34.
89. Scharenberg, C. W., M. A. Harkey, and B. Torok-Storb (2002). "The ABCG2 transporter is an efficient Hoechst 33342 efflux pump and is preferentially expressed by immature human hematopoietic progenitors." *Blood* **99**(2): 507–512.
90. Schermer, A., S. Galvin, et al. (1986). "Differentiation-related expression of a major 64K corneal keratin in vivo and in culture suggests limbal location of corneal epithelial stem cells." *Journal of Cell Biology* **103**(1): 49–62.
91. Schlotzer-Schrehardt, U. and F. E. Kruse (2005). "Identification and characterization of limbal stem cells." *Experimental Eye Research* **81**: 247–264.
92. Schwab, I. R. (1999). "Cultured corneal epithelia for ocular surface disease." *Transactions of the American Ophthalmological Society* **97**: 891–986.
93. Shanmuganathan, V. A., T. Foster, et al. (2007). "Morphological characteristics of the limbal epithelial crypt." *British Journal of Ophthalmology* **91**(4): 514–519.
94. Shimazaki, J., M. Aiba, et al. (2002). "Transplantation of human limbal epithelium cultivated on amniotic membrane for the treatment of severe ocular surface disorders." *Ophthalmology* **109**: 1285–1290.
95. Shortt, A. J., G. A. Secker, et al. (2007). "Characterization of the limbal epithelial stem cell niche: novel imaging techniques permit in vivo observation and targeted biopsy of limbal epithelial stem cells." *Stem Cells* **25**: 1402–1409.
96. Singhal, S., J. M. Lawrence, et al. (2008). "Chondroitin sulfate proteoglycans and microglia prevent migration and integration of grafted Muller stem cells into degenerating retina." *Stem Cells* **26**(4): 1074–1082.
97. Sosnova, M., M. Bradl, and J. V. Forrester (2005). "CD34+ corneal stromal cells are bone marrow-derived and express hemopoietic stem cell markers." *Stem Cells* **23**(4): 507–515.
98. Takahashi, M., T. D. Palmer, et al. (1998). "Widespread integration and survival of adult-derived neural progenitor cells in the developing optic retina." *Molecular and Cellular Neuroscience* **12**(6): 340–348.
99. Terunuma, A., K. L. Jackson, V. Kapoor, W. G. Telford, and J. C. Vogel (2003). "Side population keratinocytes resembling bone marrow side population stem cells are distinct from label-retaining keratinocyte stem cells." *Journal of Investigative Dermatology* **121**(5): 1095–1103.
100. Townsend, W. M. (1991). "The limbal palisades of Vogt." *Transactions of the American Ophthalmological Society* **89**: 721–756.

101. Triel, C., M. E. Vestergaard, L. Bolund, T. G. Jensen, and U. B. Jensen (2004). "Side population cells in human and mouse epidermis lack stem cell characteristics." *Experimental Cell Research* **295**(1): 79–90.
102. Tropepe, V., B. L. K. Coles, et al. (2000). "Retinal stem cells in the adult mammalian eye." *Science* **287**(5460): 2032–2036.
103. Tsai, R. J.-F., L.-M. Li, et al. (2000). "Reconstruction of damaged corneas by transplantation of autologous limbal epithelial cells." *The New England Journal of Medicine* **343**: 86–93.
104. Umemoto, T., M. Yamato, K. Nishida, J. Yang, Y. Tano and T. Okano (2006). "Limbal epithelial side-population cells have stem cell-like properties, including quiescent state." *Stem Cells* **24**(1): 86–94.
105. van Rossum, M. M., J. Schalkwijk, P. C. van de Kerkhof and P. E. van Erp (2002). "Immunofluorescent surface labelling, flow sorting and culturing of putative epidermal stem cells derived from small skin punch biopsies." *Journal of Immunological Methods* **267**(2): 109–117.
106. Verfaillie, C. M. (2002). "Adult stem cells: assessing the case for pluripotency." *Trends in Cell Biology* **12**(11): 502–508.
107. Watanabe, K., K. Nishida, M. Yamato, T. Umemoto, T. Sumide, K. Yamamoto, N. Maeda, H. Watanabe, T. Okano and Y. Tano (2004). "Human limbal epithelium contains side population cells expressing the ATP-binding cassette transporter ABCG2." *FEBS Letters* **565**: 6–20.
108. Wulle, K. G. (1972). "Electron microscopy of the fetal development of the corneal endothelium and Descemet's membrane of the human eye." *Investigative Ophthalmology* **11**(11): 897–904.
109. Yang, A., R. Schweitzer, et al. (1999). "p63 is essential for regenerative proliferation in limb, craniofacial and epithelial development." *Nature* **398**(6729): 714–718.
110. Zhou, S., J. D. Schuetz, K. D. Bunting, A. M. Colapietro, J. Sampath, J. J. Morris, I. Lagutina, G. C. Grosveld, M. Osawa, H. Nakauchi and B. P. Sorrentino (2001). "The ABC transporter Bcrp1/ABCG2 is expressed in a wide variety of stem cells and is a molecular determinant of the side-population phenotype." *Nature Medicine* **7**(9): 1028–1034.
111. Zieske, J. D. (2004). "Corneal development associated with eyelid opening." *The International Journal of Developmental Biology* **48**(8–9): 903–911.

Chapter 6

Colon

F. Iovino, Y. Lombardo, V. Eterno, P. Cammareri, G. Cocorullo,
M. Todaro and G. Stassi

Abstract The aim of this chapter is to show the key features of adult colon stem cells and provide a useful tool for their isolation, characterization and propagation.

In 1974, the “Unitarian theory” was proposed, according to which all the cell types within the crypt can be derived from a single stem cell [2].

The intestinal epithelium has a well defined structure ordered into crypt and villi, with a hierarchical organization that consists of cells displaying features of stem cells, rapidly dividing cell with little or no stem cells attributes (also called “transit-amplifying cells”) and differentiated cells. Intestinal epithelial stem cells are located toward the bottom of the crypt in the large intestine, and above the Paneth cells in the small intestine. Their differentiated progeny migrate upward through the transit-amplifying zone in the lower-to-middle region of the crypt, before becoming terminally differentiated, and are finally shed into the lumen [11]. In contrast, Paneth cells remain at the bottom of small intestinal crypts and play an important role in maintaining the sterility of the crypt [10]. The differentiated compartment of intestine comprises: absorptive enterocytes, hormone-secreting endocrine cells, mucus-producing goblet cells and “M” cells involved in the transport of antigens from the gut lumen into Peyer’s patches.

Stem cells are surrounded by other cells and extracellular matrix within a niche that provides an optimal environment for stem cell homeostasis [15]. Although there is evidence for a stem cell niche in the gut, little is known. The intestinal stem cell niche is thought to be covered by intestinal subepithelial myofibroblasts (ISEMFs) that create a syncytium with the lamina propria and merge with the pericytes associated with the blood vessels. The myofibroblasts play a vital role in epithelial-mesenchymal interactions and they are probably required for the regulation of epithelial cell differentiation, which might be dependent on their secretion of growth factors. Among the factors secreted by ISEMFs, the Wnt proteins [18]

G. Stassi (✉)

Cellular and Molecular Pathophysiology Laboratory, Department of Surgical and Oncological Sciences, University of Palermo, Palermo, Italy
e-mail: gstassi@tiscali.it

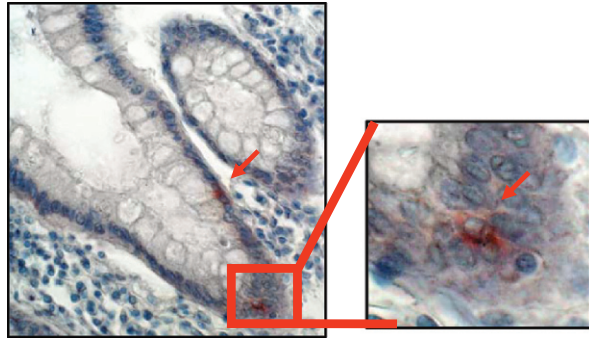
are involved in the control of colon stem cells and may maintain stem cells in a self-renewing state.

The interaction of Wnt proteins and their receptors, belonging to the Frizzled protein family, ultimately regulates the stability of the multifunctional protein beta-catenin. In the absence of Wnt, beta-catenin binds to the scaffold protein Axin in a multiprotein complex containing the tumour suppressor APC and GSK3beta leading to its proteasomal degradation. Following Wnt stimulation, Dishevelled protein is recruited to the membrane where it binds to Axin, inhibiting the degradation of the complex Axin/APC/GSK3/beta-catenin. This allows the migration of beta-catenin from the cytoplasm to the nucleus, where it regulates the expression of target genes in cooperation with the transcription factors TCF/LEF [4]. Because Wnt signals are the principal driving force behind the development of the crypt, it has been hypothesized that some Wnt target genes may be specifically expressed in the stem cells. However, it was demonstrated that most Wnt target genes were expressed in either Paneth cells or transit-amplifying cells and only LGR5 (Leucin-rich-repeat containing G-protein-coupled Receptor 5, also known as GPR49) gene has been proposed as a stem cell marker in the small intestine as well as in the colon crypts of mice [1].

Another important pathway involved in the regulation of stem cell fate is the Notch pathway. Briefly, Notch signalling is controlled by four homologous proteins in mammals, Notch1–4 that interact with several surface-bound ligands (DSL ligands: Delta, Delta like, Jagged1 and Jagged2 in vertebrates). Upon ligand binding, Notch receptors are activated by serial cleavage events involving members of the ADAM (A Disintegrin And Metalloproteinase) protease family, as well as an intramembrane cleavage regulated by γ -secretase (presenilin). This intramembrane cleavage is followed by translocation of the intracellular domain of Notch to the nucleus, where it acts on downstream targets. Musashi-1 (Msi-1) is a positive regulator of Notch signalling through an interaction with Numb mRNA and repression of its translation [5]. Musashi-1 protein was the first colon stem cell marker identified. It is a RNA-binding protein initially identified in *Drosophila* where it plays an essential role in the early asymmetric divisions of the sensory organ precursor cells. The mammalian homologue probably is involved in the early asymmetric divisions that give rise to differentiated cells from neural stem cells or progenitor cells [6]. Msi-1 positive cells localize within the deeper two thirds of the colon crypt, in the proliferating compartment [8]. Thus, Msi-1 might be a useful stem cell marker for human colon epithelium. Moreover, hairy and enhancer of split homolog-1 (Hes-1) has been proposed as a marker of intestinal stem cells [13]. Both Msi-1 and Hes1 have been demonstrated to play key roles in the maintenance of the neural stem cell state and its differentiation. Recent studies found that Msi-1 and Hes1 are expressed in the small intestine; particularly, Msi-1 in a few epithelial cells and Hes-1 in lower crypt cells above the Paneth cells. By contrast, Msi-1 and Hes-1 are not expressed in Paneth cells [7].

The rapid turnover of committed colon cells means that a homeostatic balance of stem cells in the regulation of proliferation, senescence, and apoptosis must be maintained. It is presumed that colonic epithelial stem cells are the principal cell

Fig. 6.1 Immunohistochemical analysis of CD133 on colon tissue



CD133 staining

type at risk of incurring the series of somatic mutations leading to cancer, since all other epithelial cell types are short lived.

Recently, two independent research groups have identified a population of human colon stem cells that express CD133 (CD133⁺) that can initiate and sustain tumor growth [9, 12]. CD133 is a five-transmembrane glycoprotein previously identified as a stem cell marker in the neural system and normal primitive cells of the hematopoietic, epithelial and endothelial lineages [14, 17, 19]. Our group has shown that CD133 localises at the bottom of the crypt in the putative position of stem cells (Fig. 6.1). CD133⁺ cells from colon tumors have stem-like properties and can grow exponentially *in vitro* as undifferentiated tumor spheres. Furthermore, transplantation of CD133⁺, but not of CD133⁻ cells, into nude or NOD/SCID mice is sufficient to induce tumor growth, reproducing the same morphological and antigenic pattern of the original human tumors [16].

Recent findings show that the CD133⁺ subpopulation contains cells expressing the stem cell marker Msi-1 and this expression is maintained in stem-like cells derived from xenografted tumors, suggesting that this molecule could have an active role in driving tumorigenesis.

Recent observations indicate that in the CD133⁺ population there is a restricted subset of CD44⁺ epithelial cells able to engraft *in vivo* in immunodeficient mice. Analysis of the surface molecule repertoire of EpCAM^{high}/CD44⁺ cell led to the identification of CD166 as an additional marker for colon stem cells isolation [3].

6.1 Identification of Stem Cell Markers in Colon Tissues

The identification of stem cells is difficult due to the lack of morphological criteria or specific markers. Recent studies have shown expression of several putative stem cell markers, including Musashi1, CD133 and Hes1.

Immunohistochemistry is a simple and direct method which can be used to detect the presence of specific markers on paraffin-embedded colon specimens.

The protocol depends on the type of antigen and on the primary antibody used. The introduction of antigen retrieval (AR) techniques improves the sensitivity of immunohistochemical detection of various antigens in formalin-fixed and paraffin-embedded tissues. The microwave-heating and pressure-cooking procedures are the most effective AR methods reported to date. If the visualization of the antigen depends on horseradish peroxidase it is necessary to inactivate endogenous peroxidases using H_2O_2 .

6.1.1 Immunohistochemistry

Reagents and Materials

- Xylene
- Ethanol
- Antigen retrieval solution: 10 mM sodium citrate pH 6.0, Borate pH 8.0 or Tris buffer pH 9.5
- 3% H_2O_2
- Human serum
- Saline buffer (PBS or TRIS)
- Microwave oven

Procedure

The first step is to de-wax the slides with the following solutions:

- xylene 100% 10 min (twice);
- ethanol 100% 5 min;
- xylene 100% 5 min;
- ethanol 100% 5 min;

then hydrate in:

- ethanol 96% 5 min;
- ethanol 50% 5 min;
- wash in H_2O ;
- *Optional*: heat slides for antigen retrieval in optimal AR buffer conditions depending on the antibody in a microwave oven for 1 min at 450 W followed by 5 min at 100 W.
- *Optional*: after rinsing in dH_2O , the sections are incubated in 3% H_2O_2 for 5 min to suppress endogenous peroxidase activity;
- wash in a saline buffer for 5 min (twice);
- incubate sections with 10% human serum for 20 min to block non-specific staining;
- drain excess serum;

- incubate with specific primary monoclonal antibodies against a stem cell marker, overnight at 4°C or 1 h at 37°C in humidified chamber;
- wash in a saline buffer for 5 min (twice);
- incubate with enzyme-labelled specific secondary antibody in humidified chamber 1 h at 37°C;
- develop the stain using an appropriate substrate-chromogen solution;
- coverslip with mounting medium.

6.1.1.1 Detection of CD133

Histochemical analysis of CD133 can be performed on 5 µm thick paraffin-embedded and cryostat sections of colon specimens [16].

Reagents and Materials

- 1X TRIS/saline buffer (TBS)
- Ethanol
- human serum from AB donors
- antibody CD133/2, AC133 mouse IgG₁, Miltenyi
- LSAB 2 Kit, Dako
- Hematoxylin
- ammonia water
- distilled water
- mounting medium, DAKO

Procedure

For paraffin-embedded slides:

- dewax and rehydrate the slides as previously described;
- rinse in 1X TRIS/saline buffer (TBS) for 5 min at room temperature (twice);
- add 3% H₂O₂ for 5 min;
- rinse in 1X TBS 5 min;
- incubate with 10% human serum 20 min at room temperature;
- drain excess serum;
- add primary monoclonal antibody anti CD133 dilution 1:5 in TBS overnight at 4°C;
- rinse in 1X TBS 5 min (twice);
- add biotinylated anti-mouse immunoglobulins (LSAB 2 Kit, Dako) 30 min at room temperature;
- rinse in 1X TBS 5 min (twice);
- add streptavidin-peroxidase 30 min at room temperature;
- develop the stain with AEC substrate chromogen 5–10 min room temperature;
- rinse gently with distilled water;
- counterstain nuclei with aqueous-Hematoxylin 3 min;

- rinse gently with distilled water;
- dip slides 10 times into a bath of 0.037 mM ammonia water;
- rinse gently with distilled water;
- Mount the coverslips with an aqueous based mounting medium.

For cryostat sections, fix the samples in 2% paraformaldehyde for 20 min at 37°C, wash in TBS and treat as described above.

6.1.2 Immunofluorescence

Alternatively, CD133 can be detected by immunofluorescence performed on both 5 µm thick paraffin-embedded and cryostat sections of colon specimens.

Reagents and Materials

- Xylene
- Ethanol
- PBS
- Primary monoclonal antibody anti CD133 (CD133/2, AC133 mouse IgG₁, Miltenyi)
- Rhodamine RedTM-conjugated anti-mouse
- RNA-ase
- Hoechst 33342
- Toto 3 iodide

Procedure

For paraffin-embedded slides:

- dewax and rehydrate slides as previously described;
- wash in PBS 5 min;
- add primary monoclonal antibody anti CD133 (CD133/2, AC133 mouse IgG₁, Miltenyi) dilution 1:5 in PBS was incubated overnight at 4°C;
- wash in PBS 5 min (three times);
- incubate in Rhodamine RedTM-conjugated anti-mouse diluted in PBS 1 h at 37°C;
- wash in PBS 5 min (three times);
- counterstain nuclei using Hoechst 33342
- *Optional*: counterstain nuclei with TOTO3 iodide, it need pre-treatment with RNA-ase (final concentration 200 µg/ml) for 30 min at 37°C. Proceed with the TOTO 3 staining.

Cryostat sections can be fixed in acetone for 20 min at 37°C, wash in PBS and directly incubated with primary antibody.

6.2 Isolation of Colon Stem Cells

There are various methods to isolate colon stem cells, the most popular of which is digestion of tissue followed by cell selection with cell surface stem cell marker by MACS (Magnetic Cell Sorting) or FACS (Fluorescence Activated Cell Sorting) technologies.

6.2.1 Tissue Digestion

Reagents and Materials

- Saline Buffer (PBS)
- 500 U/ml penicillin
- 500 μ g/ml streptomycin
- 1.25 μ g/ml amphotericin B
- 0.6 mg/ml amoxicillin
- 1 mg/ml metronidazole
- 5 mg/ml collagenase;
- 20 μ g/ml hyaluronidase
- sterile scissors
- rotary shaker
- centrifuge

Procedure

The tissue is transferred to PBS containing penicillin, streptomycin, amphotericin B, metronidazole and amoxicillin and extensively washed because colon, due to its anatomical site, is prone to bacterial contamination. After removing necrotic regions with sterile scissors, the tissue is cut in small pieces (about 1 mm³) and then digested with proteolytic enzymes and antibiotics for 16 h on a rotary shaker at 37°C.

The following day the material is transferred to a new tube;

- centrifuge at 800 rpm for 5 min;
- discard the supernatant;
- resuspend the pellet in an appropriate volume ($\sim 10^5$ cells/ml) of colon sphere growth medium;
- proceed with the FACS or MACS analysis and plate the cells in non-adherent conditions in colon sphere medium (Fig. 6.2).

6.2.2 Sorting of Colon Stem Cells by FACS Technology

Flow cytometry is a powerful technique for analyzing large mixed populations of single cells. Fluorescence-activated cell sorting (FACS) permits measurement of the fluorescent signal and separation of the cells from a mixed population on the basis of fluorescence intensity, size and viability. Fluorochromes with different emission

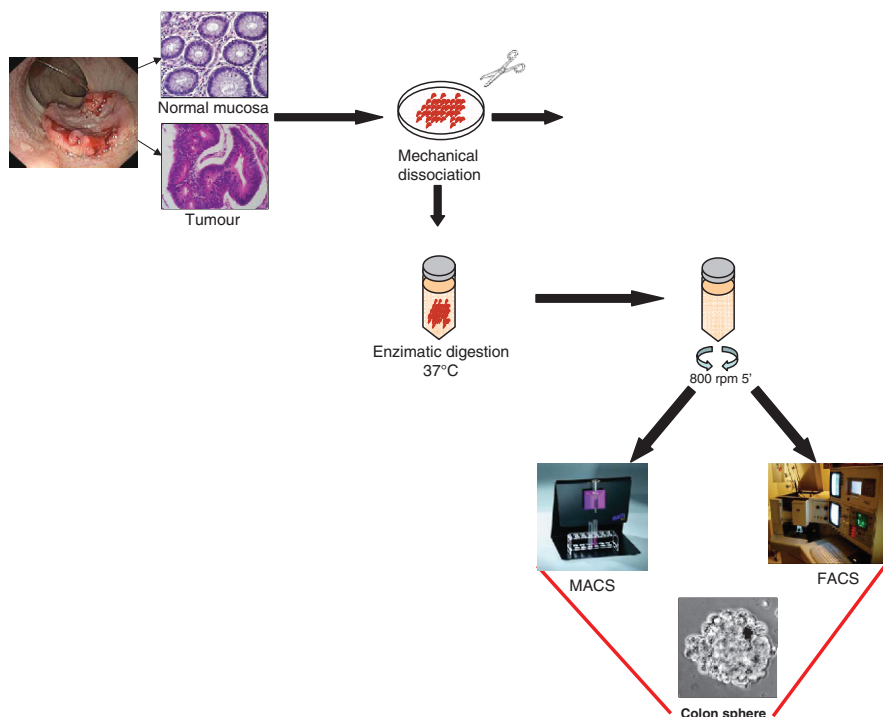


Fig. 6.2 Scheme of sphere development from colon tissue. After enzymatic digestion at 37°C of surgical specimens, the cells are centrifuged and proceeded by FACS or MACS for the detection of specific antibodies. The purified cells can be plated in Ultra-adherence flasks that permit sphere formation

wavelengths can be used concurrently, allowing for multi-parameter separations. There are two different methods for antigen detection: direct or indirect.

In direct immunofluorescence, the cells are incubated with a primary antibody specific for stem cell marker directly conjugated to a fluorochrome (e.g. phycoerythrin or fluorescein isothiocyanate). This has the advantage of requiring only one antibody incubation step and eliminates the possibility of non-specific binding from a secondary antibody.

In indirect staining, the primary antibody is not fluorochrome labelled but is detected by a second fluorochrome-labelled antibody. Alternatively, the avidin-biotin system can be used, whereby an antibody is conjugated to biotin and detected with fluorochrome-labelled avidin.

Labelled cells are analysed and sorted on the flow cytometer and the cells obtained can be cultivated in stem cell medium or utilized for further analysis.

Reagents and Materials

- Saline Buffer (PBS)
- FBS (Fetal Bovine Serum)

- Primary and secondary antibodies
- FACS tubes
- Centrifuge

Procedure for Direct Staining

- Collect the spheres by centrifugation at 800 rpm for 5 min;
- wash the cells with PBS and adjust cell suspension to a concentration of 1.5×10^6 cells/ml in ice cold PBS plus 2% FBS;
- add primary labelled antibody according to manufacturer's protocol;
- incubate for 30 min on ice;
- wash the cells two times by centrifuging at 800 rpm for 5 min and resuspend in an appropriate volume of ice cold PBS plus 2% FBS. Keep the cells in the dark on ice or at 4°C until analysis;
- for best results, analyze the cells by FACS immediately;
- *Optional:* to verify the purity of the sorted population, cells can be analyzed by flow cytometry using a conjugated antibody that recognizes a different epitope.

Procedure for Indirect Staining

- Collect the cells by centrifugation at 800 rpm for 5 min;
- wash the cells with PBS, determine the total cell number and adjust cell suspension to a concentration of 1.5×10^6 cells/ml in ice cold PBS plus 2% FBS;
- add the primary antibody against a stem cell marker;
- incubate for 30 min on ice or at 4°C;
- wash the cells three times in PBS, centrifuge at 800 rpm for 5 min and resuspend in ice cold PBS plus 2% FBS;
- add the fluorochrome-labelled secondary antibody according to manufacturer's protocol;
- incubate for 30 min on ice in the dark;
- wash the cells three times in PBS, centrifuge at 800 rpm for 5 min and resuspend in 500 μ l to 1 ml ice cold PBS;
- store the cell suspension immediately at 4°C in the dark;
- for best results, analyze the cells by FACS immediately;
- *Optional:* to verify the purity of the sorted population, cells can be analyzed by flow cytometry using a conjugated antibody that recognizes a different epitope.

6.2.3 Isolation of Colon Stem Cells by MACS Technology

An alternative method to isolate stem cells uses MACS technology (www.miltenyibiotec.com), one of the fastest and easiest techniques used to separate cells in suspension to very high purity on the basis of cell surface stem markers. Using this technology, cells of interest are separated by a positive selection strategy which takes advantage of the high specificity of monoclonal antibodies. The positively

selected cells can be immediately used for culture in stem cell medium or for further downstream applications.

Reagents and Materials

- MACS column type MS or LS depending on the cell number (up to 10^7 or 2×10^8 magnetically labelled cells);
- Buffer: PBS pH 7.2, supplemented with 0.5% bovine serum albumin and 2 mM EDTA. Keep buffer cold at 4–8°C.
- MicroBeads conjugated with antibodies.

Procedure

For optimal performance it is important to obtain a single cell suspension (10^8 cells) before magnetic separation by mechanical dissociation:

- pipette the cells until they are well dissociated or pass the cell clumps through a 30 μ m nylon mesh;
- wash disaggregated cells in PBS and resuspend in 300 μ l of Buffer;
- add 100 μ l FcR Blocking Reagent;
- label cells by adding 100 μ l of MicroBeads conjugated with a specific monoclonal antibody;
- incubate for 30 min at 4–8°C;
- wash cells by adding 10–20x the labelling volume of buffer, centrifuge at 300g for 10 min;
- pipette off the supernatant;
- resuspend cell pellet in 500 μ l buffer for up to 10^8 total cells;

Proceed to Magnetic Separation

- choose a MS or a LS Column and place it in the magnetic field of a suitable MACS Separator;
- prepare column by rinsing with appropriate amount of buffer: MS: 500 μ l LS: 3 ml;
- apply cell suspension in suitable amount of buffer onto the column: MS: 500–1000 μ l LS: 1–10 ml; allow the negative cells to pass through;
- wash with appropriate amount of buffer: MS: 4×500 μ l, LS: 4×3 ml;
- remove column from separator and place column on a suitable collection tube;
- pipette appropriate amount of buffer onto the column: MS: 1 ml, LS: 5 ml;
- firmly flush out fraction with magnetically labeled cells using the plunger supplied with the column;
- repeat magnetic separation step. Apply the eluted cells to a new prefilled positive selection column.

It is possible to control the quality of MACS sorting by flow cytometry analysis using an antibody against a different epitope. After magnetic sorting, cell viability is assessed by Trypan blue exclusion.

6.3 Propagation of Colon Stem Cells

To propagate colon stem cells it is best to culture the digest in a medium containing several factors that favour stem cell growth, such as basic Fibroblast Growth Factor (bFGF) and Epidermal Growth Factor (EGF) and without Fetal Bovine Serum (FBS). This medium selects the immature cells, while differentiated cells die through anoikis. The colon stem cells slowly proliferate, growing as non-adherent clusters, termed “spheres”. Colon spheres can be expanded by enzymatic and mechanical dissociation, followed by re-plating of single cells in complete fresh medium. All the dissociated cells expressing stem cell markers show the capacity to form secondary spheres over multiple passages.

Reagents and Materials

- Saline Buffer (PBS)
- 500 U/ml penicillin
- 500 µg/ml streptomycin
- 1.25 µg/ml amphotericin B
- 0.6 mg/ml Amoxicillin
- ultra low adhesion flasks
- Centrifuge
- Cell growth medium
- 3 mM EDTA and 0.05 mM dithiothreitol (DTT) in PBS
- 0.05% trypsin and 0.02% EDTA

Colon Spheres Growth Medium DMEM/F12 (1:1)

- 6 mg/ml Glucose
- 1 mg/ml NaHCO₃
- 5 mM Hepes
- 2 mM L-Glutamine
- 4 µg/ml Heparin
- 4 mg/ml BSA (Bovine Serum Albumin)
- 10 ng/ml bFGF
- 20 ng/ml EGF
- 100 µg/ml apotransferrin
- 25 µg/ml insulin
- 9.6 µg/ml putrescin
- 30 nM sodium selenite anhydrous
- 20 nM progesterone

Procedure

- Centrifuge colon sphere cells at 800 rpm for 5 min;
- discard the supernatant;

- resuspend the pellet in 3 mM EDTA plus 0.05 mM dithiothreitol (DTT) in PBS or in 0.05% trypsin plus 0.02% EDTA for 5 min;
- incubate at 37°C for 5 min;
- centrifuge at 800 rpm for 5 min;
- discard the supernatant;
- resuspend the pellet in the specific medium and plate in Ultra-Low flasks.

6.4 Differentiation of Cells from Colon Spheres

Differentiated cells can be obtained from spheres by changing the culture conditions using a collagen coated flask or using a 3D culture technique.

The collagen forms a thin layer of gel that favours cellular adhesion. After one day of culture, floating undifferentiated cells attach to the flask and gradually differentiate, acquiring a phenotype similar to that of differentiated epithelial colon cells.

For 3D culture, Matrigel is used (a solubilised basement membrane preparation extracted from EHS mouse sarcoma, a tumor rich in ECM proteins). The major component is laminin, followed by collagen IV, heparan sulfate proteoglycans, and entactin. At room temperature, Matrigel polymerizes to produce biologically active matrix material resembling the mammalian cellular basement membrane. It provides a physiologically relevant environment in which stem cells can generate colonies organized in crypt-like structures (Fig. 6.3) and gradually acquire colon epithelia markers.

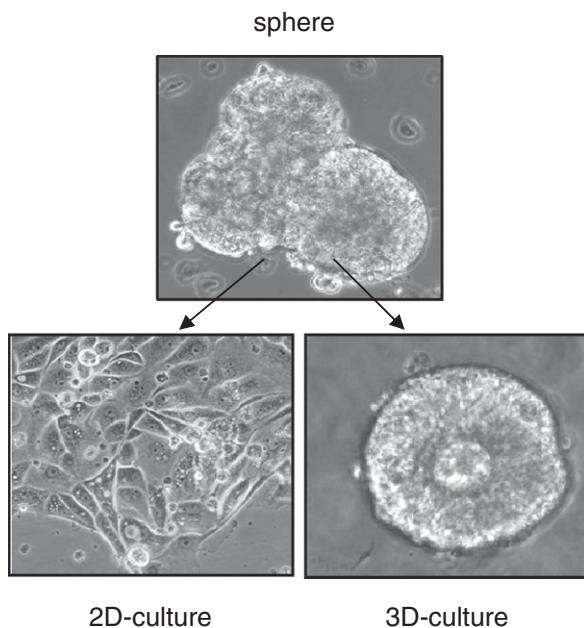


Fig. 6.3 Inverted phase contrast microscopy of purified colon cancer spheres (a) and after 7 days of culture in the presence of 10% FBS in 2-D Collagen-coated flasks (b) or in 3-D Matrigel (c) suspended cells

Reagents and Materials

- PBS
- DMEM-High Glucose
- 10% FBS (Fetal Bovine Serum)
- Collagen calf-skin
- Matrigel
- Plastic for cell culture

Procedure

The plates are coated with collagen at a concentration of 5 $\mu\text{g}/\text{cm}^2$ in PBS. The lyophilized solid collagen can be solubilised in 100 mM acetic acid (1 mg/ml) and the solution is liquid at 4°C and forms a gel at 37°C.

For coating plates:

- Add 5 ml for 75 cm^2 flasks and place at 37°C for at least 1 h;
- Wash twice with PBS to remove the acetic acid;
- Add 2–3 ml of Medium. If the colour changes it indicates that acid remains in the flask which could prevent cell growth.

To perform a 3-D cell culture with Matrigel, it is very important to keep it on ice and use pre-cooled pipettes and tubes when preparing the solution because Matrigel rapidly gels at 22–35°C. For embedding the spheres in Matrigel:

- collect the spheres by centrifugation at 800 rpm for 5 min;
- resuspend the spheres carefully in Matrigel Mix (1:3) with serum-free medium. For longer cultivation, the Matrigel concentration should be at least 60% in medium. The density of spheres should be less than 500/ml thinned Matrigel. At higher densities, they do not branch;
- incubate the cells at 37°C for 20–30 min to permit the Matrigel to solidify;
- once the Matrigel has hardened, add DMEM-High supplemented with 10% FBS carefully on top;
- every 3 days, the medium is changed by gently aspiration with a pipette (no vacuum).

Acknowledgments This work was supported by grants from AIRC to G. Stassi and M. Todaro, Programmi di Ricerca Scientifica di Rilevante Interesse Nazionale (PRIN) 2005 prot. 2005052122 to G. Stassi. Y. Lombardo is a AIRC fellowship recipient.

References

1. Barker, N. and H. Clevers (2007). “Tracking down the stem cells of the intestine: strategies to identify adult stem cells.” *Gastroenterology* **133**(6): 1755–60.
2. Cheng, H. and C. P. Leblond (1974). “Origin, differentiation and renewal of the four main epithelial cell types in the mouse small intestine. V. Unitarian Theory of the origin of the four epithelial cell types.” *Am J Anat* **141**(4): 537–61.

3. Dalerba, P., S. J. Dylla, et al. (2007). "Phenotypic characterization of human colorectal cancer stem cells." *Proc Natl Acad Sci U S A* **104**(24): 10158–63.
4. de Lau, W., N. Barker, et al. (2007). "WNT signaling in the normal intestine and colorectal cancer." *Front Biosci* **12**: 471–91.
5. Imai, T., A. Tokunaga, et al. (2001). "The neural RNA-binding protein Musashi1 translationally regulates mammalian numb gene expression by interacting with its mRNA." *Mol Cell Biol* **21**(12): 3888–900.
6. Kaneko, Y., S. Sakakibara, et al. (2000). "Musashi1: an evolutionally conserved marker for CNS progenitor cells including neural stem cells." *Dev Neurosci* **22**(1–2): 139–53.
7. Kayahara, T., M. Sawada, et al. (2003). "Candidate markers for stem and early progenitor cells, Musashi-1 and Hes1, are expressed in crypt base columnar cells of mouse small intestine." *FEBS Lett* **535**(1–3): 131–5.
8. Nishimura, S., N. Wakabayashi, et al. (2003). "Expression of Musashi-1 in human normal colon crypt cells: a possible stem cell marker of human colon epithelium." *Dig Dis Sci* **48**(8): 1523–9.
9. O'Brien, C. A., A. Pollett, et al. (2007). "A human colon cancer cell capable of initiating tumour growth in immunodeficient mice." *Nature* **445**(7123): 106–10.
10. Ouellette, M. M., M. Liao, et al. (2000). "Subsenescent telomere lengths in fibroblasts immortalized by limiting amounts of telomerase." *J Biol Chem* **275**(14): 10072–6.
11. Potten, C. S., C. Booth, et al. (1997). "The intestinal epithelial stem cell: the mucosal governor." *Int J Exp Pathol* **78**(4): 219–43.
12. Ricci-Vitiani, L., D. G. Lombardi, et al. (2007). "Identification and expansion of human colon-cancer-initiating cells." *Nature* **445**(7123): 111–5.
13. Sakakibara, S., T. Imai, et al. (1996). "Mouse-Musashi-1, a neural RNA-binding protein highly enriched in the mammalian CNS stem cell." *Dev Biol* **176**(2): 230–42.
14. Salven, P., S. Mustjoki, et al. (2003). "VEGFR-3 and CD133 identify a population of CD34+ lymphatic/vascular endothelial precursor cells." *Blood* **101**(1): 168–72.
15. Spradling, A., D. Drummond-Barbosa, et al. (2001). "Stem cells find their niche." *Nature* **414**(6859): 98–104.
16. Todaro, M., M. P. Alea, et al. (2007). "Colon cancer stem cells dictate tumor growth and resist cell death by production of interleukin-4." *Cell Stem Cell* **1**(4): 389–402.
17. Uchida, N., D. W. Buck, et al. (2000). "Direct isolation of human central nervous system stem cells." *Proc Natl Acad Sci U S A* **97**(26): 14720–5.
18. Yen, T. H. and N. A. Wright (2006). "The gastrointestinal tract stem cell niche." *Stem Cell Rev* **2**(3): 203–12.
19. Yin, A. H., S. Miraglia, et al. (1997). "AC133, a novel marker for human hematopoietic stem and progenitor cells." *Blood* **90**(12): 5002–12.

Chapter 7

Spermatogonia

Makoto C. Nagano, Jonathan R. Yeh and Khaled Zohni

Abstract Spermatogonial stem cells (SSCs) are the foundation of life-long, daily sperm production. SSCs support steady-state spermatogenesis and male fertility, thereby permitting transmission of genetic information to the next generation and maintaining the health of the species. Clinically, SSCs are a critical resource for restoration of male fertility following various testicular injuries, such as those caused by anti-cancer treatments. In vitro culture of human SSCs should provide an invaluable platform for biological and clinical studies of SSCs. Investigations into the mechanism that controls self-renewal and differentiation of human SSCs will be facilitated greatly by the use of in vitro experimentation. Human SSC culture systems should allow us to devise techniques to expand or preserve SSCs for efficient restoration of male fertility. SSC culture systems, however, have been developed only in animal models; none has been reported for human SSCs. This chapter first describes the culture methods developed for SSCs of experimental animals and then discusses issues that may be important for the development of a human SSC culture system.

7.1 Introduction

Spermatogenesis is a process in which numerous spermatozoa are produced constantly throughout life after puberty. This robust process is supported by a population of male germline stem cells, called spermatogonial stem cells (SSCs). In general, stem cells are defined by their biological activity to continuously self-renew and differentiate, leading to long-term maintenance and regeneration of normal adult tissue [1]. Based on this functional definition of stem cells, SSCs are detected unequivocally in animal models by the ability to regenerate and maintain spermatogenesis after transplantation of donor germ cells into infertile recipient testes [2–4]. A similar transplantation assay is currently not available for human SSCs,

M.C. Nagano (✉)

Department of Obstetrics and Gynecology, Royal Victoria Hospital, McGill University, Montreal, Quebec H3A 1A1, Canada

e-mail: makoto.nagano@muhc.mcgill.ca

and thus we cannot experimentally identify their presence. However, physiological characteristics of spermatogenesis indicate that a stem cell population does exist in the human male germ line. First, numerous spermatozoa are produced in the seminiferous epithelium and constantly released into male reproductive tracts but are replenished on a daily basis [5]. Second, complete regeneration of spermatogenesis can occur after sterilizing chemotherapy, sometimes after decades of azoospermia [6]. These phenomena cannot emerge without a population of cells that continuously self-renew and differentiate in the human male germ line. These facts indicate the presence of human SSCs.

Clinically, SSCs potentially hold the key to male fertility restoration in cancer survivors who may suffer from permanent infertility induced by cytotoxic anti-cancer treatment [6]. As survival rates improve, the negative impact of infertility on quality of life is experienced by more individuals, particularly preadolescent boys. While cryopreservation of sperm is commonly used to preserve fertility in adults, it is not possible for preadolescent boys, who do not yet produce sperm. However, since SSCs are present in the testis throughout life, even during childhood, fertility might be restored by (1) pharmacologically encouraging SSC survival during therapy and SSC proliferation and differentiation post-therapy, or by (2) surgically harvesting SSCs before therapy and transplanting them back to the patient's testes after therapy [7].

To accomplish these clinical goals, we need a better understanding of the mechanism that controls SSC survival, self-renewal, and differentiation. The establishment of a human SSC culture system will allow us to identify signaling cascades regulating SSC fate decision. It will also provide an important platform for investigations into discovery of novel chemical compounds that influence regeneration activity of SSCs or protect SSCs from adverse actions of anti-cancer agents. Furthermore, a human SSC culture system will solve a significant problem that SSCs are only a small subpopulation of germ cells, estimated at 0.01% in adult mouse testis [8], which causes difficulties in SSC manipulations. In animal models, SSCs can be cultured for a long time and exponentially amplified *ex vivo*, but such a system does not yet exist for human SSCs. The theme of this chapter is therefore twofold. First, the methods of SSC culture established in the mouse are described, and modifications required to adapt mouse SSC culture methods to other experimental animal species are discussed. The second theme considers issues that may be important to develop human SSC cultures. These two themes will be discussed in parallel in the following sections.

7.2 Protocols Developed for Mouse SSC Culture

Two types of mouse SSC culture protocols have been reported, the core process of which are the following (Fig. 7.1): (1) prepare a single cell suspension of heterogeneous testicular cells; (2) enrich the cells for SSCs; (3) place the enriched cells on a feeder layer; and (4) culture in serum-free or serum-reduced medium containing growth factors, notably, glial-cell-line-derived neurotrophic factor (GDNF). In both methods, SSCs form three-dimensional aggregates of germ cells, which

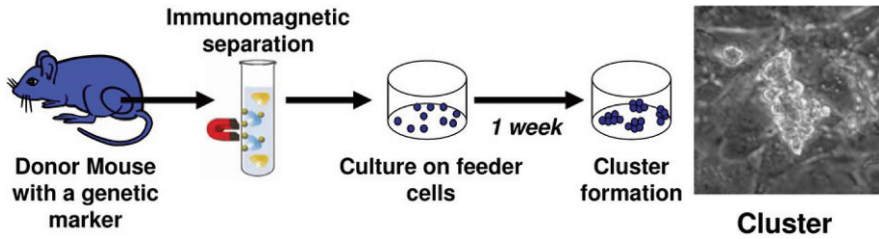


Fig. 7.1 Outline of SSC culture preparation. A single cell suspension of testis cells is enriched for SSCs using an immunological cell separation method and placed on a feeder layer of embryonic fibroblasts. SSCs are cultured in a serum-free or serum-reduced medium supplemented with growth factors, including GDNF. SSCs form three-dimensional aggregates of germ cells (clusters) on feeders. Serial passaging of clusters allows long-term culture and robust amplification of SSCs

are designated as “clusters” (Fig. 7.1). Transplantation of cluster cells results in regeneration of spermatogenesis, demonstrating the presence of SSCs [9–12]. SSCs can be amplified robustly by serially passaging the clusters [9–12].

The information obtained from mouse SSC culture systems suggests that three procedural elements may be important to develop human culture systems: (1) cell preparation, (2) medium composition, and (3) growth factors. We will briefly summarize these elements and compare them between the two protocols in the following section.

Protocol 1

The first protocol of long-term amplification culture for mouse SSCs was reported by Kanatsu-Shinohara et al. in 2003 [9]. Originally, the authors placed neonatal mouse testis cells in a gelatin-coated tissue culture well and cultured them in serum-reduced medium with growth factors and steroid hormones (see below). Testicular somatic cells proliferated and occupied the growth surface of the well on which proliferating germ cells formed clusters. Following a few passages, the proliferation ability of somatic cells diminished; thus, subsequent culture employed a feeder layer of mouse embryonic fibroblast (MEF). It is known that the clusters can also be derived from pup (~1 week old) and adult mouse testes with the highest efficiency of cluster derivation from pup cells [13].

Cell preparation: Testis cells are made into a single cell suspension using a conventional two-step enzymatic digestion; i.e., collagenase followed by trypsin [3]. While neonatal testis cells can be seeded directly into a tissue culture well [9], pup and adult testis cells are first enriched for SSCs using an anti-CD9 antibody in immunomagnetic cell sorting [13, 14] (see Section 7.4). The sorted cells are then placed on a feeder layer of MEF. This cell sorting process is essential to establish germ cell clusters from pup and adult SSCs and is also effective for neonatal SSCs [13]. Although the original protocol using neonatal cells did not include the cell sorting step [9], initial passaging with somatic cells may have enriched SSCs, since it forced somatic cells to lose proliferation activity while sustaining cluster cell proliferation.

Table 7.1 Supplements to the medium used in Protocol 1

Component*	Final concentration mouse
1. D-(+)-glucose (mg/ml)	6
2. Pyruvic acid (μ g/ml)	30
3. DL-lactic acid (ul/ml)	1
4. BSA (mg/ml)	5
5. Transferrin (μ g/ml)	100
6. L-glutamine (mM)	2
7. Na_2SeO_3 (nM)	30
8. 2-mercaptoethanol (μ M)	50
9. Insulin (μ g/ml)	25
10. Ascorbic acid (mM)	0.1
11. Putrescine (μ M)	60
12. d-biotin (μ g/ml)	10

* The base medium is StemPro-34 SFM, supplemented with StemPro supplement, MEM vitamin solution, and MEM nonessential amino acid solution.

Medium: The medium used in Protocol 1 is based on StemPro-34 SFM with StemPro supplement (both from Invitrogen, proprietary products) [9, 12]. The following components are added to this medium (Table 7.1): minimal essential medium (MEM) vitamin solution (Invitrogen), MEM nonessential amino acid solution (Invitrogen), insulin, transferrin, putrescine, sodium selenite, D-(+)-glucose, pyruvic acid, DL-lactic acid, bovine serum albumin (BSA), L-glutamine, 2-mercaptoethanol, ascorbic acid, and d-biotin. The medium is supplemented with 1% fetal bovine serum (FBS).

Growth factors: Recombinant growth factors included in the medium are 10 ng/ml GDNF, 10 ng/ml fibroblast growth factor 2 (FGF2), 20 ng/ml epidermal growth factor (EGF), and 1000 U/ml leukemia inhibitory factor (LIF). Steroid hormones, progesterone and estradiol, are also used in this protocol at 60 and 30 ng/ml, respectively.

Protocol 2

Kubota et al. reported a second protocol in 2004 [10], which we adopted in our laboratory [11]. The authors derived the germ cell clusters from pup and adult testis cells that were enriched for SSCs using immunomagnetic cell sorting. The sorted cells were seeded onto a feeder layer of a MEF-derived cell line, termed STO (SIM mouse embryo-derived, thioguanine and ouabain resistant) cells. Excellent technical reviews have been published for this protocol [15, 16].

Cell preparation: A single cell suspension of testis cells is prepared using the two-step enzymatic digestion, as in Protocol 1. These cells are enriched for SSCs by immunomagnetic cell sorting using antibodies against Thy-1 (see Section 7.4), which is known to be expressed on SSC surface [17].

Medium: The medium is based on MEM α medium (Invitrogen), supplemented with the following components (Table 7.2): insulin, transferrin, putrescine, sodium selenite, bovine serum albumin (BSA), L-glutamine, 2-mercaptoethanol, HEPES, and a mixture of free fatty acids (palmitic acid, palmitoleic acid, stearic acid, oleic acid, linoleic acid, and linolenic acid). The medium of Protocol 2 does not contain FBS.

Table 7.2 Chemically defined medium used in Protocol 2 and modified for rat SSCs

^a Component	Final concentration		^b Increase rat vs. mouse
	Mouse	Rat	
1. BSA(%)	0.2	0.6	3x
2. Iron-saturated transferrin ($\mu\text{g/ml}$)	10	100	10x
3. Free fatty acids ($\mu\text{eq/liter}$)	7.6	15.2	2x
4. Na_2SeO_3 (nM)	30	60	2x
5. L-glutamine(mM)	2	2	–
6. 2-mercaptoethanol (μM)	50	100	2x
7. Insulin ($\mu\text{g/ml}$)	5	25	5x
8. Hepes (μM)	10	10	–
9. Putrescine (μM)	60	120	2x
10. Water for dilution(%)	0	10	∞

^aThe base medium is MEM α .

^bThe concentrations of some components were increased when the medium for mouse SSCs was modified for rat SSC culture.

Growth factors: Growth factors used in this protocol are similar to but simpler than those used in Protocol 1. Recombinant growth factors included in the medium are GDNF, FGF2, and a soluble form of GDNF-family receptor alpha 1 (GFR α 1) at a final concentration of 40, 1, and 300 ng/ml, respectively. No steroid hormones are used in Protocol 2. GFR α 1 is known to potentiate the activity of GDNF [18] and promote cluster formation and long-term maintenance of SSCs [10].

7.2.1 Similarities and Differences Between the Two Protocols – What is Necessary to Develop Human SSC Culture?

Similarities: The development of a human SSC culture technique will likely incorporate the commonalities of these two protocols, namely: SSC enrichment the effect of age and/or cell cycle activity at the beginning of culture, the effect of serum, the quality of the in vitro environment and the type of growth factors to be used.

Before discussing the above five commonalities, it is useful to identify the fact that mouse SSCs behave similarly in both protocols. Under both culture conditions, SSCs form three-dimensional structures of germ cell aggregates or “clusters”. Thus, the emergence of clusters may also indicate successful initiation of human SSC culture. Importantly, however, mouse SSCs comprise only a minor subpopulation of cluster cells, estimated to be <10%, in both protocols [9–12]. This is true throughout serial passaging of clusters that leads to long-term maintenance and robust expansion of mouse SSCs ex vivo. This observation points to an important issue; the survival and proliferation of SSCs in vitro coincide with the production of non-stem, progenitor cells (i.e., cells that are primitive but committed to differentiation). In other words, both protocols do not simply

force SSCs to proliferate, but rather, generate a balance in SSC survival, self-renewal, and differentiation. This may suggest that a successful SSC culture requires an *in vitro* environment that promotes not only SSC self-renewal but also the production and survival of progenitors, thereby inducing a heterogeneous cell community in a cluster. A similar condition is anticipated to apply in a human SSC culture.

The first commonality is that the starting material is enriched for SSCs in both protocols. An increased SSC concentration is thus likely to be an important factor for successful human SSC culture. It is known that without SSC enrichment, contaminating testicular somatic cells aggressively proliferate and overwhelm the culture with time, interfering with SSC activity [15, 16]. This is the case in particular when growth factors are used, such as FGF2, or when pup or neonatal testes, in which many cell types are actively proliferating, are the source of SSCs. SSC enrichment can be accomplished using immunological cell sorting techniques, immunomagnetic cell sorting or fluorescent-activated cell sorting (FACS), which allows isolation of live cells based on the expression of cell-surface molecules. In our experience, somatic cells also proliferate aggressively in culture of testis cells from non-human primate and human origin (unpublished). Cell sorting is thus likely to be critical for successful human SSC culture (see Section 7.4).

Second, cluster formation in both protocols is dependent on the age of donor mice, with the greatest efficiency with pup testis cells. This age-dependence may arise from two characteristics of postnatal development of spermatogenesis. Related to the first commonality, while adult testes contain germ cells at all differentiation stages, pup testes contain only primitive spermatogonia as germ cells, allowing more efficient enrichment for SSCs. Further, mouse SSCs at this stage of postnatal development are rapidly dividing; those in neonatal testes are quiescent whereas they divide only slowly in adult testes [19–21]. Pup SSCs may therefore be predisposed to an active cell cycle and to an efficient response to growth factors, allowing them to compete against proliferation of somatic cells, particularly at the beginning of culture. Analogously, germ cell samples from juvenile men could yield the best results. We may thus need a robust SSC enrichment and division activation protocol that is effective regardless of age.

Third, contrary to a number of culture systems for somatic cells and embryonic stem cells, mouse SSC culture does not include serum (Protocol 2) or includes only a low level of serum (Protocol 1). Serum may contain factors that are detrimental to SSC survival and self-renewal. It is also possible that serum encourages proliferation of somatic cells and indirectly interferes with SSC activity. Successful human SSC culture is also anticipated to employ serum-free or serum-reduced medium.

The fourth similarity is the use of feeder cells. Although feeder-free mouse SSC culture has been reported, the initial induction of culture requires feeder cells [22]. A feeder layer apparently provides an *in vitro* environment that is critical to “initiate” SSC culture by expressing cell-surface and soluble factors that stimulate SSC survival, proliferation, and differentiation. In relation to the second commonality, contaminating somatic cells may also mask the function of feeder cells. The use of

a feeder layer is thus likely to be an integral component of successful human SSC culture. Since the function of feeder cells remains largely unknown, studies focusing on the role of feeder cells in mouse SSC culture should facilitate the development of human SSC culture.

Finally, it is important to note that both protocols use GDNF and FGF2. Without GDNF [9, 10], clusters do not emerge and SSCs rapidly disappear in vitro. Clinical observations support the notion that these growth factors are also essential to a human SSC culture [23, 24]. Gain-of-function mutations in FGF receptor 2 (FGFR2), FGFR3, and c-Ret (a co-receptor of GDNF) are a known cause of various familial disease syndromes; i.e., Apert, Crouzon, and Pfeiffer syndromes for FGFR mutations, and multiple endocrine neoplasia 2A for c-Ret mutation. Importantly, these syndromes are transmitted exclusively by male gametes, and the disease incidence increases with paternal age [23, 24]. Recent studies suggest a potential mechanism of this male-biased, age-dependent disease transmission. Mutations in FGFR and c-Ret may give spermatogonia, if not exclusively SSCs, a selective advantage for survival and/or proliferation that results in clonal expansion, and the cells carrying the mutations dominate spermatogenesis over time [23, 24]. It is thus likely that GDNF and FGF2 are also critical growth factors in humans to promote SSC maintenance and proliferation in vitro.

Differences: The two protocols involve two important differences, which are found in the medium composition and additional growth factors.

The medium used in Protocol 2 is completely defined in its chemical composition. The MEM α medium was chosen as a base medium in this protocol because a previous study showed that the use of another medium, DMEM, led to a rapid disappearance of SSCs [25]. The superiority of MEM α over DMEM is not clear, but DMEM is richer in nutrients (e.g., higher concentrations of glucose, amino acids, and vitamins), which might favor the proliferation of somatic cells. Since all medium components are identified, Protocol 2 provides an ideal condition to study the mechanism of SSC fate decision control. In contrast, the medium used in Protocol 1 is not completely defined, as it includes proprietary products (StemPro medium and supplements) and FBS. Kubota et al. examined the effect of FBS in Protocol 2 [10] and reported that the inclusion of 1% FBS, as used in Protocol 1, was detrimental to SSC culture. Since Protocol 1 introduces unknown elements in SSC culture, it involves a weakness when applied to the study of the SSC fate regulation mechanism.

It is noted, however, that mouse SSCs appear to proliferate more rapidly in Protocol 1. Kanatsu-Shinohara et al. report that a 10^{14} -fold expansion of SSCs can be achieved over a 5-month period, using Protocol 1 [9], which gives an estimated population-doubling time of ~ 3.2 days. Protocol 2 has been shown to induce a 5,000–10,000-fold expansion of SSCs in 10 weeks with a population-doubling time of ~ 5.5 days [10, 11]. An initial technical development for human SSC culture may therefore benefit from the condition used in Protocol 1.

Protocol 1 employs a more complex cocktail of growth factors and steroid hormones compared to Protocol 2. Additional growth factors and hormones may work together with GDNF and FGF2 and allow more rapid SSC proliferation in Protocol

1. Except for GDNF and FGF2, however, the significance of other growth factors and hormones is not clear. Further analyses using mouse SSCs is necessary to address this issue. The use of a soluble form of GFR α 1 is another difference between the two protocols. This factor promotes long-term maintenance and proliferation of SSCs in Protocol 2, whereas it apparently has no effect in Protocol 1 [10, 26]. This may also be due to the presence of additional growth factors and steroid hormones in Protocol 1, which may eliminate the requirement for GFR α 1.

7.3 Modifications of Mouse Protocols for the Application of SSC Culture from Other Species

These protocols have been successfully adapted to rat SSCs (Protocol 2) or hamster SSCs (Protocol 1). Surprisingly, even though these species are closely related in evolution, significant modifications were essential for successful SSC culture.

Two evident modifications were introduced to Protocol 2 to apply mouse SSC culture for rat SSCs [27]. One is the choice of a SSC selection marker. Rat pup testis cells are enriched for SSCs using EpCAM (epithelial cellular adhesion molecule), which is expressed on rat SSCs [28]. The other is the medium composition. When the mouse SSC medium is used for rat SSCs, rat clusters initially form but quickly disappear after a few passages [27] (unpublished). This problem is solved by increasing the concentration of several medium components (Table 7.2). A tenfold increase is made for transferrin, fivefold for insulin, threefold for BSA, and twofold for free fatty acids, sodium selenite, 2-mercaptoethanol, and putrescine. These modifications are apparently directed to encouraging cell survival, metabolism, and proliferation (transferrin, insulin, selenite, and putrescine) and to protecting proteins from oxidization (2-mercaptoethanol). Further, MEM α medium was diluted by adding water at 10% to reduce the osmolarity. This modification was introduced based on the authors' experience that decreased osmolarity was beneficial for mouse egg culture.

Despite these modifications, however, the proliferation rate of rat SSCs was at most only half the proliferation rate of mouse SSCs. This may suggest that the rat culture system is still suboptimal. It is also possible, however, that the proliferation activity of rat SSCs is inherently lower or cell cycle is longer than mouse SSCs, as the length of spermatogenic cycle is 10–13 days in rats while 8–9 days in mice [29]. The proliferation rate could thus be species-specific, and human SSCs may proliferate more slowly than rodent SSCs, since the length of the spermatogenic cycle is 16 days in humans [29].

In the application of Protocol 1 to hamster SSCs, Kanatsu-Shinohara et al. [30] enriched pup testis cells for SSCs using integrin α 6 as a marker, and reduced the FBS concentration from 1 to 0.04%. In addition, hamster SSCs were maintained more readily and proliferated more rapidly on laminin as a culture substrate, rather than on a feeder layer. A feeder-free condition thus appears to be more favorable for long-term culture of hamster SSCs. It should be noted, however, that feeder cells were required to initiate hamster SSC culture. Another modification was to use

TX-WES medium (Thrombogenics, Leuven, Belgium) for long-term maintenance of hamster SSCs, rather than StemPro medium used in mouse SSC culture. Why these modifications were required remains unclear. Apparently, some empiricism is unavoidable when developing a SSC culture system for a new species.

7.4 Issues to Be Considered for Development of Human SSC Culture

Based on animal studies, it is reasonable to expect that the initiation of human SSC culture will require a serum-free medium, a feeder layer, and growth factors, particularly GDNF and FGF2. In addition, the enrichment of testis cells for SSCs and the reduction of somatic cell numbers will likely be essential for successful human SSC culture.

Selection of live cells for SSC enrichment can be achieved using immunomagnetic cell sorting or FACS based on expression of cell-surface marker molecules [10, 11, 14, 20, 27]. Markers that are expressed on SSCs enable SSC enrichment (positive selection), whereas markers not expressed allow the reduction of unwanted cells (negative selection). Here, we describe rodent SSC markers and consider their application for human SSCs.

Cell-surface markers: Table 7.3 lists positive and negative cell-surface markers for rodent SSCs. Thy-1, CD9, EpCAM, and integrin $\alpha 6$ and $\beta 1$ have been successfully used as positive markers for rodent SSC enrichment. In all culture studies reported thus far, immunomagnetic cell sorting is preferred to FACS, because it causes less damage to the cells, is faster, requires fewer cells, and does not demand significant technical expertise with cell-sorting equipment. A disadvantage is that it is not as precise as FACS, and only one positive marker is applicable at a time, since cell selection relies on only one parameter; i.e., binding to a magnetic bead. It should be noted, however, that neither immunomagnetic sorting nor FACS purifies SSCs to 100% enrichment. At this time, no known SSC markers are expressed exclusively on SSCs. For instance, CD9 is a positive marker for SSCs, but it is also expressed on non-stem germ cells [14]. Nonetheless, these sorting techniques produce a live cell preparation with a high SSC concentration.

Table 7.3 Cell-surface molecules identified as positive and negative markers for rodent SSCs

Positive markers	Negative markers
Integrin $\alpha 6$	Integrin αv
Integrin $\beta 1$	MHC-I
Thy-1	c-Kit
CD9	Sca-1
EpCAM	
GFR $\alpha 1$	
c-Ret	
CD24	

Negative selection is also a powerful tool to reduce non-stem cells, including testicular somatic cells. Among the negative SSC markers listed in Table 7.3, MHC-I is a particularly attractive target. Although MHC-I molecules are expressed on virtually all cell types, they are known to be absent on spermatogonia in both animal models and humans [31]. It may thus be possible that antibodies against MHC-I allow us to purge or significantly reduce non-spermatogonial cells, including somatic cells, from human testis cells, and to generate a favorable in vitro environment for SSC activity.

The search for human SSC markers will be an empirical endeavor, but those identified for rodent SSCs should be the initial targets. In rodents, we have a transplantation assay to definitively determine SSC markers, a procedure not available for human SSCs. Therefore, we first need to identify the molecules expressed by human spermatogonia using immunological staining. Unfortunately, the information about cell-surface molecules expressed on human spermatogonia is scarce. Some leads could come, however, from primate studies. For example, a recent study using rhesus monkey shows that a rodent SSC marker, $GFR\alpha 1$, is expressed on a subpopulation of spermatogonia [32]. Considering a close phylogenetic relationship of the rhesus monkey to humans, $GFR\alpha 1$ could be an effective marker to enrich human SSCs, and its expression pattern should be examined in human testes.

Other potential SSC markers – Side Population: Cell-surface molecules may not be the only tool for human SSC enrichment. It has been reported that a small subpopulation of cells from various cell lineages (hematopoietic, skeletal muscle, neural, and embryonic stem cells [33, 34]) exhibits a high activity to efflux vital fluorescent dyes. The efflux occurs due to the activity of the ATP-binding cassette transporter family molecules, which confers drug resistance to a cell. This subpopulation, called “side population” (SP), is enriched for stem cells and can be sorted using FACS. The fluorescent vital dyes commonly used are Hoechst 33342 (DNA dye) and rhodamine 123 (mitochondrial dye). Using either dye, recent studies have identified a SP in mouse spermatogenic cells that is enriched for SSCs [35–37]. Therefore, human SSCs may also possess a similar dye-efflux activity and could be enriched in the SP. The advantage of this approach is that we do not need to know specific cell-surface antigens, yet may be able to isolate a SSC-enriched cell population. The disadvantage is the cytotoxicity of fluorescent dyes [17], in addition to those inherent to FACS described above.

7.4.1 How Can SSC Enrichment Be Verified? – The Necessity for a Secondary Marker

Separation of human testis cells is possible using the approaches described above. However, how can we measure an enrichment of human SSCs? In animal models we transplant sorted and unsorted cells and count the number of foci in which donor-derived spermatogenesis is regenerated in recipient testes [38]. If SSCs are enriched, the number should be higher with sorted cells than unsorted cells. A similar approach can be taken to evaluate the enrichment of human SSCs, by transplanting human cells into an animal model.

Human spermatogonia are known to colonize and survive for at least 6 months in the testes of immunodeficient nude mice after transplantation, even though no spermatogenesis is regenerated [39]. These spermatogonia are observed in the form of foci that are composed of single cells or short “chains” of cells on the basal membrane of the mouse seminiferous tubules. The chain formation is commonly seen in spermatogonia of all species, in which cells are connected with the cytoplasmic bridge that occurs due to incomplete cytokinesis of male germ cells [40]. The cell chains elongate as spermatogenic cell division and differentiation proceed, and single cells are believed to be the most primitive spermatogonia, which include SSCs. The foci of human spermatogonia are thus likely to arise from transplanted SSCs [39], and the number of foci reflects the number of human SSCs. On this basis, we should be able to estimate the degree of SSC enrichment by comparing the number of foci after transplanting sorted and unsorted cells into mouse testes.

This scheme requires visualization of human spermatogonia in mouse testes by whole-mount immunohistochemistry using antibodies against human antigens. In the rhesus monkey study [32], antibodies raised against primate testis cells were employed, which did not crossreact with mouse testis cells. For human cells, in our experience, an antibody against an oncofetal protein, MAGE A4 (known to be expressed in human spermatogonia [41]), is apparently effective, as it reacts with human spermatogonia but not with mouse testis cells (unpublished). Once various molecules are found to be expressed in human spermatogonia, they can also be used similarly, given that they do not crossreact with mouse testis cells. The experimental scheme outlined above is probably the most practical approach to assessing SSC enrichment.

With the lack of a transplantation assay, however, can we indeed determine the activity of human SSCs? In theory, it is not possible unless we have a method that allows complete regeneration of human spermatogenesis. If long-term SSC culture is established, however, we can detect SSCs based on one of two critical functions that define stem cells, i.e., self-renewal potential. The ability of germ cell clusters to continuously grow through prolonged passage generations is evidence of long-term self-renewal activity. Although this approach does not consider the differentiation activity of SSCs and thus, remains equivocal, it may be the most practical means for human SSC detection in the absence of a transplantation assay.

7.5 Feeder-Free Culture and Bioreactor: Two Techniques that Need to Be Explored in Animal Models for Clinical Application of Human SSC Culture

While culture of rodent SSCs will remain important to understand the biology of SSCs, it will also provide unique opportunities to further develop techniques for clinical applications of human SSCs. Based on the technical development related to embryonic stem cells (ESCs) and neural stem cells (NSCs), two techniques should be beneficial to this end: feeder-free culture and bioreactor.

In consideration of the clinical application of ESCs, the presence of feeder cells and serum in culture was a significant concern, because both agents can cause transmission of pathogens. For SSCs, the absence of serum has provided a favorable *in vitro* environment in animal models, which should apply to human SSCs. A feeder layer, however, has been prerequisite for the initiation of SSC culture. Interestingly, all feeder-free SSC cultures thus far reported contain serum, which might be required to compensate the lack of feeder cells [22, 26]. We therefore need to better understand the role of feeder cells in SSC culture. Cataloguing and identifying factors that feeder cells supply to the culture environment should help us eliminate the need of a feeder layer from the beginning of SSC culture, eliminating the possibility of pathogen transmission. Animal studies should generate essential information for this purpose.

Production of a large number of SSCs would be beneficial in the clinical application of human SSC culture. Male fertility should be restored more efficiently when a greater number of SSCs are transplanted. All protocols described above are based on a two-dimensional culture system; thus, the space for SSCs to proliferate is physically restricted. A three-dimensional space provided in suspension culture will enlarge the growth space. In contrast to SSCs that form clusters that are attached to two-dimensional culture substrate (e.g., a feeder layer), NSCs form spheroid cell clusters, called neurospheres, that float in culture medium. Taking this advantage, bioreactors have been developed in which neurospheres and NSCs are maintained and amplified in a three-dimensional suspension culture with automated equipment (see [42] as an example). If applicable to SSCs, such a technique will produce a large number of human SSCs for an efficient recovery of fertility upon transplantation.

In this regard, the integrity of SSCs that are exposed to an artificial, *in vitro* environment will be a significant concern in a clinical application. In animal models, no adverse phenotype has been reported in offspring produced using sperm derived from transplanted SSCs. Such analyses, however, have not been extensive, and questions still remain if genetic and epigenetic alterations occur in cultured SSCs. Since analyses of these potential alterations require a large number of cells, the development of SSC expansion culture systems should provide an effective means to address the integrity of cultured SSCs in both humans and experimental animals.

7.6 Concluding Remarks

Although the importance of human SSC culture is evident for biological studies and clinical applications, such a system has yet to be developed. Studies using animal models have generated most, if not all, techniques required for achieving this goal, and rodent SSC culture methods provide prototypes of human SSC culture. This chapter has described the essential elements that need to be considered in the efforts for establishing a human SSC culture system, and presented some issues and directions that could be useful. The most critical issue at present appears to be

the development of methods to enrich human SSCs and to remove or significantly reduce somatic cells. Even though empiricism is unavoidable in any types of technical development, with rapid and extensive advances seen in the research of rodent SSCs, we can be optimistic for the success of human SSC culture in the near future.

Acknowledgments The authors are indebted to Riaz Farookhi, Ludovic Marcon, and Frances Clerk for their suggestions for this manuscript. The work done in the authors' laboratory was supported by the Canadian Institute of Health Research (MOP-86532 and 49444), Fraser Foundation, and Department of Obstetrics and Gynecology at McGill University. M.C.N. is a Fondation pour la Recherche en Sante du Quebec scholar, and K.Z. is supported by the Mission Department, Egyptian Ministry of Higher Education.

References

1. Weissman IL (2000) Translating stem and progenitor cell biology to the clinic: barriers and opportunities. *Science* 287:1442–1446
2. Brinster RL, Avarbock MR (1994) Germline transmission of donor haplotype following spermatogonial transplantation. *Proc Natl Acad Sci U S A* 91:24:11303–11307
3. Nagano M, Avarbock MR, Brinster RL (1999) Pattern and kinetics of mouse donor spermatogonial stem cell colonization in recipient testes. *Biol Reprod* 60:1429–1436
4. Orwig KE, Shinohara T, Avarbock MR et al. (2002) Functional analysis of stem cells in the adult rat testis. *Biol Reprod* 66:944–949
5. Amann RP, Howards SS (1980) Daily spermatozoal production and epididymal spermatozoal reserves of the human male. *J Urol* 124:211–215
6. Meirou D, Dro J (2004) Epidemiology and infertility in cancer patients. In: Tulandi T, Gosden RG (eds) *Preservation of Fertility*, Taylor & Francis, London
7. Nagano MC (2004) A surgical strategy using spermatogonial stem cells for restoring male fertility. In: Tulandi T, Gosden RG (eds) *Preservation of Fertility*, Taylor & Francis, London
8. Nagano MC (2003) Homing efficiency and proliferation kinetics of male germ line stem cells following transplantation in mice. *Biol Reprod* 69:701–707
9. Kanatsu-Shinohara M, Ogonuki N, Inoue K et al. (2003) Long-term proliferation in culture and germline transmission of mouse male germline stem cells. *Biol Reprod* 69:612–616
10. Kubota H, Avarbock MR, Brinster RL (2004) Growth factors essential for self-renewal and expansion of mouse spermatogonial stem cells. *Proc Natl Acad Sci U S A* 101:16489–16494
11. Yeh JR, Zhang X, Nagano MC (2007) Establishment of a short-term in vitro assay for mouse spermatogonial stem cells. *Biol Reprod* 77:897–904
12. Kanatsu-Shinohara M, Ogonuki N, Iwano T et al. (2005) Genetic and epigenetic properties of mouse male germline stem cells during long-term culture. *Development* 132:4155–4163
13. Kanatsu-Shinohara M, Inoue K, Ogonuki N et al. (2007) Leukemia inhibitory factor enhances formation of germ cell colonies in neonatal mouse testis culture. *Biol Reprod* 76:55–62
14. Kanatsu-Shinohara M, Toyokuni S, Shinohara T (2004) CD9 is a surface marker on mouse and rat male germline stem cells. *Biol Reprod* 70:70–75
15. Kubota H, Brinster RL (2008) Culture of rodent spermatogonial stem cells, male germline stem cells of the postnatal animal. *Methods Cell Biol* 86:59–84
16. Oatley JM, Brinster RL (2006) Spermatogonial stem cells. *Methods Enzymol* 419:259–282
17. Kubota H, Avarbock MR, Brinster RL (2003) Spermatogonial stem cells share some, but not all, phenotypic and functional characteristics with other stem cells. *Proc Natl Acad Sci U S A* 100:6487–6492
18. Paratcha G, Ledda F, Baars L et al. (2001) GFR α 1 potentiates downstream signaling, neuronal survival, and differentiation via a novel mechanism of recruitment of c-Ret to lipid rafts. *Neuron* 29:171–184

19. McCarrey JR (1993) Development of the germ cell. In: Desjardins C, Ewing LL (eds) *Cell and Molecular Biology of the Testis*, Oxford University Press, New York
20. Nagano M, Shinohara T, Avarbock MR et al. (2000) Retrovirus-mediated gene delivery into male germ line stem cells. *FEBS Lett* 475:7–10
21. Nagano M, Watson DJ, Ryu BY et al. (2002) Lentiviral vector transduction of male germ line stem cells in mice. *FEBS Lett* 524:111–115
22. Kanatsu-Shinohara M, Miki H, Inoue K et al. (2005) Long-term culture of mouse male germline stem cells under serum-or feeder-free conditions. *Biol Reprod* 72:985–991
23. Crow JF (2000) The origins, patterns and implications of human spontaneous mutation. *Nat Rev Genet* 1:40–47
24. Crow JF (2003) There's something curious about paternal-age effects. *Science* 301:606–607.
25. Nagano M, Ryu BY, Brinster CJ et al. (2003) Maintenance of mouse male germ line stem cells in vitro. *Biol Reprod* 68:2207–2214
26. Kanatsu-Shinohara M, Inoue K, Lee J et al. (2006) Anchorage-independent growth of mouse male germline stem cells in vitro. *Biol Reprod* 74:522–529
27. Ryu BY, Kubota H, Avarbock MR et al. (2005) Conservation of spermatogonial stem cell self-renewal signaling between mouse and rat. *Proc Natl Acad Sci U S A* 102:14302–14307
28. Ryu BY, Orwig KE, Kubota H et al. (2004) Phenotypic and functional characteristics of spermatogonial stem cells in rats. *Dev Biol* 274:158–170
29. Russell LD, Ettlir RA, Sinha Hikim AP et al. (1990) *Histological and Histopathological Evaluation of the Testis*, Cache River Press, Clearwater
30. Kanatsu-Shinohara M, Muneto T, Lee J et al. (2008) Long-term culture of male germline stem cells from hamster testes. *Biol Reprod* 78:611–617
31. Klein, J. (1986) *Natural History of Major Histocompatibility Complex*, Wiley, New York
32. Hermann BP, Sukhwani M, Lin CC et al. (2007) Characterization, cryopreservation, and ablation of spermatogonial stem cells in adult rhesus macaques. *Stem Cells* 25:2330–2338
33. Bunting KD (2002) ABC transporters as phenotypic markers and functional regulators of stem cells. *Stem Cells* 20:11–20
34. Zhou S, Schuetz JD, Bunting KD (2001) The ABC transporter Bcrp1/ABCG2 is expressed in a wide variety of stem cells and is a molecular determinant of the side-population phenotype. *Nat Med* 7:1028–1034
35. Lassalle B, Bastos H, Louis JP et al. (2004) 'Side Population' cells in adult mouse testis express Bcrp1 gene and are enriched in spermatogonia and germinal stem cells. *Development* 131:479–487
36. Falcatori I, Borsellino G, Haliassos N et al. (2004) Identification and enrichment of spermatogonial stem cells displaying side-population phenotype in immature mouse testis. *FASEB J* 18:376–378
37. Lo KC, Brugh VM 3rd, Parker M et al. (2005) Isolation and enrichment of murine spermatogonial stem cells using rhodamine 123 mitochondrial dye. *Biol Reprod* 72:767–771
38. Zhang X, Ebata KT, Nagano MC. (2003) Genetic analysis of the clonal origin of regenerating mouse spermatogenesis following transplantation. *Biol Reprod* 69:1872–1878
39. Nagano M, Patrizio P, Brinster RL (2002) Long-term survival of human spermatogonial stem cells in mouse testes. *Fertil Steril* 78:1225–1233
40. Meistrich ML, van Beek MEAB (1993) Spermatogonial stem cells. In: Desjardins C, Ewing LL (eds) *Cell and Molecular Biology of the Testis*, Oxford University Press, Oxford
41. Jungbluth AA, Busam KJ, Kolb D et al. (2000) Expression of MAGE-antigens in normal tissues and cancer. *Int J Cancer* 85:460–465
42. Gilbertson JA, Sen A, Behie LA, Kallos MS (2006) Scaled-up production of mammalian neural precursor cell aggregates in computer-controlled suspension bioreactors. *Biotechnol Bioeng* 94:783–792

Chapter 8

Hair Follicle Pluripotent Stem (hfPS) Cells

Robert M. Hoffman

Abstract Our laboratory has discovered that nestin, a protein marker for neural stem cells is also expressed in hair follicle stem cells and their immediate, differentiated progeny. The fluorescent protein, GFP, whose expression is driven by the nestin regulatory element in transgenic mice (ND-GFP mice), served to mark hair follicle stem cells and enabled us to make this observation. The ND-GFP hair-follicle stem cells are positive for the stem cell marker CD34 but negative for keratinocyte marker keratin 15, suggesting their relatively undifferentiated state. We have shown that these hair follicle stem cells can differentiate into neurons, glia, keratinocytes, smooth muscle cells and melanocytes in vitro. In vivo studies show the hair follicle stem cells can differentiate into blood vessels and neural tissue after transplantation to the subcutis of nude mice. Hair follicle stem cells implanted into the gap region of severed sciatic or tibial nerves greatly enhance the rate of nerve regeneration and the restoration of nerve function. When transplanted to severed nerves in mice, the follicle cells transdifferentiate largely into Schwann cells, which are known to support neuron regrowth. The transplanted mice regain the ability to walk normally. We have also shown that hair follicle stem cells can affect the functional joining of the severed spinal cord. When the hair follicle stem cells are injected into the severed spinal cord, they differentiate into Schwann cells enabling the cord to rejoin and the mouse to regain function of its rear legs. Thus, hair follicle pluripotent stem (hfPS) cells can provide an effective, accessible, autologous source of stem cells for treatment of peripheral nerve injury and appear to be a paradigm for adult stem cells.

R.M. Hoffman (✉)

Department of Surgery, University of California, and AntiCancer, Inc., 7917 Ostrow Street, San Diego, CA 92111, USA
e-mail: all@anticancer.com

8.1 Introduction

8.1.1 The Hair Follicle as a “Mini-Organ”

The hair follicle produces a terminally differentiated keratinized end product, the hair shaft, that is eventually shed. The follicle undergoes cyclical regeneration with at least 10 different epithelial and mesenchymal cell lineages [1]. Hair is formed by rapidly proliferating matrix keratinocytes in the bulb located at the base of the growing (anagen) follicle. The duration of anagen varies greatly between hairs of differing lengths. Nevertheless, matrix cells eventually stop proliferating, and hair growth ceases at catagen when the lower follicle regresses (telogen). After telogen, the lower hair-producing portion of the follicle regenerates, starting the new anagen phase [1].

Hair follicle stem cells, located in the hair follicle bulge, possess stem cell characteristics, including multipotency, high proliferative potential, and ability to enter quiescence. Lineage analysis has demonstrated that all epithelial layers within the adult follicle and hair originate from bulge cells [1, 2]. The hair follicle stem cells, therefore appear to be responsible for regenerating the hair follicle in each hair cycle.

After wounding, hair follicles form *de novo* in adult mice. The nascent follicles arise from epithelial cells outside of the hair follicle stem cell niche, suggesting that epidermal cells in the wound assume a hair follicle stem cell phenotype. The newly generated hair follicles establish a stem cell population, express known molecular markers of follicle differentiation, produce a hair shaft, and progress through all stages of the hair follicle cycle [3].

8.1.2 Tracking Hair Follicle Stem Cells In Vivo

The insufficiency of markers to identify and track hair follicle stem cells in the bulge area has hindered the study of hair follicle stem cells. CD34 expression, as first defined by Trempus et al. [4], is a marker for hair follicle stem cells. Antibodies recognizing CD34 were used to collect viable bulge cells by fluorescent activated cell sorting [4, 5]. K15 is expressed at high levels in the bulge, but lower levels of expression can be present in the basal layers of the lower follicle outer-root sheath (ORS) and the epidermis [6, 7]. A K15 promoter used for generation of transgenic mice was active only in the bulge in the adult mouse [8].

A breakthrough occurred with the use of transgenic mice in which the neural stem cell marker, nestin, drove the expression of green fluorescent protein (GFP) (ND-GFP). We observed in these mice that nestin was also a marker for hair follicle stem cells which suggested that hair follicle stem cells could form neurons and were pluripotent [9]. The hair follicle stem cells could then be tracked by their green fluorescence. These relatively small, oval-shaped, ND-GFP-expressing cells in the bulge area surround the hair shaft and are interconnected by short dendrites. In mid- and late anagen, the ND-GFP-expressing cells are located in the upper outer-root

sheath as well as in the bulge area but not in the hair matrix bulb. These observations show that the ND-GFP-expressing cells form the outer-root sheath. Following our report that ND-GFP can serve as a marker for hair follicle stem cells to track them in the live animal, Morris et al. [10] subsequently used GFP to isolate hair follicle stem cells in transgenic mice. Fuchs' group also subsequently used GFP to identify hair follicle stem cells and possibly other skin stem cells in transgenic mice [11, 12]. Mignone et al. [13] have confirmed our results that hair follicle stem cells express nestin. Yu et al. [14] showed that nestin was present in human hair follicle stem cells also confirming our original observation [9].

The evidence that nestin-expressing cells in the hair follicle bulge are hair follicle stem cells rather than a population of stem cells that reside in the hair follicle whose purpose is to regenerate the neuronal and endothelial components associated with the pilosebaceous unit is that the nestin-expressing (and GFP-expressing) cells have been imaged over time to regenerate a large portion of the hair follicle as described above [9]. The ND-GFP marker may have enabled the identification and isolation of the most pluripotent cells in the hair follicle bulge area.

8.1.3 The Ability of Hair Follicle Stem Cells to Differentiate to Follicular and Non-Follicular Cell Types

Hair follicle stem cells from adult mice, when combined with neonatal dermal cells, formed hair follicles after injection into immunodeficient mice [5, 10]. Cultured, individually cloned bulge cells from adult mice also were shown to form hair follicles in skin reconstitution assays [5].

Taylor et al. [15] reported that hair follicle bulge stem cells are potentially bipotent because they can give rise to not only cells of the hair follicle but also to epidermal cells. However, hair follicle stem cells may form epidermal stem cells only when the epidermis is wounded [16]. Other experiments [17] also have provided new evidence that the upper outer-root sheath of vibrissal (whisker) follicles of adult mice contains multipotent stem cells, which can differentiate into hair follicle matrix cells, sebaceous gland basal cells, and epidermis. Toma et al. [18] reported that multipotent adult stem cells isolated from mammalian skin dermis, termed skin-derived precursors (SKP), can proliferate and differentiate in culture to produce neurons, glia, smooth muscle cells, and adipocytes. However, the exact location of these stem cells in skin is unknown, and their functions are still unclear. They may have arisen in hair follicles.

8.1.4 Blood Vessels Derived from Hair-Follicle Stem Cells

We observed that in ND-GFP mice, skin blood vessels express ND-GFP and appear to originate from hair follicles and form a follicle-linking network. This was seen most clearly by transplanting ND-GFP-labeled vibrissa (whisker) hair follicles to

unlabeled nude mice. New vessels grew from the transplanted follicle, and the number of vessels increased when the local recipient skin was wounded. The ND-GFP-expressing blood vessels display the characteristic endothelial-cell-specific markers CD31 and von Willebrand factor [19].

8.1.5 Differentiation of Hair Follicle Stem Cells to Neural and Other Cell Types

ND-GFP hair follicle stem cells can differentiate into neurons, glia, keratinocytes, smooth muscle cells, and melanocytes in vitro. These pluripotent ND-GFP stem cells are positive for the stem cell marker CD34, and negative for keratin 15, suggesting their relatively undifferentiated state as mentioned above. The apparent primitive state of the ND-GFP stem cells is compatible with their pluripotency. The ND-GFP hair follicle stem cells may be more primitive than those hair follicle stem cells previously isolated [2]. Furthermore, we showed that the hair follicle stem cells differentiated into neurons after transplantation to the subcutis of nude mice [20].

Mignone et al. [13] confirmed our data that hair follicle stem cells are pluripotent when isolated from the ND-GFP mice. In addition, the hair follicle stem cells formed neuronal cells when implanted in chick embryos. Transcriptional profiling showed that the nestin-expressing hair follicle stem cells are similar to neural stem cells.

Li et al. [21] have reported that nuclei from hair follicle stem cells can be successfully used as nuclear transfer (NT) donors, resulting in live cloned mice. Thus, the nuclei of hair follicle stem cells can be reprogrammed to the pluripotent state by exposure to the cytoplasm of unfertilized oocytes. These results confirm our earlier results demonstrating the pluripotency of hair follicle stem cells [9].

8.1.6 Hair Follicle Stem Cells Can Effect Nerve Repair

When the GFP hair follicle stem cells were implanted into the gap region of a severed sciatic nerve they greatly enhanced the rate of nerve regeneration and the restoration of nerve function. After transplantation to severed nerves, the hair follicle stem cells differentiated largely into Schwann cells, which are known to support neuron regrowth. Function of the rejoined sciatic nerve was measured by contraction of the gastrocnemius muscle upon electrical stimulation. The transplanted mice recovered the ability to walk normally [22].

8.1.7 Hair Follicle Stem Cells Can Effect Spinal Cord Repair

We severed the thoracic spinal chord of C57BL/6 immunocompetent mice and transplanted mouse GFP-expressing hair follicle stem cells to the injury site. Most of the transplanted cells also differentiated into Schwann cells that apparently facilitated

repair of the severed spinal cord. The rejoined spinal cord reestablished extensive hind-limb locomotor performance. These results suggest that hair follicle stem cells can promote the recovery of spinal cord injury. Thus, hair follicle stem cells provide an effective accessible, autologous source of stem cells for the treatment of peripheral nerve and spinal cord injury [23].

8.2 Discussion

Sieber-Blum et al. [24] showed that neural crest cells grew out when the hair follicle was explanted, resulting in differentiation to a variety of cell types including neurons, smooth muscle cells, rare Schwann cells, and melanocytes. The location of these cells within the follicle was not determined. Sieber-Blum et al. [25] characterized the behavior of implanted neural crest stem cells from the hair follicle in the contusion-lesioned murine spinal cord. The grafted neural crest cells survived, integrated, and intermingled with host neurites in the lesioned spinal cord. They did not proliferate and did not form tumors. Subsets expressed neuron-specific beta-III tubulin, the GABAergic marker glutamate decarboxylase 67 (GAD67), the oligodendrocyte marker, RIP, or myelin basic protein (MBP). However, glial fibrillary acidic protein (GFAP) was not detected by immunofluorescence.

This apparent puzzle is probably due to different cell types transplanted by Sieber-Blum et al. [25] compared to the cell types we transplanted to the lesioned spine. Sieber-Blum et al. explanted the bulge area of a whisker (vibrissa) *in vitro*. Within 3–4 days, cells migrated from the explanted bulge area and grew on the surface of the culture dish. Glial markers were not expressed or expressed only at low levels in the migrating cells. Four days after onset of migration, these cells were harvested and further expanded in culture for another four days. After four days of expansion, the cells were implanted in the lesioned spinal cord. Although neurons and oligodendrocytes formed after transplantation, glial cells did not appear.

Our approach was to actually isolate the vibrissa stem cells, culture them for two months and then implant the cells in the lesioned spinal cord. In contrast to Sieber-Blum et al., in our study, the vast majority of the implanted cells (82%) formed glial cells in the lesioned spinal cord. Our hypothesis is that the glial cells promoted axon growth and recovery of spinal cord function. Perhaps the outgrowth method of Sieber-Blum et al. [25] did not allow for recovery of sufficient numbers of cells capable of glial differentiation, which in turn did not allow for sufficient axon growth for spinal cord recovery.

Toma et al. [18] reported that multipotent adult stem cells isolated from mammalian skin dermis, the SKP mentioned above, can proliferate and differentiate in culture to produce neurons, glia, smooth muscle cells, and adipocytes. However, while the exact source of the skin-derived precursors was not identified, it is possible they originated in the hair follicles. This same laboratory then observed that the SKPs could form myelinating Schwann cells when injected into the injured sciatic nerve [26] which is similar to our earlier results with the nestin-expressing hair follicle stem cells [22]. The same laboratory then showed that SKPs could promote

spinal cord repair. The SKPs were released from skin by collagenase treatment of the skin which produced a mixture of cells [27]. The origin of SKPs within the skin is thus unclear. In contrast, our results show that the hair follicle stem cells, a defined population, can functionally repair the severed spinal cord. It should also be noted that our studies as well as the studies with SKPs used fluorescent proteins to track the transplanted cells, a technology pioneered in our laboratory [28–32].

Soluble factors secreted from host cells as well as hair follicle stem cells may play a role in the regeneration of spinal cord injury. For example, brain-derived neurotrophic factor (BDNF) and insulin-like growth factor (IGF-1) were shown to be involved in nerve regeneration [33]. Future experiments will examine this issue in the case of hair follicle stem cells.

Cell-replacement therapies show particular promise in the nervous system, where transplanted embryonic or bone marrow stem cells have been shown to promote recovery of function in animal models of spinal cord or peripheral nerve injury [34, 35]. Although the therapeutic potential of such transplants is clear, a number of problems remain. In particular, fetal tissue is the current tissue source for human neuron-specific and embryonic stem cells, raising significant ethical issues. Moreover, the use of human tissue involves heterologous transplantation with attendant immune response. The requisite accompanying immuno-suppression is particularly problematic in individuals with long-term neuron-specific problems. Recently, induced pluripotent stem (iPS) cells have been derived from skin and other organs by gene transfer [36–38]. However, the vectors used for gene transfer have made these stem cells potentially malignant. In this regard, nestin-expressing hair follicle pluripotent stem (hfPS) cells are available from autologous, accessible adult tissue source, normal skin and they do not form tumors. hfPS cells can readily generate neuron and glial cells and provide a potential solution to these problems.

8.3 Conclusions

We have shown that the hair follicle bulge area is an abundant, easily accessible source of actively growing pluripotent adult stem cells that could serve a clinical source in humans. The availability of the ND-GFP mice has enabled the identification, isolation, and characterization of the hfPS cells. These hair follicle stem cells express the stem cell marker CD34 and nestin but are negative for the keratinocyte marker keratin 15, indicating their relatively undifferentiated state. The hair follicle stem cells can differentiate into neurons, glia, keratinocytes, smooth muscle cells and melanocytes *in vitro*. *In vivo* studies show the nestin-driven GFP hair follicle stem cells can differentiate into blood vessels and neural tissue after transplantation to the subcutis of nude mice. Hair follicle stem cells implanted into the gap region of a severed sciatic or tibial nerve greatly enhance the rate of nerve regeneration and the restoration of nerve function. After transplantation to the severed nerve, the follicle cells transdifferentiate largely into Schwann cells, which are known to support neuron regrowth. The transplanted mice regain the ability to walk normally.

Thus, hfPS cells provide an effective, accessible, autologous source of stem cells for treatment of peripheral nerve injury.

The hfPS cells thus have the potential as an alternative to the use of embryonal stem cells or fetal cells for regenerative medicine. The hfPS cells do not have the ethical problems that embryonal or fetal stem cells have. Even more important, the hfPS cells are much more easily accessible than other stem-cell types and offer the potential for autologous treatment as they can be readily expanded in culture after isolation from the patient. The fact that Yu et al. [14] have shown nestin expression and pluripotency of human hair follicle stem cells further suggests the clinical potential of hair follicle stem cells for regenerative medicine. Hair follicle stem cells also have great potential for hair restoration [1].

Li et al. [21] have shown that nuclei from hair follicle stem cells can be used to clone mice, further demonstrating the pluripotency of these stem cells.

It is also important to note that the dermal papilla is a potential source of multipotent stem cells that may have use in regenerative medicine. For example, Jahoda's group has demonstrated that hair follicle dermal cells repopulate the mouse haematopoietic system [39], can differentiate into adipogenic and osteogenic lineages [40] and participate in wound healing and induction [41].

8.4 Materials and Methods

8.4.1 *GFP-Expressing Transgenic Mice (Green Mice)*

Transgenic C57/B6-GFP mice were originally obtained from Professor M. Okabe at the Research Institute for Microbial Diseases (Osaka University, Osaka). The C57/B6-GFP mice expressed the *Aequorea victoria* GFP under the control of the chicken β -actin promoter and cytomegalovirus enhancer (β -actin-driven GFP). All of the tissues from this transgenic line, with the exception of erythrocytes and hair, express GFP [22].

8.4.2 *ND-GFP Transgenic Mice*

Transgenic mice carrying GFP under the control of the nestin second-intron enhancer (9, 19) were obtained from G. Enikolopov (Cold Spring Harbor Laboratory, Cold Spring Harbor, NY) [20].

8.4.3 *GFP-Expressing, Hair Follicle Stem Cells Cultured from Isolated Vibrissa Follicles*

To isolate the vibrissa follicles, the upper lip containing the vibrissa pad was cut, and its inner surface was exposed. The vibrissa follicles were dissected under a binocular microscope and plucked from the pad by pulling them gently by the neck with fine forceps. The follicles were then washed in DMEM-F12 (GIBCO/BRL,

Grand Island, NY) containing B-27 (GIBCO/BRL) and 1% penicillin-streptomycin (GIBCO/BRL). All surgical procedures were made in a sterile environment. The GFP-expressing vibrissa follicular stem cells located under the sebaceous gland (9) were isolated under a binocular microscope and suspended in 1 ml of DMEM-F12-containing B-27 with 1% methylcellulose (Sigma-Aldrich). The culture was supplemented every 2 days with basic FGF at 20 ng·ml⁻¹ (Chemicon). Cells were cultured in 24-well tissue culture dishes (Corning) in a 37°C, 5% CO₂/95% air tissue-culture incubator. After 4 weeks, GFP-expressing vibrissa follicle stem cells formed GFP-expressing colonies. For differentiation, GFP-expressing cell colonies were centrifuged, the growth factor-containing supernatant was removed, and the colonies were resuspended in fresh RPMI medium 1640 (Cellgro, Herndon, VA) containing 10% FBS in SonicSeal four-well chamber slides (Nunc). After 8 weeks of expansion, the GFP-expressing cell colonies were switched to RPMI medium 1640 containing 10% FBS in the SonicSeal four-well chamber slides and then differentiated [22].

8.4.4 Nestin-, CD34-, and K15-Expression in Vibrissa Follicles of Green Mice

Skin samples were dissected from 6- to 8-week-old β-actin-driven GFP mice. These mice were anesthetized with tribromoethanol (i.p. injection of 0.2 ml per 10 g of body weight of a 1.2% solution), and samples were excised from the skin containing vibrissa follicles. Immediately after excision, the vibrissa follicle samples were frozen in liquid nitrogen, embedded in tissue-freezing embedding medium (Triangle Biomedical Sciences, Durham, NC) and stored at -80°C until further processing. Frozen vibrissa follicle sections (5 μm thick) were cut with a Leica CM1850 cryostat and were air-dried. The sections were directly observed by fluorescence microscopy and used for immunofluorescence (nestin and K15) and immunohistochemical (CD34) staining [22].

8.4.5 Transplantation of GFP-Expressing Hair Follicle Stem Cells to the Thoracic Region of the Severed Spinal Cord in C57BL/6 Immunocompetent Mice

The GFP-expressing stem cells, cultured for two months in DMEM-F12 containing B-27 and 1% methylcellulose, were used for transplantation. Six- to eight-week old C57BL/6 immunocompetent mice (Harlan, San Diego, CA) were anesthetized with tribromoethanol. Using a binocular microscope, a laminectomy was made at the 10th thoracic spinal vertebra, followed by transversal cut. The GFP-expressing hair follicle stem cells were transplanted between the severed thoracic region (spinal level T10) of the spinal cord in C57BL/6 immunocompetent mice. After 2 months, the spinal cords of the transplanted mice were directly observed by fluorescence

microscopy under anesthesia. A total of 12 mice were transplanted with hair follicle stem cells [22].

8.4.6 Transplantation of GFP-Expressing Hair Follicle Stem Cells Between Severed Sciatic or Tibial Nerve Fragments In Immunocompetent C57BL/6 Mice

The GFP-expressing hair follicle stem cell colonies from the vibrissa follicle bulge area were transplanted between the severed sciatic or tibial nerve fragments in immunocompetent C57BL/6 mice under tribromoethanol anesthesia. The skin incision was closed with nylon sutures (6–0). After 2 months, the sciatic nerve of the transplanted mouse was directly observed by fluorescence microscopy under anesthesia. The sciatic nerve samples were embedded in tissue freezing embedding medium and frozen at -80°C overnight. Frozen sections $5\ \mu\text{m}$ thick were cut with a Leica CM1850 cryostat and air dried. The sections were first directly observed under fluorescence microscopy. The frozen sections were then used for the immunofluorescence staining of β -III-tubulin, glial fibrillary acidic protein, K15, and smooth muscle actin as described above. For quantification of the percentage of cells producing a given marker protein in any given experiment, at least three fields were photographed, and the number of positive cells determined relative to the total number of cells [22].

8.4.7 Histology and Immunohistochemistry

Spinal cord or nerve biopsies of the transplanted mice were excised under anesthesia. Tissues were embedded in tissue-freezing embedding medium (Triangle Biomedical Sciences, Durham, NC) and frozen at -80°C overnight. Frozen sections, $5\ \mu\text{m}$ thick, were cut with a Leica CM1850 cryostat, and were air-dried. The sections were directly observed by fluorescence microscopy. The sections were then used for immunofluorescence (IF) staining of β III-tubulin, GFAP, CNPase, K15, and SMA. The primary antibodies used were: anti- β III-tubulin monoclonal (1:500; Tuj1 clone; Covance Research Products, Inc., Berkeley, CA), anti-glial fibrillary acidic protein (GFAP) monoclonal (1:200; Lab Vision, Fremont, CA), anti-2'-3'-cyclic nucleotide 3'-phosphodiesterase (CNPase) monoclonal (1:50; Lab Vision), anti-K15 monoclonal (1:100; Lab Vision), and anti-smooth muscle actin (SMA) monoclonal (1:200; Lab Vision). Secondary antibodies were Alexa Fluor[®] 568 goat anti-mouse (1:200; Molecular Probes, Eugene, OR), or Alexa Fluor[®] 568-conjugated goat anti-rabbit (1:200; Molecular Probes). For quantification of the percentage of cells producing a given marker protein, in any given experiment at least three fields were photographed, and the number of positive cells determined relative to the total number of GFP-expressing cells. For each mouse, a minimum of three fields of 400x were photographed and analyzed.

8.4.8 Basso-Beattie-Bresnahan (BBB) Locomotor Rating Scale

Behavioral analyses of mice with nerves or spinal cords repaired by hfPS cells were conducted for 12 weeks using the BBB locomotor rating scale [42, 43]. Each experimental group consisted of seven mice.

8.4.9 Fluorescence Microscopy

The spinal cord or peripheral nerve in the live mouse, transplanted with GFP-expressing hfPS cells, was directly observed under an Olympus IMT-2 inverted fluorescence microscope equipped with a mercury lamp power supply. The microscope had a GFP filter set (Chroma Technology, Brattleboro, VT).

8.4.10 Statistical Analysis

The experimental data are expressed as the mean \pm SD. Statistical analysis was performed using the two-tailed Student's t test.

Acknowledgments This study was supported in part by NIAMSD grant AR050933 to Anti-Cancer, Inc.

References

1. Cotsarelis G. (2006) Epithelial stem cells: a folliculocentric view. *J Invest Dermatol* 126:1459–1468.
2. Cotsarelis G, Sun TT, Lavker RM. (1990) Label-retaining cells reside in the bulge area of pilosebaceous unit: implications for follicular stem cells, hair cycle, and skin carcinogenesis. *Cell* 61:1329–1337.
3. Ito M, Yang Z, Andl T, et al. (2007) Wnt-dependent de novo hair follicle regeneration in adult mouse skin after wounding. *Nature* 447:316–320.
4. Trempus C, Morris R, Bortner C, et al. (2003) Enrichment for living murine keratinocytes from the hair follicle bulge with the cell surface marker CD34. *J Invest Dermatol* 120:501–511.
5. Blanpain C, Lowry We, Geoghegan A, et al. (2004) Self-renewal, multipotency, and the existence of two cell populations within an epithelial stem cell niche. *Cell* 118:635–648.
6. Lyle S, Christofidou-Solomidou M, Liu Y, et al. (1998) The C8/144B monoclonal antibody recognizes cytokeratin 15 and defines the location of human hair follicle stem cells. *J Cell Sci* 111:3179–3188.
7. Waseem A, Dogan B, Tidman N, et al. (1999) Keratin 15 expression in stratified epithelia: downregulation in activated keratinocytes. *J Invest Dermatol* 112:362–369.
8. Liu Y, Lyle S, Yang Z, Cotsarelis G. (2003) Keratin 15 promoter targets putative epithelial stem cells in the hair follicle bulge. *J Invest Dermatol* 121:963–968.
9. Li L, Mignone J, Yang M, et al. (2003) Nestin expression in hair follicle sheath progenitor cells. *Proc Natl Acad Sci USA* 100:9958–9961.

10. Morris RJ, Liu Y, Marles L, et al. (2004) Capturing and profiling adult hair follicle stem cells. *Nat Biotechnol* 22:411–417.
11. Tumber T, Guasch G, Greco V, et al. (2004) Defining the epithelial stem cell niche in skin. *Science* 303:359–363.
12. Rhee H, Polak L, Fuchs E. (2006) *Lhx2* maintains stem cell character in hair follicles. *Science* 312:1946–1949.
13. Mignone JL, Roig-Lopez JL, Fedtsova N, et al. (2007) Neural potential of a stem cell population in the hair follicle. *Cell Cycle* 6:2161–2170.
14. Yu H, Fang D, Kumar SM, et al. (2006) Isolation of a novel population of multipotent adult stem cells from human hair follicles. *Am J Pathol* 168:1879–1888.
15. Taylor G, Lehrer MS, Jensen PJ, et al. (2000) Involvement of follicular stem cells in forming not only the follicle but also the epidermis. *Cell* 102:451–461.
16. Ito M, Liu Y, Yang Z, Nguyen J, et al. (2005) Stem cells in the hair follicle bulge contribute to wound repair but not to homeostasis of the epidermis. *Nat Med* 11:1351–1354.
17. Oshima H, Rochat A, Kedzia C, Kobayashi K, Barrandon Y. (2001) Morphogenesis and renewal of hair follicles from adult multipotent stem cells. *Cell* 104:233–245.
18. Toma JG, Akhavan M, Fernandes KJ, et al. (2001) Isolation of multipotent adult stem cells from the dermis of mammalian skin. *Nat Cell Biol* 3:778–784.
19. Amoh Y, Li L, Yang M, et al. (2004) Nascent blood vessels in the skin arise from nestin-expressing hair follicle cells. *Proc Natl Acad Sci USA* 101:13291–13295.
20. Amoh Y, Li L, Katsuoka K, Penman S, Hoffman RM. (2005) Multipotent nestin-positive, keratin-negative hair-follicle-bulge stem cells can form neurons. *Proc Natl Acad Sci USA* 102:5530–5534.
21. Li J, Greco V, Guasch G, Fuchs E, Mombaerts P (2007) Mice cloned from skin cells. *Proc Natl Acad Sci USA* 104:2738–2743.
22. Amoh Y, Li L, Campillo R, et al. (2005) Implanted hair follicle stem cells form Schwann cells that support repair of severed peripheral nerves. *Proc Natl Acad Sci USA* 102:17734–17738.
23. Amoh Y, Li L, Katsuoka K, Hoffman RM. (2008) Multipotent hair follicle stem cells promote repair of spinal cord injury and recovery of walking function. *Cell Cycle* 7:1865–1869.
24. Sieber-Blum M, Grim M, Hu YF, Szeder V. (2004) Pluripotent neural crest stem cells in the adult hair follicle. *Dev Dyn* 231:258–269.
25. Sieber-Blum M, Schnell L, Grim M, et al. (2006) Characterization of epidermal neural crest stem cell (EPI-NCSC) grafts in the lesioned spinal cord. *Mol Cell Neurosci* 32:67–81.
26. McKenzie IA, Biernaskie J, Toma JG, Midha R, Miller FD. (2006) Skin-derived precursors generate myelinating Schwann cells for the injured and dysmyelinated nervous system. *J Neurosci* 26:6651–6660.
27. Biernaskie J, Sparling JS, Liu J, et al. (2007) Skin-derived precursors generate myelinating Schwann cells that promote remyelination and functional recovery after contusion spinal cord injury. *J Neurosci* 27:9545–9559.
28. Hoffman RM. (2005) The multiple uses of fluorescent proteins to visualize cancer in vivo. *Nat Rev Cancer* 5:796–806.
29. Glinsky GV, Glinskii AB, Berezovskaya O, et al. (2006) Dual-color-coded imaging of viable circulating prostate carcinoma cells reveals genetic exchange between tumor cells in vivo, contributing to highly metastatic phenotypes. *Cell Cycle* 5:191–197.
30. Jiang P, Yamauchi K, Yang M, et al. (2006) Tumor cells genetically labeled with GFP in the nucleus and RFP in the cytoplasm for imaging cellular dynamics. *Cell Cycle* 5:1198–1201.
31. Berezovska OP, Glinskii AB, Yang Z, et al. (2006) Essential role for activation of the Polycomb Group (PcG) protein chromatin silencing pathway in metastatic prostate cancer. *Cell Cycle* 5:1886–1901.
32. Yamauchi K, Yang M, Hayashi K, et al. (2007) Imaging of nucleolar dynamics during the cell cycle of cancer cells in live mice. *Cell Cycle* 6:2706–2708.
33. Salie R, Steeves JD. (2005) IGF-1 and BDNF promote chick bulbospinal neurite outgrowth in vitro. *Int J Dev Neurosci* 23:587–598.

34. Wichterle H, Lieberam I, Porter JA, Jessell TM. (2002) Directed differentiation of embryonic stem cells into motor neurons. *Cell* 110:385–397.
35. Cummings BJ, Uchida N, Tamaki SJ, et al. (2005) Human neural stem cells differentiate and promote locomotor recovery in spinal cord-injured mice. *Proc Natl Acad Sci USA* 102:14069–14074.
36. Aoi T, Yae K, Nakagawa M, Ichisaka T, et al. (2008) Generation of pluripotent stem cells from adult mouse liver and stomach cells. *Science* 321:699–702.
37. Takahashi K, Tanabe K, Ohnuki M, et al. (2007) Induction of pluripotent stem cells from adult human fibroblasts by defined factors. *Cell* 131:861–872.
38. Yu J, Vodyanik MA, Smuga-Otto K, et al. (2007) Induced pluripotent stem cell lines derived from human somatic cells. *Science* 318:1917–1920.
39. Lako M, Armstrong L, Cairns PM, Harris S, Hole N, Jahoda CA. (2002) Hair follicle dermal cells repopulate the mouse haematopoietic system. *J Cell Sci.* 115(Pt 20):3967–3974.
40. Jahoda CA, Whitehouse J, Reynolds AJ, Hole N (2003) Hair follicle dermal cells differentiate into adipogenic and osteogenic lineages. *Exp Dermatol* 12:849–859.
41. Gharzi A, Reynolds AJ, Jahoda CA. (2003) Plasticity of hair follicle dermal cells in wound healing and induction. *Exp Dermatol* 12:126–136.
42. Basso DM, Beattie MS, Bresnahan JC. (1996) Graded histological and locomotor outcomes after spinal cord contusion using the NYU weight-drop device versus transection. *Exp Neurol* 139:244–256.
43. Wells JE, Rice TK, Nuttall RK, et al. (2003) An adverse role for matrix metalloproteinase 12 after spinal cord injury in mice. *J Neurosci* 23:10107–10115.

Chapter 9

Pancreas

Fang-Xu Jiang and Grant Morahan

Abstract Type 1 diabetes and some forms of type 2 diabetes are caused by deficiency of insulin-secreting islet β cells. Although diabetes may be treated with exogenous insulin replacement, this is not a cure, and this therapy may be associated with some devastating complications, such as nephropathy, retinopathy and neuropathy. An ideal treatment for diabetes would be to transplant donated islets or to regenerate endogenous β cells. However, the poor availability of donor islets has severely restricted the broad clinical use of islet transplantation. The ability to differentiate embryonic stem cells into insulin-expressing cells initially showed great promise, but the generation of functional β cells has proven extremely difficult and far slower than originally thought. Pancreatic stem cells (PSC) or transdifferentiation of other cell types in the pancreas may therefore provide an alternative renewable source of surrogate β cells.

The term “stem cell” was initially used in embryology in the late 19th century in the context of the origin of blood system and gametes (see [53]). Stem cells are undifferentiated cells that are capable of both self-renewal and giving rise to specialized functional cells. Depending on the developmental stages of their origin, stem cells can be divided into embryonic stem cells (derived from the inner cell mass of pre-implanted embryos) [18, 40]; epiblast stem cells (derived from post-implanted epiblast-stage embryos) [10, 70]; germline-derived stem cells (derived from embryonic gonadal ridges or postnatal testes) [22, 35, 64]; induced pluripotent stem cells (from foetal or adult cells) [2, 25, 47, 69] or adult stem cells (derived from postnatal tissues). Adult stem cells are a rare population in specific tissues but show powerful potential for regeneration. They can be further divided based on their tissue origin into a number of categories such as haematopoietic stem cells, neuronal stem cells, skin stem cells, as well as mesenchymal stem cells. Unlike other tissue-specific stem cells, pancreatic stem cells (PSC) were proposed relatively recently

F.X. Jiang (✉)

Western Australian Institute for Medical Research, Centre for Diabetes Research, and
Centre for Medical Research, University of Western Australia, 50 Murray St (Rear),
Perth, WA 6000, Australia
e-mail: jiang@waimr.uwa.edu.au

[54]. In order to understand the role and potential of PSC, a knowledge of pancreas development is required.

9.1 Pancreas Development and Function

The pancreas is an endoderm-derived organ. The endoderm is one of the three primary germ layers formed during the early embryo stage known as gastrulation. Taking the mouse as an example, the pancreas originates from the thickened endodermal epithelium along the dorsal and ventral surfaces of the posterior foregut. These thickenings can be identified histologically at 9.0–9.5 days postcoitum (dpc) [49]. Subsequently, these epithelia evaginate into the surrounding mesoderm-derived mesenchymal tissue and form dorsal and ventral pancreatic buds. These buds continue to expand, branch and fuse as a result of gut rotation bringing the buds together. The fused developing pancreas continues to proliferate, differentiate and, ultimately, develop into mature pancreas. In humans, the dorsal bud can be detected as early as 26 dpc (an equivalent stage to 9.5 dpc mouse embryos), but insulin-positive cells are first visible at 52 dpc, approximately 2 weeks later than the equivalent stage seen in mice. The appearance of human insulin-positive cells precedes that of glucagon-positive cells at 8–10 weeks of development [51]. All islet cells are detectable at the end of the first trimester in humans [51], but at later stages in mice [29]. These data indicate a human-mouse temporal difference in lineage development [55], and this is supported by differences in gene expression patterns during developmental and disease processes in these two species [19]. More studies of the development of human pancreas can be found elsewhere [15, 39, 52].

During the last decade or two, our knowledge of pancreas development, including key transcriptional controls, has increased exponentially. Transcriptional regulation of specification and differentiation of the various lineages in the pancreas has been extensively reviewed [4, 24, 30, 44, 63, 75] and is briefly summarised in Fig. 9.1.

The adult pancreas consists of digestive enzyme-secreting exocrine tissue, digestive enzyme-transporting ductal tissue and hormone-secreting tissue found in the islets of Langerhans. The islets are composed mainly of α , β , δ , ϵ and PP cells (Fig. 9.1) that secrete glucagon, insulin, somatostatin, ghrelin and pancreatic polypeptide respectively [34]. These hormones are generally responsible for the regulation of glucose homeostasis. The β cells sense the fluctuation of blood glucose levels and secrete insulin in a manner dependent on the glucose concentration. In adult humans, there are 2000–3000 β cells/islet of Langerhans, with approximately 1 million islets scattered throughout the pancreas [66]. Insulin regulates circulating blood glucose concentrations through its actions on peripheral tissues, such as to inhibit hepatic glucose release and stimulate glucose uptake and storage by skeletal muscle and adipocyte tissue. Insulin insufficiency or unresponsiveness leads to diabetes, which has recently manifested a global prevalent trend and has been a major public health problem in the world, not only in Western developed countries, but also in developing countries, such as China and India. Diabetes currently

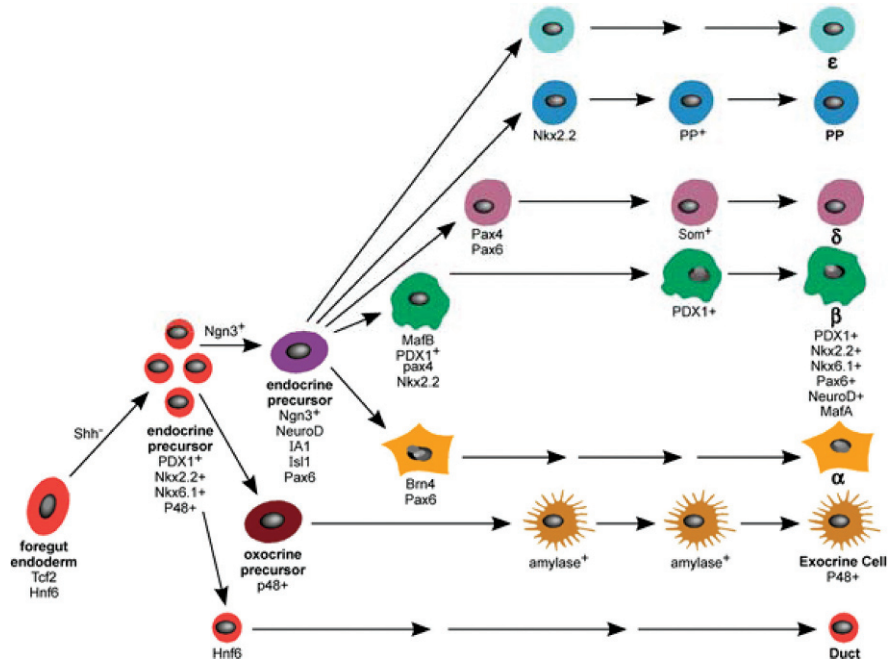


Fig. 9.1 Lineage development in the pancreas showing role of defined transcription factors. Progenitors within a defined domain of foregut endoderm express Tcf2 (*T cell factor 2*, also known as *hepatocyte nuclear factor 1b*, *Hnf1b*) and *Hnf6*. Suppression of *sonic hedgehog* (*Shh*) signalling leads to the development of pancreatic precursor cells, which are marked by expression of a number of transcription factors, especially Pdx1 (pancreas and duodenum transcription factor 1), pancreas transcription factor 1a (Ptf1a), Nkx2.2 (Nk family homeobox factor 2.2) and Nkx6.1. Up-regulation of *neurogenin-3* (*Ngn3*) allows these pancreatic precursors to commit to progenitors of the endocrine islet lineages; these endocrine progenitors also express *NeuroD* (*neural differentiation 1*), *IA1* (*insulinoma associated 1*), *Isl1* (*Islet 1*) and *Pax6* (*paired box factor 6*). The endocrine progenitors then may differentiate into five types of islet cells (α , β , δ [somatostatin], PP [pancreatic polypeptide] and ϵ [ghrelin]). For example, whereas cells that express *Brn4* (the brain-specific POU-box factor) and *Pax6* are destined to become glucagon-secreting cells, a group of *MafB*- (musculoaponeurotic fibrosarcoma oncogene family protein B), *Pdx1*-, *Pax4*- and *Nkx2.2*-expressing cells give rise to mature insulin-secreting β cells

affects approximately 200 million people, and is likely to increase to 400 million by 2030 [38]. Absolute deficiency of β cells results in type 1 diabetes, which represents approximately 10% of diabetes cases. The best prospect for a cure of type 1 diabetes is to transplant donated islets or to regenerate β cells of people with this disease, provided that autoimmunity to β cells can be controlled. However, the poor availability of donor islets has severely restricted the broad clinical use of islet transplantation. This is why much attention has been paid to stem cells, including PSC, as a renewable source of insulin-producing β cells. However, despite intensive research, the presence and origin of human PSC (hPSC) both are still hotly debated.

9.2 Regeneration of β Cells Occurs Physiologically and Pathophysiologically

β cells are regenerated during pregnancy, partial pancreatectomy and obesity. These observations led to the birth of the PSC concept [7]. The existence of PSC is also inferred from the continued function of islets after transplantation [58, 59]. Since there is no convincing evidence of contribution of haematopoietic stem cells to islet cells [74] nor that β cells are long-lived [5], the continued function of transplanted islets suggests that either hPSC reside inside the islets or the β cells are capable of self-renewal (or some combination of these).

9.2.1 Regeneration of β Cells During Pregnancy

To cope with physiological demand, pancreatic β cells regenerate during pregnancy in humans and experimental animals. For example, the uptake of bromodeoxyuridine (BrdU), a thymidine analogue that may be incorporated into DNA during S-phase, increases 3-fold at 10 dpc and 10-fold at 14 dpc in islets of pregnant rats [48], providing indirect evidence that proliferation of islet cells contributes significantly to the increase of islet volume [28, 72]. However, there only is a 2-fold increase in islet volume and a 3-fold increase in BrdU labelling in 15.5 dpc maternal mouse islets [36]. This discrepancy may reflect a species difference in regeneration capacity or a difference in sensitivity of detection methods. During human pregnancy, both an increase in volume of maternal islets and hyperplasia of “ β ” cells have also been observed [73], but direct evidence of proliferation in these islets is still lacking. Furthermore, in rodents and humans, prolactin and placental lactogens may stimulate β -cell proliferation [45], via suppression of the transcriptional co-activator menin, encoded by the gene *multiple endocrine neoplasia type 1 (MEN1)*. This was demonstrated by experiments in which a short infusion of prolactin was sufficient to reduce menin expression and stimulate proliferation of mouse islet cells [36]. However, it is still unknown whether proliferation comes from functional β cells and/or from PSC. Future research should be directed to recapitulate this effect in vitro with purified islet cells, in which novel stimuli and molecular pathways may be identified. Defining these pathways may establish a platform on which novel strategies can be developed for a cure of type 1 diabetes.

9.2.2 Regeneration of β Cells During Obesity

β cells regenerate in response to pathological processes such as obesity. For example, up to 10-fold increase in β -cell mass has been observed in obese rodents, responding to their insulin resistance [11]. Double staining of pancreas sections from obese mice and humans can detect insulin-producing cells that express Ki-67, a marker strictly associated with cell proliferation [11, 12], indicating that

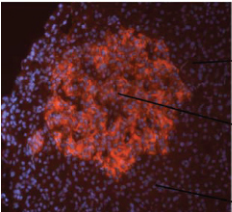
regeneration may occur in the islets. Again, the regeneration capacity seems to be significantly greater in mice than in humans, although the underlying mechanism is unclear yet. Studies of one obese mutant mouse line, termed A^y , showed that reduction of menin contributes to adaptive β -cell proliferation [36]. Taken together, these data suggest that a similar mechanism for β -cell regeneration may operate in physiological pregnancy and pathophysiological obesity in mice. It would be interesting to determine whether this mechanism is also at work during human pregnancy or obesity.

9.2.3 Regeneration of β Cells After Partial Pancreatectomy

Like many other organs in the body, islets do regenerate in response to injury, in this case, pancreatectomy. In rats 4 weeks after 90% pancreatectomy, for example, there is a regeneration to 27 and 45% of sham-operated pancreas and islet mass, respectively [7]. However, there are species differences in regeneration capacity. Even a 50% pancreatectomy in adult dogs would cause impaired fasting glucose in the short term [41] and diabetes in the longer term [65]. Likewise, a 50% pancreatectomy in adult humans also leads to subsequent obesity and diabetes [56]. These studies again indicate that there is a difference between species in their capacity to mount islet regeneration: this is much more powerful in rodents than in larger mammals. Additional studies are needed to confirm this capacity difference and understand its underlying mechanism. Furthermore, it is less clear to what extent islet regeneration contributes to maintain β -cell mass in adult humans from existing islet cells and how much is from cells of any other origins. This knowledge is critical for a viable strategy to promote β -cell regeneration both in vivo and in vitro. Additionally, it is unknown whether PSC also contribute to this type of regeneration. In the following sections, we will examine several possible mechanisms that may lead to β -cell generation and regeneration.

9.3 Evidence that β Cells Are Generated from PSC

In addition to the observations of long-term survival of transplanted islets mentioned above, substantial in vitro evidence has indicated that “pluripotent PSC” may be present in all three major pancreas compartments, i.e. the ductal epithelium [14, 54, 68], islets, and acinar tissue [60, 77] (Fig. 9.2). This evidence comes from studies of both rodent and human pancreas. For example, a potential PSC candidate has been purified by flow cytometry in the developing and adult mouse pancreas. These cells are identified by expression of the receptor for hepatocyte growth factor, c-Met, and absence of blood cell surface markers such as CD45, TER119, c-Kit, and Flk-1. These cells can differentiate into multiple pancreatic lineage cells from individual cells in vitro and give rise to pancreatic endocrine and acinar cells in vivo following transplantation [67]. However, the molecular characteristics of



	Marker	Colony	Self-renewal	Ref.
→ Duct	Yes	?	?	1
	ND	Yes	?	2
	Yes	ND	ND	3
→ Islet	ND	Yes	?	2
	Yes	ND	ND	4
	ND	Yes	?	5
→ Acinar	Yes	ND	ND	6

Fig. 9.2 Pancreatic stem cells (PSC) were found in the duct, islet or acinar tissue. ND=not done; ?=questionable; 1=Suzuki et al. [67]; 2=Seaberg et al. [60]; 3=Bonner-Weir et al. [6]; 4=Zulewski et al. [27]; 5=Gershengorn et al. [21]; 6=Minami et al. [43]

these c-met expressing cells are largely unknown and clonogenesis at the single cell level has not been established.

9.3.1 PSC May Be Found in Ductal Epithelium

We investigated the differentiation and proliferation of foetal mouse pancreatic cells, a rich source for potential PSC. We first demonstrated in vitro that bone morphogenetic proteins-2, -4, -5 and -6, members of the transforming growth factor β superfamily, can promote the proliferation of pancreatic progenitors and the development of pancreatic cystic epithelial colonies containing β cells [31, 33], a process recapitulating the in vivo developmental process. In addition, we also revealed that various isoforms of epidermal growth factors stimulate colony formation [32]. These data indicate that extracellular signalling molecules, including various families of growth factors, modulate fate changes of pancreas progenitor/stem cells. However, currently these colony-forming cells may at most be considered progenitors because their self-renewal has not been demonstrated in vitro (F.X.J. unpublished observations).

Recently, in vitro and in vivo experiments have indicated that PSC are localized in the ductal epithelium. Bonner-Weir and colleagues were the first to report that adult human pancreatic ductal epithelial cells can form islet-like clusters and differentiate into insulin-secreting β cells [8]. Ramiya and colleagues reported that transplantation of in vitro generated islet-like structures from mouse PSC in the ductal epithelium can reverse diabetes [54]. Another set of experiments used cultures of “pancreatic ductal cell aggregates” that were left over from pancreas digests after purification of human islets for transplantation. From these cultures fibroblast-like cells grew out and have been termed “pancreatic mesenchymal stem cells (pMSC)”. These cells can undergo at least 12 passages and express a range of bone marrow-derived MSC markers including CD13, CD29, CD44, CD54, CD105, α_6 integrin subunit (also known as CD49f) and Thy1 (also known as CD90). These pMSC can give rise to cells of at least two germ layer origins including endoderm-derived cells, but not convincingly pancreatic lineage cells [61]. In vivo, the large, small, and centrolobular ducts of the rat pancreas contain foci of cells that express the neural

stem cell-specific marker, nestin, but do not express the ductal marker cytokeratin 19 (CK19) [77], suggestive of islet progenitor cells.

However, all the above studies have used mixed cell populations and failed to demonstrate clonogenesis. Using culture conditions suitable for generating neurospheres *ex vivo*, mouse pancreatic ductal cells gave rise to neurosphere-like structures that can subsequently be differentiated into several types of islet cells including β cells [60]. The molecular phenotype of progenitor cells for these islet cells remains unknown. On the other hand, after pancreatic duct ligation, numerous CK19⁺ ductal cells are regenerated and then give rise to islet progenitor cells (namely Ngn3⁺ cells), transplantation of the latter has further resulted in their differentiation into functional β cells [76], suggesting that the regeneration process may resemble that of embryonic pancreas development.

These studies did not explore the origin of Ngn3⁺ cells in adult pancreas and whether the cells that give rise to these Ngn3⁺ cells possess PSC features. Recently, the use of the *in vivo* genetic tracing Cre-loxP system has generated further knowledge in this regard. In these experiments, Cre expression was directed by the promoter of carbonic anhydrase II, a marker of mature ductal cells, resulting in the excision of the stop cassette in the transgenic Rosa26. Therefore β -galactosidase activity is expressed in the cells that express Cre. At 4 weeks, β -galactosidase is detected in many ducts, patched acinar cells and 35–40% of islet cells [6]. These data provide direct evidence that adult ductal epithelial cells can give rise to islet cells, at least in mice. It is still unknown whether the carbonic anhydrase II-expressing cell population is homogenous or heterogenous, and whether this is a differentiation process from PSC or a transdifferentiation process from mature ductal cells. Anyway, these results should be repeated by independent research laboratories and even in other experimental animals.

9.3.2 PSC May Reside in the Islets

Accumulated *in vitro* evidence suggests that a subpopulation of islet cells has PSC potential. A well-planned *in vitro* study found that uncharacterized cells of mouse islets give rise to neurosphere-like structures and subsequently could differentiate into islet β cells. This was a minor property, as they mostly developed into neural lineage cells [60].

In rat and human islets, a distinct population of nestin⁺ cells that do not express the hormones insulin, glucagon, somatostatin or pancreatic polypeptide has been identified. When cultured *in vitro*, these cells proliferate extensively (~8 months), give rise to cells that express liver and exocrine pancreas markers, such as α -fetoprotein and pancreatic amylase, and display a ductal/endocrine phenotype with expression of CK19, neural-specific cell adhesion molecule, insulin, glucagon, and PDX1 (pancreas and duodenum homeobox factor 1). These nestin⁺ putative progenitor cells may therefore participate in the neogenesis of islet endocrine cells [77], mediated at least partially by glucagon-like peptide-1, an incretin hormone

derived from processing proglucagon [1]. However, recent studies *in vivo* indicate that nestin⁺ cells are mostly restricted in non-endothelial-derived cells [37, 62]. In addition, from donated adult human islets, outgrown fibroblast-like cells do not express hormones, but proliferate readily and give rise *in vitro* to hormone-expressing cell aggregates, characteristics of typical islet cells [21]. Nevertheless, a rigorous genetic-based lineage tracing in mice under the control of Pdx1 or rat insulin promoter (RIP) demonstrated that neither PDX1- nor RIP-expressing cells contribute significantly to these fibroblast-like cells *in vitro* [13]. Because of its critical importance, such tracing experiments should be reproduced by independent research groups. Further investigations are required to resolve the inconsistent results from the current studies.

9.3.3 PSC May Be Present in the Exocrine Tissue

In the clinic, a large population of nonendocrine pancreatic acinar cells are discarded after purification of islets from donated pancreas for transplantation. The best way to make use of these cells has attracted significant interest in recent years. After co-transplantation with foetal pancreatic cells under the kidney capsule of immunodeficient mice, these nonendocrine pancreatic epithelial cells are capable of endocrine differentiation though without evidence of β -cell replication or cell fusion. These experiments suggest the existence of PSC or progenitor cells within the acinar compartment of the adult human pancreas [26]. More recently, analysis using the Cre/loxP-based tracing system demonstrated that amylase/elastase-expressing acinar cells can give rise to insulin-positive cells in a suspension culture [43]. However, because clonal assay of these amylase/elastase-expressing cells and their intermediate steps have not been investigated, this study may simply reveal that mouse and rat pancreatic acinar cells are able to transdifferentiate into surrogate insulin-expressing cells [3, 42]. On the other hand, similar lineage tracing experiments *in vivo* demonstrate that after 70–80% pancreatectomy, pre-existing mouse pancreatic acinar cells do not contribute to regeneration of islet β cells [16]. The contradiction of *in vitro* and *in vivo* findings requires further reconciliation.

9.4 Evidence that Islet β Cells Are Capable of Self-Replication

There are several pieces of strong evidence demonstrating that islet β cells can reproduce themselves. Using the RIP to genetically trace the fate of insulin-expressing cells, Dor and colleagues [17] first revealed that adult mouse pancreatic β cells are duplicated by RIP-expressing cells within the islets, either physiologically or after partial pancreatectomy. This study assumed that all RIP-expressing cells in adult islets are functional β cells and did not exclude the presence of PSC. Similarly, by using a transgenic model, in which the expression of diphtheria toxin was

directed by RIP to β cells, diphtheria expression results in apoptosis of 70–80% of β cells, destruction of islet architecture and, finally, diabetes. Withdrawal of diphtheria expression leads to a significant regeneration of β -cell mass and a spontaneous normalization of blood glucose levels and islet architecture. Simultaneously, RIP-based lineage tracing analysis indicates that the proliferation of 20–30% surviving “ β ” cells played a major role in this regeneration and in recovery of euglycemia [46]. More recently with human islets, RIP-expressing cells could be dedifferentiated and proliferate in vitro up to 16 population doublings [57]. As the β -cell population in the adult islets is in fact functionally heterogeneous [27, 50], studies designed to address whether the RIP-expressing cells or the remaining 20–30% cells are unambiguously functional β cells will be critical.

Using a more sophisticated genetic mosaic analysis with a double marker system in mice known as RIP-CreER; Rosa26^{GR}/ Rosa26^{RG}, each RIP-expressing clone has been demonstrated to consist of 5.1 ± 5.4 or 8.2 ± 6.9 cells after one or two months of chase [9]. These RIP-expressing clones have been interpreted as further evidence of regeneration of functional β cells. Additional loss-of-function study following knockout of the Hnf4 α (hepatocyte nuclear factor 4 α) gene suggests that this regeneration may involve the Ras/Erk signalling cascade [23] and ultimately regulated by cycling modulators including cyclin D2 [20]. Taken together, further identification and characterization of the so-called self-replicative or dedifferentiative RIP-expressing cells both in vivo and in vitro will be urgently needed because they may hold the key for a regenerative therapy for type 1 diabetes.

Again using thymidine-based lineage tracing, β cells were demonstrated to be produced within an islet by rare self-renewing cells with a slow replication-refractory period [71], although the identity of these unique cells and the length of their replication-refractory period remain to be determined. The frequency of these self-renewal cells can be significantly increased after partial pancreatectomy or during pregnancy. Further studies should determine the molecular signature and biological potential of these replicating self-renewal cells. Because of ethical issues, similar studies cannot be performed in human islet tissues, but such investigation should at least be repeated in larger mammals.

9.5 The Identity of PSC is Inconclusive

Whereas investigation to characterize β -cell duplication as a mechanism of islet regeneration has attracted great attention in recent years, much progress has been made to identify PSC but their identity is still inconclusive. This is due at least partially to lack of the following factors: specific cell surface markers to characterize and purify cells that may have PSC potential; a simple, effective and reproducible in vitro assay to examine self-renewal and differentiation potential of a purified cell population; in vivo functional assays to determine biological function for both experimental animals and humans. Finally, well-agreed general criteria for defining a PSC are required.

9.6 Future Directions for PSC Research

We believe that future work should reach a consensus that PSC at least satisfy the following criteria: (1) clonogenesis can be demonstrated at the level of single cells sorted by flow cytometry; (2) sorted single cells can self-renew in vitro; (3) clonogenic cells can give rise in vitro to more than one specialized cell lineage and (4) these cells can differentiate in vivo into several functional cell types after transplantation. In the future, the investigation of PSC should be particularly encouraged based on three considerations. First, differentiation of embryonic stem cells into insulin-expressing cells was initially exciting and promising, but safety consideration aside, the generation of functional β cells proves extremely difficult and progress has been far slower than originally expected. PSC and dedifferentiation or transdifferentiation of other cell types in the pancreas may therefore provide an alternative renewable source of surrogate β cells. Second, the β -cell duplication theory was mostly established from rodent models. It cannot completely exclude the existence of PSC, and it assumed that all insulin-expressing cells in the adult islets are uniformly functional β cells, but in fact these cells are heterogeneous. Last, as there is a significant difference in regeneration capacity between rodent and human islets, it may be wise not to directly extrapolate regeneration data from rodents to humans. Unlike previous studies that were only performed on in vivo or in vitro experiments without targeting specific cell types, future PSC work may need to employ integrated approaches, for example, applying cell surface markers to target particular cell populations; examining in vitro their potential of self-renewal and clonogenesis, using genetic approaches to dissect molecular mechanisms of their phenotypic changes and finally to examine their lineage contribution and biological function. Performing such integrated research is likely beyond the capacity of most individual laboratories, and therefore requires multi-discipline, multi-laboratory and even multi-national collaborations including the participation of the pharmaceutical sector to generate a therapeutic grade of surrogate β cells for a replacement therapy to diabetes.

Acknowledgments The authors are grateful to Dr Anne Bonser for critical reading of the manuscript. The authors are supported by grants from the Diabetes Research Foundation of Western Australia, the University of Western Australia, and the National Health and Medical Research Council of Australia (No. 305500).

Abbreviations

PSC:	pancreatic stem cells
dpc:	days postcoitum
hPSC:	human pancreatic stem cells
BrdU:	bromodeoxyuridine
MEN1:	multiple endocrine neoplasia type 1
pMSC:	pancreatic mesenchymal stem cells

Ngn3: neurogenin3
PDX1: pancreas and duodenum homeobox factor 1
RIP: rat insulin promoter

References

1. Abraham EJ, Leech CA, Lin JC, Zulewski H, and Habener JF, (2002) Insulinotropic hormone glucagon-like peptide-1 differentiation of human pancreatic islet-derived progenitor cells into insulin-producing cells. *Endocrinology* 143, 3152–61.
2. Aoi T, Yae K, Nakagawa M, Ichisaka T, Okita K, Takahashi K, Chiba T, and Yamanaka S, (2008) Generation of pluripotent stem cells from adult mouse liver and stomach cells. *Science* DOI: 10.1126/science.1154884.
3. Baeyens L, De Breuck S, Lardon J, Mfopou JK, Rooman I, and Bouwens L, (2005) In vitro generation of insulin-producing beta cells from adult exocrine pancreatic cells. *Diabetologia* 48, 49–57.
4. Best M, Carroll M, Hanley NA, and Piper Hanley K, (2008) Embryonic stem cells to beta-cells by understanding pancreas development. *Mol Cell Endocrinol* 288, 86–94.
5. Bonner-Weir S, (2000) Life and death of the pancreatic beta cells. *Trends Endocrinol Metab* 11, 375–8.
6. Bonner-Weir S, Inada A, Yatoh S, Li WC, Aye T, Toschi E, and Sharma A, (2008) Trans-differentiation of pancreatic ductal cells to endocrine beta-cells. *Biochem Soc Trans* 36, 353–6.
7. Bonner-Weir S, and Sharma A, (2002) Pancreatic stem cells. *J Pathol* 197, 519–26.
8. Bonner-Weir S, Taneja M, Weir GC, Tatarkiewicz K, Song KH, Sharma A, and O’Neil JJ, (2000) In vitro cultivation of human islets from expanded ductal tissue. *Proc Natl Acad Sci USA* 97, 7999–8004.
9. Brennand K, Huangfu D, and Melton D, (2007) All beta cells contribute equally to islet growth and maintenance. *PLoS Biol* 5, e163.
10. Brons IG, Smithers LE, Trotter MW, Rugg-Gunn P, Sun B, Chuva de Sousa Lopes SM, Howlett SK, Clarkson A, Ahrlund-Richter L, Pedersen RA, and Vallier L, (2007) Derivation of pluripotent epiblast stem cells from mammalian embryos. *Nature* 448, 191–5.
11. Butler AE, Janson J, Bonner-Weir S, Ritzel R, Rizza RA, and Butler PC, (2003a) Beta-cell deficit and increased beta-cell apoptosis in humans with type 2 diabetes. *Diabetes* 52, 102–10.
12. Butler AE, Janson J, Soeller WC, and Butler PC, (2003b) Increased beta-cell apoptosis prevents adaptive increase in beta-cell mass in mouse model of type 2 diabetes: evidence for role of islet amyloid formation rather than direct action of amyloid. *Diabetes* 52, 2304–14.
13. Chase LG, Ulloa-Montoya F, Kidder BL, and Verfaillie CM, (2007) Islet-derived fibroblast-like cells are not derived via epithelial-mesenchymal transition from Pdx-1 or insulin-positive cells. *Diabetes* 56, 3–7.
14. Cornelius JG, Tchernev V, Kao KJ, and Peck AB, (1997) In vitro-generation of islets in long-term cultures of pluripotent stem cells from adult mouse pancreas. *Horm Metab Res* 29, 271–7.
15. De Krijger RR, Aanstoot HJ, Kranenburg G, Reinhard M, Visser WJ, and Bruining GJ, (1992) The midgestational human fetal pancreas contains cells coexpressing islet hormones. *Dev Biol* 153, 368–75.
16. Desai BM, Oliver-Krasinski J, De Leon DD, Farzad C, Hong N, Leach SD, and Stoffers DA, (2007) Preexisting pancreatic acinar cells contribute to acinar cell but not islet beta cell regeneration. *J Clin Invest*, 117, 971–7.
17. Dor Y, Brown J, Martinez OI, and Melton DA, (2004) Adult pancreatic beta-cells are formed by self-duplication rather than stem-cell differentiation. *Nature* 429, 41–6.
18. Evans MJ, and Kaufman MH, (1981) Establishment in culture of pluripotential cells from mouse embryos. *Nature* 292, 154–6.

19. Foucherousse F, Bullen P, Herasse M, Lindsay S, Richard I, Wilson D, Suel L, Durand M, Robson S, Abitbol M, Beckmann JS, and Strachan T, (2000) Human-mouse differences in the embryonic expression patterns of developmental control genes and disease genes. *Hum Mol Genet* 9, 165–73.
20. Georgia S, and Bhushan A, (2004) Beta cell replication is the primary mechanism for maintaining postnatal beta cell mass. *J Clin Invest* 114, 963–8.
21. Gershengorn MC, Hardikar AA, Wei C, Geras-Raaka E, Marcus-Samuels B, and Raaka BM, (2004) Epithelial-to-mesenchymal transition generates proliferative human islet precursor cells. *Science* 306, 2261–4.
22. Guan K, Nayernia K, Maier LS, Wagner S, Dressel R, Lee JH, Nolte J, Wolf F, Li M, Engel W, and Hasenfuss G, (2006) Pluripotency of spermatogonial stem cells from adult mouse testis. *Nature* 440, 1199–203.
23. Gupta RK, Gao N, Gorski RK, White P, Hardy OT, Rafiq K, Brestelli JE, Chen G, Stoeckert CJ, Jr, and Kaestner KH, (2007) Expansion of adult beta-cell mass in response to increased metabolic demand is dependent on HNF-4alpha. *Genes Dev* 21, 756–69.
24. Habener JF, Kemp DM, and Thomas MK, (2005) Minireview: transcriptional regulation in pancreatic development. *Endocrinology* 146, 1025–34.
25. Hanna J, Markoulaki S, Schorderet P, Carey BW, Beard C, Wernig M, Creyghton MP, Steine EJ, Cassady JP, Foreman R, Lengner CJ, Dausman JA, and Jaenisch R, (2008) Direct reprogramming of terminally differentiated mature B, lymphocytes to pluripotency. *Cell* 133, 250–64.
26. Hao E, Tyrberg B, Itkin-Ansari P, Lakey JR, Geron I, Monosov EZ, Barcova M, Mercola M, and Levine F, (2006) Beta-cell differentiation from nonendocrine epithelial cells of the adult human pancreas. *Nat Med* 12, 310–6.
27. Heimberg H, De Vos A, Vandercammen A, Van Schaftingen E, Pipeleers D, and Schuit F, (1993) Heterogeneity in glucose sensitivity among pancreatic beta-cells is correlated to differences in glucose phosphorylation rather than glucose transport. *EMBO J* 12, 2873–9.
28. Hellman B, (1960) The islets of Langerhans in the rat during pregnancy and lactation with special reference to the changes in the B/A, cell ratio. *Acta Obstet Gynecol Scand* 39, 331–42.
29. Herrera PL, Huarte J, Sanvito F, Meda P, Orci L, and Vassalli JD, (1991) Embryogenesis of the murine endocrine pancreas; early expression of pancreatic polypeptide gene. *Development* 113, 1257–65.
30. Jensen J, (2004) Gene regulatory factors in pancreatic development. *Dev Dyn* 229, 176–200.
31. Jiang FX, and Harrison LC, (2005a) Convergence of bone morphogenetic protein and laminin-1 signaling pathways promotes proliferation and colony formation by fetal mouse pancreatic cells. *Exp Cell Res* 308, 114–22.
32. Jiang FX, and Harrison LC, (2005b) Laminin-1 and epidermal growth factor family members co-stimulate fetal pancreas cell proliferation and colony formation. *Differentiation* 73, 45–9.
33. Jiang FX, Stanley EG, Gonez LJ, and Harrison LC, (2002) Bone morphogenetic proteins promote development of fetal pancreas epithelial colonies containing insulin-positive cells. *J Cell Sci* 115, 753–60.
34. Jorgensen MC, Ahnfelt-Ronne J, Hald J, Madsen OD, Serup P, and Hecksher-Sorensen J, (2007) An illustrated review of early pancreas development in the mouse. *Endocr Rev* 28, 685–705.
35. Kanatsu-Shinohara M, Inoue K, Lee J, Yoshimoto M, Ogonuki N, Miki H, Baba S, Kato T, Kazuki Y, Toyokuni S, Toyoshima M, Niwa O, Oshimura M, Heike T, Nakahata T, Ishino F, Ogura A, and Shinohara T, (2004) Generation of pluripotent stem cells from neonatal mouse testis. *Cell* 119, 1001–12.
36. Karnik SK, Chen H, McLean GW, Heit JJ, Gu X, Zhang AY, Fontaine M, Yen MH, and Kim SK, (2007) Menin controls growth of pancreatic beta-cells in pregnant mice and promotes gestational diabetes mellitus. *Science* 318, 806–9.
37. Lardon J, Rooman I, and Bouwens L, (2002) Nestin expression in pancreatic stellate cells and angiogenic endothelial cells. *Histochem Cell Biol* 117, 535–40.

38. Lock LT, and Tzanakakis ES, (2007) Stem/Progenitor cell sources of insulin-producing cells for the treatment of diabetes. *Tissue Eng* 13, 1399–412.
39. Lukinius A, Ericsson JL, Grimelius L, and Korsgren O, (1992) Ultrastructural studies of the ontogeny of fetal human and porcine endocrine pancreas with special reference to colocalization of the four major islet hormones. *Dev Biol* 153, 376–85.
40. Martin GR, (1981) Isolation of a pluripotent cell line from early mouse embryos cultured in medium conditioned by teratocarcinoma stem cells. *Proc Natl Acad Sci USA* 78, 7634–8.
41. Matveyenko AV, Veldhuis JD, and Butler PC, (2006) Mechanisms of impaired fasting glucose and glucose intolerance induced by an approximate 50% pancreatectomy. *Diabetes* 55, 2347–56.
42. Minami K, Okano H, Okumachi A, and Seino S, (2008) Role of cadherin-mediated cell–cell adhesion in pancreatic exocrine-to-endocrine transdifferentiation. *J Biol Chem* 283, 13753–61.
43. Minami K, Okuno M, Miyawaki K, Okumachi A, Ishizaki K, Oyama K, Kawaguchi M, Ishizuka N, Iwanaga T, and Seino S, (2005) Lineage tracing and characterization of insulin-secreting cells generated from adult pancreatic acinar cells. *Proc Natl Acad Sci USA* 102, 15116–21.
44. Murtaugh LC, (2007) Pancreas and beta-cell development: from the actual to the possible. *Development* 134, 427–38.
45. Nielsen JH, Svensson C, Galsgaard ED, Moldrup A, and Billestrup N, (1999) Beta cell proliferation and growth factors. *J Mol Med* 77, 62–6.
46. Nir T, Melton DA, and Dor Y, (2007) Recovery from diabetes in mice by beta cell regeneration. *J Clin Invest* 117, 2553–61.
47. Park IH, Zhao R, West JA, Yabuuchi A, Huo H, Ince TA, Lerou PH, Lensch MW, and Daley GQ, (2008) Reprogramming of human somatic cells to pluripotency with defined factors. *Nature* 451, 141–6.
48. Parsons JA, Brelje TC, and Sorenson RL, (1992) Adaptation of islets of Langerhans to pregnancy: increased islet cell proliferation and insulin secretion correlates with the onset of placental lactogen secretion. *Endocrinology* 130, 1459–66.
49. Pictet RL, Clark WR, Williams RH, and Rutter WJ, (1972) An ultrastructural analysis of the developing embryonic pancreas. *Dev Biol* 29, 436–67.
50. Pipeleers D, Kiekens R, Ling Z, Wilikens A, and Schuit F, (1994) Physiologic relevance of heterogeneity in the pancreatic beta-cell population. *Diabetologia* 37 Suppl 2, S57–64.
51. Piper K, Brickwood S, Turmpenny LW, Cameron IT, Ball SG, Wilson DI, and Hanley NA, (2004) Beta cell differentiation during early human pancreas development. *J Endocrinol* 181, 11–23.
52. Polak M, Bouchareb-Banaei L, Scharfmann R, and Czernichow P, (2000) Early pattern of differentiation in the human pancreas. *Diabetes* 49, 225–32.
53. Ramalho-Santos M, and Willenbring H, (2007) On the origin of the term “stem cell”. *Cell Stem Cell* 1, 35–8.
54. Ramiya VK, Maraist M, Arfors KE, Schatz DA, Peck AB, and Cornelius JG, (2000) Reversal of insulin-dependent diabetes using islets generated in vitro from pancreatic stem cells. *Nat Med* 6, 278–82.
55. Richardson MK, Hanken J, Gooneratne ML, Pieau C, Raynaud A, Selwood L, and Wright GM, (1997) There is no highly conserved embryonic stage in the vertebrates: implications for current theories of evolution and development. *Anat Embryol (Berl)* 196, 91–106.
56. Robertson RP, Lanz KJ, Sutherland DE, and Seaquist ER, (2002) Relationship between diabetes and obesity 9 to 18 years after hemipancreatectomy and transplantation in donors and recipients. *Transplantation* 73, 736–41.
57. Russ HA, Bar Y, Ravassard P, and Efrat S, (2008) In vitro proliferation of cells derived from adult human beta-cells revealed by cell-lineage tracing. *Diabetes* 57, 1575–83.
58. Ryan EA, Lakey JR, Paty BW, Imes S, Korbitt GS, Kneteman NM, Bigam D, Rajotte RV, and Shapiro AM, (2002) Successful islet transplantation: continued insulin reserve provides long-term glycemic control. *Diabetes* 51, 2148–57.

59. Ryan EA, Paty BW, Senior PA, Bigam D, Alfarhli E, Kneteman NM, Lakey JR, and Shapiro AM, (2005) Five-year follow-up after clinical islet transplantation. *Diabetes* 54, 2060–9.
60. Seaberg RM, Smukler SR, Kieffer TJ, Enikolopov G, Asghar Z, Wheeler MB, Korbitt G, and van der Kooy D, (2004) Clonal identification of multipotent precursors from adult mouse pancreas that generate neural and pancreatic lineages. *Nat Biotechnol* 22, 1115–24.
61. Seeberger KL, Dufour JM, Shapiro AM, Lakey JR, Rajotte RV, and Korbitt GS, (2006) Expansion of mesenchymal stem cells from human pancreatic ductal epithelium. *Lab Invest* 86, 141–53.
62. Selander L, and Edlund H, (2002) Nestin is expressed in mesenchymal and not epithelial cells of the developing mouse pancreas. *Mech Dev* 113, 189–92.
63. Servitja JM, and Ferrer J, (2004) Transcriptional networks controlling pancreatic development and beta cell function. *Diabetologia* 47, 597–613.
64. Shamblott MJ, Axelman J, Wang S, Bugg EM, Littlefield JW, Donovan PJ, Blumenthal PD, Huggins GR, and Gearhart JD, (1998) Derivation of pluripotent stem cells from cultured human primordial germ cells. *Proc Natl Acad Sci USA*, 95, 13726–31.
65. Stagner JJ, and Samols E, (1991) Deterioration of islet beta-cell function after hemipancreatectomy in dogs. *Diabetes* 40, 1472–9.
66. Stefan Y Orci L, Malaisse-Lagae F, Perrelet A, Patel Y, and Unger RH, (1982) Quantitation of endocrine cell content in the pancreas of nondiabetic and diabetic humans. *Diabetes* 31, 694–700.
67. Suzuki A, Nakauchi H, and Taniguchi H, (2004) Prospective isolation of multipotent pancreatic progenitors using flow-cytometric cell sorting. *Diabetes* 53, 2143–52.
68. Suzuki A, Oyama K, Fukao K, Nakauchi H, and Taniguchi H, (2002) Establishment of clonal colony-forming assay system for pancreatic stem/progenitor cells. *Cell Transplant* 11, 451–3.
69. Takahashi K, and Yamanaka S, (2006) Induction of pluripotent stem cells from mouse embryonic and adult fibroblast cultures by defined factors. *Cell* 126, 663–76.
70. Tesar PJ, Chenoweth JG, Brook FA, Davies TJ, Evans EP, Mack DL, Gardner RL, and McKay RD, (2007) New cell lines from mouse epiblast share defining features with human embryonic stem cells. *Nature* 448, 196–9.
71. Teta M, Rankin MM, Long SY Stein GM, and Kushner JA, (2007) Growth and regeneration of adult beta cells does not involve specialized progenitors. *Dev Cell* 12, 817–26.
72. Van Assche FA, (1974) Quantitative morphologic and histoenzymatic study of the endocrine pancreas in nonpregnant and pregnant rats. *Am J Obstet Gynecol* 118, 39–41.
73. Van Assche FA, Aerts L, and De Prins F, (1978) A morphological study of the endocrine pancreas in human pregnancy. *Br J Obstet Gynaecol* 85, 818–20.
74. Wagers AJ, Sherwood RI, Christensen JL, and Weissman IL, (2002) Little evidence for developmental plasticity of adult hematopoietic stem cells. *Science* 297, 2256–9.
75. Wilson ME, Scheel D, and German MS, (2003) Gene expression cascades in pancreatic development. *Mech Dev* 120, 65–80.
76. Xu X, D'Hoker J, Stange G, Bonne S, De Leu N, Xiao X, Van De Casteele M, Mellitzer G, Ling Z, Pipeleers D, Bouwens L, Scharfmann R, Gradwohl G, and Heimberg H, (2008) Beta cells can be generated from endogenous progenitors in injured adult mouse pancreas. *Cell* 132, 197–207.
77. Zulewski H, Abraham EJ, Gerlach MJ, Daniel PB, Moritz W, Muller B, Vallejo M, Thomas MK, and Habener JF, (2001) Multipotential nestin-positive stem cells isolated from adult pancreatic islets differentiate ex vivo into pancreatic endocrine exocrine and hepatic phenotypes. *Diabetes* 50, 521–33.

Chapter 10

Prostate

C. Foley, K.T. Brouillette, C. Kane, H. Patel, H. Yamamoto
and A. Ahmed

Abstract Evidence for stem cells in the adult prostate comes from studies performed in rodents. Isaacs and Coffey [20] showed that castration in male rats resulted in the involution of prostate gland with persistence of the basal layer. On replacement of androgens, the prostate regained its original size [20]. It was concluded that a population of cells in the basal layer is capable of reconstituting the prostate in the presence of androgens. Since then good evidence of the existence and characterization of stem or stem like cells has been shown for mouse prostate [2, 23, 58]. Stem-like cells have also been described in cell lines derived from human prostate [34, 46] and from transplantation studies of human malignant prostate in mice [35]. In contrast to some tissues [10, 11, 28, 48, 49], isolation and characterization of stem cells from freshly procured human prostate tissue has proved difficult. Although there are numerous studies that have attempted to isolate, propagate and characterize human prostate derived stem cells; conclusive evidence for the existing of self-renewing, multipotential human prostate stem cells has proved elusive [46].

10.1 Properties of Stem Cells

Adult stem cells are a small fraction of cells within tissues and are responsible for maintaining and replenishing the cells within that tissue [4, 47]. Stem cells possess the capability, unlike differentiated cells, of self-renewal. Self-renewal is defined as a cell division in which one or both of the daughter cells are stem cells that retain the same developmental potential as the mother cell [33]. The demonstration of the capacity of a single cell to self-renew is a benchmark for the validation of stem cell isolation and characterization. Another important criterion is pluripotency (i.e. the

A. Ahmed (✉)

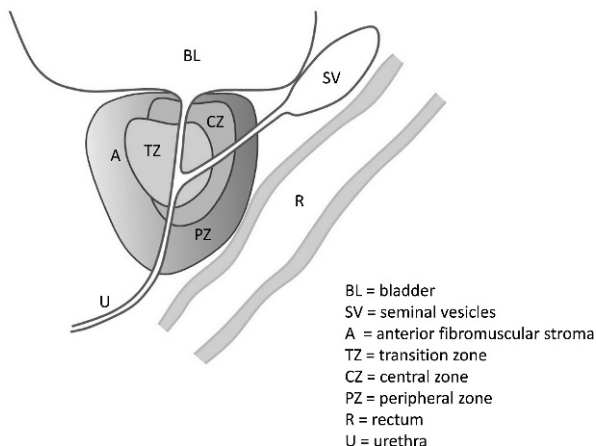
Division of Surgery and Interventional Sciences, Charles Bell House Laboratories, Prostate Cancer Research Centre, University College London, 67 Riding House Street, London, UK
e-mail: aamir.ahmed@ucl.ac.uk

ability to differentiate into specialized cells given an appropriate environment with a specific genetic program) [4, 38, 45].

10.2 Anatomy of the Prostate Gland

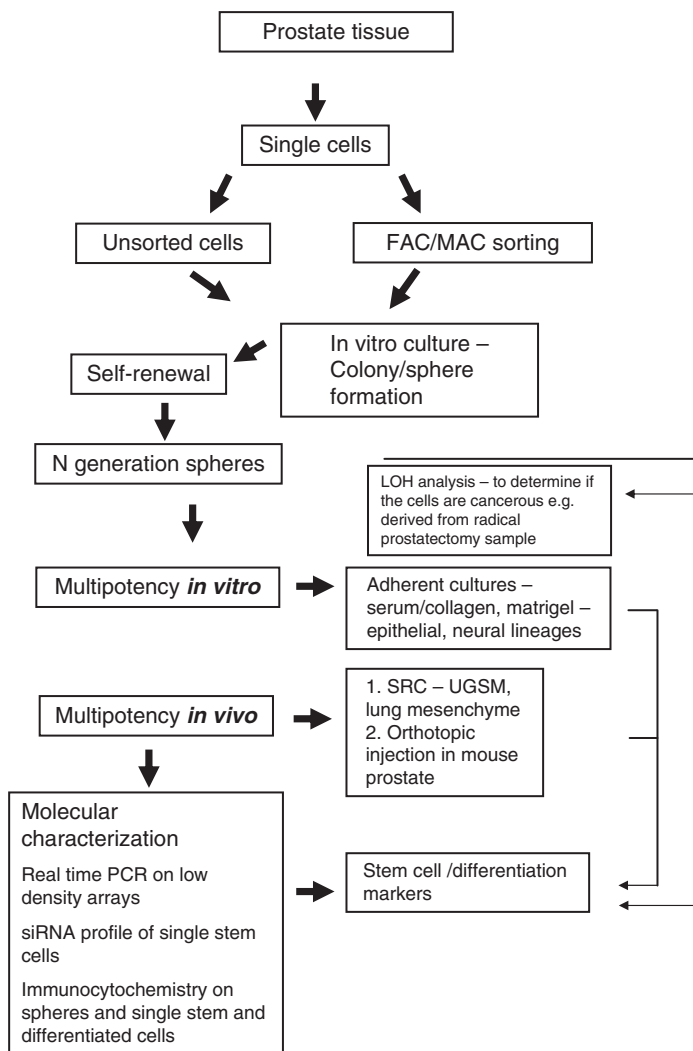
Stem cells reside within a specific microenvironment (or niche) within organs [13]. The composition and function of the organ can therefore be critical for the isolation and maintenance of stem cells *in vitro*. The prostate gland is situated below the bladder, surrounding the urethra and ejaculatory ducts. The anatomy of the prostate is illustrated in Fig. 10.1. It can be described as an inverted pyramid surrounding the urethra as it exits the bladder; the apex of the pyramid pointing towards the penis and the base adjacent to the bladder. The ejaculatory ducts, the conduits of sperm from the testes to the urethra, also pass through the prostate gland, meeting the urethra at the verumontanum. An anatomical model of the prostate that superseded earlier anatomical models [12, 27, 52], was proposed by McNeal [29] and divides the human prostate into three glandular zones (transition, central, peripheral) [29, 52]. The zonal model of the prostate has been supported by evidence from various different investigations utilizing, for example, histochemistry [1, 24], histology [8], computed tomography [31], ultrasound [53] and histopathology [30].

Fig. 10.1 A model of the zonal anatomy of human prostate [30]



10.3 Prostate Stem Cells – Isolation and Characterization

A basic approach, common to the isolation of stem cells from most studies of human or mouse tissue, including prostate is described in Scheme 10.1.



Scheme 10.1 A workflow for the isolation of adult human prostate stem cells

10.4 Sources of Human Prostate Tissue

The main sources for obtaining human prostate are from surgical procedures for diagnosis or treatment of prostatic diseases such as BPH or cancer. Prior ethical permission and patient consent is a pre-requisite. Tissue can be obtained from radical prostatectomy, cystoprostatectomy, Trans-Urethral Resection of the Prostate (TURP) and TRAnsrectal UltraSound (TRUS) biopsy.

10.5 Tissue Handling

It is critical that there is minimal delay between procurement and processing of the prostate obtained at surgery. Wherever possible, tissue should remain in sterile buffered solution (PBS, RPMI 1640 or HBSS) containing antibiotics (10 U/ml) / streptomycin (10 μ g/ml) / fungizone (Amphotericin B 2.5 μ g/ml) from the time of procurement until the time of processing.

10.6 Tissue Processing

To obtain a single cell suspension, prostate tissue is washed in HBSS or PBS and is processed using enzymatic digestion and mechanical dispersion in digestion buffer (HBSS + 5 mM CaCl₂ containing 0.5% bovine serum albumin and collagenase IV (400–600 U/ml), Worthington, UK). The tissue (1 g/15 ml of digestion buffer) is minced using fine scissors into < 1 mm³ pieces. The sample is incubated overnight at 37°C on a shaker. After incubation, 2 ml HBSS is added and the collagenase mixture centrifuged at 300 \times g for 15 min. The pellet is resuspended in 100 μ l of 0.025% DNase and incubated for 5 min. HBSS (3 ml) is added and the suspension passed through a 40 μ m cell strainer (BD Falcon) to remove cell debris and the resulting suspension is centrifuged at 300 \times g for 15 min. The pellet containing the cells is resuspended in 100–200 μ l medium, and cells counted using an haemocytometer. Regular pipetting during collagenase exposure improves the dispersion of epithelial organoids into single cells.

Collagenase I or IA has been used in previous prostate cell isolation protocols [3, 7, 19, 22, 26, 51]. Collagenase IV has a low tryptic activity and is thought to maintain the integrity of cell surface proteins [55]. These properties are important if cells are subsequently used for fluorescence activated cell sorting (FACS) or immunomagnetic cell sorting (MACS) based upon expression of cell membrane proteins. Although it is convenient to leave the tissue to digest in collagenase for 16 h [3, 18, 22, 26], about 40% of the total yield of single cells can be obtained in the first 4 h of a 16 h digestion protocol. It is also useful to select a batch of collagenase after optimization [55]; some suppliers can supply sample batches for optimization and thereafter hold a batch that provides the best yield of viable cells and greatest digestion efficiency.

10.7 Identification and Characterization of Putative Prostate Stem Cells

After obtaining a single cell suspension various approaches can be used to identify and characterize putative prostate and other stem cells. These include cell sorting and in vitro and growth and characterization.

10.8 Cell Sorting

FACS and MACS or side-population analysis (based upon the exclusion of Hoechst 33342 dye) [14] have been used for the isolation of putative stem cells from tissue derived cell populations.

Numerous combinations of cell surface markers have been used to isolate putative stem cells from various mammalian tissues. A list is posted on <http://stemcells.nih.gov/info/scireport/appendixE.asp>. Some robust markers (e.g. Sca1 in combination with other cell surface proteins and side-population analysis) have been used to isolate and characterize putative mouse prostate stem cells and stem-like cells from prostate cancer cell lines. For example, Witte and colleagues [23, 58] and Tang and colleagues [46] have used FACS to isolate and characterize stem and stem-like cells from adult mouse prostate and prostate cancer cell lines, respectively.

Liu and colleagues [26] used antibodies against CD44 and CD57 to separate epithelial cells from TURP derived benign prostate samples using FACS. Bhatt et al. [3] used the Hoechst 33342 exclusion assay [14] to identify side populations of prostate cells obtained from BPH tissue. Hoechst 33342 is extruded by stem cells via the multi-drug resistance protein (MDR-1) family [14]. As stem cells divide slowly and are thought to express a multidrug resistant transporter to exclude Hoechst 33342, a small side population of these cells can be isolated. Based upon this reasoning, Bhatt et al. [3] suggested that a sub-population that accounts for less than 2% of the total cell population, could contain the prostate stem cells. MACS has also been used to identify putative stem cells in whole tissue cell population from diseased human prostate [7, 40, 46]. Collins and colleagues [7, 40] have also isolated cells expressing $\alpha 2\beta 1^{\text{hi}}/\text{CD}44^+$ or $\text{CD}133^+$ enriched $\alpha 2\beta 1^{\text{hi}}/\text{CD}44^+$ for characterization in colony formation assay to assess proliferative capacity (see below).

10.9 In Vitro Cell Culture Techniques for Maintenance and Characterization of Stem Cells

Peehl et al. [36] first described the colony forming ability of primary cultures of human prostate epithelial cells. Hudson et al. [19] plated single cell suspensions (1000 cells/6 cm) of human prostate cells onto a layer of irradiated NIH 3T3 cells on collagen, resulting in the growth of two morphologically distinct colony types. Type I colonies were small and irregular and constituted about 90% of the colonies and expressed either K8 and K14 or just K8 in the smallest colonies. Type II colonies were larger and more regular and constituted about 10% of the colonies and expressed K14. Type II colonies were proposed to be the progeny of basal layer stem cells, while type I cells derived from transit amplifying (TA) cells. However, no attempt was made to test whether the cells from the large colonies possess the ability to self-renew.

Collins and colleagues [7] also used an adherent in vitro growth assay to propagate putative human prostate cells. Prostate cells from TURP derived tissue were

selected on the basis of rapid adhesion to type I collagen. Basal prostate cells (selected by their expression of CD44) were plated onto type I collagen for five minutes. In agreement with Hudson and colleagues [18], different colony types were noted. Adherent cells were $\alpha_2\beta_1$ integrin bright and showed 3.8-fold greater colony forming efficiency compared to non-selected basal cells. 15% of basal cells showed strong $\alpha_2\beta_1$ -integrin expression and high levels of α_2 -integrin staining were also seen in 1% of human basal cells in vivo. However, like other previous attempts to isolate prostate stem cells, no direct evidence of self-renewal of individual cells within this heterogeneous cell fraction was provided.

Non-adherent, sphere forming assay has been employed to isolate and characterize adult stem cells from solid tissues such as the brain and breast [10, 41] although not from prostate. Most sphere formation assays use a variation of chemically defined DMEM/F12 medium containing 2 mM, L-glutamine, 0.6% glucose, 9.6 mg/ml putrescine, 6.3 ng/ml progesterone, 5.2 ng/ml sodium selenite, 0.025 mg/ml insulin, 0.1 mg/ml transferrin, and 2 mg/ml heparin (sodium salt, grade II; Sigma) with growth factors (FGF2 20 ng/ml and EGF human recombinant, 20 ng/ml) [16]. A similar formulation for growth of spheres in suspension is available from Stem Cell Technologies. Using this approach, self-renewal of visually verifiable, single putative stem cells, could be monitored [39]. Spheres are dissociated and individual cells plated into single wells and observed for the formation of new clonal spheres [39]. This procedure is repeated at least up to five generations to validate self-renewal capability of individual cells [39].

10.10 In Vitro Differentiation Potential of Self-Renewing Stem Cells

Differentiation into multiple cell types of the tissue of origin, is a critical in vitro test for the characterization of putative stem cells. Hudson and colleagues [18] used a 3D culture system to determine the differentiation potential of putative stem like cells from type II colonies. Cells derived from type II colonies were grown in 3D Matrigel cultures and formed spherical structures connected by ducts reminiscent of the two-layered architecture of the prostate in vivo. The spheres consisted of a basal layer of cells expressing K5 and K14 and one or more luminal layers of larger, flatter cells expressing weak K5 and K14 and strong K17, K19 and K8 arranged around a lumen. Shed cells within the lumen expressed AR, but no staining for PSA or PAP was seen in this androgen free culture.

10.11 Molecular Characterization of Putative Prostate Stem Cells

Immunochemistry, gene expression microarrays and PCR can be employed to study stem cell markers [10, 37]. The prostate gland epithelium in humans consists of neuroendocrine cells and two types of epithelial cells: basal and luminal. A list of

Table 10.1 Summary of cell marker expression by the different cell populations in normal human prostate epithelium

Histological location	Basal /intermediate	Basal epithelial	Luminal epithelial	
Cell type	Putative stem cell	Transit amplifying	Secretory luminal	
Marker	CD133 ⁺ ABCG2 ⁺ $\alpha 2\beta 1^{\text{Hi}}$	K14 ⁺ K5 ⁺ K15 ⁺ K17 ⁺ K19 ⁺ p63 ⁺ $\alpha 2\beta 1^{\text{Hi}}$ CD44 ⁺ Bcl-2 ⁺ ETS-2 ⁺ pp32 ⁺ , Telomerase ⁺ GSTP1 ⁺ Ki67 ⁺	K8 ⁺ K18 ⁺ K5 ⁺ K15 ⁺ K17 ⁺ K19 ⁺ K7 ⁺ CD44 ⁺ PSCA ⁺ p63 ⁺	AR ⁺ PSA ⁺ K8 ⁺ K18 ⁺ PAP ⁺ PSA ⁺ CPP32 ⁺ CD57 ⁺ p21 ^{Kip1+}
	p63 ⁻ PSCA ⁻ AR ⁻ PSA ⁻	CD133 ⁻ ABCG2 ⁻ PSCA ⁻ AR ⁻ PSA ⁻ p21 ^{Kip1-} K8 ⁻ K18 ⁻	CD133 ⁻ ABCG2 ⁻ $\alpha 2\beta 1^{\text{Lo}}$ p63 ⁻ AR ⁻ PSA ⁻ p21 ^{Kip1-}	CD133 ⁻ ABCG2 ⁻ $\alpha 2\beta 1^{\text{Lo}}$ p63 ⁻ PSCA ⁻ K5 ⁻ K14 ⁻

prostate specific, putative stem cell and differentiated epithelial markers is given in Table 10.1. Some of these markers have been used to characterize putative prostate stem cells. The utility of these markers was discussed in a recent review by Tang and colleagues [46].

A number of genes have been suggested as markers of ‘stemness’ in stem cells from various tissues [22, 35]. These markers include CD34, mCD24a, CD10, Bmi-1, Bcrp1, nestin, Bcrp1 and PNA [15, 41, 50]. Furthermore, in a series of publications [9, 17, 32, 59] transfection of 4 genes (Oct 4, KLF 4, SOX2 and c-MYC) has been shown to reprogramme adult human and mouse cells to an earlier pluripotent, stem-like state. We have investigated the expression of numerous known stem cells markers using global gene expression analysis on an Affymetrix chip using the putative stem cells from type II colonies. The rationale was as follows: if type II colonies are derived from stem like cells and type I from transient amplifying cells, there should be differential expression of known stem cell markers in cells derived from these colonies [21]. Global gene expression profiling of type I and II colonies (Fig. 10.2) did not reveal any difference in expression for any known stem cell marker (including CD133, Bmi1, CD18, CD34).

Collins et al. [7] suggested that some basal cells that show rapid adhesion and are capable of differentiation in vivo express CK18, 34 β E12, CK19, PAP and PSA. In another study of putative prostate stem cell identification, Litvinov et al.

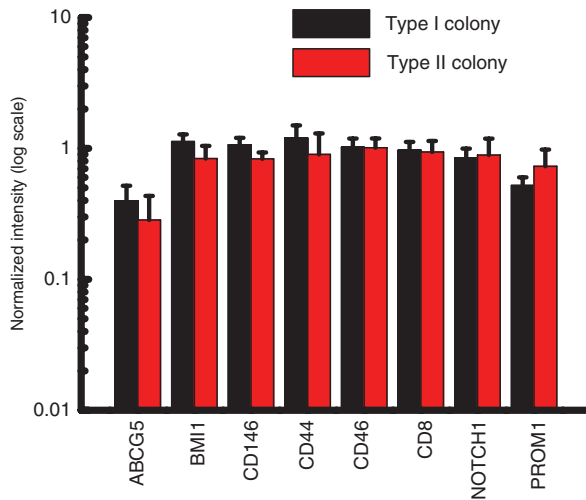


Fig. 10.2 No significant difference in the gene expression of 25 known stem cell markers was found in type I and type II colonies. A representative graph for normalized expression of BMI1, CD44, CD146, CD46, CD8, PROM1, ABCG5, NOTCH1. Gene expression analysis was performed on 5 pairs of type I and type II colonies using an Affymetrix gene chip array (HGU 133 Plus 2.0). Microarray data was analyzed using GeneSpring (Agilent) version 7.2 using relaxed statistics ($p < 0.1$) and 1.5 fold difference

[25] investigated the prostate epithelial stem cell population in vitro that they defined as $CD133^+/ABCG2^+/\alpha2\beta1^{Hi}/p63^-/PSCA^- /AR^-/PSA^-$. Their working model describes a prostate epithelial differentiation process in which cells proceed down a neuroendocrine or luminal lineage. Cells destined for the luminal epithelium become TA cells with the phenotype $CD133^- /ABCG2^- /\alpha2\beta1^{Hi}/p63^+/PSCA^- /AR^- /PSA^-$ as well as expressing K5 and K14 and amplify through a number of divisions. At some point these cells acquire the ‘intermediate’ (TA) cell phenotype of $CD133^- /ABCG2^- /\alpha2\beta1^{Lo}/p63^-/PSCA^+/AR^- /PSA^-$ expressing K8 and K18 also. However, whether these are functional stem cells with regards to self-renewal and pluripotency was not investigated.

10.12 Techniques for In Vivo Characterization of Putative Human Prostate Stem Cells

In vivo assays are crucial in determining the veracity of stem cells isolated in vitro. For prostate stem cells there is a lack of quantitative, in vivo, assays similar to those established for hematopoietic and other solid tissue adult stem cells [42–44, 47, 54], to assess self-renewal, differentiation potential and frequency of stem cells. This has proved a major impediment for the purification and physiological characterization of adult human prostate stem cells.

For putative prostate stem cells, Collins et al. [7] provided strong evidence of pluripotency of a cell population isolated from adult prostate using mouse xenograft assays. Basal epithelial cells (1×10^5 to 1×10^6 cells) in a 1:1 ratio with stromal cells were injected subcutaneously into nude mice. Grafts were removed after 6 weeks, formalin fixed and embedded in paraffin and sectioned. Microscopic examination of the grafts indicated development of glandular structures. The capacity of the grafted cells to differentiate in vivo was measured by the expression of androgen receptor, prostate specific antigen and prostatic acid phosphatase. Other committed progenitor and differentiated cells present may also have contributed to the glandular structures [46].

Prostate development has been studied in vivo by a tissue recombination method initially developed by Bogden et al. [5]. This was subsequently modified for prostate by Cunha and colleagues [6]. The 'subrenal capsule assay' (SRC) involved transplantation of adult mouse prostate tissue fragments under the renal capsule of an immunodeficient mouse with rodent urogenital sinus mesenchyme (UGSM). This technique, initially applied to whole tissue fragments, was later applied to enzymatically dissociated cells. This approach had the advantage that specific subpopulations of cells could be selected on the basis of their cell surface markers prior to transplantation [23, 56]. An interpretational problem arises from the fact that thousands of cells from a heterogeneous population need to be injected and therefore the origin of cells giving rise to the glandular structure is difficult to ascertain. For mouse derived stem cells, this problem can be limited using mice expressing GFP or dsRED. Witte and colleagues have utilized this method to show that ductal structures may be clonal [57]. Techniques to determine single stem cell self-renewal and differentiation in vivo, as used in breast and skeletal muscle stem cells studies [42, 44], have not yet been applied to putative stem cells from the prostate.

References

1. Arenas MI, Romo E, de G, I, de Bethencourt FR, Sanchez-Chapado M, Fraile B and Paniagua R. A lectin histochemistry comparative study in human normal prostate, benign prostatic hyperplasia, and prostatic carcinoma. *Glycoconj J* 16: 375–382, 1999.
2. Azuma M, Hirao A, Takubo K, Hamaguchi I, Kitamura T and Suda T. A quantitative matrigel assay for assessing repopulating capacity of prostate stem cells. *Biochem Biophys Res Commun* 338: 1164–1170, 2005.
3. Bhatt RI, Brown MD, Hart CA, Gilmore P, Ramani VA, George NJ and Clarke NW. Novel method for the isolation and characterisation of the putative prostatic stem cell. *Cytometry* 54A: 89–99, 2003.
4. Blau HM, Brazelton TR and Weimann JM. The evolving concept of a stem cell: entity or function? *Cell* 105: 829–841, 2001.
5. Bogden AE, Haskell PM, LePage DJ, Kelton DE, Cobb WR and Esber HJ. Growth of human tumor xenografts implanted under the renal capsule of normal immunocompetent mice. *Exp Cell Biol* 47: 281–293, 1979.
6. Chung LW and Cunha GR. Stromal-epithelial interactions: II. Regulation of prostatic growth by embryonic urogenital sinus mesenchyme. *Prostate* 4: 503–511, 1983.

7. Collins AT, Habib FK, Maitland NJ and Neal DE. Identification and isolation of human prostate epithelial stem cells based on alpha(2)beta(1)-integrin expression. *J Cell Sci* 114: 3865–3872, 2001.
8. Colombel M, Vacherot F, Diez SG, Fontaine E, Buttyan R and Chopin D. Zonal variation of apoptosis and proliferation in the normal prostate and in benign prostatic hyperplasia. *Br J Urol* 82: 380–385, 1998.
9. Dimos JT, Rodolfa KT, Niakan KK, Weisenthal LM, Mitumoto H, Chung W, Croft GF, Saphier G, Leibel R, Goland R, Wichterle H, Henderson CE and Eggan K. Induced pluripotent stem cells generated from patients with ALS can be differentiated into motor neurons. *Science* 321: 1218–1221, 2008.
10. Dontu G, Abdallah WM, Foley JM, Jackson KW, Clarke MF, Kawamura MJ and Wicha MS. In vitro propagation and transcriptional profiling of human mammary stem/progenitor cells. *Genes Dev* 17: 1253–1270, 2003.
11. Dontu G, Al Hajj M, Abdallah WM, Clarke MF and Wicha MS. Stem cells in normal breast development and breast cancer. *Cell Prolif* 36 Suppl 1: 59–72, 2003.
12. Franks LM. Benign nodular hyperplasia of the prostate: a review. *Ann R Coll Surg* 14: 92–106, 1954.
13. Fuchs E, Tumber T and Guasch G. Socializing with the neighbors: stem cells and their niche. *Cell* 116: 769–778, 2004.
14. Goodell MA, Brose K, Paradis G, Conner AS and Mulligan RC. Isolation and functional properties of murine hematopoietic stem cells that are replicating in vivo. *J Exp Med* 183: 1797–1806, 1996.
15. Goto K, Salm SN, Coetzee S, Xiong X, Burger PE, Shapiro E, Lepor H, Moscatelli D and Wilson EL. Proximal prostate stem cells are programmed to regenerate a proximal-distal ductal axis. *Stem Cells* 24: 1859–1868, 2006.
16. Gritti A, Frolichsthal-Schoeller P, Galli R, Parati EA, Cova L, Pagano SF, Bjornson CR and Vescovi AL. Epidermal and fibroblast growth factors behave as mitogenic regulators for a single multipotent stem cell-like population from the subventricular region of the adult mouse forebrain. *J Neurosci* 19: 3287–3297, 1999.
17. Huangfu D, Maehr R, Guo W, Eijkelenboom A, Snitow M, Chen AE and Melton DA. Induction of pluripotent stem cells by defined factors is greatly improved by small-molecule compounds. *Nat Biotechnol* 26: 795–797, 2008.
18. Hudson DL, Guy AT, Fry P, O'Hare MJ, Watt FM and Masters JR. Epithelial cell differentiation pathways in the human prostate: identification of intermediate phenotypes by keratin expression. *J Histochem Cytochem* 49: 271–278, 2001.
19. Hudson DL, O'Hare M, Watt FM and Masters JR. Proliferative heterogeneity in the human prostate: evidence for epithelial stem cells. *Lab Invest* 80: 1243–1250, 2000.
20. Isaacs JT and Coffey DS. Etiology and disease process of benign prostatic hyperplasia. *Prostate Suppl* 2: 33–50, 1989.
21. Ivanova NB, Dimos JT, Schaniel C, Hackney JA, Moore KA and Lemischka IR. A stem cell molecular signature. *Science* 298: 601–604, 2002.
22. Kassen A, Sutkowski DM, Ahn H, Sensibar JA, Kozlowski JM and Lee C. Stromal cells of the human prostate: initial isolation and characterization. *Prostate* 28: 89–97, 1996.
23. Lawson DA, Xin L, Lukacs RU, Cheng D and Witte ON. Isolation and functional characterization of murine prostate stem cells. *Proc Natl Acad Sci U S A* 104: 181–186, 2007.
24. Leung CS and Srigley JR. Distribution of lipochrome pigment in the prostate gland: biological and diagnostic implications. *Hum Pathol* 26: 1302–1307, 1995.
25. Litvinov IV, Vander Griend DJ, Xu Y, Antony L, Dalrymple SL and Isaacs JT. Low-calcium serum-free defined medium selects for growth of normal prostatic epithelial stem cells. *Cancer Res* 66: 8598–8607, 2006.
26. Liu AY, True LD, LaTray L, Nelson PS, Ellis WJ, Vessella RL, Lange PH, Hood L and van den EG. Cell-cell interaction in prostate gene regulation and cytodifferentiation. *Proc Natl Acad Sci U S A* 94: 10705–10710, 1997.

27. Lowsley OS. The development of the human prostate gland with reference to the development of other structures at the neck of the urinary bladder. *Am J Anat* 13: 299–349, 1912.
28. McKay R. Stem cells in the central nervous system. *Science* 276: 66–71, 1997.
29. McNeal JE. The zonal anatomy of the prostate. *Prostate* 2: 35–49, 1981.
30. McNeal JE, Redwine EA, Freiha FS and Stamey TA. Zonal distribution of prostatic adenocarcinoma. Correlation with histologic pattern and direction of spread. *Am J Surg Pathol* 12: 897–906, 1988.
31. Mirowitz SA and Hammerman AM. CT depiction of prostatic zonal anatomy. *J Comput Assist Tomogr* 16: 439–441, 1992.
32. Park IH, Zhao R, West JA, Yabuuchi A, Huo H, Ince TA, Lerou PH, Lensch MW and Daley GQ. Reprogramming of human somatic cells to pluripotency with defined factors. *Nature* 451: 141–146, 2008.
33. Park IK, Morrison SJ and Clarke MF. Bmi1, stem cells, and senescence regulation. *J Clin Invest* 113: 175–179, 2004.
34. Patrawala L, Calhoun T, Schneider-Brossard R, Zhou J, Claypool K and Tang DG. Side population is enriched in tumorigenic, stem-like cancer cells, whereas ABCG2+ and A. *Cancer Res* 65: 6207–6219, 2005.
35. Patrawala L, Calhoun-Davis T, Schneider-Brossard R and Tang DG. Hierarchical organization of prostate cancer cells in xenograft tumors: the CD44+alpha2beta1+ cell population is enriched in tumor-initiating cells. *Cancer Res* 67: 6796–6805, 2007.
36. Peehl DM and Stamey TA. Serial propagation of adult human prostatic epithelial cells with cholera toxin. *In Vitro* 20: 981–986, 1984.
37. Ramalho-Santos M, Yoon S, Matsuzaki Y, Mulligan RC and Melton DA. “Stemness”: transcriptional profiling of embryonic and adult stem cells. *Science* 298: 597–600, 2002.
38. Reya T, Morrison SJ, Clarke MF and Weissman IL. Stem cells, cancer, and cancer stem cells. *Nature* 414: 105–111, 2001.
39. Reynolds BA and Rietze RL. Neural stem cells and neurospheres – re-evaluating the relationship. *Nat Methods* 2: 333–336, 2005.
40. Richardson GD, Robson CN, Lang SH, Neal DE, Maitland NJ and Collins AT. CD133, a novel marker for human prostatic epithelial stem cells. *J Cell Sci* 117: 3539–3545, 2004.
41. Rietze RL, Valcanis H, Brooker GF, Thomas T, Voss AK and Bartlett PF. Purification of a pluripotent neural stem cell from the adult mouse brain. *Nature* 412: 736–739, 2001.
42. Sacco A, Doyonnas R, Kraft P, Vitorovic S and Blau HM. Self-renewal and expansion of single transplanted muscle stem cells. *Nature* 456: 502–506, 2008.
43. Schneider TE, Barland C, Alex AM, Mancianti ML, Lu Y, Cleaver JE, Lawrence HJ and Ghadially R. Measuring stem cell frequency in epidermis: a quantitative in vivo functional assay for long-term repopulating cells. *Proc Natl Acad Sci U S A* 100: 11412–11417, 2003.
44. Stingl J, Eirew P, Ricketson I, Shackleton M, Vaillant F, Choi D, Li HI and Eaves CJ. Purification and unique properties of mammary epithelial stem cells. *Nature* 439: 993–997, 2006.
45. Takahashi K and Yamanaka S. Induction of pluripotent stem cells from mouse embryonic and adult fibroblast cultures by defined factors. *Cell* 126: 663–676, 2006.
46. Tang DG, Patrawala L, Calhoun T, Bhatia B, Choy G, Schneider-Brossard R and Jeter C. Prostate cancer stem/progenitor cells: identification, characterization, and implications. *Mol Carcinog* 46: 1–14, 2007.
47. Till JE and McCulloch EA. A direct measurement of the radiation sensitivity of normal mouse bone marrow cells. *Radiat Res* 14: 213–222, 1961.
48. Toma JG, Akhavan M, Fernandes KJ, Barnabe-Heider F, Sadikot A, Kaplan DR and Miller FD. Isolation of multipotent adult stem cells from the dermis of mammalian skin. *Nat Cell Biol* 3: 778–784, 2001.

49. Tropepe V, Coles BL, Chiasson BJ, Horsford DJ, Elia AJ, McInnes RR and van der KD. Retinal stem cells in the adult mammalian eye. *Science* 287: 2032–2036, 2000.
50. Uchida S, Yokoo S, Yanagi Y, Usui T, Yokota C, Mimura T, Araie M, Yamagami S and Amano S. Sphere formation and expression of neural proteins by human corneal stromal cells in vitro. *Invest Ophthalmol Vis Sci* 46: 1620–1625, 2005.
51. Uzgare AR, Xu Y and Isaacs JT. In vitro culturing and characteristics of transit amplifying epithelial cells from human prostate tissue. *J Cell Biochem* 91: 196–205, 2004.
52. Villers A, Steg A and Boccon-Gibod L. Anatomy of the prostate: review of the different models. *Eur Urol* 20: 261–268, 1991.
53. Villers A, Terris MK, McNeal JE and Stamey TA. Ultrasound anatomy of the prostate: the normal gland and anatomical variations. *J Urol* 143: 732–738, 1990.
54. Weissman IL. The road ended up at stem cells. *Immunol Rev* 185: 159–174, 2002.
55. Worthington CC. *Worthington enzyme manual: enzymes and related biochemicals*. Free Hold: Worthington Biochemical Corp, 1988.
56. Xin L, Ide H, Kim Y, Dubey P and Witte ON. In vivo regeneration of murine prostate from dissociated cell populations of postnatal epithelia and urogenital sinus mesenchyme. *Proc Natl Acad Sci U S A* 100 Suppl 1: 11896–11903, 2003.
57. Xin L, Lawson DA and Witte ON. The Sca-1 cell surface marker enriches for a prostate-regenerating cell subpopulation that can initiate prostate tumorigenesis. *Proc Natl Acad Sci U S A* 102: 6942–6947, 2005.
58. Xin L, Lukacs RU, Lawson DA, Cheng D and Witte ON. Self-renewal and multilineage differentiation in vitro from murine prostate stem cells. *Stem Cells* 25: 2760–2769, 2007.
59. Zhou Q, Brown J, Kanarek A, Rajagopal J and Melton DA. In vivo reprogramming of adult pancreatic exocrine cells to beta-cells. *Nature* 455: 627–632, 2008.